Biofilm formation in the thermoacidophilic crenarchaea *Sulfolobus spp.*

Dissertation
zur Erlangung des Doktorgrades
der Naturwissenschaften
(Dr. rer. nat.)

dem
Fachbereich Biologie
der Philipps-Universität Marburg
vorgelegt von

Andrea Koerdt
aus Wickede

Marburg / Lahn, August 2011

Die Untersuchungen zur vorliegenden Arbeit wurden von Oktober 2008 bis Juli 2011 am Max-Planck-Institut für terrestrische Mikrobiologie unter der Leitung von Dr. Sonja-Verena Albers durchgeführt.

Vom Fachbereich Biologie der Philipps-Universität Marburg als Dissertation angenommen am:

Erstgutachter: Dr. Sonja-Verena Albers
Zweitgutachter: Prof. Dr. Martin Thanbichler

Tag der mündlichen Prüfung:

Die während der Promotion erzielten Ergebnisse sind zum Teil in folgenden Originalpublikationen veröffentlicht:

1. Zolghadr, B., A. Klingl, **A. Koerdt**, A. J. Driessen, R. Rachel, and S. V. Albers. 2010. Appendage mediated surface adherence of *Sulfolobus solfataricus*. J Bacteriol 192:104-110.

2. **A. Koerdt**, J. Godeke, J. Berger, K. M. Thormann, and S. V. Albers. 2010. Crenarchaeal biofilm formation under extreme conditions. PLoS One 5:e14104.

3. **A. Koerdt**[#], A. Orell[#], T. K. Pham, J. Mukherjee, A. Wlodkowski, E. Karunakaran, C. A. Biggs, P. C. Wright, and S. V. Albers. 2011. Macromolecular Fingerprinting of *Sulfolobus* Species in Biofilm: A Transcriptomic and Proteomic Approach Combined with Spectroscopic Analysis. J Proteome Res. (DOI: 10.1021/pr2003006)

Die während der Promotion erzielten Ergebnisse die zum Zeitpunkt der Einreichung der Arbeit im anerkannten Journal eingereicht wurden:

1. **A. Koerdt**[#], AL. Henche[#], A. Ghosh and SV Albers. 2011. Influence of cell surface structures on crenarchaeal biofilm formation (Submitted in Environmental Microbiology)

2. **Koerdt A**., Jachlewski S., Ghosh A., Wingender J., Siebers B., Albers SV. 2011. Complementation of *Sulfolobus solfataricus* PBL2025 with an α-mannosidase: effects on surface attachment and biofilm formation (Submitted in Extremophiles)

Beide Autoren trugen gleichermaßen zur Erlangung der Ergebnisse bei

Meinem Großvater
(For my grandfather)

Contents

Abbreviations

CLSM	Confocal laser scanning microscopy
ConA	Concavalin A
DAPI	6-diamidino-2-phenylindole
DDAO	7-hydroxy-9H-(1,3-dichloro-9,9-dimethylacridin-2-one)
EDTA	Ethylendiamine tetra-acetic acid
EM	Electron microscopy
EPS	Exopolymeric substances
GFP	Green fluorescence protein
GS-II	Lectin GS-II from *Griffonia simplicifolia*
h	Hours
IB_4	Isolectin GS-IB4 from *Griffonia simplicifolia*
LB	Lysogenic broth
$\log_2 FC$	log2 fold change
Mbp	Mega base pairs
min	Minute
OD	Optical density
PCR	Polymerase chain reaction
rpm	Rounds per minute
RT	Room temperature
SDS-PAGE	Sodium dodecyl sulfate polyacrylamide gel electrophoresis
TE	Tris-EDTA

1   Introduction

1.1   Biofilm- A choice between the planktonic or biofilm style of life

The social activities and organization of microorganisms are keys to their ecological success in natural environments. In nature microorganisms adapt different survival strategies to thrive under different environmental conditions. They can survive either as solitary uni-cellular life form called „planktonic life style or free swimming life style' or they can opt for conglomeration of different genus and/or species to form a colonized multi-cellular form called „biofilms'. In the planktonic life style or free swimming life style cells can translocate (swim or swarm) from one location to the other in order to reach the most suitable conditions (food, light etc.) for survival. On the other hand microbial association in biofilms is an efficient means of surviving in a favorable microenvironment rather than being swept away by natural disturbances. In general, biofilm formation is one of the most common life styles found in all three domains of life.

Biofilms are cellular clusters, containing single or/and multiple species and are embedded in a wide range of self-produced extracellular polymeric substances (EPS) (43, 108). The produced EPS, also known as the matrix of biofilms, is an important characteristic feature in the biofilm life style and is necessary for the close contact between the cells and between the cells and biotic or abiotic surfaces. An additional feature of the EPS is that it maintains the close connection of cells and therefore ensures improved interaction and communication with each other. Furthermore, in such cellular communities the ability of protection against environmental changes or harsh conditions is highly improved (169, 288). Occasionally, biofilm influences the course of human life in significant manner. The most common biofilm life style known in the human body is dental plaque (104). Additionally, biofilms can occur in other medical conditions (catheters, implants), (12, 106, 120, 297) industry (pipe line, tanks) (68) and of course in environmental habitats (e.g. river, ocean, soil). The formation of biofilm is a reversible dynamic process and highly abundant on earth. However, under natural conditions this life style of microorganisms has both beneficial as well as detrimental effects in nature. Understanding why, when and how biofilms are formed and how they influence nature as well as human lives, might provide new insights, which possibly lead to high scientific as well as public benefits.

1.2   Development of the biofilm

One of the most controversial topics during the early phases of biofilm research was how to determine whether a microbial community is forming a biofilm or not. The most commonly used definition was formulated by Costerton et al. (63) and supported by other groups independently (158, 186, 199, 203). They described biofilm as community of microorganisms, embedded into a matrix in which the cells tightly connect to each other and to a surface or interface. In short, biofilm can be considered as "living material" ("bio") which forms a layer ("film"). However, this layer of "living material" can be composed of a number of different species (e.g. 300-700 for dental plaque (1)). The number of known surfaces colonized by biofilm is uncountable, but can be simply categorized into two classes, biotic surfaces that include plants, animals or other microbes and abiotic surfaces that include minerals, metals, glass, PVC, catheter or the air-water interface. So far in all domains of life biofilm formation has been observed and follows a general process of development. For eukarya several studies about fungal biofilm have been performed (57, 165), whereas very limited information is available about archaeal biofilm (20, 243). However, bacterial biofilms, especially those of pathogens like *Pseudomonas aeruginosa* (86, 92, 166, 173, 293) or *Escherichia coli* (29, 94, 125, 175, 216), are the most explored amongst all three domains of life.

The current model of biofilm formation divides its development into five distinct steps (Figure 1-1) (63, 186, 199). The initial surface attachment is the first step in which extracellular components of planktonic cells converge to a surface (40, 176, 182, 216). The cells attach weakly to the surface and are at this point still motile. As cells at this stage can still detach it is termed transient attachment. Subsequently, the attachment of a subpopulation becomes irreversible and is then referred to as permanent attachment (110, 130, 286, 291). The following steps of the development follow a strict scheme. Microcolonies accumulate during the first maturation phase and the production of EPS is observed (187). The next step referred to as the Maturation 2 represents the phenotype of a fully developed biofilm (29, 166). In this stage the biofilm attains the maximum thickness and typical shape and/or morphology. Following the maturation cells stay in the biofilm life style until a subtle change in the environmental conditions such as depletion of nutrients is sensed, which triggers the release of the cells called dispersal, the final step of the development. Throughout the dispersal stage cells produce hydrolyzing enzymes that decompose the extracellular matrix (38, 41, 294), eventually become motile and escape the old biofilm (126, 239, 307). Free cells are then preparing themselves for a next round of fresh colonization to form biofilm. The entire process of biofilm formation is heavily regulated at different developmental

stages; however, the mechanisms are still largely unknown. Furthermore, many of the characteristics of the different steps exhibit a high variety depending on the presence of different species and conditions under which the biofilm is formed.
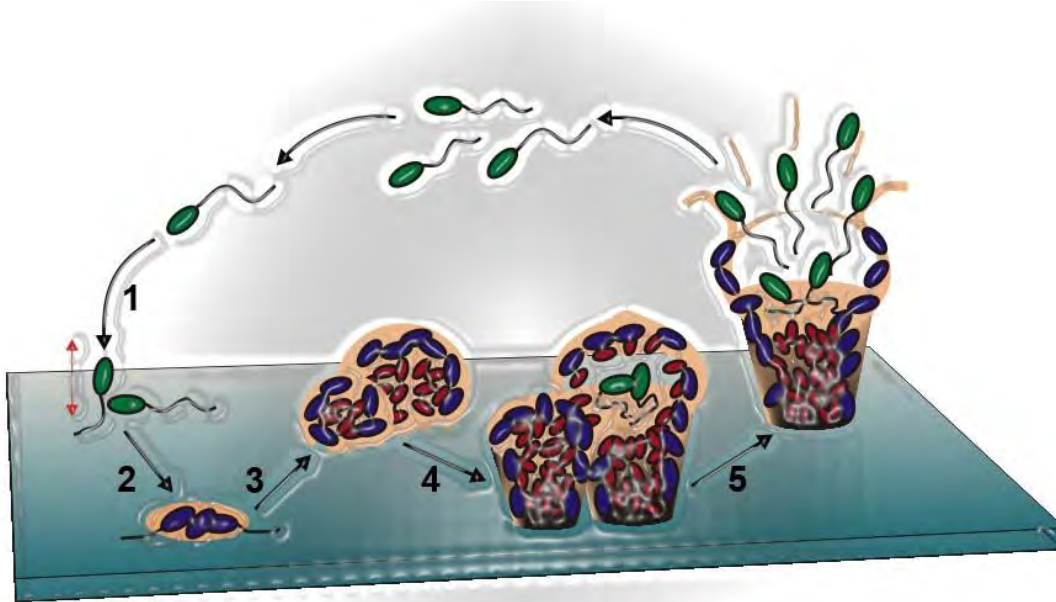

Figure 1-1: The five stages of biofilm development: The current model of the development of biofilm formation includes five distinct steps and is based mainly on results obtained with *P. aeruginosa*. (1) Initial surface attachment: Motile cells (green) get attached to a surface via surface structures. This step is reversible (indicated by the red arrow) and cells can still leave the surface. (2) Irreversible surface attachment: The cells get attached strongly to the surface, the motility gets lost (blue cells) and EPS is synthesized. (3) Maturation 1: The cells start to form microcolonies and produce special proteins needed for the biofilm life style. Cells which are deeply embedded in the cluster have lower access to nutrients leading to a reduction of the metabolic flux (red cells). (4) Maturation 2: The growth and the final morphology of the colonies are achieved. The protein expression pattern changes and cells start secreting matrix degradation proteins. In the cluster some cells become motile. (5) Dispersal: As a result of environmental changes, the cells synthesize more degradation proteins. More motile cells appear in the cluster. The degradation proteins break the matrix and the motile cells are released into the medium. The cells are now again in planktonic life style and ready to start new micro colony formation.

In archaea most of the biofilm related research that has been performed is related to initial surface attachment. Only one study discovered some components of the matrix and the reaction to stress of the euryarchaeote *Archaeoglobus fulgidus* (152) and the other revealed ten proteins which were differently regulated in *Ferroplasma acidarmanus* biofilm in comparison to planktonic cells (20), however, this studies have provided only basic insights on archaeal surface attachment and biofilm (in comparison to these what is known in bacteria). Consequently, less information is available for the development of wildtype (Chapter 3.2, (146)) or mutant biofilms (Chapter 3.1 (327); 3.4), the composition of EPS (Chapter 3.2, (146)) and transcriptomic or proteomic analyses (Chapter 3.3). Indeed, information of later stages of biofilm maturation in

archaea is only available for *Sulfolobales*, and will be described and presented in this work. These further detailed analyses might provide a detailed view of the way archaea cope with a variety of different environmental conditions.

1.3 The Domain of archaea

All life forms are divided into three domains of life (eukarya, bacteria and archaea; Figure 1-2). The most recently identified one is called „archaea' which was introduced by Woese and co-workers in 1990 (311-312). Archaea are often termed as extremophiles as they were initially cultivated only from different extreme environments.
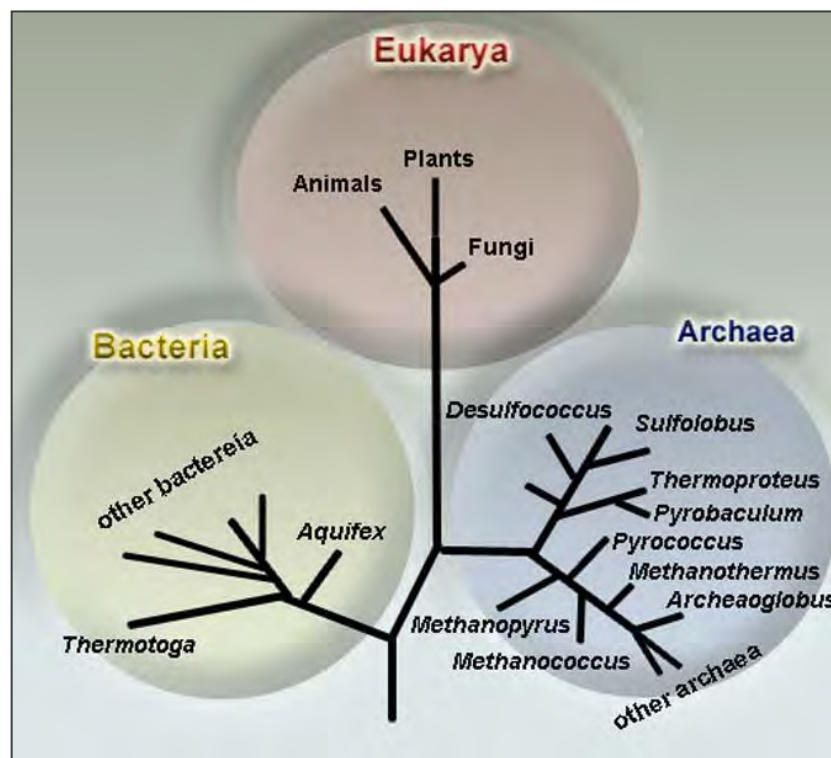
Figure 1-2: Phylogenic tree of life. Three domains, bacteria, eukarya and archaea are depicted. For each domain is exemplarily shown some families or kingdoms.

However, recent studies have confirmed their occurrence in almost every ecological niche known (53, 71, 139). In 1972, the first hyperthermophilic archaeon, *Sulfolobus acidocaldarius* was isolated from Yellow Stone National Park by Thomas Brock *et.al.* and was considered as a bacterium at the beginning (47). The idea of the third domain of life, e.g., archaea appeared after the pioneering work of Carl Woese in 1990. Immediately after the settlement of Woese's work, *S. acidocaldarius* and many other isolates were classified into the archaeal domain of life. Archaea in general can easily

be separated from bacteria by comparing 16S rRNA gene sequences and also considering the absence of the bacterial murein layer (134). Additionally, the lipids of the archaeal membrane are composed of polyisoprenyl groups ether-linked to a polar head group of a glycerol backbone whereas those in either bacteria or eukarya are ester-linked (45, 69). Interestingly, many characteristic molecules in archaea show similarities to eukaryotic homologs, e.g., the DNA-depending RNA polymerase of *S. acidocaldarius*, *Halobacterium halobium* or *Thermoplasma acidophilum* is more similar to these of eukarya (326). In general the transcription as well as the translation machinery is more similar to the eukaryotic system whereas the metabolism is more related to the bacterial one. Initially, the archaeal domain was divided into two main kingdoms namely the euryarchaeota and crenarchaeota (312). However, with the advancement of archaeal research, new strains have been isolated and compared with already existing isolates. Recently based on the available SSu rRNA gene sequences three additional kingdoms were introduced: korarchaea, nanoarchaea and thaumarchaea (46, 76, 121). In the last two decades most of the archaeal research was dedicated to organisms belonging to either of the kingdoms crenarcheaota or euryarchaeota. Consequently, most of the available information is restricted to these two kingdoms. Members of the kingdom euryarchaea mostly constitute methanogens, halophiles and hyperthermophiles (82, 242). In contrast, most of the hyperthermoacidophilic archaea belong to the kingdom crenarchaea (47, 326), e.g., *Acidilobus aceticus* (218), *Caldisphaera lagunensis* (124) or *Sulfolobus islandicus* (325).

1.3.1 The genus *Sulfolobus*

Thermoacidophilic crenarchaea *Sulfolobus spp.* are commonly isolated from extreme habitats (60°C-90°C and pH 2-4) such as solfataric fields, hot water or mud pools. Members of the *Sulfolobales* are found to be spread over the whole world. *S. acidocaldarius* was the first discovered member of the *Sulfolobales* and isolated from a hot spring in Yellowstone National Park (USA) (47). Two other isolated species are *Sulfolobus solfataricus* P2, first found in Pozzuoli (Italy) (326) and *Sulfolobus tokodaii*, isolated in Japan (269). These closely related strains are the basis for the in this work described research on biofilm formation (Figure 1-3). Noteworthy, *S. solfataricus* PBL2025 is derived from *S. solfataricus* 98/2, an original Yellowstone National park isolate, and lacks ~50 genes (SSO3004-SSO3050) in the genome. One of the missing genes is the β-glycosidase (*lacS*) (SSO3019) which has proven to be useful as a selectable marker for genetic manipulations in *Sulfolobales* (5, 240, 299). A

closely related strain to *S. solfataricus* is *S. islandicus* which was isolated from the Reykjanes sulfataric field in Iceland (325) and many other places all around the world (308).
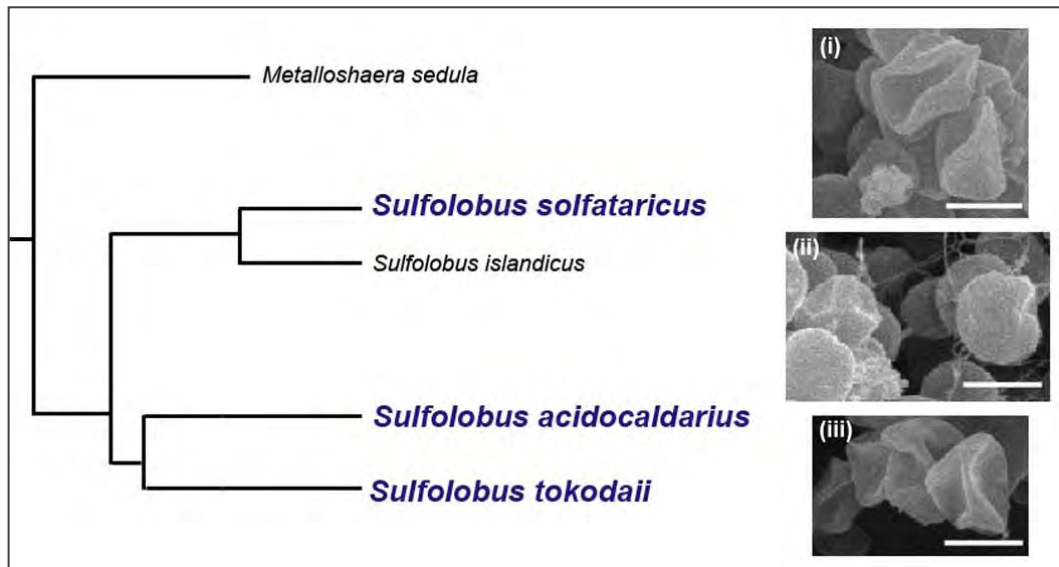

Figure 1-3: Phylogenetic tree of related species based on multiple-genome alignment: *Metalloshaera sedula* is used as an out-group. The, for this work important, *Sulfolobus* strains are highlighted in blue. On the right side the SEM pictures of biofilm cells of (i) *S. solfataricus* (7 days old), (ii) *S. acidocaldarius* (6 days old) and (iii) *S. tokodaii* (7 days old). Bars are 1 µm in length.

However, the three *Sulfolobus* strains have properties and aspects in common along with features specific to each of these species. Commonalities are such as the typical cell shape (lobed and irregular coccoid-shaped, see above Figure 1-3), cell size (0.8 - 2 µm) and growth conditions (aerobically at 75°-80°C and an optimal pH of 2.5).

Until now several *Sulfolobus spp.* have been sequenced and the genomes are publically available. Moreover, genetic tools (e.g. deletion, expression vectors) are available for *S. solfataricus, S. islandicus* and *S. acidocaldarius* (157). Data about the genomic sequences of the three *Sulfolobus* strains used in this study are summarized in Table 1-1 (59, 140, 247). The genome size of the three strains differs and *S. solfataricus* exhibits the highest number of open reading frames (ORFs). Indeed, *S. solfataricus* exhibits the broadest metabolic spectrum and can take up and utilize for instance a variety of carbon sources, in contrast to the other *Sulfolobales ssp.* (103). Although the basic house-keeping genes that encode proteins involved in the nonphosphorylated Entner–Doudoroff pathway exist in *S. acidocaldarius* as well as *S. tokodaii* (250), several sugar uptake systems are missing in these two species and are present in *S. solfataricus* (7, 75). Several carbon sources can be utilized by all three species, for instance xylose, dextrin, sucrose and maltose.

Table 1-1: Basic Information about the genetic context of three *Sulfolobus ssp*.: Comparative demonstration of genome size, open reading frames (ORF), GC-content and number of identified insertion sequence element (IS-element) of three *Sulfolobales spp.*. The listed information based on the genome sequencing studies for *S. solfataricus* (She et al., 2001 (247)), *S. acidocaldarius* (Chen et al., 2005 (59)) and *S. tokodaii* (Kawarabayasi et al., 2001 (140)).

Strain	Genome size (Mbp)	ORFs	GC-content (%)	IS-Elements
S. solfataricus	2.9	2997	35.8	201
S. acidocaldarius	2.2	2292	37.7	0
S. tokodaii	2.7	2826	32.8	34

Another interesting aspect is that the genome of *S. solfataricus* contains several IS-elements (247) whereas the number in *S. tokodaii* is less (140) and for *S. acidocaldarius* no active "jumping" IS-element could be detected (59).

1.4 Cell surfaces and surface appendages of archaea

In prokaryotes, a variety of surface exposed macro- and supra-molecular structures exist (e.g. glycocalyx, S-Layer, outer membrane proteins, pili, flagella). These structures are often involved in different physiological phenomena such as motility, DNA-uptake/exchange, protection or in attachment. The outer components of the cell can be involved in formation of bacterial biofilm (40, 176, 182, 216) and also in surface attachment in archaea (190, 275, 281). In archaea, the influence of surface appendages in attachment to a surface was extensively demonstrated for *S. solfataricus* (Chapter 3.1 (327)) as well as for *S. acidocaldarius* (Chapter 3.4).

In the domain of archaea several surfaces structures have been identified and especially flagella and pili were in the main focus of interest. Interestingly, some archaea-related extracellular structures were discovered which seem to be exclusive for this domain. One of these unique structures is formed by *Pyrodictium abyssi* and termed cannulae, which can appear as a very dense network (195, 226). The cannulae tubes are formed by three homologous glycoproteins and are highly resistance to denaturizing conditions. They can achieve a length of 30- 150 µm (119) with a diameter of 25 nm (195). Furthermore, it was shown that the cannulae keep the cells connected even during cell division (119). By 3D reconstruction it was shown that the cannulae penetrate the periplasmatic space, but do not enter the cytoplasmic membrane (195). However, the function of the cannulae is not yet resolved and it remains to be seen if they are perhaps involved in communication, adherence (cell to cell and/or cell to surface) or in utilization of nutrients. The other unique filamentous appendage is called hamus and is produced by the euryarchaeon SM1, which was isolated in cold (10°C)

sulphurous marsh water (183, 232). An intriguing circumstance was that this organism is living closely together with a bacterium of the genus *Thiothrix* and together they form a string-of-pearls like structure (macroscopically visible with a diameter of up to 3 mm) (183). The inner part of these pearl like structure contains mainly SM1 whereas the outer part is composed of *Thiothrix*. However, SM1 produces approximately 100 hami per cell. A single hamus has a diameter of 7 to 8 nm with three hooks after every 4 nm. The end of the hamus contains so called, "tripartite barbed grappling hook" which has a diameter of 60 nm. The chemical analysis of the hami showed that they are stable over a broad range of different pH-values as well as temperatures (183).

Flagella and pili are the most famous and known appendages in prokaryotes reported in both bacteria and archaea. Both bacterial and archaeal flagella are involved in swimming as well as in initial phases of surface attachments. In archaea, flagella mediated swimming was demonstrated for *Halobacterium salinarum*, *Methanococcus voltae*, *M. maripaludis, S. solfataricus* and *S. acidocaldarius* (21, 55, 202, 270, 276). In contrast, concerning the structure of the archaeal flagella, they are incomparable with those in bacteria. The bacterial flagellum is composed of three main structures (the filament, the hook and the basal body) and empowered by the ionic gradient over the membrane (e.g. proton motive force). A torque is shown to be generated which leads to the rotation of the bacterial flagella (31, 127). The bacterial flagella-driven movement is a highly regulated system. Quite a number of proteins have been identified to be involved in either in the process of assembly or in rotation of bacterial flagellum, e.g., in *Salmonella enterica serovar* Typhimurium more than 60 genes are involved in this process (91). However, archaeal flagella assembly systems resemble bacterial type IV pili assembly systems. Several components in archaeal flagella assembly have homologs in type IV pili assembly systems. With, so far only one identified exception (pilus of *Methanothermobacter thermoautotrophicus* (275)), all identified pili of archaea are assembled by the type IV-like assembly system as well (133, 271). However, in contrast to bacteria, few genes are necessary for the flagella formation in archaea; for example in case of euryarchaeota 10 to 15 genes and in the case of crenarchaeota 7 genes were identified in operons encoding the flagella. Moreover, for *H. salinarum* it was demonstrated that the rotation of the flagellum is ATP-dependent, although the mechanism of rotation is still not known (172). The flagella are also present in the, for this study used, *Sulfolobus* strains (exemplary *S. acidocaldarius* Figure: 1-4; A (i)).

All *Sulfolobus* strains so far sequenced possess also another surface structure, which are called the UV-induced-pili (Ups-pili). The Ups-pili are highly expressed upon UV treatment in *S. acidocaldarius* and *S. solfataricus* (89-90, 98) (Figure 1-4; A (ii)). In *S. solfataricus*, it was demonstrated that the exposure to UV-light as well as treatment

with agents like bleomycin (induces double strand breaks of DNA) resulted in a drastic increase of UV-induced pili on the cell surface followed by cell-cell aggregation (89). Furthermore, recent data from our laboratory demonstrated that the UV-induced pili are involved in exchanging DNA between the cells upon UV treatment (Ajon et al, unpublished). The other important surface structures available in *Sulfolobus* are the Aap-pili and the bindosome. The Aap-pili are found to be exclusive for *S. acidocaldarius* and highly abundant on its cell surface (Figure 1-4; A (i)). The Aap-pilus has a diameter of 8 to 10 nm and is involved in surface attachment and biofilm formation (Chapter 3.4). Therefore these pili are termed archaeal adhesive (aap) pili. The genes responsible for the assembly of the Aap-pili are clustered in an operon called *aap*-operon and this operon encodes two putative pilin subunits. Interestingly, the transcriptional start sites for these two pilins are in the opposite direction with respect to the rest of the genes in the operon which are probably transcribed monocistronically.

The other surface component is called the bindosome and present in *S. solfataricus* and *S. islandicus,* and is shown to be involved in binding and up-take of different sugars (glucose, arabinose‑ and trehalose) (6, 9, 329). Using genetic analysis it has been shown that the macromolecular bindosome structure contributes to the typical lobed shape of *S. solfataricus* cells and might be structurally connected to the S-Layer (328).
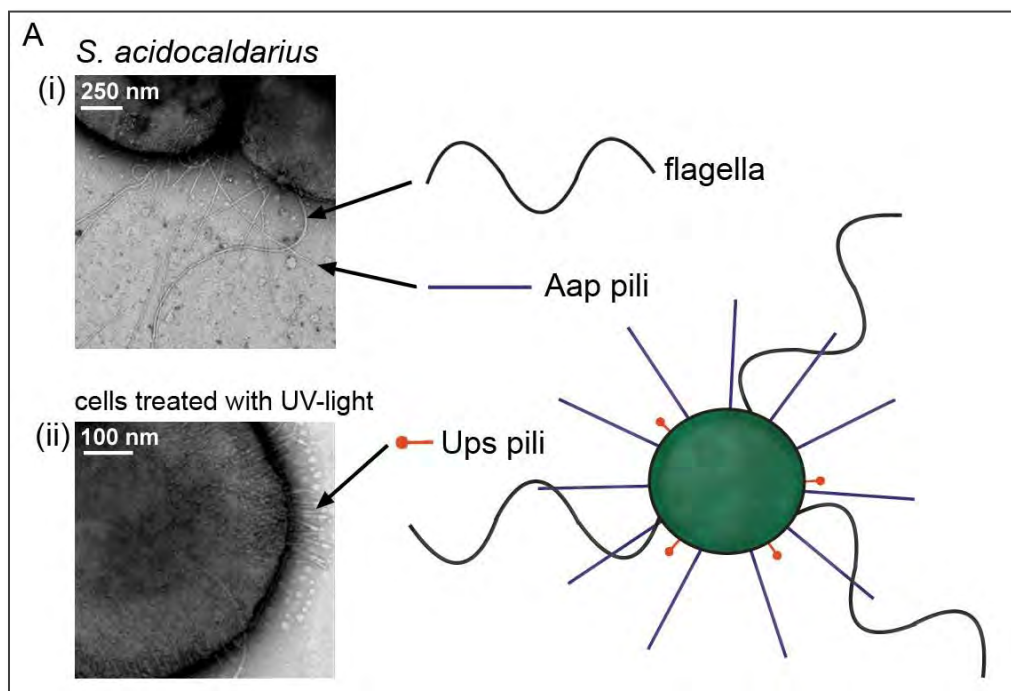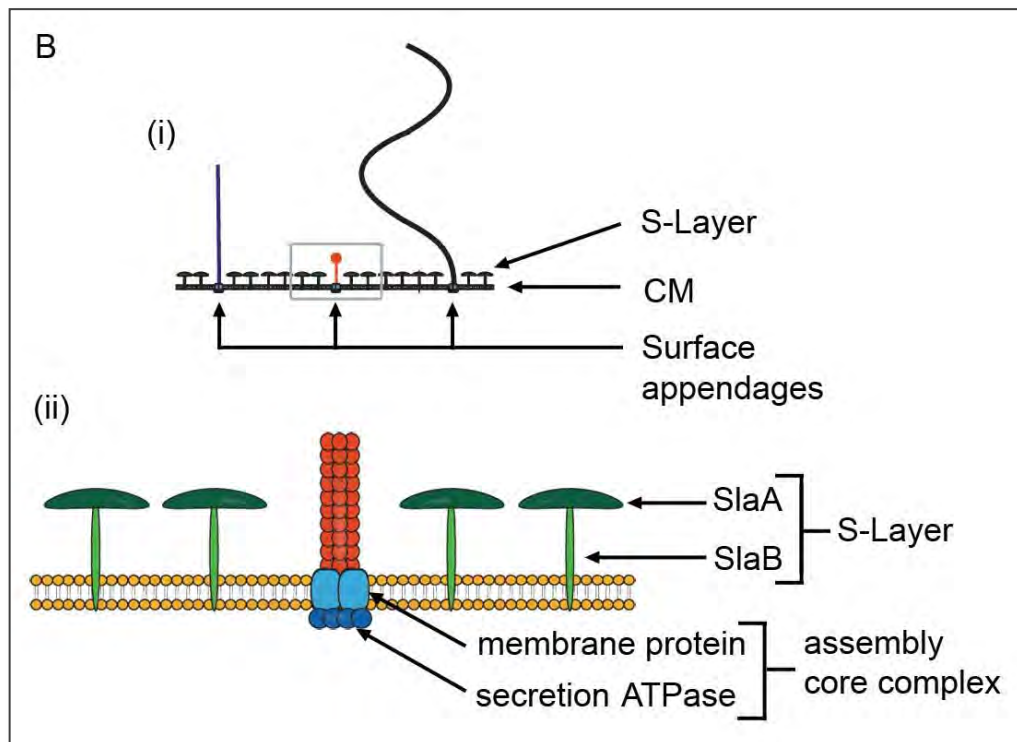
Figure 1-4: Surface and surface structures of archaea. For the exemplary representation of surface structures in archaea, structures of *S. acidoacaldarius* are chosen of which the coding genes are known. (A) Model-like illustration of *S. acidocaldarius* cell with the appendages: flagella (black), Aap pili (blue) and Ups pili (orange). The diameter of the cell is around 1 µM and the abundance of the distinct structures was taken into account. (A, (ii)) Electron microscopy picture of *S. acidocaldarius* cells with flagella and Aap-Pili: The curved thick filament are the flagella with a diameter of 14 nm and the straight thinner ones are the Aap pili with an approximate diameter of 8- 10 nm. (A (ii)) Electron microscopy picture of *S. acidocaldarius* cells 3 hours after UV treatment: at the cell surface a high number of Ups pili are visible. (B (i)) Detail of the cell surface: The cytoplasmic membrane (CM) with the overlying S-Layer is shown. The different appendages are integrated into the membrane by a membrane protein complex. (B (ii) Model of the cytoplasmic membrane: an enlarged representation of the grey box of B (i). The S-Layer is composed of the outer protein SlaA (dark green) and the membrane bound part, SlaB (light green). The distinct appendages build up by a specific assembly core complex which is homolog to bacterial type-IV-pili assembly systems. The complex is composed of a membrane protein (light blue) and a secretion ATPase (dark blue).

The type IV pili-like assembly systems of the archaeal flagella and pili are homologous to the bacterial IV pili assembly system (192, 210). All these surface appendages are anchored into the membrane by a conserved core complex and pass across the S-Layer (Figure 1-4; B (i)). The major structural protein subunit that constitute the flagella or pili (e.g. Ups-Pili, Aap-pili) possess a class III signal peptide at the N-terminus of the protein. In general, both the pili and the flagella are composed of a membrane protein and a secretion ATPase which together form the assembly core complex (25, 192) (Figure 1-4; B (ii)) in these systems. The prepilins/preflagellins are transported via the Sec-pathway across the cytoplasmic membrane (192) and thereafter the signal peptide of the pre-subunits is cleaved by a specific signal peptidase (PibD/FlaK) (214). The assembly of the processed pilins/flagellins takes place at the bottom of the growing

filament and it has been shown that this process is controlled by the respective core membrane complex in an ATP dependent manner (8). This is in contrast to the bacterial flagella where the assembly occurs at the tip of the filament (77, 123, 205) and is rather dependent on the H^+-ion gradient across the membrane.

Recent experiments showed that surface appendages can influence the surface attachment as well as biofilm formation in bacteria and in archaea. However, other physical parameters such as surface hydrophobicity, surface charge, outer membrane proteins (OMPs) or substrate properties (81, 228, 284) can also influence the surface attachment and biofilm formation as it was demonstrated for bacteria; the S-Layer of *Sulfolobales* might influences these factors as well. In fact, the S-Layer is a common feature in some bacteria (32, 236) where they were predicted to be involved in adhesion and contribute to surface attachment (182, 246, 253). With just few exceptions almost all archaea possess a S-Layer proteins as a component of the cell wall (148). Usually, the S-Layer is composed of one single protein which assembles into a two dimensional crystalline layer covering the whole cytoplasmic membrane. The S-Layer is responsible for the cell surface integrity/stability and in addition involved in the protection against different environmental conditions (e.g. osmotic/ mechanical stress, pH/ temperature shift) (33, 78-79, 237). In contrast to most archaea, the S-Layer of *Sulfolobales* (and some other exceptions) is composed of two proteins, SlaA (120kDa) and SlaB (45kDa) (101, 295) (Figure 1-4; B (ii)). SlaB is an integral membrane protein with strong affinity to SlaA indicating a co-complex formation which might be responsible for the stability of the S-layer. The S-Layer is arranged in a repetitive crystalline lattice with p3 symmetry (24, 220). In this crystalline lattice pores are present with a distance of 21 nm to maintain the p3 symmetry in the S-layer. The SlaA protein is connected to the membrane via SlaB, whereby a space of around 25 nm is formed between the membrane and the S-layer and is called pseudoperiplasmic space (Figure 1-4; B (ii)). Interestingly, both these S-layer proteins are glycosylated, which is however common to most of the surface exposed proteins in *Sulfolobales* and other archaea (6, 75, 102, 213). Due to the fact that cell charge as well as hydrophobicity of the cells influences attachment, glycosylation of proteins might play an important role in the process of attachment and biofilm formation.

1.4.1 N-glycosylation in *Sulfolobales*

The glycosylation of proteins is one of the major post-translational modifications known in all three domains of life. Long time it was thought that glycosylation of proteins is a feature restricted only to the domain of eukarya. However, recent studies revealed that

glycosylation is a very common post-translational modification of proteins and is universal in all forms of life. The glycosylation of proteins has been shown to be important in different physiological processes, e.g., correct folding of proteins (56, 97, 99), attachment to a surface (151, 163, 181), protection against proteolytic activity, (111) and protection against harsh environmental conditions/stress (3, 137, 320). Two different modes of glycosylation are known, e.g., the N-glycosylation (glycan covalently bound to the nitrogen of an Asn residue) and the O-glycosylation (glycan bound to the hydroxyl oxygen of a Ser or Thr residue). It has been shown that these two modes of glycosylation are common in all three domains of life.

O-glycosylation in archaea was so far only found on the S-layer proteins of *H. salinarum* and *H. volcanii*, but the O-glycosylation pathway has not been studied (179, 266). With the exception of two main characteristics in eukarya, the general mechanism of N-glycosylation is similar in all three domains. The first exception is that the sugar composition of the glycan tree in eukarya is conserved (Glc3Man9GlcNAc2) and mainly branched whereas the arrangement of the sugars in the other two domains are often linear and show a high diversity in their composition (70). Secondly, it is common for eukarya that the glycan tree undergoes after the transfer to the protein several modifications (glycan trimming) by several glycosidases. These modifications take place during the transport of proteins from the ER and the Golgi apparatus. This glycan trimming is needed for the transport to the right cell compartment (112). So far, this kind of modification is only demonstrated for eukarya.

It has been shown that most of the extracellular proteins in archaea are glycosylated, e.g., flagellins (192), pilins (193) or S-Layer proteins (179, 213, 266). Probably because of an adaption to the harsh conditions the number of potential glycosylation sites in hyperthermophilic organisms is higher than in mesophilic organisms. It is noteworthy that the sugar composition along the archaea species is different. The glycan tree of the flagellins of the halophilic euryarchaeon *H. salinarum* are linear oligosaccharides (glucose and sulphated glucuronic and iduronic acids)(265). For the flagellin of the thermophilc methanogenic *M. voltae* a trisaccharide (N-acetylglucosamine, di-acetylated glucuronic acid and a modified mannuronic) which is linked to a threonine residue was identified (296). In the crenarchaeota - or more accurately in *S. acidocaldarius*, the glycan composition of two proteins (cytochrome b$_{558/566}$ (320) and the S-Layer protein SlaA (213)) was solved. The glycan tree is composed of a highly branched hexasaccharide chain containing sulfoquinovose which is an uncommon sugar (320). Furthermore, the S-Layer protein is glycosylated at 9 of the 11 predicted glycosylation residues (213).

The enzymes, which are involved in the process of N-glycosylation are encoded by the archaeal *gl*ycosylation (*agl*) gene clusters and have been studied in details for *M. voltae* (54, 296) and *H. volcanii* (4, 168, 318). The process of N-glycosylation in archaea is initiated at the inner side of the cytoplasmic membrane on the lipid carrier dolichol. The oligosaccharides are enzymatically transferred from the nucleotide-activated sugar precursors in a stepwise manner on the lipid carrier. After the complete assembly of the branched sugar tree the lipid attached glycan is flipped across the membrane with the help of a flippase enzyme and finally the sugar tree is transferred to the target protein by oligosaccharide transferase (51, 319) at the outer side of the cytoplasmic membrane.

1.4.2 Glycosyltransferases and -hydrolases

During the assembly of the glycan tree glycosyltransferases are instrumental for the stepwise addition of sugars to the glycan. This process is highly coordinated and deletions of glycosyltransferases early in the pathway lead to an abolishment of the glycan assembly (51, 200). The gene disruption however proved not to be lethal to the organism although it altered the resistance against environmental changes or the ability adhere to surface or host (138, 272).

In biofilm formation, glycosylated proteins are found to play an important role. This was observed for eukarya and bacteria. The fungal biofilms of *Candida ssp.* and *Pneumocystis spp.* contain high levels of glycosylated proteins within the matrix. In several *E. coli* strains it was discovered that the glycoproteins Ag43, AIDA and TibA support biofilm formation (64, 248-249). *Microbacterium* (MC3B-10) produces an EPS which contains a high amount of a so far not identified glycoprotein (207). Indeed, in other bacteria the involvement of glycoproteins, such as Fab1 (fimbria-associated glycoprotein) in biofilm formation have been studied extensively (293, 314, 323-324). *Streptococcus parasanguinis* causes dental plaque and is a so called first colonizer of the tooth surface. The serine-rich glycoprotein Fab1 of *S. parasanguinis* is essential for adhesion and biofilm formation. This high molecular weight protein (the matured protein have a molecular mass of 200 kDa) is found in several streptococcal and staphylococcal species and the impact of this protein for interaction with the host components was demonstrated for these species as well (245, 322). However, the deletion of *fab1* resulted in a mutant were the ability for biofilm is abolished, thus the impact of the appendages itself is evinced (88). As it is mentioned the Fab1 is a glycoprotein for which studies has been performed to analyze the importance of the posttranslational modification (glycosylation) of this protein for biofilm formation. Two

gene clusters next to *fab1* are identified to be involved in the glycosylation of those. The downstream gene cluster (seven genes) encodes glycosyltransferase which are essential for the first step of glycosylation and for the accessory secretion proteins (49, 60, 162, 212, 314). The gene cluster upstream to *fab1* codes for four genes while all of them are glycosyltransferases (Gly, GalT1, GalT2 and Nss (reclassified recently as Gtf3)). For two of them it is demonstrated that they are responsible for the glycosylation of Fab1 (314, 324). The deletion of GalT2 reveals that *S. parasanguinis* still attached to a surface but they were forming a thin biofilm with decreased mass accumulation (314). Similarly, Gtf3 deletion led to decreased biofilm formation (324). Indeed, the influence of glycosylated proteins for attachment, biofilm formation and to be part of the matrix is evinced while obviously next to the protein, the glycan tree itself supports for the biofilm formation.

With respect to the pathway of glycosylation other proteins might be important as well for the construction of the entire glycan tree, the glycosylhydrolases. This class of proteins is common in all domains of life, but their involvement in glycosylation is so far studied only in eukarya. In all domains the glycan tree is assembled in a similar manner. For bacteria the assembly of glycoproteins is finalized after the addition of the last sugar by the glycosyltransferases whereas in eukarya a so called glycan trimming follows. During the process of glycan trimming, the cleavage of before added distinct sugars occurs. Glycan trimming of glycoproteins is common in eukarya and responsible for correct transport of proteins to the targeted cellular compartment (96, 279). The cleavage of these sugars is catalyzed by different glycosylhydrolases, e.g., α-mannosidases. Usually, in bacteria the catalyzed reactions by α-mannosidase reflects a high diversity with respect to the substrates and it seems they are not directly involved in processing of the glycan tree (171, 188, 235). Interestingly, the α-mannosidase of pathogen *Mycobacterium tuberculosis* is used for the synthesis of mannose containing glycoconjugates. The expression of α-mannosidase was down-regulated during intra cellular growth which indicates that the pattern of the glycoconjugates changed in different environmental conditions. It is assumed that this organism can exhibit a kind of glycan trimming with the function to escape the immune response of the host and could be used as kind of mimicry of the bacterial cell surface (230). Nevertheless, for eukarya, the involvement of α-mannosidase in trimming of the glycan tree which has been demonstrated recently (112). The function of α-mannosidase in archaea is so far less analyzed. Quite recently, a study has been carried out, which demonstrated the in vitro function of an α-mannosidase (SSO3006, Ssα-man). It was demonstrated, that Ssα-man catalyzes the degradation of α(1,2), α(1,3), and α(1,6)-D-mannobiose (61). Additionally, it was shown that the Ssα-man of

S. solfataricus demannosylates a glycosylated protein and an involvement in glycosylation was postulated (61). *S. solfataricus* can attach to different surfaces, forms biofilm and produces EPS (Chapter 3.1; 3.2: (146, 327)). In contrary to *S. solfataricus* P2 cells, a considerable amount of extracellular material was produced by PBL2025 during surface attachment. The PBL2025 strain was derived from *S. solfataricus* 98/2 and lacks 50 genes which are predicted to be involved in sugar metabolism and transport (240). It has been postulated, that these phenotypic differences in biofilms are related to these missing genes in the PBL2025 genome. The α-mannosidase (SSO3006, Ssα-man) is one of the 50 missing genes in PBL2025. Considering the biochemical nature of the enzyme and the defined functions of its homologs in eukarya, Cobucci-Ponzano et al. (61) have postulated that the Ssα-man has a functional role in glycosylation in *S. solfataricus*. In general, *Sulfolobus spp.* contains a high number of N-glycosylated extra-cellular proteins and for *S. acidocaldarius* it was shown that the glycan tree of the S-layer proteins contains large amounts of mannose (213). The fluorescence signal of the labeled lectin ConA (specific for mannose-/glucose residues) for PBL2025 under surface attached as well as biofilm conditions demonstrated a higher mannosylation than for *S. solfataricus* P2 (327) (Chapter 3.1; 3.5). By complementation studies in PBL2025 it was demonstrated that the Ssα-man of *S. solfataricus* reduces the mannose concentration of the EPS. Consequently, it is assumed that the Ssα-man is involved in glycosylation and maybe even in glycan trimming.

1.5   The role of surface appendages in attachment and biofilm

The attachment of cells to a surface is divided in two steps; the reversible attachment (transient attachment) followed by the irreversible attachment (permanent attachment). Initially, cells move actively until they find a suitable position and thereafter attach themselves via weak forces to the surface. These forces include van der Waals forces (London force of interaction), electrostatic forces and hydrophobic interactions (290). The attachment can, however, be mediated by several different extracellular components (e.g. flagella, pili, membrane, S-Layer (40, 176, 182, 216)) or even by special properties of the cell (e.g. hydophobicity, cell surface charge (229, 287)). Nevertheless, the properties of the substratum are also important for an accurate attachment (81, 201). At the initial phase of attachment, cells can still leave the attachment site either because of their intrinsic motility (swimming, swarming or sliding) or indirectly depending on the presence of shearing forces. With time the attachment is,

however, increasingly strengthened resulting in a permanent attachment of a subpopulation of the cells. It is assumed that the environmental signals induce the transformation from transiently attached cells to the permanently attached cells. The reason for the transition is still not completely understood. For *Vibrio cholerae*a it was demonstrated, that during the step from transient to permanent attachment, the membrane potential ($\Delta\psi$) changes, which might be responsible for the switch (286). In support of this several studies have conclusively demonstrated that adhesions are important for attachment and required for the generation of strong forces, e.g., covalent, hydrogen bonds and strong hydrophobic interaction (110, 130, 291). The involvement of pili and flagella in attachment has also been demonstrated for the members of the domain archaea (190, 275, 281). Most of the information regarding biofilm formation in archaea is dealing with the initial attachment stage while nothing has so far been documented about the transition to the permanently attached state.

The involvement of pili (also called fimbriae) in bacterial attachment was demonstrated in several studies (26, 37, 135, 178, 216). For example, under special growth condition some *E. coli* cells produce special pili, termed curli fimbriae (42), which are involved in attachment to different surfaces. Moreover, these pili are highly expressed under stress conditions and curli-producing strains can attach faster to surfaces (62).

Flagella are the most well studied surface structures that have repeatedly been shown to influence surface attachment in bacteria. For example, the flagella of *E. coli* and *Aeromonas caviae* mediate the attachment to host cells (94, 143). In 1998, O`Toole and Kolter demonstrated for the first time that for flagella deficient mutants of *P. aeruginosa* and *Pseudomonas fluorescens*, the ability to form biofilm was reduced (203-204). Interestingly, following investigations on biofilm and attachment revealed quite a controversial situation with respect to the involvement of flagella in attachment and biofilm formation. A detailed study by Klausen and coworkers (145) revealed that biofilm formation can occur in two distinct conditions called static or hydrodynamic. They further proposed that the work of O`Toole and Kolter mostly relied on static biofilm formation where flagella played an important role in initiation of biofilms. Furthermore, they suggested that in nature, biofilm formation is a complex regulated mechanism. They could successfully show, that the previously used flagella mutants (used before by O`Toole and Kolter) are capable in forming biofilm under hydrodynamic conditions (113). They analyzed *P. aeruginosa*, flagella-mutants (Δ*fliM*) and pili-mutants (Δ*pilA*) under static/hydrodynamic conditions and each system with different carbon sources. The results indicated that the impact of flagella in the formation of biofilm is depending on the hydrodynamics as well as on the nutrient composition (145). It became more and more apparent that flagella as well as flagella

driven motility play an important role in biofilm development. For example, *Listeria monoctogenes*, *P. aeruginosa* and *E. coli* require flagella driven motility for biofilm formation (159, 175, 203). However, *V. cholerae* does not need the flagella itself for biofilm formation, rather the flagella motor is required (153, 286). Surface attachment has been studied in archaea. Similar to bacteria, some surface appendages exhibit controversial functions with respect to their role in attachment to different surfaces. On one hand, in some archaea the flagella are required for attachment (e.g. *P. furiosus, S. solfataricus, M. maripaludis* (128, 190, 327)) where as in some others flagella are not involved in attachment (e.g. *H. volcanii*) (281). In *P. furiosus* it was shown, that the flagella are essential for their attachment to different solid surfaces such as gold, copper, nickel, nylon or plexiglas; however, a lack of genetic tools has not allowed researchers to study the exact role of flagella in attachment in this organism. Further studies on *P. furiosus* showed that cells used their flagella to attach to the "first colonizer" *Methanopyrus kandleri*. In this bi-species biofilm, the *M. kandleri* cells first attached to the surface followed by colonization of *P. furiosus* (243). During attachment the *P. furiosus* flagella bundled together as cable like structures (190). These cable-like bundles of flagella between the cells were observed for *Methanocaldococcus villosus* as well. Furthermore, in contrast to planktonic *M. villosus* cells, the attached ones were heavily flagellated (27). Recent advancement in the development of genetic tools for different archaeal species has allowed researchers to analyze surface attachment studies with flagella- as well as pili- deletions mutants. These studies have provided detailed insights into the role that these surface structures play during the process of attachment and biofilm formation. In *H. volcanii* it has recently being demonstrated that the type IV pili like surface structures are responsible for surface attachment (281). In *M. maripaludis* the deletion of either flagella or pili, or even both, resulted in a defect in attachment for all the mutants (128). Indeed, deletion of the flagella in *S. solfataricus* PBL2025 and *S. acidocaldarius* MW001 (a Δ*pyrE* knockout strain (Wagner et al., unpublished)) shows a similar phenotypic trend with no attachment of flagella mutant of *S. solfataricus* PBL2025 (Chapter 3.1; (327)) and a reduced attachment in the flagella mutant of *S. acidocaldarius* MW001 (Chapter 3.4). Additionally, with respect to the involvement of Ups-Pili of *Sulfolobales* an interesting observation has recently been made in our laboratory. While in *S. solfataricus* PBL2025 the Δ*upsE* cannot attach to a surface (Chapter 3.1; (327)), the Δ*upsE* of *S. acidocaldarius* MW001 showed an increased initial surface attachment.

The effect of the deletions of different surface appendages in *Sulfolobales* on later stages of biofilm has recently been examined in our laboratory. Interestingly, compared to wildtype cells, a three days old static biofilm of *S. solfataricus* Δ*upsE* shows slight

differences to the wild type, whereas the Δ*flaJ* strain exhibited no changes with respect to the morphology to the wildtype (Chapter 3.2; (146)). Similar experiments have been performed also for the later stages of biofilm lifestyle where commonly a dispersal of the attached cells was observed and a consequent reduction of the height and density of the biofilm was evident. However, the Δ*flaJ* strain was found to be the only exception with random clustering of the cells visible even after eight days biofilm growth (Koerdt et al., unpublished).

However, the most detailed study was performed for *S. acidocaldarius* MW001, which is the *Sulfolobus* strain with the most stable biofilm (146). In *S. acidocaldarius* three surface appendages, flagella, Ups pili and Aap pili are present. For the analysis of surface attachment and biofilm, all of the appendages were deleted and besides this all possible combinations of deletion such as double as well as triple knockout were constructed (Δ*aapF*/Δ*flaJ*, Δ*aapF*/Δ*upsE*, Δ*upsE*/Δ*flaJ*, Δ*aapF*/Δ*flaJ*/Δ*upsE*). First of all the surface attachment of these mutants was tested and the main outcome was that the single deletion mutants showed just more or less slight differences with respect to the number of cells, which were attached. Although, the number of attached cells of the Δ*aapF* -mutant showed a slight increase, they attached in clusters of cells. This might correlate with the fact, that these mutants exhibit much more flagella than the MW001 wild type and indicates that the flagella are responsible for this property. Nevertheless, the deletion of more than one appendage led to stronger changes in the number of attached cells and the conclusion that the attachment occurs because the different appendages interact. With the exception of Δ*upsE*/Δ*flaJ* which showed a dramatic increase of attachment (more than 150% increase), the attachment of the Δ*aapF*/Δ*flaJ* and Δ*aapF*/Δ*upsE* deletion strain were decreased. Lastly, for the triple knockout a strong reduction of attachment was observed (Chapter 3.4).

Moreover, the mutants showed a change in biofilm formation as well (Figure 1-5; A): mainly, three distinct phenotypes were detected (Figure 1-5; B; Chapter 3.4). The MW001 biofilm architecture presented an appearance which is comparable with those of *S. acidocaldarius* wild type (Chapter 3.2 (146)), although it produced less clusters and had a lower EPS production. The Δ*flaJ* deletion strain exhibited the same phenotype as MW001 and was therefore classified in the same group of phenotypes (Figure 1-5; Chapter 3.4). The second class of phenotypes is marked by the attributes of high cell density and slightly reduced height, which is due to the deletion of *aapF*. In fact, this morphology occurs in all mutants which were deleted for the Aap pili (Δ*aapF*/Δ*flaJ*, Δ*aapF*/Δ*upsE* and Δ*aapF*/Δ*upsE* /Δ*flaJ*).
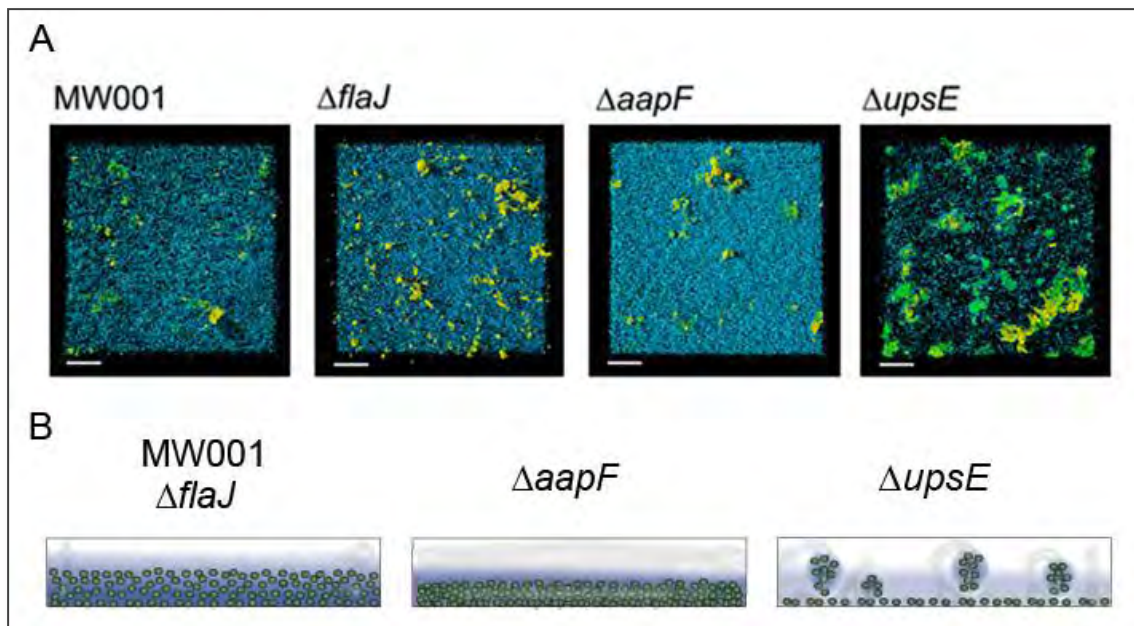
Figure 1-5: Biofilm phenotype of surface appendages mutants of *S. acidocaldarius* MW001. (A) Confocal laser scanning microscopy (CLSM) of 3 days old biofilms of MW001 (wt), ΔflaJ, ΔaapF and ΔupsE strains stained with DAPI (blue) and the lectins ConA (green) and IB$_4$ (yellow). Bars are 40 µM in length. (B) Model-like representation of the observed biofilm phentotypes during CLSM. Three distinct phenotypes were detected "wildtype phenotype" (first column), "ΔaapF-phenotype" (second column) and the "ΔupsE-phenotype".

The last phenotype was observed manifested by the ΔupsE strain. Even though the bottom was covered with cells at a higher level the general cell density of the biofilm was decreased. Tower-like structures were present which were composed of a high amount of EPS while the numbers of cells embedded within these towers of EPS were low (Figure 1-5; Chapter 3.4).

1.6   The matrix of the biofilm

During the course of biofilm formation the cells arrive at a point, shortly after the surface attachment, at which the production of the matrix of the biofilm sets in. The matrix is the extracellular material of the biofilm and termed as <u>extrap</u>olymeric <u>s</u>ubstances (EPS). The matrix is a key characteristic component for formed biofilms. The matrix is highly hydrated and it is believed that around 97% of the biofilm is composed of water (268). In fact, only 10% of the matrix constitutes the cell material and the rest of the 90% is composed of EPS. The matrix can be compared with a sponge, which allows small molecules to enter and to leave the biofilm. Moreover, the matrix contributes to the stability of the immobilized cell community. Cells are completely embedded in the self-produced matrix, which is used for different purposes: a better cell to cell contact/interaction, adhesion to the surface or other cells, protection against toxic agents or harsh environmental conditions (63, 136, 187). Furthermore, the

matrix can function as storage as it can absorb metals and minerals or organic compounds. An additional feature is that the matrix can concentrate nutrients, enzymes, and growth factors (83-84, 253). The matrix consists of an accumulation of different biopolymers such as proteins, glycoproteins, glycolipids, exopolysaccharides or DNA (eDNA) (83, 267). The composition and the proportion of each of these compounds can differ between species. Furthermore, the growth conditions (carbon source, temperature, pH e.g.) can influence and change the EPS production and its composition (87, 141-142, 145, 293, 300, 313).

In bacteria the main component of the matrix/EPS are exopolysaccharides, e.g., for instance a famous polysaccharide in biofilm of *P. aeruginosa* is alginate (67), for *S. enteric serovar* Enterititis it is cellulose (255) and for *E. coli* it is colonic acid (65). The deletion of genes for exopolysaccharide synthesis or export leads to cells which still attach to a surface, but are not able to form multilayered biofilms (11, 65, 305). In the domain archaea exopolysaccharides synthesis has also been demonstrated. One of the first analyzed archaea was *Haloferax mediterranei* which produces extracellular polysaccharides when grown on solid plates and a mucous appearance of the colonies was observed (231); The polymers consisted of mannose, glucose, an unidentified sugar, amino sugars, uronic acids and large amounts of sulphate (16). *Natronococcus occultis* exhibits L-glutamat in the cell wall (197) and *Natrialba aegyptiaca* possesses poly-γ-D-(glutamtat) (PGA) (115), which is a common sugar for several bacterial species as well (136). Moreover, a study carried out by Rinker and Kelly (227) has analyzed the exopolysaccharide composition of *Thermococcus litoralis* grown as biofilm on polycarbonate filters or glass slides. They discovered a mannan-like exopolysaccharide and assumed that this sugar might be involved in biofilm formation. *A. fulgidus* biofilm produced an EPS which contained protein, polysaccharide, and metals (152).

Regarding the sugar composition of exopolysaccharides in *Sulfolobales* just little information is available. *S. solfataricus* and *S. acidocaldarius* were grown consecutively in a fermenter as well as in a static batch culture and the produced exopolysaccharides were analyzed and found to be composed of glucose, mannose, glucosamine and galactose. Furthermore, the exopolysaccharides was found to be sulfated (196).

In spite of the fact that the biofilms of three *Sulfolobales* were stained with lectins (IB$_4$ (galactosyl-residues), GS-II (N-acetyl-Dglucosamine) and ConA (glucose/mannose)), which bind to sugar residues, it cannot be concluded that the obtained signal was due to the presence of secreted exopolysaccharides (Chapter 3.2; (146)). Rather, the used lectins could also bind to the sugar residues of glycosylated proteins. Recently, it was shown that the glycan tree of *S. acidocaldarius* the S-layer protein contained two

terminal mannoses (213) and the *S. acidocaldarius* biofilm exhibited a strong ConA signal (ConA binds to mannose and glucose) (Chapter 3.2; (146)). Furthermore, the matrix of *Sulfolobus* biofilm contained direct connections between the cells, which were composed either of exopolysaccharides or glycosylated proteins (Chapter 3.2; (146)). Different *Sulfolobus* strains exhibited a different distribution of sugars (exopolysaccharides or glycoproteins) during biofilm formation when compared with each other (Chapter 3.2; 3.3; (146)).

For bacteria it was demonstrated, that eDNA plays an important role in biofilm formation. These eDNA supports the integrity and stability of the biofilm (136).

It is thought that the source of eDNA is mainly because of induced autolysis, however there exists reports demonstrating the release of vesicles containing the DNA (10, 166, 277). Besides this, another amazing function for eDNA was demonstrated for *P. aeruginosa*. Here, the cells of the stalks released eDNA and obviously contribute to the stability. Interestingly this eDNA can also be used for a special kind of movement. The secreted eDNA forms lattice-like structure in the stalk of the cluster and is taken up from cells next to the bottom by type IV Pili. Due to tractive forces the cells climb up the stalk and form the cup of the stalks and the typically tower-structure appear (10, 292). In contrast to bacteria the *Sulfolobus* biofilm matrix contains just little amounts of eDNA. In addition, this eDNA is not supporting the stability of the biofilm as evident from the DNase digestion experiment (Chapter 3.2; (146)).

1.7   Biofilm specific transcription or protein pattern

During the last decade several studies have been performed to determine whether common mechanisms exist that lead to biofilm formation by microorganisms. Consequently, proteomic as well as transcriptomic analyses have been performed to shed light on this question. To understand the biofilm lifestyle, these studies mainly aimed to find out whether there are specifically expressed genes during the course of the transition from the planktonic to the biofilm lifestyle. These experiments were performed mainly within different bacterial species. For the analysis the cells were grown on different surfaces, in a static or hydrodynamic system and under several environmental conditions, for instance different carbon sources, temperatures, pH and with or without stress.

The differences observed between planktonic and biofilm cells point at large changes of gene expression. Indeed, changes of the expression pattern of biofilm cells were observed for different species but also within one species. As one example, an early study discovered by using random insertion mutagenesis that 38% of the genes were

differentially expressed in *E. coli* biofilms (217), while another found out that just 5.8% were differently expressed (225). Nevertheless, it is assumed that these differences within one species are mainly due to the techniques used in these studies. The major differences, however, include differences in the medium composition, small temperature shifts of the incubator or differences in the RNA isolation/cDNA-synthesis methods. However, the results based on gene expression or protein translation of biofilm give at least strong indications how gene expression in the biofilm cells differs from planktonic cells and which components might be important.

With respect to the development of biofilm Sauer and coworkers (239) compared the protein pattern of *P. aeruginosa* biofilm to each distinct stage of biofilm. They demonstrated that during the transitions from planktonic growth to irreversible attachment 29% of the detectable proteins changed, from attachment to full maturated biofilm 40% and lastly during the dispersal again 35% of the whole cell protein showed changes (239). Recent studies showed that around 1-15% of the genes underwent a significant change during bacterial biofilm formation (30, 225, 241, 257, 310). In archaea, it was revealed that for *S. acidocaldarius* 15%, for *S. solfataricus* 3.4% and for *S. tokodaii* ~1% was differentially expressed in biofilm cells (Chapter 3.3; (147)). Additionally, only one other archaeal (*F. acidarmanus* Fer1) proteome analysis has been so far performed on biofilms and will be discussed below (20).

So far no expression profile could be identified that is common for all microorganisms that change their life style from planktonic to form biofilms, however, trends were observed. Usually, in the early stages of bacterial biofilm maturation the flagella gene expression was repressed whereas gene/proteins involved in the production of the matrix, related to stationary growth phase, environmental stress or anaerobic growth were up-regulated (14, 28, 136).

Whilst the demand of the flagella for initial attachment still is a controversial topic, usually flagella are not important at the later stages in biofilm maturation as evident from several studies in different bacteria (217, 238, 257). *S. acidocaldarius* exhibits an increased expression of genes involved in flagella synthesis while in the proteome analysis none of the flagella-related proteins have been identified at the second day of biofilm maturation (Chapter 3.3). However, in some bacteria flagella gene expression is up-regulated even at the later stages of biofilm formation (132). Another result supporting the need of flagella or maybe other different surface appendages of *S. acidocaldarius* was the up-regulation of PibD (Chaper 3.3; (147)). PibD is required for the assembly of both flagella and pili; therefore an up-regulation might imply a higher need/amount as more appendages are assembled. The appendages are evidently responsible for maintenance of the typically architecture of the

S. acidocaldarius MW001 biofilm (Chapter 3.4). However, another gene for surface appendages, which was differentially expressed, belonged to the ups pili operon. Interestingly, it was up-regulated in three days biofilm of *S. solfataricus* for which the ups pili were shown to be essential for initial attachment and seemingly were also required for biofilm maturation (Chapter 3.1; (327))

In *S. acidocaldarius*, the NAD-dependent epimerase/dehydratase homolog was found to be up-regulated in biofilm (Chapter 3.3). In *Metallosphaera sedula* this protein has been postulated to be involved in exopolysacchraides synthesis (19). Moreover, glycosyltransferases of *S. acidocaldarius* were up-regulated in biofilm and this observation was in congruence with what has been shown in bacteria, where glycosyltransferases were also found to be up-regulated in biofilm. Besides, gene disruption of the glycosyltransferases showed a profound effect with subtle change in the EPS of bacterial biofilm (149).

In general, it is thought that anaerobic conditions are common in biofilm. In particular, the deeply embedded cells of the biofilm do not have the same access to oxygen in comparison to either the cells at the outer surface of the biofilm or the planktonic cells. An increased expression of proteins involved in maintenance of the anaerobic lifestyle is frequently observed in bacterial biofilm (66, 206) as well as for some archaea like *F. acidarmanus* Fer1. In *F. acidarmanus* Fer1 biofilm six to ten fold up-regulation was evident for the proteins involved in the growth under anaerobic conditions (20). Interestingly, the over-expression of genes encoding components of the Sox complex in *Sulfolobales* implies that no limited oxygen stress existed (Chapter 3.3; (147)). However, other stress response related changes in *Sulfolobus spp.* biofilm were observed. Apart from respiratory function of the Sox complex it was also shown that the SoxM complex recognizes the pH in the periplasmic space and actively reduces the pH (146). This information is further supported by the observation that the pH increases up to ~pH 5 during the development of *Sulfolobus ssp*. biofilm (Koerdt et al., unpublished) which might be sensed by the SoxM complex to keep/regulated the pH in a optimal level for *Sulfolobus spp.*. Two identified proteins or complexes with chaperon activities were found regulated in biofilm. One of them corresponded to the heat stress response element, the thermosome (131, 280) and the other one is the heat shock protein Hsp20 (273). These proteins seem to have a so far unknown function in *Sulfolobales* biofilm development as they were commonly regulated in the three tested *Sulfolobus* strains as evidenced by means of the proteomic analysis.

Additionally, the fact that some other commonly regulated genes or proteins in *Sulfolobus* biofilm was searched, as this might indicate their relevance within the biofilm lifestyle. From this analysis few genes were found to be commonly regulated in

Sulfolobus biofilm. A transcriptional regulator Lrs14-like protein (from the proteomic data) and an ABC transporter ATP-binding protein (from the transcriptomic data) were found to be up-regulated in all three strains, whereas one subunit of the V-ATPase (proteomic) and 3-oxoacyl-(acyl carrier protein) reductase (fabG-1) (transcriptomic) were shown to be down-regulated. Both of these candidate proteins possibly might play a crucial role in the transition from planktonic to biofilm lifestyle (Chapter 3.3; (147)).

Nevertheless, as it was already mentioned biofilm formation allows cells to live as a community, where cells interactions take place. In bacteria it has been broadly described that Quorum sensing (QS) phenomena provides the means to coordinate the activities of cells so that they function as a multi-cellular community. In general QS phenomena involves the secretion of signal molecules, autoinducer (AI), to the extracellular environment. Thus, AI molecules accumulate reaching a threshold level, which consequently undergoes several gene/protein profile changes allowing the adaptation to the new environmental situation. In gram-negative bacteria, depending on the AI molecule, two QS processes have been described: type AI-1, which is involved mainly in intraspecies communication, and type AI-2, which is related to interspecies communication (13, 23, 95). Indeed, it has been described that QS plays an important role influencing biofilm formation. Moreover, some studies reveal a close relationship between the extracellular regulation by QS and the intracellular regulation by the second messenger 3',5'-cyclic diguanylic acid (c-di-GMP). c-di-GMP specifically regulates multiple cellular processes by binding to diverse target molecules. c-di-GMP is synthesized by diguanylate cyclase (GGDEF protein domain) and the following degradation by specific phosphodiesterases (EAL- or HD-GYP protein domains) (233). It has been reported that c-di-GMP acts a central regulator for gram-negative bacteria promoting that the transition from planktonic to sessile lifestyle. Usually, high levels of c-di-GMP lead to reduced motility and biofilm formation (180, 251). The mechanism behind the biofilm formation inducement via c-di-GMP can differ even in related organisms (129, 316). For example, while in *P. fluorescence* high levels of c-di-GMP increase the production of the adhesin LapA (184), in *P. aeruginosa* EPS production is increased (50, 150). A direct connection between QS and the concentration of cellular c-di-GMP was demonstrated in *P. aeruginosa* and *V. cholera*. In *P. aeruginosa* the transcriptional regulator LasR is activated by AI's and lead to the synthesis of TpbA (Tyrosine Phosphatase) which in turn lead to reduction of the intracellular c-di-GMP-level (283). In both cases high cell density leads to an accumulation of the extracellular autoinducer (AI) which leads at a certain threshold level to the expression of special genes. For example, in *P. aeruginosa* the transcriptional regulator LasR is activated by AI's and induces the synthesis of TpbA (Tyrosine Phosphatase) which in turn leads to

the reduction of the intracellular c-di-GMP-level (283). Moreover, in a similar manner, in *V. cholera*, high levels of AI result in the expression of HapR which reduces the c-di-GMP-level as well (304). As a consequence of the low c-di-GMP-levels cell motility is recovered promoting bacterial dispersal and biofilm formation impairment. In *P. aeuroginosa*, type AI-1 QS involves the production of 3-oxo-C12-HSL by LasI synthase activity and the 3-oxo-C12-HSL-responsive DNA-binding regulator LasR. The 3-oxo-C12-HSL derives its invariant lactone rings from *S*-adenosylmethionine and their variable acyl chains from the cellular acyl-acyl carrier protein (ACP) pool. It has been determined that 3-oxoacyl-(acyl-carrier-protein) reductase (FabG) is a determining factor of 3-oxo-C12-HSL chain lengths (116). Interestingly, the levels of FabG were also found to be accumulated by both *P. aeuruginosa* (198) and in *Sulfolobus* spp. planktonic cells in comparison to their biofilm counterparts. Although, it seems that *Sulfolobus* genomes do not encode for a LasI homologous proteins, a different and unknown activity might be involved together with FabG in the production of putative archaeal AI molecules. In this regard, studies in biofilms of the archaeon *F. acidarmanus* Fer1 showed no evidence for quorum sensing and the signalling molecules (20). However, the production of AI molecules by *Sulfolobus* cells needs to be proven. Furthermore, in the future it will be of interest to determine the potential occurrence of cell signalling and communication within *Sulfolobus* biofilm communities.

On the other hand, it is well known that transcriptional regulators play an pivotal role in the adaptation of environmental changes by means of coordinating expression of distinct genes (215). This mechanism is needed for the fast as well as specific production of proteins required for the present situation. In Bacteria, the sigma factors (σ), a class of transcriptional initiation factors, are used for the coordinated synthesis of specific genes. So far several regulators belonging to this classed have been identified and functionally analyzed, among others σ^{70} (housekeeping sigma factor) (36), σ^{28} (flagella synthesis) (258) or σ^{32} (heat shock) (17). Thus, several studies have demonstrated the specific role of some transcriptional regulators on the biofilm development process.

Indeed, for biofilm formation several studies have been demonstrating a similar regulation which induces the production of biofilm specific proteins and the repression of genes which are needed for the planktonic lifestyle. The transcriptional regulator Nrg1p of the eukaryote *Candida albicans* is required for biofilm formation and dispersal (285). AphA of *V. cholerae* is a transcriptional activator which induces biofilm formation by the expression of VpsT which is a biofilm activator (315).

From our proteomic data of *Sulfolobus* biofilm, we found that all three analysed strains displayed increased levels of putative transcriptional regulators belonging to the Lrs14-

like proteins. Thus, the expression of these homologous transcriptional regulators seems to be a common response when *S. acidocaldarius*, *S. solfataricus* and *S. tokodaii* grow in biofilms and might constitute a key regulatory factor during biofilm development. Furthermore, these regulators show high homology to each other, and to several other homologs which are spread over the whole genome of each of the investigated *Sulfolobus* strains. One of the homologous is Lrs14 of *S. solfataricus* has been functionally characterized. It was shown that this regulator is negatively autoregulated and accumulates in the midexponential and late growth phase (189), which might reflect the situation in biofilm. Lrs14-like proteins of archaea are related to the Lrp-AsnC bacterial transcriptional regulator family (leucine-responsive regulatory protein) (189). Lrs14-like proteins are present in bacteria as well as archaea. The Lrp regulator of *E. coli* is involved in the regulation of up to 75 different genes (52), and it might be that the archaeal version has a similar global function. Consequently, further research is on going to shed light on this open question.

1.8   Stress and resistance

It is known that cells, which are embedded into the biofilm community are more resistant against toxic agents or physical and chemical stress (169, 288). The resistance is largely caused by the EPS (detailed discussed above), which covers the cells and can inhibit the access of toxic substances. Furthermore, the EPS can act as a buffer to decrease the disruptive forces (e.g. temperatures shift). On the other hand it is thought that biofilm cells behave as in the stationary-phase, which means that the growth is slow and the number of persistent cells is high (18, 274). Consequently, the effect of antibiotics is abolished, especially for antibiotics of which the mode of action is dependent upon their intervention on the metabolic activity, for instance penicillin or chloramphenicol (118, 254). The resistance property differs largely from one bacterial strain to the other against the same chemical (100, 194, 219). In fact, there is also no rule how or when biofilm is formed. Some organisms initiate biofilm growth for instance if nutrients become limited (93) while other form biofilms if the concentration of nutrients is high (317). The stress-induced biofilm formation is very common in bacteria. In *P. aeruginosa* and *E. coli* a high concentration of the antibiotic aminoglycoside promotes biofilm formation (117), while osmotic stress increases the biofilm formation of *Staphylococcus aureus* (222). Similar observations are also evident in the domain archaea. The biofilm formation was found to be enhanced in *A. fulgidus* at high metal concentration, under extreme pH and temperature, and with the addition

of xenobiotics, antibiotics, and also oxygen concentration (152). In *Sulfolobales* the biofilm formation is influenced by pH, temperature, iron concentration or the combination of pH and iron concentration, while the response to the stress exhibits differences along the related species. *S. acidocaldarius* for instance forms the most efficient biofilm at low temperatures whereas *S. solfataricus* at high temperatures. A combination of high pH and iron concentration led to a dramatically reduction of biofilm and seemed to be toxic while *S. acidoacaldarius* (~50 times more) and *S. tokodaii* (~10 times more) biofilm increases in comparison to the standard conditions (Chapter 3.2; (146)). Due to the fact that already the architecture of the biofilm is different it might be that also the differences regarding to stress a kind of specialization along the three species.

2   Objectives of this work

Over the past decade research about microbial community formation has attracted immense attention. It is becoming clear that under different environmental conditions microbes survive by forming either homogeneous or heterogeneous communities. This form of microbial life style is called „biofilm' and reflects the natural scenario for an organism in the environment. In the field of medicine and biotech industries, biofilm research is attracting attention mostly because of the fact that the advancement of our understanding of community life style might be useful in combating human disease as well as to solve several industrial bottlenecks. However, our knowledge on biofilm lifestyle is mostly restricted to the domain bacteria while it has been shown that this lifestyle is common in all domains of life.

In the present study we have focused on understanding the biofilm lifestyle of *Sulfolobales*. The order *Sulfolobales* belongs to the subkingdom crenarchaeota in the domain archaea. These are aerobic thermoacidophilic microorganisms. The genome sequence for several species is available (e.g., *S. solfataricus*, *S. acidocaldarius*, and *S. tokodaii*) and most interestingly genetic tools are available for *S. solfataricus* and *S. acidocaldarius*, which makes these species attractive model systems. Additionally, these strains were isolated from different habitats over the whole world and therefore a comparative study might have provided valuable insights.

Previous studies from our laboratory had demonstrated the initial surface attachment of *S. solfataricus* indicating that this organism might involve in biofilm formation. However, the ability to form a biofilm still had to be demonstrated. In the present thesis it was demonstrated biofilm that the crenarchaeota *S. solfataricus*, *S. acidocaldarius* and *S. tokodaii* form biofilms. We aimed to focus on the characteristic features (development, maturation and dispersal) of the biofilm in all these three strains. To achieve these goals a static biofilm assay method was developed, which was adapted to high temperature and low pH (75°C, pH3) to analyze *Sulfolobus spp*. biofilm. During the course this work it was tried to address the following questions as a part of this study objectives:

1. How does crenarchaeal biofilm develop? What influences the biofilm formation and which structures are involved in the composition of the EPS?

The developed methods (e.g. high temperature microtiter assay and, static biofilm assay) were used in combination with fluorescent microscopy to shed light on these questions (Chapter 3.2).

2. Which genes or proteins are involved in crenarchaeal biofilm formation? Is there a global way of regulation occurring, which may be shared among the three *Sulfolobus* species? Does the transcription pattern change during the development of the biofilm?

To answer this question a comparative proteomic and transcriptomic analysis of two days old biofilms of *S. acidocaldarius*, *S. tokodaii* and *S. solfataricus* was performed Chapter 3.3).

3. Are there surface structures in *Sulfolobales* which might be important for biofilm formation,?

The deletion mutants of the three surface appendages of *S. acidocaldarius* were constructed and a detailed analysis of surfaces attachment as well as the biofilm formation was carried out (Chapter 3.4).

Within this study the resulting observation of the different EPS production of PBL2025 in comparison to *S. solfataricus* lead to the following question (Chapter 3.1).

4. Which of the missing 50 genes in PBL2025 could be responsible or at least is supporting this phenotype?

The complementation of one of the genes, with the most promising effect (Ssα-man), was the primary target (Chapter 3.5).

3   Results

The next chapter is divided into five sections where each of these represents an independent study describing separate objectives of the entire thesis and they are either published in or submitted to a peer reviewed journal. At the beginning of each section, the results and a short interpretation are incorporated including authors contributions have been outlined.

3.1   Appendages for the attachment in *Sulfolobus solfataricus*

Zolghadr, B., A. Klingl, A. Koerdt, A. J. Driessen, R. Rachel, and S. V. Albers. 2010. **Appendage mediated surface adherence of *Sulfolobus solfataricus***. J Bacteriol 192:104-110

The impact of extracellular macro-molecular structures (e.g. flagella, pili or other extracellular structures) in attachment to a surface was demonstrated for several bacteria and archaea. The ability to attach to a surface is the first indication for an organism to form biofilm. Before this study it was unknown if strains belonging to the genus of *Sulfolobus spp.* are competent for an attachment or biofilm formation. However, the appearance of different surface structures like the flagella or Ups-pili has been shown for this organism. Aim of this work was to figure out if these surface appendages of *S. solfataricus* PBL2025 are involved or required for the attachment to surfaces. Therefore, the attachment to different abiotic surfaces (mica, glass, pyrite and gold-grids) of *S. solfataricus* P2, *S. solfataricus* PBL2025, Δ*upsE* and Δ*flaJ* (mutants derived from PBL2025) was tested. The comparative analysis showed the requirement of flagella and Ups-Pili for attachment to all analysed surfaces. Additionally, differences in the production of extracellular surface structures between PBL2025 and P2 were analysed by electron microscopy. The observed phenotypic differences including differential EPS production in these two strains are presumably reside in the 50 missing genes involved in sugar metabolism and transport in PBL2025. Therefore, the study was extended for a comparable analysis of the sugar composition between P2 and PBL2025 and the change of the expression level of distinct genes within the aforementioned gene cluster of P2 in planktonic and biofilm lifestyles. With fluorescence microscopy it was revealed that in both these strains, e.g., P2 and PBL2025, the EPS contains the sugars glucose, α-D-mannose, α-D-galactose, and N-acetyl-D-glucosamine. It was also confirmed from the analysis that the EPS production is higher in PBL2025 and contains higher amounts of glucose and mannose, respectively. Furthermore, via q-PCR and comparative analysis of planktonic and

attached P2 cells, it was evident that a number of genes, which are missing in PBL2025, are up-regulated under surface attached conditions. This might explain the differences in the morphology at the attached state of P2 and PBL2025.

All the results describing an analysis of the sugar composition of *S. solfataricus* P2 and PBL2025 cells were performed by Andrea Koerdt. The electron microscopy was performed by Andreas Klingl (Supervisor and supporting material: Reinhard Rachel) and Behnam Zolghadr (Supervisor and supporting material: Arnold J. M. Driessen and Sonja-Verena Albers). All other experiments like q-PCR and surface attachment studies on different abiotic surfaces were performed by Behnam Zolghadr. The manuscript was written by Sonja-Verena Albers and revised by all authors.

Appendage-Mediated Surface Adherence of *Sulfolobus solfataricus*[▽]

Behnam Zolghadr,[1,3]† Andreas Klingl,[2]† Andrea Koerdt,[1] Arnold J. M. Driessen,[3]
Reinhard Rachel,[2] and Sonja-Verena Albers[1]*

*Independent Junior Research Group Molecular Biology of Archaea, Max-Planck-Institute for Terrestrial Microbiology,
Karl-von-Frisch-Strasse, 35043 Marburg, Germany[1]; Universitaet Regensburg, Centre for Electron Microscopy, Institute for
Anatomy, Universitaetsstr. 31, 93053 Regensburg, Germany[2]; and Department of Microbiology,
Groningen Biomolecular Sciences and Biotechnology Institute, and the Zernike Institute for
Advanced Materials, University of Groningen, Kerklaan 30, 9751 NN Haren, The Netherlands[3]*

**Attachment of microorganisms to surfaces is a prerequisite for colonization and biofilm formation. The
hyperthermophilic crenarchaeote *Sulfolobus solfataricus* was able to attach to a variety of surfaces, such as
glass, mica, pyrite, and carbon-coated gold grids. Deletion mutant analysis showed that for initial attachment
the presence of flagella and pili is essential. Attached cells produced extracellular polysaccharides containing
mannose, galactose, and *N*-acetylglucosamine. Genes possibly involved in the production of the extracellular
polysaccharides were identified.**

In microbiology, organisms are isolated from their natural habitats and typically cultivated in the laboratory as planktonic species. Though this method has been essential for understanding the concept of life, it remains unclear how microbial ecosystems operate. For bacteria, it is well known that they are able to form large cellular communities with highly complex cellular interactions and symbioses between different microbial or eukaryotic species. Biofilm formation is an essential component of such communities, and studies have shown that bacteria within biofilms are physiologically different from planktonic ones (20, 21). They can exhibit extensive networks of pili on their surfaces and produce and secrete extracellular polysaccharides (EPS), their growth rate is decreased, and cells are much more resistant to physical stresses and antibiotics (19).

The study of surface colonization and cellular communities of archaea is crucial for understanding their ecological properties. The only detailed study showed that the hyperthermophilic organism *Archaeoglobus fulgidus* produced biofilms when challenged with heavy metals and pentachlorophenol (10). *Pyrococcus furiosus* was able to adhere to different surfaces, such as mica and carbon-coated gold grids, and cells were connected via cable-like bundles of flagella (12). *Methanopyrus kandleri* was shown to adhere to glass, but *P. furiosus* could colonize only by attaching to *M. kandleri* cells, using flagella and direct cell contacts (16).

Here we report on the function of cell surface appendages in initial attachment to surfaces of archaea, using directed gene inactivation mutants. The crenarchaeote *Sulfolobus solfataricus* P2 is a thermoacidophile which grows optimally at 80°C and pH values of 2 to 4 (22). *S. solfataricus* possesses cell surface structures such as flagella and UV-induced pili (1, 2). The flagellum operon of *S. solfataricus* encodes, in addition to the structural subunit FlaB, four proteins of unknown function, the ATPase FlaI, and the only integral membrane protein, FlaJ. Previously, we isolated a Δ*flaJ* mutant which was nonflagellated and had lost its ability for surface motility on Gelrite plates (17). Recently, we described UV-inducible pili in *S. solfataricus* that directed cellular aggregation after UV stress (8). Deletion of the central ATPase UpsE, responsible for pilus assembly, rendered cells devoid of pili and defective in cellular aggregation after UV treatment (8). In this study, wild-type cells and deletion strains were tested for the ability to attach to a variety of surfaces and the formed structures and extracellular material were analyzed.

MATERIALS AND METHODS

Strains and growth conditions. *S. solfataricus* P2, *S. solfataricus* PBL2025 (15), and Δ*flaJ* (17) and Δ*upsE* (8) mutants were grown aerobically at 80°C in the medium described by Brock et al. (5), adjusted to pH 3 with sulfuric acid, and supplemented with 0.1% (wt/vol) tryptone under moderate agitation. Growth of cells was monitored by measuring the optical density at 600 nm.

Sample preparation for electron microscopy. Samples on 200-mesh carbon-coated gold grids were negatively stained with 2% uranyl acetate and analyzed by transmission electron microscopy on a Philips CM12 electron microscope (LaB6 cathode, 120 keV; FEI Co., Eindhoven, The Netherlands). Samples for scanning electron microscopy were freeze-dried for 2 h at −80°C (CFE 50; Cressington Ltd., Watford, United Kingdom), rotary shadowed with platinum-carbon (1 to 2 nm), and analyzed with an FEI Quanta 400 scanning electron microscope (FEG cathode; 4 to 25 keV).

Fluorescence microscopy. Cells were grown for 3 days in 0.1% tryptone medium in the presence of a glass slide. After cooling down of the culture, the cells were fixed with 4% formaldehyde for 30 min. The glass slides were washed with Brock medium (pH 5) to remove planktonic cells. Cells on the lower side of the glass slides were removed with ethanol. Lectins were applied to the glass slides, evenly spread with Parafilm, and incubated for 30 min at room temperature in the dark. Fluorescently labeled lectins used were concanavalin A (ConA)-fluorescein conjugate (1 mg/ml), GS-II–Alexa Fluor 594 from *Griffonia simplicifolia* (1 mg/ml), and GS-IB4–Alexa Fluor 594 from *G. simplicifolia* (1 mg/ml). Unbound lectins were removed by washing with Brock medium (pH 5). All lectins were obtained from Molecular Probes. The samples were analyzed by fluorescence microscopy, using a red-filter 750-ms exposure and green-filter 250-ms exposure.

* Corresponding author. Mailing address: Independent Junior Research Group Molecular Biology of Archaea, Max-Planck-Institute for Terrestrial Microbiology, Karl-von-Frisch-Strasse, 35043 Marburg, Germany. Phone: 496421178300. Fax: 496421178309. E-mail: albers @mpi-marburg.mpg.de.
† B. Zolghadr and A. Klingl contributed equally to this paper.
▽ Published ahead of print on 23 October 2009.

TABLE 1. Primers used for RT-PCRs and qPCRs

Primer	Sequence (5′–3′)
UpsA-rt-forward	GCTGGGTGGTCTACTTTAT
UpsA-rt-reverse	AGTACTGCCCAGCAGTTA
UpsA-rt-forward	TCTCACTCATCGTTCCATTA
UpsA-rt-reverse	CAGAGTTTCCCTCAATGAAT
FlaB-rt-forward	AGACAGCGTCAACAGACTA
FlaB-rt-reverse	ACCTGCACTTGTCTGCTGAT
sso3002-rt-forward	TGTTGGAGATGGGTGTGATG
sso3002-rt-reverse	AGCTGGGTCTGTCGTAATTG
sso3012-rt-forward	CCCAACTTCCTCGTTGTTAG
sso3012-rt-reverse	TGCCCTCGCAATACTTAACC
sso3042-rt-forward	TTTGCGGTACTGATAGGGAG
sso3042-rt-reverse	CTGAAGCGCCTGTAGTATCG
sso3043-rt-forward	TACTTCACTGACGGCACACC
sso3043-rt-reverse	CCGTGGGATTCAAGCAACTG
SSO3041-rt-forward	CTGGTCTGCCTGGTTCATAC
SSO3041-rt-reverse	CACATCCCTCTGCCTTATTG
SSO3039-rt-forward	GAGAAGACTACGCAGTTCCA
SSO3039-rt-reverse	GCGTTCCTAGCAACCTCATA
SSO3036-rt-forward	CCTATGGGCACCTAAAGGTA
SSO3036-rt-reverse	CTGCAACCTCACGTATATCG
SSO302-rt-forward	ACTCTAAAGGTCGCTGAGTG
SSO3021-rt-reverse	GGAAATTGGCTTGCCTCTTG
SSO3017-rt-forward	GGGTGAGTAGGAATAGTAGG
SSO3017-rt-reverse	GGAATCAGATAGGGCGTAAG
SSO3010-rt-forward	GCGAACTTCGGTTGGTTACT
SSO3010-rt-reverse	TACCCACGAGCCTCTGTAAT
SSO3007-rt-forward	ATATGATAGGAGCGCGGGAT
SSO3007-rt-reverse	CCCTACTTCCTGCTGGATTA
SSO3014-rt-forward	CCAGACCCAGATACTCCAAA
SSO3014-rt-reverse	CAACATCCTTGAGGCCTAAC
SSO3038-rt-forward	TTAGGCGTGTAGGAGGACAA
SSO3038-rt-reverse	ACCAGCCATCTATCCCTGAA
secY-rt-forward	GGATCGGGAGTTAGTCTGTT
secY-rt-reverse	GAAGCTGAGGGTGAGACATA

Gene expression analysis. *S. solfataricus* P2 cultures were incubated with pieces of mica for 2 days. Total RNAs were then isolated from planktonic cells and cells attached to the mica. Total RNA isolation and cDNA synthesis were performed as described previously (23). Gene-specific primer sets (Table 1) were used to detect the presence of selected genes in the SSO3002-3050 genomic region. PCR products were analyzed on 0.8% agarose gels.

Quantitative PCR (qPCR) analysis was carried out according to the protocol and chemicals provided by Applied Biosystems. For each gene of interest, a duplicate setup of 26 μl PCR mixture was prepared from 13 μl Sypro green master mix, 2 μl of a 5 μM primer pair stock solution, 2 μl cDNA, and 9 μl nucleotide-free water. The negative control assays were done with RNA mixtures that were prepared for cDNA synthesis. Primer efficiencies were calculated from the average slope of the linear regression curves according to the calculation model advised by Applied Biosystems. The fluorescence quantities of the reactions were measured with an ABI 7500 instrument (Applied Biosystems, Foster City, CA).

RESULTS

Attachment of *S. solfataricus* to various surfaces. For initial attachment to different materials, we tested *S. solfataricus* P2, *S. solfataricus* PBL2025, and the Δ*flaJ* and Δ*upsE* mutants derived from this strain. Carbon-coated gold grids were incubated in shaking cultures for 2 days in tryptone medium. PBL2025 adhered to the carbon-coated gold grids, and some flagella and more straight pili were present (Fig. 1A and C). In contrast, only very few cells of the Δ*flaJ* (Fig. 1B) and Δ*upsE* (Table 2) strains attached to the carbon grids, implying an important role for both the flagella and UV-induced pili for this process. The same experiment was

repeated with the addition of sulfur to the tryptone medium to mimic the natural habitat of *Sulfolobus* species. Considerably more PBL2025 cells were found attached to the carbon film than to tryptone medium alone (Fig. 1D). Moreover, the cells clustered around the sulfur particles (Fig. 1E) and developed some extracellular sheet-like structure connecting the cells (Fig. 1F). Other materials tested for attachment of cells were glass, pyrite, and mica, a layered aluminum silicate which forms extremely smooth and clean surfaces when cleaved with a razor blade (for an overview, see Table 2). *S. solfataricus* P2 and PBL2025 grew very differently on mica surfaces. PBL2025 formed microcolonies and produced very large, thin layers of extracellular material in which cells were embedded (Fig. 2A and B). *S. solfataricus* P2 formed a more regular, extended network of extracellular appendages containing some other material between the structures (Fig. 2C and D). As shown for carbon-coated grids, cells of the Δ*flaJ* and Δ*upsE* strains were also unable to adhere to mica (data not shown). *S. solfataricus* P2 grew best on glass surfaces, yielding more cells than on mica or carbon-coated grids. Obviously, the cells attached to the surfaces by using flagella and pili (Fig. 2E and F), but they did not produce the extensive network of extracellular material and appendages observed on mica. The Δ*flaJ* and Δ*upsE* strains were also not able to grow on glass (Table 2).

Analysis of extracellular material from attached cells. It is well known that extracellular proteins of *Sulfolobales* are glycosylated. Glucose, mannose, galactose, and *N*-acetylglucosamine have previously been identified in the glycans of sugar-binding proteins (7). Moreover, the same sugars were found in extracellular polysaccharides that are produced mainly in the stationary growth phase of *S. solfataricus* MT3 and MTA4 (13). Therefore, fluorescently labeled lectins were used to determine the nature of the extracellular material produced by the attached *S. solfataricus* cells. Glass slides were incubated for 3 days in shaking *S. solfataricus* P2 and PBL2025 cultures. After fixation, the samples were incubated with fluorescently labeled lectins directed against terminal α-D-galactosyl residues (isolectin-IB4), α- or β-linked *N*-acetyl-D-glucosamine (GS-II), or α-mannopyranosyl and α-glucopyranosyl residues (ConA). In *S. solfataricus* P2, all three lectins reacted with the extracellular material, indicating the presence of the different sugars recognized by the different lectins (Fig. 3A to H). ConA and isolectin-IB4 also bound to cells staining the cell envelope, whereas GS-II only attached to the extracellular material. As shown by the scanning electron images (Fig. 2), PBL2025 formed a denser-appearing extracellular material, which was also visible by light microscopy (Fig. 3I to P). Also with PBL2025, all three lectins bound to the extracellular material; interestingly, and in contrast to the case with *S. solfataricus* P2, the lectin GS-II also bound to the cell envelope. From this analysis, it can be concluded that *Sulfolobus* strains produce EPS when attached to a glass surface.

Analysis of differentially expressed genes in attached *S. solfataricus* P2 cells. As shown in Fig. 2, attachment of *S. solfataricus* P2 and PBL2025 to mica resulted in diverse structures; in particular, the extracellular material formed had a different appearance. In contrast to *S. solfataricus* P2, strain PBL2025 lacks genes SSO3004 to -3050 (15). This region includes a diverse set of genes possibly involved in sugar degradation and
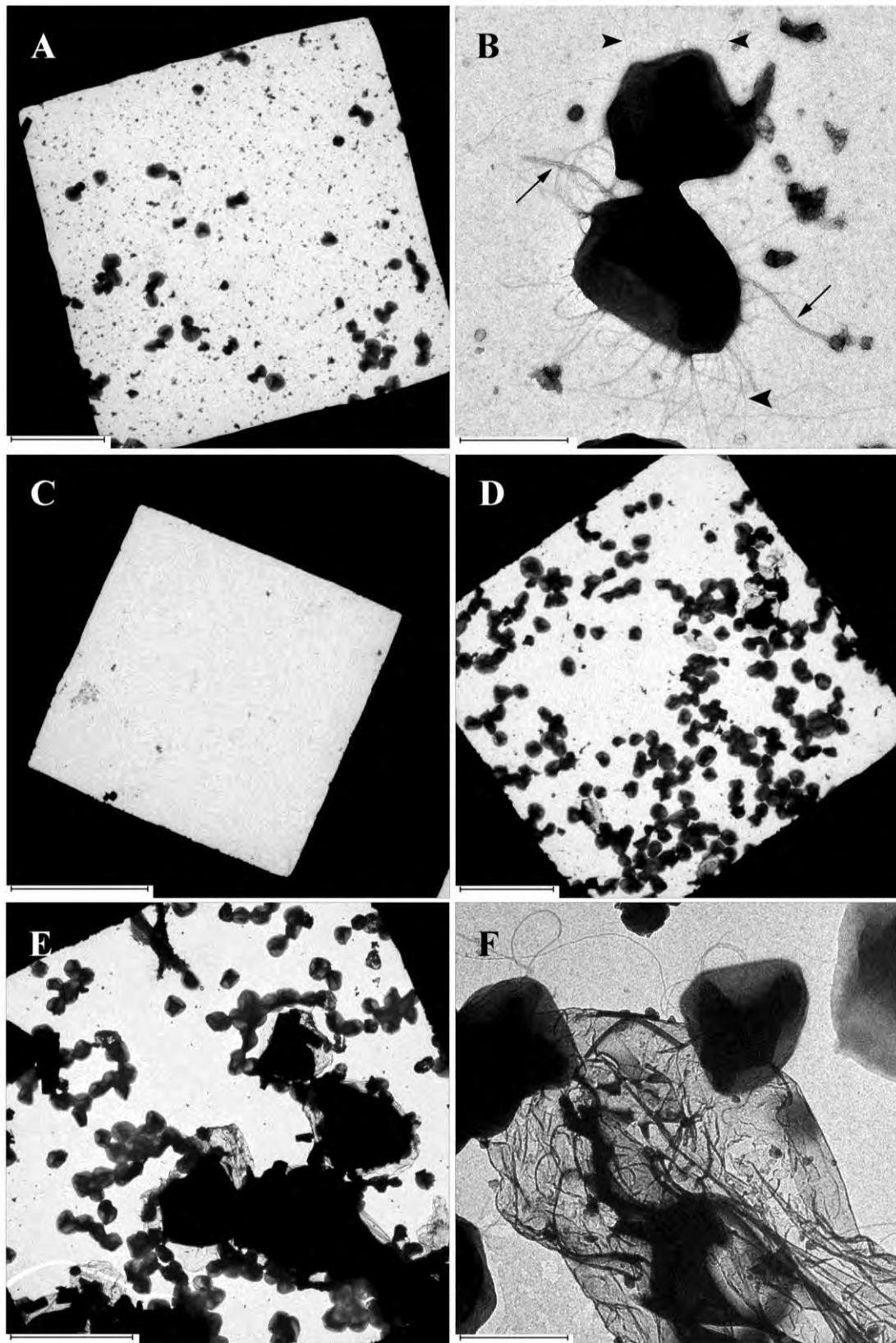
FIG. 1. Attachment of strain PBL2025 to carbon-coated gold grids. (A and B) Transmission electron micrographs of PBL2025 attached to carbon. (B) At higher magnifications, flagella (arrows) and pili (arrowheads) could be detected. (C) The Δ*flaJ* strain was not able to adhere under these conditions. When sulfur was added to the medium, considerably more PBL2025 cells attached to the carbon film (D), adhered to the sulfur particles (E), and produced an extracellular sheet-like material (F). Bars: 10 μm (A, D, and E), 1 μm (B and F), and 20 μm (C).

TABLE 2. Different materials tested for attachment of *Sulfolobus* strains

| Surface | Growth of *S. solfataricus* strain | | | |
	P2	PBL2025	Δ*upsE*	Δ*flaJ*
Mica (glimmer)	Growth on surface with many flagella and pili	Growth on surface with pili	No growth	No growth
Glass	Growth on surface; cells are connected with a mesh of flagella/pili	Growth on surface; no pili or flagella visible	No growth	No growth
Pyrite (FeS$_2$)	Growth on surface	No growth	No growth	No growth
Gold grids coated with carbon	Growth on surface with pili and flagella	Growth on surface with pili and flagella	Only very few cells present	Only very few cells present

lipid metabolism (Table 3). Since the EPS produced by the two strains differed significantly, we explored whether the genes in the aforementioned region are involved in the production or modulation of EPS during growth of *Sulfolobales* on surfaces and whether the expression of the flagellin and pilin genes, the structural subunits of the flagella and the pili, respectively, is altered after attachment. Shaking *S. solfataricus* P2 cultures were incubated with pieces of mica for 2 days. Quantitative
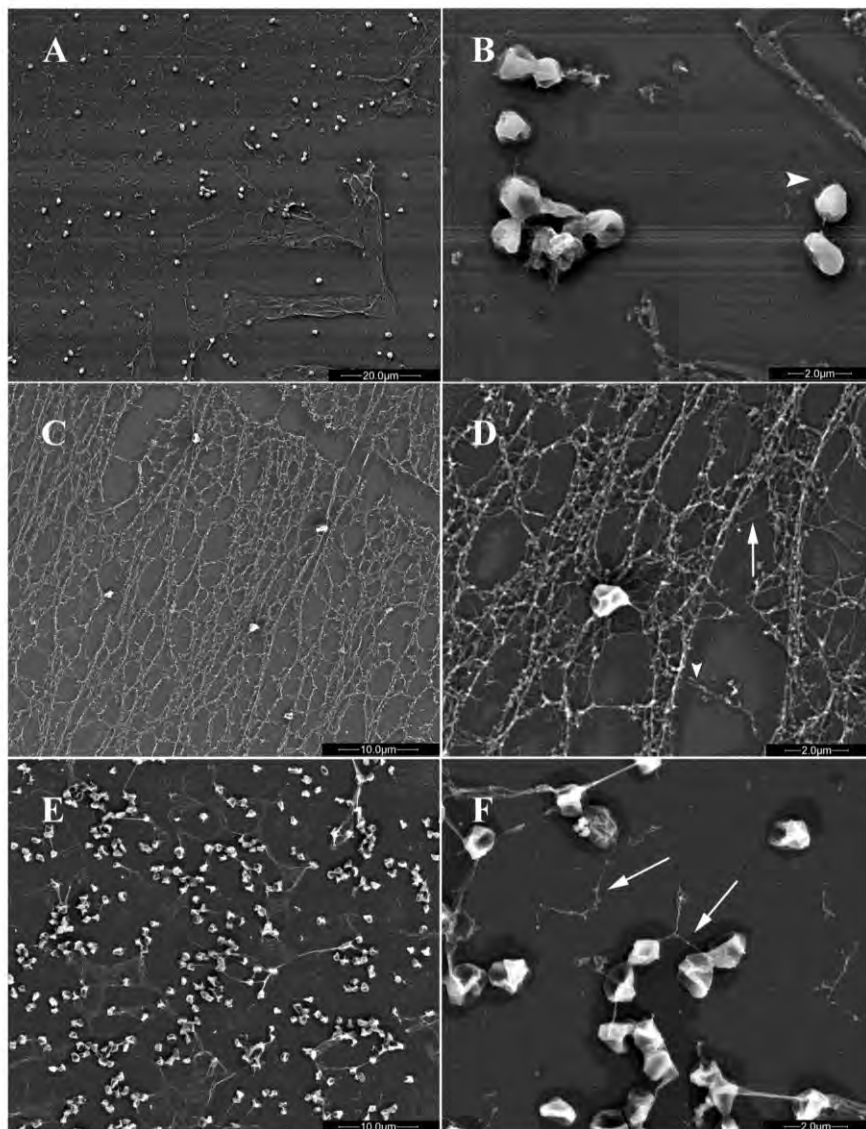
FIG. 2. Attachment of *S. solfataricus* P2 and PBL2025 to mica and glass. PBL2025 attached to mica and produced extracellular sheet-like structures (A and B), whereas P2 adhered via an extensive network of flagella/pili (C and D; panel D is an enlargement of panel C). Attachment of *S. solfataricus* P2 to glass was very different from that to mica (E and F; panel F is an enlargement of panel E). Pili (arrowheads) and flagella (arrows) are indicated. Bars: 20 μm (A), 2 μm (B, D, and F), and 10 μm (C and E).

108   ZOLGHADR ET AL.   J. BACTERIOL.

S. solfataricus P2

DIC   ConA   GS-II/ IB$_4$ Overlay

S. solfataricus PBL2025

DIC   ConA   GS-II/ IB$_4$ Overlay

FIG. 3. Fluorescence microscopy using fluorescein-coupled ConA (green) and either Alexa-coupled GSII or IB4 lectin (both red) on *S. solfataricus* P2 (A to H) and *S. solfataricus* PBL2025 (I to P) attached to glass. (A, E, I, and M) Differential interference contrast; (B, F, J, and N) green channel; (C, G, K, 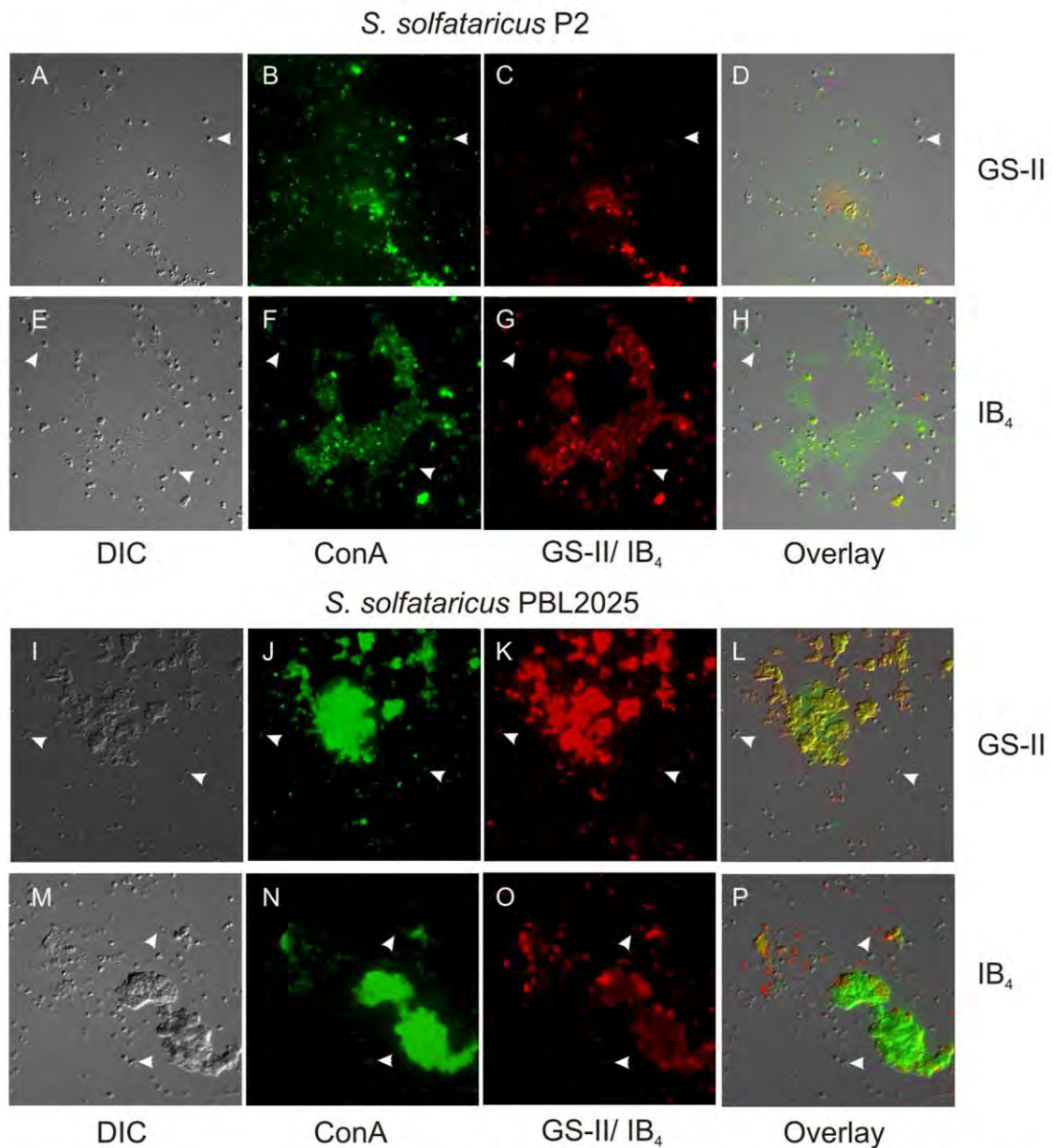and O) red channel; (D, H, L, and P) overlay of differential interference contrast and fluorescence images. White arrowheads indicate the positions of cells.

RT-PCR was performed on cDNAs obtained from total mRNAs isolated from planktonic and mica-attached cells.

Using qPCR, we determined that the expression of the flagellin FlaB was repressed 12-fold in attached cells in comparison to planktonic cells, whereas the UV-induced pilins, UpsA and UpsB, were upregulated 5- and 2-fold, respectively. Among the 18 tested genes in the genomic region of SSO3002 to SSO3050, 10 genes were not expressed in attached cells, whereas 8 were clearly induced (Fig. 4A and B). The genes induced strongly are predicted to be involved in sugar degradation and metabolism, such as a β-mannosidase (SSO3007); LacS, a β-galactosidase

(SSO3019); two carbohydrate transporters (SSO3010/17); a glucose-1 dehydrogenase (SSO3009); and a gluconolactonase (SSO3041). An oxidoreductase (SSO3014) and a dihydrodipicolinate synthase (SSO3035), which is part of the lysine synthesis pathway, were induced as well.

DISCUSSION

In this study, we have shown that the hyperthermophilic archaea *S. solfataricus* P2 and PBL2025 are able to attach to a variety of surfaces, such as glass, mica, pyrite, and carbon-

TABLE 3. Putative functions of ORFs SSO3002 to SSO3048 and
their induction patterns in attached cells

ORF	Putative function	Induction in attached cells[a]
SSO3002	Glycosyltransferase	−
SSO3003	Glucose 1-dehydrogenase	ND
SSO3004	3-Oxoacyl-(acyl carrier protein) reductase	ND
SSO3006	α-Mannosidase	−
SSO3007	Endo-β-mannanase	+
SSO3008	Dehydrogenase	ND
SSO3009	Carbon monoxide dehydrogenase, large chain	+
SSO3010	Carbohydrate transporter	+
SSO3011	Dehydrogenase	ND
SSO3012	ABC-type multidrug transporter	−
SSO3013	Dehydrogenase	ND
SSO3014	Oxidoreductase	+
SSO3015	Dehydrogenase	ND
SSO3016	Amino hydrolase	ND
SSO3017	Carbohydrate transporter	+
SSO3019	β-Glycosidase (LacS)	+
SSO3021	Zn-dependent hydrolase	−
SSO3022	α-Xylosidase	−
SSO3029	Sugar phosphate isomerase	ND
SSO3032	β-Xylosidase	ND
SSO3034	Hypothetical	ND
SSO3035	Dihydrodipicolinate synthase	+
SSO3036	β-Glucuronidase	−
SSO3037	Hypothetical	−
SSO3038	Hypothetical	−
SSO3039	Bile acid β-glucosidase	−
SSO3041	Gluconolactonase	+
SSO3042	Glucose dehydrogenase	−
SSO3043	ABC transporter, dipeptide binding protein	−
SSO3045	ABC transporter, ATP-binding protein	ND
SSO3046	ABC transporter, ATP-binding protein	ND
SSO3047	ABC transporter, permease	ND
SSO3048	ABC transporter, permease	ND

[a] ND, not determined.

coated gold grids, from shaking cultures, in a flagellum- and pilus-dependent manner. Cells lacking either the flagella or UV-inducible pili were unable to attach to the tested surfaces. The pili assembled by the *ups* operon so far have only been implicated in cellular aggregation after UV exposure. Our studies demonstrate that these pili are also expressed upon contact with surfaces and that there is an interplay with flagella in surface adhesion. Flagella have also been implicated in mediating surface adhesion and cell-cell contacts in the archaea *P. furiosus* and *M. kandleri* (12, 16), but our deletion mutant analysis demonstrated the requirement of these surface structures for attachment from shaking cultures. The qPCR data confirmed that the expression of the UV-induced pilins, UpsA and -B, was indeed upregulated in surface-attached cells. However, the expression of FlaB was drastically reduced in immobilized cells, from which the mRNA for the expression-level analysis was isolated after 2 days of incubation. Most probably the flagella are necessary for initial attachment and possibly "recognition" of surfaces, but not for persistence once the cells are attached.

PBL2025 formed extensive sheets of extracellular material, whereas *S. solfataricus* P2 synthesized an extensive network of flagella and pili in order to attach to glass and mica. We utilized fluorescent lectins to study the composition of the EPS formed by these two strains. Glucose, α-D-mannose, α-D-galactose, and *N*-acetyl-D-glucosamine are the minimal components of EPS, since a selective reaction was observed with ConA, GS-II, and isolactin-IB4 (Fig. 3). This sugar composition matches the sugars found in extracellular glycoproteins of *S. solfataricus* and EPS isolated from shaking *S. solfataricus* MT4 cultures (7, 13). We could not observe flagella and Ups
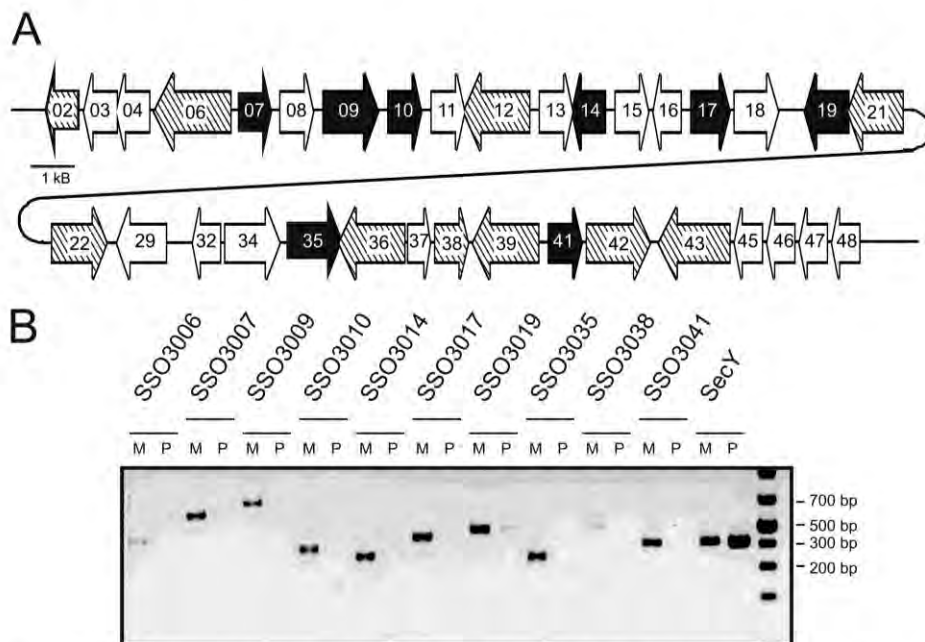
FIG. 4. Expression analysis of the genomic region SSO3002 to SSO3048. (A) Schematic view of the genomic region SSO3002 to SSO3048. Genes indicated by hatched arrows were not expressed in attached cells, whereas filled black arrows indicate genes induced under attached conditions. (B) Agarose gel of RT-PCRs performed on cDNAs from planktonic cells (P) and mica-attached cells (M). *secY* was used as a quality control for the isolated RNA and as a housekeeping gene.

pili on mica and glass as clearly as in the transmission electron micrographs from carbon-coated grids. A possible explanation is that both flagella and Ups pili are structural components within the EPS network. A recent study on surface attachment of an *Escherichia coli* K-12 strain to glass demonstrated that α-D-mannose-rich EPS structures on glass surfaces are essential for lateral biofilm maturation of the cells (14). The EPS coat on the hydrophilic glass creates a template for the hydrophobic type 1 fimbria filaments of *E. coli* and subsequent development of biofilm. In the case of *S. solfataricus*, the EPS was produced in large amounts during the attachment of cells to mica and glass, while on carbon-coated grids similar EPS structures were absent. Both glass and mica surfaces are hydrophilic, and the carbon films on electron microscopy grids are hydrophobic. One possible explanation is that *S. solfataricus* EPS creates a template on a hydrophilic surface which is more suitable for other cell surface structures, such as the S-layer envelope or other glycosylated components of the cell surface, during the following development of cells.

S. solfataricus P2 and PBL2025 differed in the amount and form of the EPS secreted after 3 days of surface attachment. Since PBL2025 lacks a quite large genomic region present in *S. solfataricus* P2, we demonstrated that at least 10 of these genes were upregulated upon surface attachment. The majority of these genes are predicted to be involved in sugar degradation and transport. These proteins might be involved in the efficient degradation of the produced EPS or in its modification and modulation, which might explain why with PBL2025 an extensive surface labeling of the EPS was observed. Among the upregulated proteins was LacS, a very-well-characterized β-galactosidase, and its cognate lactose transporter, which have both been shown to be essential for *S. solfataricus* for growth on lactose (3). Since we detected glucose and galactosyl residues by lectin staining, lactose might be present as a breakdown product of the EPS. Studies on bacterial EPS in biofilm suggest that glycosylation functions as a means for nutrition storage (4, 6, 9, 11, 18). Therefore, it will be interesting to determine the purpose of EPS in archaea and whether it is composed only of sugars or contains proteins besides the flagellins and pilins. We have demonstrated that flagella and UV-induced pili are essential for initial attachment of *S. solfataricus*, and it will be vital to determine which role they play in the development and consolidation of biofilms. Future gene inactivation studies will therefore focus on the role of surface structures, EPS production, and degradation in this process.

REFERENCES

1. **Albers, S. V., and M. Pohlschroder.** 2009. Diversity of archaeal type IV pilin-like structures. Extremophiles **13:**403–410.

2. **Albers, S. V., Z. Szabo, and A. J. Driessen.** 2006. Protein secretion in the Archaea: multiple paths towards a unique cell surface. Nat. Rev. Microbiol. **4:**537–547.

3. **Bartolucci, S., M. Rossi, and R. Cannio.** 2003. Characterization and functional complementation of a nonlethal deletion in the chromosome of a beta-glycosidase mutant of *Sulfolobus solfataricus.* J. Bacteriol. **185:**3948–3957.

4. **Bejarano, E. M., and R. P. Schneider.** 2004. Use of fluorescent lectin probes for analysis of footprints from *Pseudomonas aeruginosa* MDC on hydrophilic and hydrophobic glass substrata. Appl. Environ. Microbiol. **70:**4356–4362.

5. **Brock, T. D., K. M. Brock, R. T. Belly, and R. L. Weiss.** 1972. Sulfolobus: a new genus of sulfur-oxidizing bacteria living at low pH and high temperature. Arch. Microbiol. **84:**54–68.

6. **Decho, A. W., and T. Kawaguchi.** 1999. Confocal imaging of in situ natural microbial communities and their extracellular polymeric secretions using Nanoplast resin. Biotechniques **27:**1246–1252.

7. **Elferink, M. G. L., S. V. Albers, W. N. Konings, and A. J. M. Driessen.** 2001. Sugar transport in *Sulfolobus solfataricus* is mediated by two families of binding protein-dependent ABC transporters. Mol. Microbiol. **39:**1494–1503.

8. **Frols, S., M. Ajon, M. Wagner, D. Teichmann, B. Zolghadr, M. Folea, E. J. Boekema, A. J. Driessen, C. Schleper, and S. V. Albers.** 2008. UV-inducible cellular aggregation of the hyperthermophilic archaeon *Sulfolobus solfataricus* is mediated by pili formation. Mol. Microbiol. **70:**938–952.

9. **Hassan, A. N., J. F. Frank, and K. B. Qvist.** 2002. Direct observation of bacterial exopolysaccharides in dairy products using confocal scanning laser microscopy. J. Dairy Sci. **85:**1705–1708.

10. **Lapaglia, C., and P. L. Hartzell.** 1997. Stress-induced production of biofilm in the hyperthermophile *Archaeoglobus fulgidus.* Appl. Environ. Microbiol. **63:**3158–3163.

11. **Laue, H., A. Schenk, H. Li, L. Lambertsen, T. R. Neu, S. Molin, and M. S. Ullrich.** 2006. Contribution of alginate and levan production to biofilm formation by *Pseudomonas syringae.* Microbiology **152:**2909–2918.

12. **Nather, D. J., R. Rachel, G. Wanner, and R. Wirth.** 2006. Flagella of *Pyrococcus furiosus*: multifunctional organelles, made for swimming, adhesion to various surfaces, and cell-cell contacts. J. Bacteriol. **188:**6915–6923.

13. **Nicolaus, B., M. C. Manca, I. Romano, and L. Lama.** 2003. Production of an exopolysaccharide from two thermophilic archaea belonging to the genus Sulfolobus. FEMS Microbiol. Lett. **109:**203–206.

14. **Rodrigues, D. F., and M. Elimelech.** 2009. Role of type 1 fimbriae and mannose in the development of Escherichia coli K12 biofilm: from initial cell adhesion to biofilm formation. Biofouling **25:**401–411.

15. **Schelert, J., V. Dixit, V. Hoang, J. Simbahan, M. Drozda, and P. Blum.** 2004. Occurrence and characterization of mercury resistance in the hyperthermophilic archaeon *Sulfolobus solfataricus* by use of gene disruption. J. Bacteriol. **186:**427–437.

16. **Schopf, S., G. Wanner, R. Rachel, and R. Wirth.** 2008. An archaeal bi-species biofilm formed by *Pyrococcus furiosus* and *Methanopyrus kandleri*. Arch. Microbiol. **190:**371–377.

17. **Szabó, Z., M. Sani, M. Groeneveld, B. Zolghadr, J. Schelert, S. V. Albers, P. Blum, E. J. Boekema, and A. J. Driessen.** 2007. Flagellar motility and structure in the hyperthermoacidophilic archaeon *Sulfolobus solfataricus.* J. Bacteriol. **189:**4305–4309.

18. **Tsuneda, S., H. Aikawa, H. Hayashi, A. Yuasa, and A. Hirata.** 2003. Extracellular polymeric substances responsible for bacterial adhesion onto solid surface. FEMS Microbiol. Lett. **223:**287–292.

19. **Vu, B., M. Chen, R. J. Crawford, and E. P. Ivanova.** 2009. Bacterial extracellular polysaccharides involved in biofilm formation. Molecules **14:**2535–2554.

20. **Watnick, P., and R. Kolter.** 2000. Biofilm, city of microbes. J. Bacteriol. **182:**2675–2679.

21. **Watnick, P. I., and R. Kolter.** 1999. Steps in the development of a *Vibrio cholerae* El Tor biofilm. Mol. Microbiol. **34:**586–595.

22. **Zillig, W., K. O. Stetter, S. Wunderl, W. Schulz, H. Priess, and I. Scholz.** 1980. The Sulfolobus-"Caldariella" group: taxonomy on the basis of the structure of DNA-dependent RNA polymerases. Arch. Microbiol. **125:**259–269.

23. **Zolghadr, B., S. Weber, Z. Szabó, A. J. M. Driessen, and S. V. Albers.** 2007. Identification of a system required for the functional surface localization of sugar binding proteins with class III signal peptides in Sulfolobus solfataricus. Mol. Microbiol. **64:**795–806.

3.2 First insides into biofilm formation of *Sulfolobus spp.*

Only few studies have been performed to understand biofilm formation in archaea while the most of the information available is related to the surface attachment. Only two studies have been performed demonstrating the proteomic and stress induced changes occurred during the biofilm formation in euryarchaeota. However, no information was available on the biofilm formation in crenarchaeota. Therefore, the goal of this study was to develop methods to study biofilm formation in *Sulfolobus spp.* which grows under thermoacidophilic conditions (e.g. microtiter assay, optimal conditions for the growth of biofilm, staining of biofilm or CLSM). Furthermore, a comparative analysis of the three related strains, *S. solfataricus*, *S. acidocaldarius* and *S. tokodaii*, in respect to biofilm formation was demonstrated in the present study. It was clearly evident that they exhibit differences in morphology (ranging from simple carpet structure for *S. solfataricus* to a towel-structure of *S. acidocaldarius*) and also responsiveness against the environmental stress (e.g. temperature, pH and iron concentration). Furthermore, basic information of the EPS compositions in biofilm was obtained where it was evident that each of these strains possesses different amounts of extracellular substances. The matrix contains mainly sugars like glucose, galactose, mannose and N-D-acetylglucosamine. We could observe the direct cell-cell connections under SEM and also could detect the presence of glycosylation even at the level of these connections. We found little eDNA in the biofilm matrix of these strains indicating minor role of eDNA in the development of biofilm in *Sulfolobus spp.*. In a parallel study we analyzed surface appendage(s) mutant(s) of *S. solfataricus* for biofilm formation. We found that they show no (Δ*flaJ*) or little (Δ*upsE*) changes compared to the wildtype P2 and PBL2025, respectively.

PLoS one

Crenarchaeal Biofilm Formation under Extreme Conditions

Andrea Koerdt[1], Julia Gödeke[2], Jürgen Berger[3], Kai M. Thormann[2], Sonja-Verena Albers[1]*

1 Molecular Biology of Archaea, Max Planck Institute for Terrestrial Microbiology, Marburg, Germany, 2 Department of Ecophysiology, Max Planck Institute for Terrestrial Microbiology, Marburg, Germany, 3 Electron Microscopy, Max Planck Institute for Developmental Biology, Tübingen, Germany

Abstract

Background: Biofilm formation has been studied in much detail for a variety of bacterial species, as it plays a major role in the pathogenicity of bacteria. However, only limited information is available for the development of archaeal communities that are frequently found in many natural environments.

Methodology: We have analyzed biofilm formation in three closely related hyperthermophilic crenarchaeotes: *Sulfolobus acidocaldarius*, *S. solfataricus* and *S. tokodaii*. We established a microtitre plate assay adapted to high temperatures to determine how pH and temperature influence biofilm formation in these organisms. Biofilm analysis by confocal laser scanning microscopy demonstrated that the three strains form very different communities ranging from simple carpet-like structures in *S. solfataricus* to high density tower-like structures in *S. acidocaldarius* in static systems. Lectin staining indicated that all three strains produced extracellular polysaccharides containing glucose, galactose, mannose and N-acetylglucosamine once biofilm formation was initiated. While flagella mutants had no phenotype in two days old static biofilms of *S. solfataricus*, a UV-induced pili deletion mutant showed decreased attachment of cells.

Conclusion: The study gives first insights into formation and development of crenarchaeal biofilms in extreme environments.

Introduction

In nature, most microbes are assumed to exist predominantly in surface-associated communities, encased in a self-produced matrix, termed biofilms [1,2,3]. Thus, the formation of biofilms reflects the native growth conditions for most microbial species. Cells within biofilms differ substantially from their planktonic counterparts, particularly with regard to an increased resistance towards numerous environmental perturbations. Thus, the mechanism of biofilm formation and its importance for microbial survival in natural habitats has attracted increasing interest in recent years.

To date, studies on microbial biofilms have mainly been conducted on bacteria, in particular with regard to pathogenic species in which biofilms play an important role in disease development [4,5]. In sharp contrast, for the archaeal domain only very limited information is available on this topic. Archaea are frequently detected in biofilm communities from many different environments [6,7], but biofilm formation by archaea has only been sparsely studied. So far, all studies have dealt with the formation of biofilms by euryarchaeotes. The first archaeal biofilm was described for the hyperthermophilic *Thermococcus litoralis*. The *T. litoralis* biofilm developed in rich media on hydrophilic surfaces, such as polycarbonate filters, and was accompanied by

mannose-type extracellular polysaccharides production [8]. *Archaeoglobus fulgidus* biofilm formation, measured as attachment to the sides of cultivation vessels, was found to be increased in response to unfavorable environmental conditions, including high metal concentrations, pH and temperature changes [9]. Upon adhesion to (a)biotic surfaces, mediated by flagella or pili, *Pyrococcus furiosus* and *Methanobacter thermoautotrophicus* formed monospecies biofilms, respectively [10,11]. Development of *P. furiosus* and *Methanopyrus kandlerii* bi-species biofilms was shown to be established within less than 24 hours on biotic surfaces [12]. However, the formation of a layered biofilm was dependent on the initial colonization of the surface by *M. thermoautotrophicus* cells to which *P. furiosus* could adhere by using its flagella and establishing cell-to-cell contacts. Very recently, two distinct biofilm morphologies were described in the extremely acidophilic euryarchaeote *Ferroplasma acidarmanus* Fer1, a multilayered film forming on glass and pyrite surfaces and up to 5 mm-long filaments that were also found in natural environments [13]. Proteomic studies on these biofilms showed that 6 out of the 10 up-regulated proteins were involved in the adaptation to anaerobic growth indicating anaerobic zones in the multilayered *Ferroplasma* biofilms.

In this study, we use the crenarchaeal model organism *Sulfolobus spp.* to initiate comprehensive studies on archaeal biofilms. *Sulfolobus* species are hyperthermoacidophiles growing optimally

at 70–85°C and pH 2–3 that are found worldwide in geothermically active environments such as solfataric fields. They express a variety of surface structures including flagella and type IV-like pili [14,15,16] which have been shown to be involved in motility and UV light-induced cell aggregation [16,17]. A recent study indicated that flagella and pili are also essential for initial surface attachment [18]. The same study demonstrated that *Sulfolobus* can attach to a variety of surfaces including glass, mica, pyrite and gold coated carbon grids. An initiation of microcolony formation by the attached cells was observed, indicating that *Sulfolobus* may be able to develop into structured microbial communities reminiscent to that of many eubacteria.

To further assess the ability to form biofilms, *S. solfataricus*, an European isolate from Italy [19], *S. acidocaldarius*, originally isolated from Yellowstone National Park [20] and *S. tokodaii*, an isolate from Japan [21], were chosen for a comparative study. Using an adapted microtitre plate assay, the impact of multiple environmental conditions on biofilm formation by these three *Sulfolobus* species was tested. Confocal laser scanning microscopy (CLSM) was employed to study the formed microbial communities in detail. We demonstrate that all three *Sulfolobus* species develop into distinct three-dimensional communities. The adapted methods will enable further detailed studies on how archaeal biofilms are formed and how their structures develop.

Materials and Methods

Strains and growth conditions

Sulfolobus solfataricus P2 (DSM1617), *S. acidocaldarius* (DSM639), *S. tokodaii* (DSM16993), *S. solfataricus* PBL2025 [22], flagella deletion mutant $\Delta flaJ$ [16] and the ups pili deletion mutant $\Delta upsE$ [17] were grown in Brock medium at 76°C, pH adjusted to 3 using sulphuric acid, and supplemented with 0.1% w/v tryptone [20]. For biofilm formation, cultures were inoculated in standing Petri dishes and grown for 2–3 days at 76°C in a metal box which was supplemented with a small amount of water to minimize evaporation of the media. For these assays *Sulfolobus* strains were inoculated with specific starting OD_{600} of 0.03 for *S. solfataricus*, 0.01 for *S. acidocaldarius* and 0.06 for *S. tokodaii*.

Microtitre plate assay

The assay was performed in polystyrol 96-well tissue culture plates (flat bottom cell+, Sarstedt) to screen for the efficiency of biofilm formation under different environmental conditions. To avoid evaporation of the medium, the plates were covered with a gas-permeable sealing membrane (Breathe-Easy, Diversified Biotech, Boston, USA). After two days incubation the microtitre plate was cooled down to room temperature and the OD_{600} of cell cultures from each well was measured using a luminometer (InfiniteM200, TECAN, Switzerland) at a wavelength of 600 nm. 10 μl of a 0.5% solution of crystal violet (CV) was added and incubated at room temperature for 10 minutes. Subsequently, the liquid supernatant was removed from each well and the biofilm cells attached to the well were washed with water. 100% ethanol was added to release the crystal violet from the biofilm. The absorbance of crystal violet from each well was measured at a wavelength of 570 nm. The efficiency of biofilm formation was determined by the correlation between the growth of the cells ($OD_{600\,nm}$) and the absorbance of crystal violet ($OD_{570\,nm}$).

To determine how much biomass was present as biofilm, biofilms were grown and either resuspended by prolonged vortexing to obtain the $OD_{600\,nm}$, or stained with crystal violet to obtain the corresponding $OD_{570\,nm}$ values. This relation was used to calculate the percentage of cells within the biofilm related to the total amount of cells in biofilm and planktonic cells (see Fig. S2 and Table S1).

Confocal laser scanning microscopy (CLSM)

For CLSM images the cells were grown for three days in uncoated plastic dishes (μ-Dishes, 35 mm high; Ibidi, Martinsried). To prevent evaporation at the high incubation temperature, the lids of the dishes were closed. The medium was carefully exchanged every 24 hours to ensure aerobic growth conditions. Prior to confocal microscopy, the liquid supernatant of the biofilm, with the planktonic cells, was removed and 2 ml fresh medium was added. Images were recorded on an inverted TCS-SP5 confocal microscope (Leica, Bensheim, Germany).

DAPI (4′,6-diamidino-2-phenylindole), dissolved in water to 300 μg/ml, was used to visualize the cells of the biofilm. 6 μl of the DAPI stock solution was added to the biofilm and incubated at room temperature for at least 10 minutes. Images were taken at an excitation wavelength of 345 nm and an emission wavelength of 455 nm.

A 100 μM stock solution of 7-hydroxy-9H-1,3-dichloro-9,9-dimethylacridin-2-one (DDAO; Invitrogen, Karlsruhe, Germany), in demineralised water, was used at a final concentration of 4 μM. Incubation times varied between 20 and 300 minutes. DDAO has an excitation wavelength of 646 nm and an emission wavelength of 659 nm.

Fluorescently labelled lectins were employed to visualize the EPS (extracellular polymeric substances) of the biofilms. Before adding lectins to the biofilm, the growth medium was replaced with medium adjusted to pH 5 to ensure that binding of lectins was not inhibited by low pH. Fluorescein-conjugated concavalin A (ConA) (5 mg/ml; Invitrogen, Karlsruhe, Germany), which binds to α-mannopyranosyl and α-glucopyranosyl residues, was dissolved in 20 mM sodium bicarbonate (pH 8) to a final concentration of 10 μg/ml. Fluorescein-conjugated ConA has an excitation wavelength of 494 nm and an emission wavelength of 518 nm.

Alexa Fluor® 594-conjugated GS-II, specific for N-acetyl-D-glucosamine (lectin GS-II from *Griffonia simplicifolia*, 1 mg/ml; Invitrogen, Karlsruhe, Germany), and IB$_4$, specific for α-D-galactosyl residues (isolectin GS-IB4 from *Griffonia simplicifolia* 1 mg/ml; Invitrogen, Karlsruhe, Germany), were dissolved in 100 mM Tris-HCl pH 7.4 and 0.5 mM $CaCl_2$ to final concentrations of 8 μg/ml.

The Alexa Fluor-conjugated lectins, which have an excitation wavelength of 591 nm and an emission wavelength of 618 nm, were used in concert with ConA. The lectin-biofilm mixtures were incubated at room temperature for 20–30 minutes in the absence of light. After incubation, the biofilm was washed with Brock media (pH 5) to remove excess label and images were taken by CSLM. Image data obtained were processed by using the IMARIS software package (Bitplane AG, Zürich, Switzerland).

Scanning electron microscopy

S. acidocaldarius was grown as a standing culture under the described biofilm conditions in Petri dishes with 30 ml brock media adjusted with 0.1% trypton together with polylysin treated glass coverslips. The cells were fixed with 2.5% glutaraldehyde and incubated for 5 min at room temperature. The coverslips were carefully removed and stored at 4°C in 24 well plates with PBS-buffer with 2,5% glutaraldehyde.

The samples were then postfixed with 1% osmium tetroxide for 1 h on ice. After washing the cells were dehydrated in ethanol and critical-point-dried from CO_2. The samples were sputter-coated with 7 nm Au/Pd and examined at 20 kV accelerating voltage in an Hitachi S-800 field emission electron microscope.

Results

Adaptation of microtitre plate assay

To enable rapid quantification of surface-attached biomass, we adapted the commonly used microtitre plate assay based on crystal violet binding [23] for use at high temperatures. To prevent evaporation of the medium it was essential to cover the plates with gas permeable sealing membranes. For incubation at 76°C the plates were placed into a metal container to further prevent evaporation of the medium. The requirements for adherence to abiotic surfaces can vary greatly among microorganisms, therefore, different plates with hydrophilic and hydrophobic surfaces were tested. All three strains, *S. acidocaldarius*, *S. solfataricus* and *S. tokodaii*, attached preferentially to hydrophilic surfaces at the well's walls (data not shown). The conditions for biofilm formation were further optimized for each of the strains. The amount of biomass detected after two days was strongly dependent on the starting OD_{600} of the inoculum and differed for each strain (Fig. S1). Based on these results, for all subsequent experiments the starting OD for *S. acidocaldarius* was 0.01, for *S. solfataricus* was 0.03 and for *S. solfataricus* was 0.06. It was confirmed that the crystal violet values reflected the amount of biomass formed, as the obtained values correlated with the OD values measured from resuspended biofilm cells (data not shown). For the presentation of the microtitre plate assay results we show the correlation of the crystal violet release of the biofilm cells ($OD_{570\ nm}$) divided by the growth of the planktonic cells ($OD_{600\ nm}$) to emphasize the fraction of the cells which grow as biofilm under each condition in Fig. 1 and the absolute amount of surface-associated cells in Fig. S2.

Influence of pH, temperature, and iron concentration on *Sulfolobus* biofilm formation

Using the adapted microtitre plate assay the influence of a variety of conditions on the biofilm formation of the three *Sulfolobus* strains was tested. The pH values of a hot spring may be subject to change, for example by incoming rain or changes in the pH of fluid entering the hot spring. Therefore, the effect of pH values ranging from 2 to 7 on biofilm formation were evaluated. As expected, growth of all three strains was optimal around pH 3–4, but at pH 6 up to 80 and 70% of the total biomass of *S. acidocaldarius* and *S. tokodaii*, respectively, was present in biofilm (Fig. 1, second column and Fig. S2, C). Based on the correlation between OD values and the amount of surface-attached biomass, it was evident that in both species biofilm formation protects cells against alkaline pH, as the optimum pH for biofilm formation was much higher than the growth optimum.

As the temperature in a hot spring may also be subject to rapid changes, biofilm formation in the microtitre plates were tested at temperatures ranging from 60–85°C. In the range from 65 to 80°C *S. tokodaii* formed equal amounts of biofilm, with decreased levels only observed at 60 and 85°C, although at 60°C the amount of cells present in biofilms was the highest (50%)(Fig. 1, first column and Fig. S2,B). In contrast, *S. acidocaldarius* and *S. solfataricus* displayed increased biofilm formation at both extremes of the temperature gradient; at 60°C *S. acidocaldarius* and *S. solfataricus* showed a 5-fold and 4-fold increase biofilm formation, respectively, when compared with the optimal growth temperature of 75°C.

The natural habitats of *Sulfolobales* are acidic geothermal springs which are rich in As, S and Fe [24,25]. In these springs hydrous ferric oxide (HFO) microbial mats are found which contain a variety of members of the *Sulfolobales* indicating that these microorganisms might play a role in mediating the oxidation of iron in these environments [24]. Therefore, the influence of iron concentration on biofilm formation was tested.

Whereas the normal iron concentration in the medium of *Sulfolobales* is 0.02 g/L, we tested 0.015 g/L to 0.065 g/L. Biofilm formation by *S. acidocaldarius* and *S. tokodaii* was not significantly influenced by the different concentrations of iron, but *S. solfataricus* displayed an optimum curve with the highest biofilm formation at 0.045 g/L (Fig. 1, third column and Fig. S2, D). When different pH values and iron conditions were combined, it was interesting to see that *S. solfataricus* was unable to resist the higher pH in the presence of high iron concentrations and, subsequently, biofilm formation was abolished. In contrast *S. tokodaii* and *S. acidocaldarius* biofilm formation was additionally stimulated (Fig. 1, last column and Fig. S2, E). At pH 6 and 0.065 g/L iron, biofilm formation increased 4-fold for *S. tokodaii* and 10-fold for *S. acidocaldarius* which compared with normal levels reaching 63 and 83% of cells, respectively, in biofilm compared to the total cell mass (Table S1 and Fig. S2, E).

In general, the amount of formed biofilm in microtitre plates is much less for *S. solfataricus* than for the other two species, most probably due to the more anaerobic conditions as compared to the static biofilm assay in Petri dishes.

Structural determination of static biofilms of the three *Sulfolobus* strains by confocal laser scanning electron microscopy

All three *Sulfolobus* strains were inoculated in uncoated plastic μ-dishes and incubated without agitation at 76°C. Evaporation was prevented by placing the Petri dishes in a humidified metal box and the medium was carefully exchanged every 24 hrs with fresh, prewarmed medium to ensure nutrient and oxygen availability. After three days the formed biofilms were stained with DAPI, as described in the Materials and Methods section and analyzed by confocal laser scanning microscopy (CLSM). We employed DAPI staining to visualize cells as there is currently no fluorescent protein available that is stably expressed under the growth conditions of *Sulfolobus* spp.. *S. solfataricus* formed biofilms (20–30 μm thick) with a carpet like structure covering the whole surface of the Petri dish with a low density of cells (Fig. 2, middle column). The biofilm structure of *S. tokodaii* was 25–35 μm thick and also exhibited a carpet like structure but, in contrast to *S. solfataricus*, these had a high cell density and, occasionally, cell aggregates were visible (Fig. 3, overlay picture, last row). *S. acidocaldarius* readily formed biofilms (25–35 μm thick) which contained a high density of cells and large aggregates, forming towering structures above the surface of attached cells (Fig. 3, first row).

For bacteria it is well known that extracellular DNA can play an essential role in the formation and stabilization of the three-dimensional structure of biofilms [26]. To examine whether extracellular DNA was present in biofilms of the three *Sulfolobus* strains, three days old biofilms were stained concomitantly with DAPI and the membrane-impermeable DNA-binding dye DDAO. In all three strains the DDAO signal was only present at locations in the biofilm where aggregates were also visible (Fig. 2, middle panels C and D). The weak DDAO signal was further reduced following DNase treatment indicating that the extracellular DNA was removed, but had no effect on the structure of the biofilms. Therefore, at this stage of the biofilm maturation, extracellular DNA does not appear to play a structural role in biofilms of these three *Sulfolobus* strains.

To estimate the amount of living and dead cells three days old biofilms were stained with the LIVE/DEAD stain. In *S. solfataricus* and *S. tokodaii* it was evident that throughout the biofilm less then ~2% of the cells were dead whereas in *S. acidocaldarius* up to ~8% of cells were dead (data not shown).
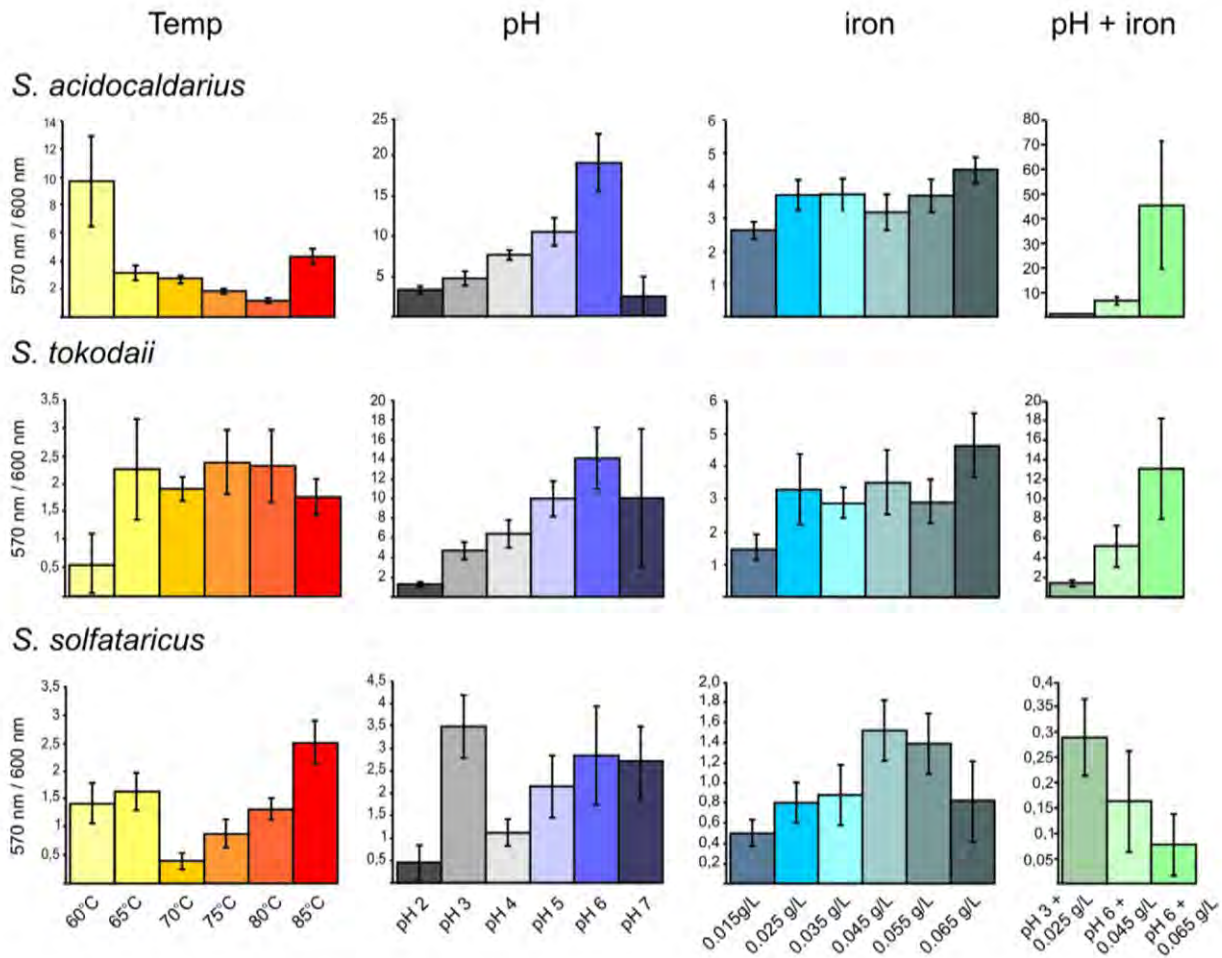
Figure 1. Effect of varying conditions on biofilm formation of the three *Sulfolobus* strains in microtitre plates. *S. acidocaldarius* (first row), *S. tokodaii* (second row) and *S. solfataricus* (third row) were incubated at different temperatures (first column), pH values (second column), iron concentrations (third column) and a combination of different iron concentrations and pH values (fourth column). The graphs show the correlation of the measured cristal violet absorbance of attached cells ($OD_{570\ nm}$) and the growth of the planktonic cells ($OD_{600\ nm}$) to emphasize the amount of cells in a sessile lifestyle at the tested condition. Each point and standard deviation is the mean of 8 samples per condition. Temp, temperature. doi:10.1371/journal.pone.0014104.g001

Analysis of *Sulfolobus* matrix components

The extracellular matrix that connects the cells and enables three-dimensional structuring of the communities is thought to be composed of (glyco)proteins, lipids, extrallular DNA (eDNA), and polymeric carbohydrates [27]. We therefore tested, whether eDNA, proteins, and polysaccharides play an important structural role in *Sulfolobus* biofilms. Experiments to inhibit biofilm formation by the addition of Proteinase K or DNase did not give conclusive results. Irrespective of the time at which DNase or Proteinase K was added, no effect on biofilm formation was observed although both enzymes showed enzyme activity under the conditions tested (data not shown).

Recently, it has been described that *S. solfataricus* cells, particularly when surface-attached, produce extracellular polymeric substances (EPS) containing glucose, mannose, galactose and N-acetyl-glucosamine [18,28]. To test whether cells also produce EPS during biofilm formation, three days maturated biofilms of all three *Sulfolobus* species were stained with DAPI, and two different fluorescently labeled lectins (Fig. 3). The lectins

selected were concanavalin A (ConA), specific for terminal glucose and mannose residues and either IB4 (specific for galactosyl residues) or GSII (specific for N-acetylglucosamine residues). In all three strains it was observed that the ConA signal (green signal) corresponded to the DAPI signal (blue signal, Fig. 3). *Sulfolobus* cells are covered by an S-layer and is has been described that the S-layer proteins are glycosylated and can be purified by ConA affinity chromatography [29,30,31]. Whereas in *S. solfataricus* the ConA-derived signal did, in fact, completely overlap with the DAPI signal, in *S. tokodaii* and *S. acidocaldarius* GSII and IB4 lectin (yellow channel) stained matter was observed on top of the cell layer and, as no DAPI signal was found in this accumulated material, we concluded that these two strains secrete EPS. In both strains, these clouds of EPS also reacted with the other two lectins indicating the presence of not only mannose and glucose, but also galactose and N-acetylglucosamine (Fig. S3). In *S. solfataricus*, only marginal GSII- and IB$_1$-mediated staining of cell attached sugar residues was observed, indicating a different glycosylation of extracellular proteins than in the other two strains.
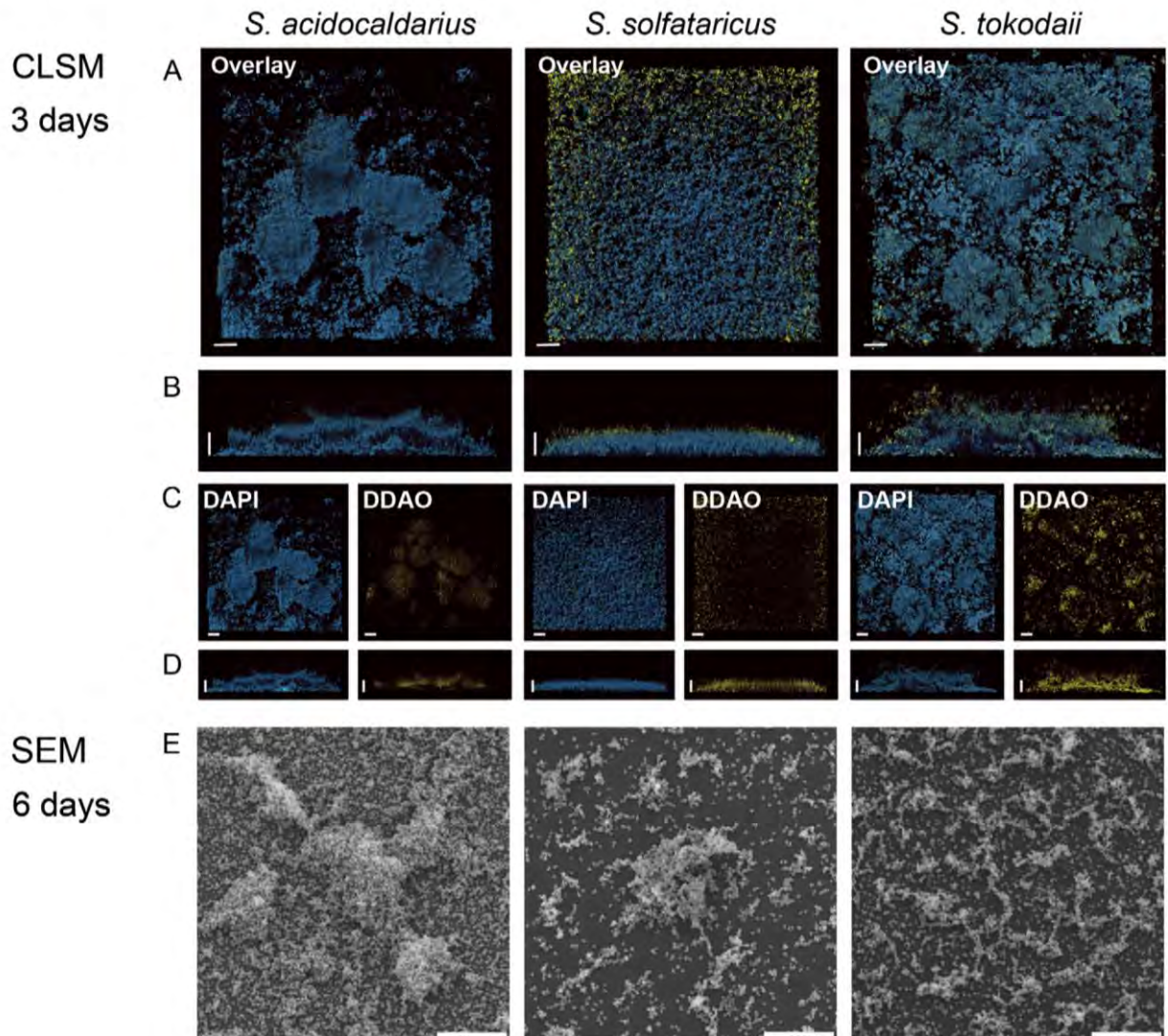
Figure 2. Different structures of static biofilms formed by three *Sulfolobus* strains *S. acidocaldarius*, *S. solfataricus* and *S. tokodaii* visualized by CLSM and SEM. A (top views) and B (side views) display the overlays of the images of three day old biofilms treated with DAPI and DDAO. The bar is 20 μm in length. C (top view) and D (side views) show the single channels of the overlays. DAPI signal: blue; DDAO signal: yellow. E, SEM images of biofilms of the three *Sulfolobus* strains incubated for 6 days. CLSM: confocal laser scanning microscopy; SEM: scanning electron microscopy.
doi:10.1371/journal.pone.0014104.g002

A detailed analysis of a biofilm formed by *S. tokodaii* and *S. acidocaldarius* showed extensive cell-cell connections. These connections became visible when the *S. tokodaii* sample was incubated with ConA and analysed by CLSM (Fig. 4). The connection might be a string of sugars or flagella/pili in which the subunits are glycosylated. In *S. acidocaldarius* and *S. solfataricus* biofilms the lectin GSII also stained thin connections between the cells (Fig. 4) which were clearly visible also in SEM pictures (Fig. 5D).

Maturation of *S. acidocaldarius* over a range of seven days

All experiments described so far were performed using 2–3 days old biofilms of *Sulfolobus* spp.. In order to monitor further community development under static conditions, biofilms of *S. acidocaldarius* were allowed to develop for seven days. Each day one

sample was treated with DAPI and analyzed by CLSM. The thickness of the biofilm increased from 30 μM in height on day three to 150 μM (including EPS structures) on day seven (Fig. 5AB). For a more detailed analysis of the maturation of biofilm formation by *S. acidocaldarius* the cells were inoculated in large Petri dishes in which polylysine covered glass slides had been placed. These slides were then analyzed by scanning electron microscopy (SEM). Only 15 minutes after the addition of the cell suspension a few cells attached to the surface, and some budding of vesicles was visible (Fig. S4A). After two hours there was not an apparent increase in the number of attached cells, but nearly all attached cells had formed filamentous structures adhering the cells to the surface or neighboring cells (Fig. S4B). After 36 hours, microcolonies started to form with only a few cells remaining on the rest of the surface whereas after 48 hours the surface of the
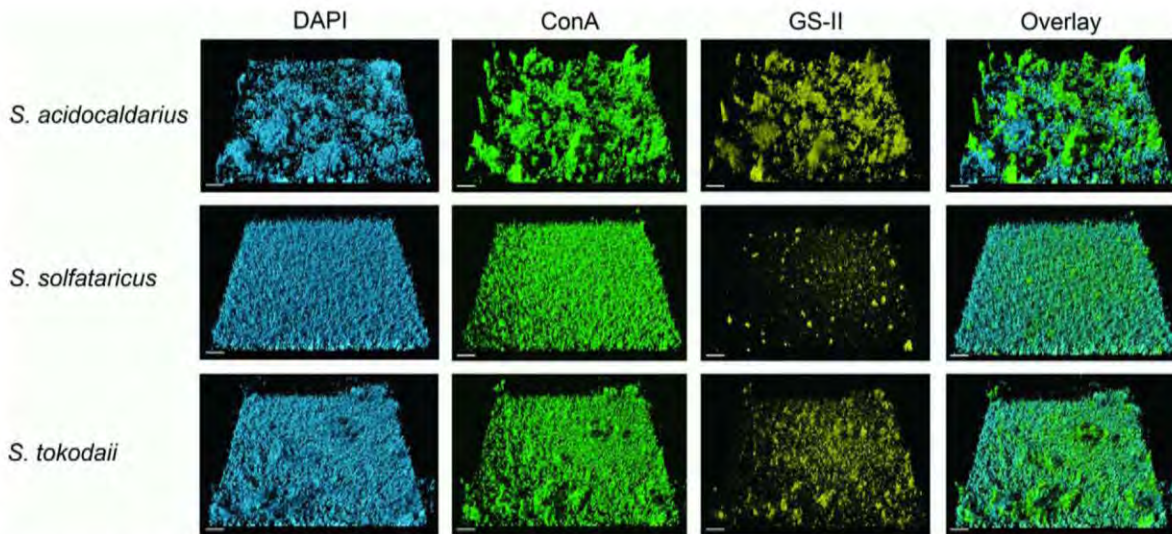
Figure 3. CSLM analysis of three day old static biofilms of *S. acidocaldarius*, *S. solfataricus* and *S. tokodaii* by lectin-staining. After three days the biofilms of *S. acidocaldarius* (first row), *S. solfataricus* (second row) and *S. tokodaii* (last row) were incubated with DAPI and different lectins and were analyzed by CSLM. The first column displays the DAPI signal (blue), the second column the ConA signal (green), the third column the GSII signal (yellow) and the last column the overlay of the other three channels. Bars are 20 μm in length.
doi:10.1371/journal.pone.0014104.g003

glass plates was completely covered with cells. In the microcolonies, cells appeared to be connected by a network of filamentous structures as was observed previously following lectin staining (Fig. 5D). These connections grew denser and also increasing extracellular material accumulated in the later stages of the biofilm formation (Fig. 5D). Interestingly, on the seventh day the layer of cells at the surface of the glass slide apparently disappeared and the density of cells in the detailed view was reduced compared with the sixth day (Fig. 5C/D). To test whether the extracellular material visible in the closer SEM view of the towering structures did indeed consist of EPS, *S. acidocaldarius* biofilms were incubated for seven days, stained with lectins, as described above, and analyzed by CLSM (Fig. 6). Towering structures were formed which were initiated by the secretion of EPS and then colonized by cells.

The secretion of certain sugars apparently progressed in a sequential manner: initially the ConA (glucose and mannose) derived signal was much stronger, but in later stages both the GSII (galactose) and the IB4 (N-acetylgucosamine) signal increased (Fig. 6 and Fig. S5), after which the secretion of mannose-rich sugars increases again as detected by ConA. This indicates that these sugars play an important role in biofilm maturation.

Role of surface appendages on static biofilm formation in *S. solfataricus*

Attachment of *S. solfataricus* cells from shaking cultures to different surfaces is mediated by flagella and UV induced pili. Deletion mutants in which either the *flaJ* gene, encoding the integral membrane protein of the flagella operon, or the *uspE*
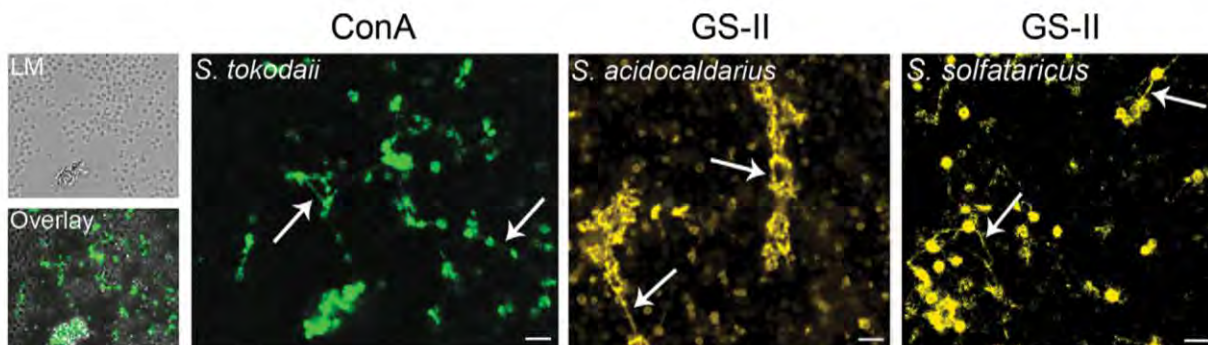
Figure 4. Connections between cells in three days matured static biofilms of *S. acidocaldarius*, *S. tokodaii* and *S. solfataricus*. The left three pictures show the CLSM analysis of a ConA treated *S. tokodaii* biofilm (LM: light microscopy picture, ConA: green channel, Overlay: overlay of the ConA signal and the LM picture). Middel panel: CLSM analysis of GS-II (yellow) treated *S. acidocaldarius* biofilm. Right panel: CLSM analysis of GS-II (yellow) treated *S. solfataricus* biofilm. Arrows indicate the connections. Bars are 4,5 μm in length. CLSM: confocal laser scanning microscopy; LC: light microscopy.
doi:10.1371/journal.pone.0014104.g004
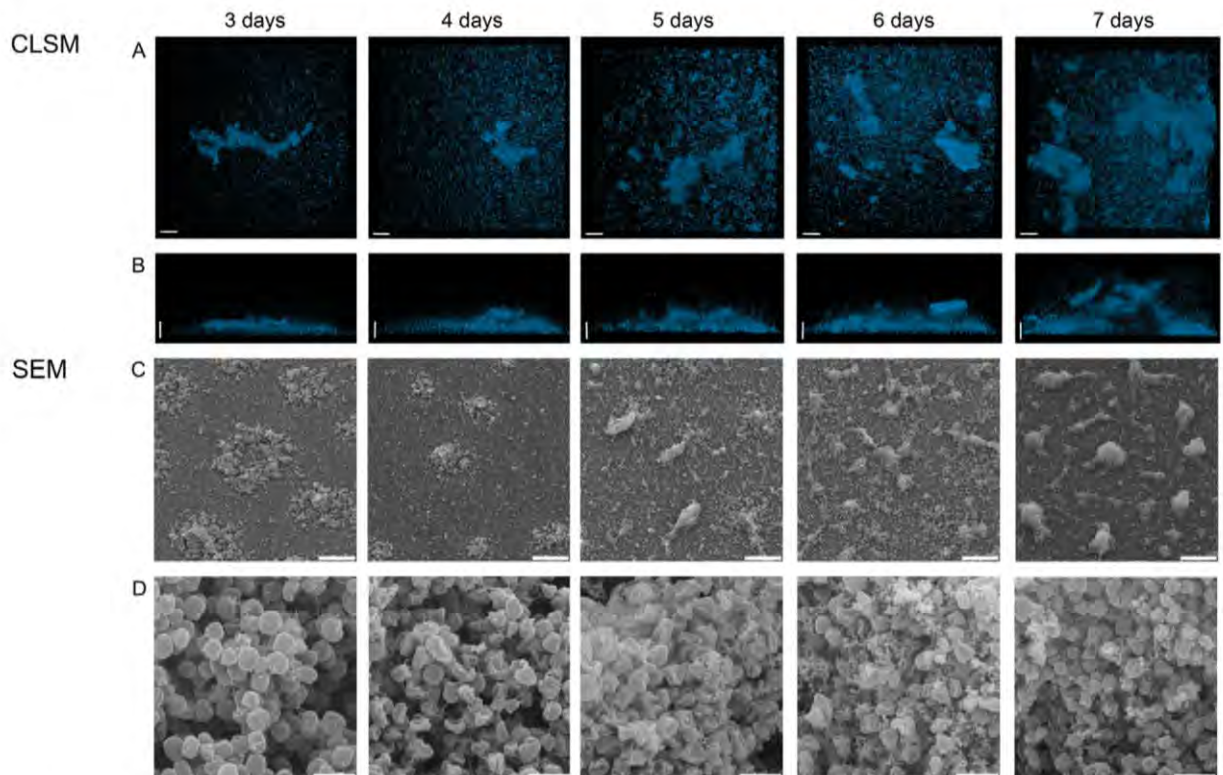
Figure 5. CLSM and SEM analysis of the development of a static biofilm of *S. acidocaldarius* during a time course of seven days. DAPI signal (blue) in the top view (A) and the side view (B). SEM analysis showing an overview (C) and enlarged view (D) of the developing biofilm. Size standards are 20 µM in length for A and B, 40 µM in C and 2 µM in D. CLSM: confocal laser scanning microscopy; SEM: scanning electron microscopy.
doi:10.1371/journal.pone.0014104.g005

gene, encoding the ATPase of the UV-induced pili operon were incapable of attachment to glass surfaces, gold-coated carbon grids or mica [18]. In bacterial biofilm development, filaments such as type IV pili and flagella have a strong effect on the dynamics of biofilm formation. Therefore, we tested the Δ*flaJ* and Δ*upsE* mutants and the wild type *S. solfataricus* PBL2025 strain for their ability to form static biofilms in three days. PBL2025 is a *S. solfataricus* strain which lacks 50 genes predicted to be involved in sugar metabolism and uptake and is the only currently available *S. solfataricus* strain which can be genetically manipulated [22].

The PBL2025, Δ*flaJ* and Δ*upsE* strains were grown in petri dishes and tested in the microtitre plate assay. After three days the matured biofilms in the petri dishes were stained with DAPI and analyzed by CLSM. The biofilms of PBL2025 and the Δ*flaJ* strain were comparable to three day old biofilms of *S. solfataricus* in height, density and structure, and showed mainly a carpet like appearance (Fig. 7A and B). However, in biofilms from the Δ*upsE* strain, the surface of the petri dish was not as completely covered with cells and the biofilm was less dense as compared to PBL2025 and the Δ*flaJ* mutant strain. Furthermore, slightly more aggregates were visible in the biofilms of the Δ*upsE* strain. These observations were supported by the results of the microtitre plate assay showing that only the Δ*upsE* strain produced significantly less biofilm than *S. solfataricus*, PBL2025 and Δ*flaJ*. We therefore concluded that cell appendages do not to play an important role in the early development of static biofilm formation in *S. solfataricus* strains.

Discussion

It is well known that archaea and bacteria coexist in natural biofilms, playing essential roles in the Earth's biogeochemical cycles as well as in human disease [2]. The formation of bacterial biofilms has been very well documented. Studies have been carried out on euryarchaeal biofilm formation whereas we presented here the first detailed insights into crenarchaeal biofilm formation.

We chose the thermoacidophilic crenarchaeotes *Sulfolobus* spp as a model to establish methods for the analysis of hyperthermophilic archaeal biofilm formation. *Sulfolobus* spp. exist in acidic, mostly muddy, hot springs all over the world in which the hydrological dynamics result in rapid variations in temperature, pH and geochemical conditions. Therefore, these organisms must quickly adapt to these changing conditions or exist in a state that enables them remain undisturbed by such changes. As fully maturated biofilms protect their inhabitants from environmental disturbances, this form might be a way for *Sulfolobus* spp to survive in their habitats. The three selected strains were originally isolated from well separated geographical locations and each of the strains did, in fact, behave differently following the initiation of biofilm formation. Of the three strains, *S. acidocaldarius* most readily engaged in community formation either in microtitre plate assays or in static biofilm conditions when compared with the other *Sulfolobus* strains. In particular, when challenged with low temperature (60°C) or the combination of near neutral pH and low iron concentrations, *S. acidocaldarius* responded with highly
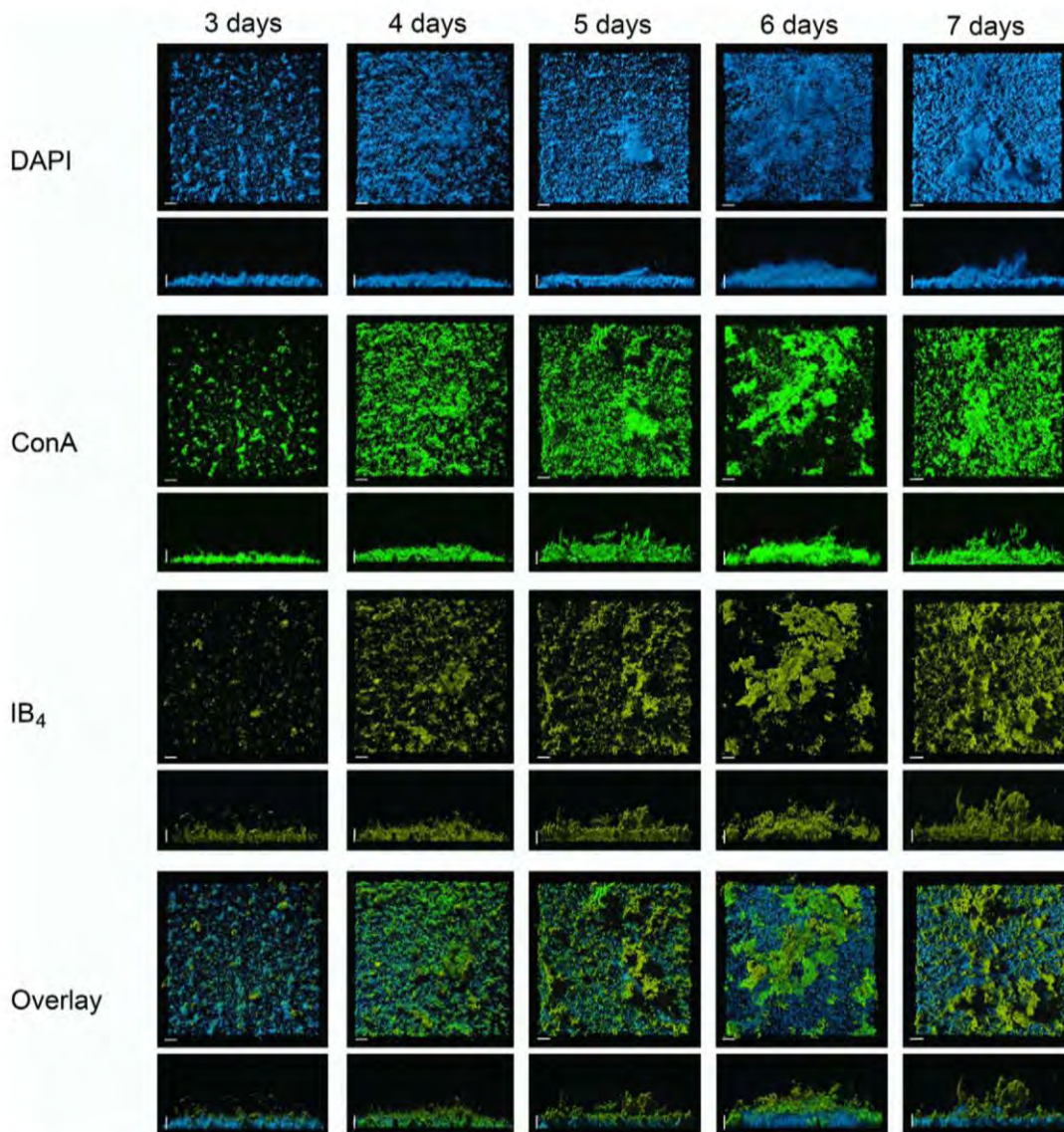
Figure 6. Lectin-based analysis of developing static biofilm of *S. acidocaldarius* during a time course of seven days. Samples were treated with DAPI (blue channel), Con A (green channel) and IB$_4$ (yellow channel) and analyzed by CSLM. For each channel the top view and the side view is presented. An overlay shows all three channels. Bars are 20 μm in length. CLSM: confocal laser scanning microscopy.
doi:10.1371/journal.pone.0014104.g006

increased biofilm formation demonstrating the ability of this strain to adapt to rapid changes in temperature and pH.

The maturation of bacterial biofilms proceeds via defined steps including initial attachment and further development into microcolonies secreting extrapolymeric substances [32]. During maturation multilayered biofilm structures are shaped and kept together by the secretion of EPS, extracellular DNA, and proteins [27,33]. Cells can be released from matured biofilms at any time point to proceed with a planktonic life style. Very recently, we have shown that *S. solfataricus* displays flagella and pili-dependent attachment to abiotic surfaces [18]. After two days of attachment to a glass slide in a shaking culture the cells started to produce EPS which contained glucose, mannose, galactose and

N-acetylglucosamine demonstrating the first phase of biofilm formation. Similar to bacterial biofilm formation, it is evident that after initial attachment *Sulfolobus* cells start to form microcolonies that are surrounded by an extracellular matrix, containing EPS and, most probably, proteins. The function of EPS formation in these *Sulfolobus* strains may serve a variety of purposes. A natural deletion mutant of *S. solfataricus* which lacks 50 genes overproduced EPS when attached to a glass slide [18]. The deleted region contains genes mainly involved in sugar degradation and transport and these were shown to be upregulated in attached *S. solfataricus* cells, implying that they play an important role in the modulation of the EPS. One might speculate that the EPS is used as a carbohydrate reservoir which might also be the case when the
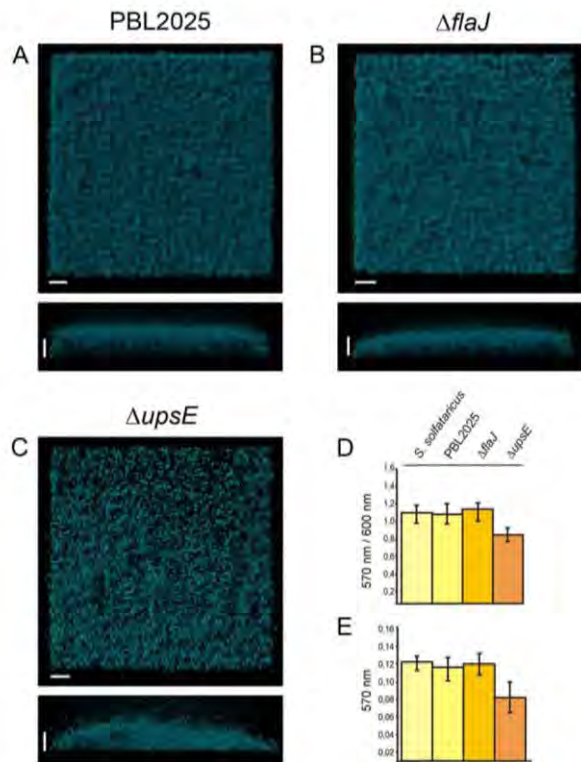
Figure 7. Three day matured static biofilms of S. solfataricus PBL2025, ΔflaJ and ΔupsE. Biofilms of PBL2025, ΔflaJ and ΔupsE were stained with DAPI and analyzed by CLSM (A–C, respectively). Complementary, a microtitre plate assay was performed for 72 hrs with all three strains and biofilm formation is presented in D as the correlation of the crystal violet absorbance (OD$_{570 nm}$) divided by the optical density of the planktonic cells (OD$_{600 nm}$) and in E the crystal violet absorbance (OD$_{570 nm}$) is indicated. Bars are 20 μm in lengt. doi:10.1371/journal.pone.0014104.g007

cells are engaged in biofilm formation. When the *S. acidocaldarius* biofilm was incubated for seven days it was evident that the different sugars were produced in a consecutive manner implying that they may serve different purposes. Moreover, a layer of EPS was produced which enabled the formation of three-dimensional tower-like structures, especially in *S. acidocaldarius*. It appeared that after seven days the *S. acidocaldarius* biofilms detached by releasing attached cells to the planktonic phase.

In bacteria, cell appendages such as type IV pili and flagella are very well known for their influence and importance in the dynamics and development of static and hydrodynamically grown biofilms [34]. Like in *Vibrio cholerae* and *Shewanella oneidensis* MR-1, the *S. solfataricus* pili mutant ΔupsE exhibited decreased biofilm formation in the microtitre plate assay [35,36]. Also more dense aggregates were observed as in *Pseudomonas aeruginoasa* and *S. oneidensis* MR-1 type IV pili mutants [36,37]. However, the flagella mutant showed no obvious differences in static biofilm formation to the wild type, As the *S. solfataricus* flagella and pili mutant could not attach to several different surfaces in shaking culture [18], it will be interesting for future studies whether flagella and pili have a greater impact on biofilm formation in flow chamber systems.

Taken together, we demonstrated that *Sulfolobus* species can engage in biofilm formation and developed methods to study

these in more detail. Of the three strains, *S. acidocaldarius* formed the largest amounts of biomass and was able to evade unfavorable conditions most successfully by choosing this life style. Interestingly, these data support the observation that *S. acidocaldarius* is mainly sampled from the crusts surrounding acidic hot springs and mud holes (Karl-Otto Stetter, personal communication) whereas *S. solfataricus* and *S. tokodaii* are primarily isolated from the midst of these types of hot springs, where the hot fluids are bubbling up to the surface [38] (Christa Schleper, personal communication).

In the future, it will be interesting to study how *Sulfolobus* strains behave in mixed biofilms and even in communities including other inhabitants of these acidic hot springs.

Supporting Information

Table S1
Found at: doi:10.1371/journal.pone.0014104.s001 (0.12 MB DOC)

Figure S1 Optimization of inoculation conditions for biofilm formation of S. acidocaldarius, S. solfataricus and S. tokodaii. The strains were inoculated with different OD 600 and incubated in a microtitre plate for three days. The correlation of the measured crystal violet absorbance of the formed biofilm and the OD600 values of the planktonic cells is presented. Each bar represents the mean of 8 different samples.
Found at: doi:10.1371/journal.pone.0014104.s002 (0.23 MB TIF)

Figure S2 Data shown in Figure 1 presented as calculated percentage of cells within the biofilm related to the total amount of cells in biofilm and planktonic cells. (A) Biofilms were grown and either resuspended by prolonged vortexing to obtain the OD600nm, or stained with crystal violet to obtain the OD570nm values. This relation was used to calculate the percentage of cells within the biofilm related to the total amount of cells in biofilm and planktonic cells for (B) different temperatures, (C), different pH values, (D) different iron concentrations, and (E) a combination of different iron concentrations and pH values (D). S. acidocaldarius (blue), S. tokodaii (green) and S. solfataricus (red) are indicated by different colors.
Found at: doi:10.1371/journal.pone.0014104.s003 (0.49 MB TIF)

Figure S3 CSLM analysis of three day old static biofilms of S. acidocaldarius, S. solfataricus and S. tokodaii by lectins. After three days the biofilms of S. acidocaldarius (first row), S. solfataricus (second row) and S. tokodaii (last row) were incubated with DAPI and different lectins and were analyzed by CSLM. The first column shows the DAPI signal (blue), the second column the Con A signal (green), the third column the IB4 signal (yellow) and the last column the overlay of the other three channels. Bars are 20 μm in length. CLSM: confocal laser scanning microscopy.
Found at: doi:10.1371/journal.pone.0014104.s004 (5.80 MB TIF)

Figure S4 SEM pictures from early stages of S. acidocaldarius biofilm formation from 15 minutes to 48 hours after incubation. (A) shows the overviews and (B) and (C) more detailed views of the respective picture in A in the same column of the developing biofilms. The length of the bars is indicated in the images. SEM: scanning electron microscopy.
Found at: doi:10.1371/journal.pone.0014104.s005 (7.76 MB TIF)

**Figure S5** Lectin based analysis of developing static biofilm of S. acidocaldarius. Samples were treated with DAPI (blue channel), Con A (green channel) and GSII (yellow channel) and analyzed by CSLM. For each channel the top view and the side view is

presented. Overlay shows all three channels again including top- and side views. Bars are 20 μm in length.
Found at: doi:10.1371/journal.pone.0014104.s006 (9.90 MB TIF)

References

1. Costerton JW, Lewandowski Z, Caldwell DE, Korber DR, Lappin-Scott HM (1995) Microbial biofilms. Annu Rev Microbiol 49: 711–745.
2. Hall-Stoodley L, Costerton JW, Stoodley P (2004) Bacterial biofilms: from the natural environment to infectious diseases. Nat Rev Microbiol 2: 95–108.
3. Moons P, Michiels CW, Aertsen A (2009) Bacterial interactions in biofilms. Crit Rev Microbiol 35: 157–168.
4. Hall-Stoodley L, Stoodley P (2005) Biofilm formation and dispersal and the transmission of human pathogens. Trends Microbiol 13: 7–10.
5. Parsek MR, Singh PK (2003) Bacterial biofilms: an emerging link to disease pathogenesis. Annu Rev of Microbiol 57: 677–701.
6. Kruger M, Blumenberg M, Kasten S, Wieland A, Kanel L, et al. (2008) A novel, multi-layered methanotrophic microbial mat system growing on the sediment of the Black Sea. Environ Microbiol 10: 1934–1947.
7. Zhang CL, Ye Q, Huang Z, Li W, Chen J, et al. (2008) Global occurrence of archaeal amoA genes in terrestrial hot springs. Appl Environ Microbiol 74: 6417–6426.
8. Rinker KD, Kelly RM (1996) Growth physiology of the hyperthermophilic archaeon Thermococcus litoralis: Development of a sulfur-free defined medium, characterization of an exopolysaccharide, and evidence of biofilm formation. Appl Environ Microbiol 62: 4478–4485.
9. Lapaglia C, Hartzell PL (1997) Stress-induced production of biofilm in the hyperthermophile Archaeoglobus fulgidus. Appl Environ Microbiol 63: 3158–3163.
10. Näther DJ, Rachel R, Wanner G, Wirth R (2006) Flagella of Pyrococcus furiosus: multifunctional organelles, made for swimming, adhesion to various surfaces, and cell-cell contacts. J Bacteriol 188: 6915–6923.
11. Thoma C, Frank M, Rachel R, Schmid S, Nather D, et al. (2008) The Mth60 fimbriae of Methanothermobacter thermoautotrophicus are functional adhesins. Environ Microbiol 10: 2785–2795.
12. Schopf S, Wanner G, Rachel R, Wirth R (2008) An archaeal bi-species biofilm formed by Pyrococcus furiosus and Methanopyrus kandleri. Arch Microbiol 190: 371–377.
13. Baker-Austin C, Potrykus J, Wexler M, Bond PL, Dopson M (2010) Biofilm development in the extremely acidophilic archaeon 'Ferroplasma acidarmanus' Fer1. Extremophiles.
14. Albers SV, Pohlschroder M (2009) Diversity of archaeal type IV pilin-like structures. Extremophiles 13: 403–410.
15. Fröls S, Ajon M, Wagner M, Teichmann D, Zolghadr B, et al. (2008) UV-inducible cellular aggregation of the hyperthermophilic archaeon Sulfolobus solfataricus is mediated by pili formation. Mol Microbiol 70: 938–952.
16. Szabo Z, Sani M, Groeneveld M, Zolghadr B, Schelert J, et al. (2007) Flagellar motility and structure in the hyperthermoacidophilic archaeon Sulfolobus solfataricus. J Bacteriol 189: 4305–4309.
17. Fröls S, Ajon M, Wagner M, Teichmann D, Zolghadr B, et al. (2008) UV-inducible cellular aggregation of the hyperthermophilic archaeon Sulfolobus solfataricus is mediated by pili formation. Mol Microbiol 70: 938–952.
18. Zolghadr B, Klingl A, Koerdt A, Driessen AJM, Rachel R, et al. (2010) Appendage-mediated surface adherence of Sulfolobus solfataricus. J Bacteriol 192: 104–110.
19. Zillig W, Stetter KO, Wunderl S, Schulz W, Priess H, et al. (1980) The Sulfolobus – " Caldariella " Group: Taxonomy on the basis of the structure of DNA-dependent RNA polymerases. Arch Microbiol. pp 259–269.

Author Contributions

Conceived and designed the experiments: AK SVA. Performed the experiments: AK JG JB. Analyzed the data: SVA. Contributed reagents/materials/analysis tools: JG. Wrote the paper: KMT SVA.

20. Brock TD, Brock KM, Belly RT, Weiss RL (1972) Sulfolobus: a new genus of sulfur-oxidizing bacteria living at low pH and high temperature. Arch Microbiol 84: 54–68.
21. Suzuki T, Iwasaki T, Uzawa T, Hara K, Nemoto N, et al. (2002) Sulfolobus tokodaii sp. nov. (f. Sulfolobus sp. strain 7), a new member of the genus Sulfolobus isolated from Beppu Hot Springs, Japan. Extremophiles 6: 39–44.
22. Schelert J, Dixit V, Hoang V, Simbahan J, Drozda M, et al. (2004) Occurrence and characterization of mercury resistance in the hyperthermophilic archaeon Sulfolobus solfataricus by use of gene disruption. J Bacteriol 186: 427–437.
23. O'Toole GA, Kolter R (1998) Initiation of biofilm formation in Pseudomonas fluorescens WCS365 proceeds via multiple, convergent signalling pathways: a genetic analysis. Mol Microbiol 28: 449–461.
24. Macur RE, Langner HW, Kocar BD, Inskeep WP (2004) Linking geochemical processes with microbial community analysis: successional dynamics in an arsenic-rich, acid-sulfate-chloride geothermal spring. Geobiology 2: 163–177.
25. Inskeep WP, Macur RE, Harrison G, Bostick BC, Fendorf S (2004) Biomineralization of As(V)-hydrous ferric oxyhydroxide in microbial mats of an acid-sulfate-chloride geothermal spring, Yellowstone National Park. Geochim Cosmochim Acta 68: 3141–3155.
26. Allesen-Holm M, Barken KB, Yang L, Klausen M, Webb JS, et al. (2006) A characterization of DNA release in Pseudomonas aeruginosa cultures and biofilms. Mol Microbiol 59: 1114–1128.
27. Flemming HC, Neu TR, Wozniak DJ (2007) The EPS matrix: the "house of biofilm cells". J Bacteriol 189: 7945–7947.
28. Nicolaus B, Manca MC, Romano I, Lama L (2003) Production of an exopolysaccharide from two thermophilic archaea belonging to the genus Sulfolobus. FEMS Microbiol Lett 109: 203–206.
29. Grogan DW (1996) Isolation and fractionation of cell envelope from the extreme thermo-acidophile Sulfolobus acidocaldarius. J Microbiol Meth 26: 35–43.
30. Veith A, Klingl A, Zolghadr B, Lauber K, Mentele R, et al. (2009) Acidianus, Sulfolobus and Metallosphaera surface layers: structure, composition and gene expression. Mol Microbiol 73: 58–72.
31. Ellen AF, Albers SV, Huibers W, Pitcher A, Hobel CF, et al. (2009) Proteomic analysis of secreted membrane vesicles of archaeal Sulfolobus species reveals the presence of endosome sorting complex components. Extremophiles 13: 67–79.
32. Sauer K, Camper AK, Ehrlich GD, Costerton JW, Davies DG (2002) Pseudomonas aeruginosa displays multiple phenotypes during development as a biofilm. J Bacteriol 184: 1140–1154.
33. Sutherland IW (2001) The biofilm matrix—an immobilized but dynamic microbial environment. Trends Microbiol 9: 222–227.
34. Karatan E, Watnick P (2009) Signals, regulatory networks, and materials that build and break bacterial biofilms. Microbiol Mol Biol Rev 73: 310–347.
35. Watnick PI, Kolter R (1999) Steps in the development of a Vibrio cholerae El Tor biofilm. Mol Microbiol 34: 586–595.
36. Thormann KM, Saville RM, Shukla S, Pelletier DA, Spormann AM (2004) Initial phases of biofilm formation in Shewanella oneidensis MR-1. J Bacteriol 186: 8096–8104.
37. Chiang P, Burrows LL (2003) Biofilm formation by hyperpiliated mutants of Pseudomonas aeruginosa. J Bacteriol 185: 2374–2378.
38. Zillig W, Kletzin A, Schleper C, Holz I, Janekovic D, et al. (1994) Screening for Sulfolobales, their plasmids and their viruses in Icelandic solfataras. Syst Appl Microbiol 16: 609–628.

3.2.1 Supplementary material

Table and figure legends: see main manuscript

Table S1: Calculation of OD_{600} values from OD_{570} values from two days old biofilms

Condition		$^{P}OD_{600}$ planktonic cell	crystal violet absorbance [570 nm]	$^{B}OD_{600}$ biofilm cells [y=5.99x]	Total biomass $[^{B}OD_{600}+^{P}OD_{600}]$	Cells in biofilm [%]
Temperature [°C]						
S. acidocaldarius	60	0.004	0.039	0.007	0.011	61.9
	65	0.049	0.154	0.026	0.075	34.4
	70	0.077	0.207	0.035	0.112	31.0
	75	0.11	0.204	0.034	0.144	23.6
	80	0.12	0.138	0.023	0.143	16.1
	85	0.05	0.209	0.035	0.085	41.1
S.solfataricus	60	0.012	0.018	0.003	0.015	20.0
	65	0.035	0.058	0.010	0.045	21.7
	70	0.064	0.025	0.004	0.068	6.1
	75	0.066	0.058	0.010	0.076	12.8
	80	0.062	0.081	0.014	0.076	17.9
	85	0.071	0.177	0.030	0.101	29.4
S.tokodaii	60	0.01	0.055	0.009	0.019	47.9
	65	0.03	0.067	0.011	0.041	27.2
	70	0.054	0.103	0.017	0.071	24.2
	75	0.06	0.141	0.024	0.084	28.2
	80	0.061	0.139	0.023	0.084	27.6
	85	0.096	0.167	0.028	0.124	22.5
pH						
S. acidocaldarius	2	0.051	0.172	0.029	0.080	36.0
	3	0.048	0.232	0.039	0.087	44.7
	4	0.032	0.251	0.042	0.074	56.7
	5	0.013	0.136	0.023	0.036	63.6
	6	0.006	0.121	0.020	0.026	77.1
	7	0.006	0.012	0.002	0.008	25.0
S.solfataricus	2	0.042	0.019	0.003	0.045	7.0
	3	0.041	0.137	0.023	0.064	35.8
	4	0.045	0.049	0.008	0.053	15.4
	5	0.038	0.077	0.013	0.051	25.3
	6	0.035	0.097	0.016	0.051	31.6
	7	0.019	0.051	0.009	0.028	30.9
S.tokodaii	2	0.059	0.079	0.013	0.072	18.3
	3	0.049	0.231	0.039	0.088	44.0
	4	0.036	0.225	0.038	0.074	51.1
	5	0.021	0.21	0.035	0.056	62.5
	6	0.012	0.167	0.028	0.040	69.9
	7	0.004	0.026	0.004	0.008	52.0
Iron [g/L]						
S. acidocaldarius	0.015	0.103	0.3	0.050	0.153	32.7
	0.025	0.076	0.281	0.047	0.123	38.2
	0.035	0.078	0.286	0.048	0.126	38.0
	0.045	0.093	0.292	0.049	0.142	34.4
	0.055	0.085	0.311	0.052	0.137	37.9
	0.065	0.07	0.313	0.052	0.122	42.7
S.solfataricus	0.015	0.06	0.03	0.005	0.065	7.7
	0.025	0.045	0.036	0.006	0.051	11.8
	0.035	0.043	0.035	0.006	0.049	12.0
	0.045	0.042	0.077	0.013	0.055	23.4
	0.055	0.037	0.051	0.009	0.046	18.7
	0.065	0.035	0.027	0.005	0.040	11.4
S.tokodaii	0.015	0.068	0.096	0.016	0.084	19.1
	0.025	0.037	0.094	0.016	0.053	29.8
	0.035	0.044	0.122	0.020	0.064	31.6
	0.045	0.036	0.12	0.020	0.056	35.8
	0.055	0.05	0.147	0.025	0.075	32.9
	0.065	0.034	0.156	0.026	0.060	43.4
pH/Iron [g/L]						
S. acidocaldarius	3/0.02	0.148	0.165	0.028	0.176	15.7
	6/0.045	0.051	0.329	0.055	0.106	51.9
	6/0.065	0.006	0.188	0.031	0.037	84.0
S.solfataricus	3/0.02	0.108	0.032	0.005	0.113	4.7
	6/0.045	0.051	0.008	0.001	0.052	2.6
	6/0.065	0.024	0.002	0.000	0.024	1.4
S.tokodaii	3/0.02	0.089	0.122	0.020	0.109	18.6
	6/0.045	0.029	0.125	0.021	0.050	41.8
	6/0.065	0.007	0.071	0.012	0.019	62.9
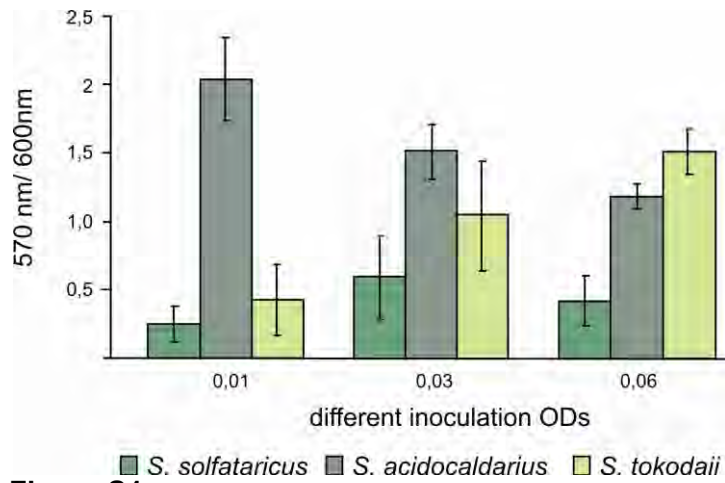
Figure S1
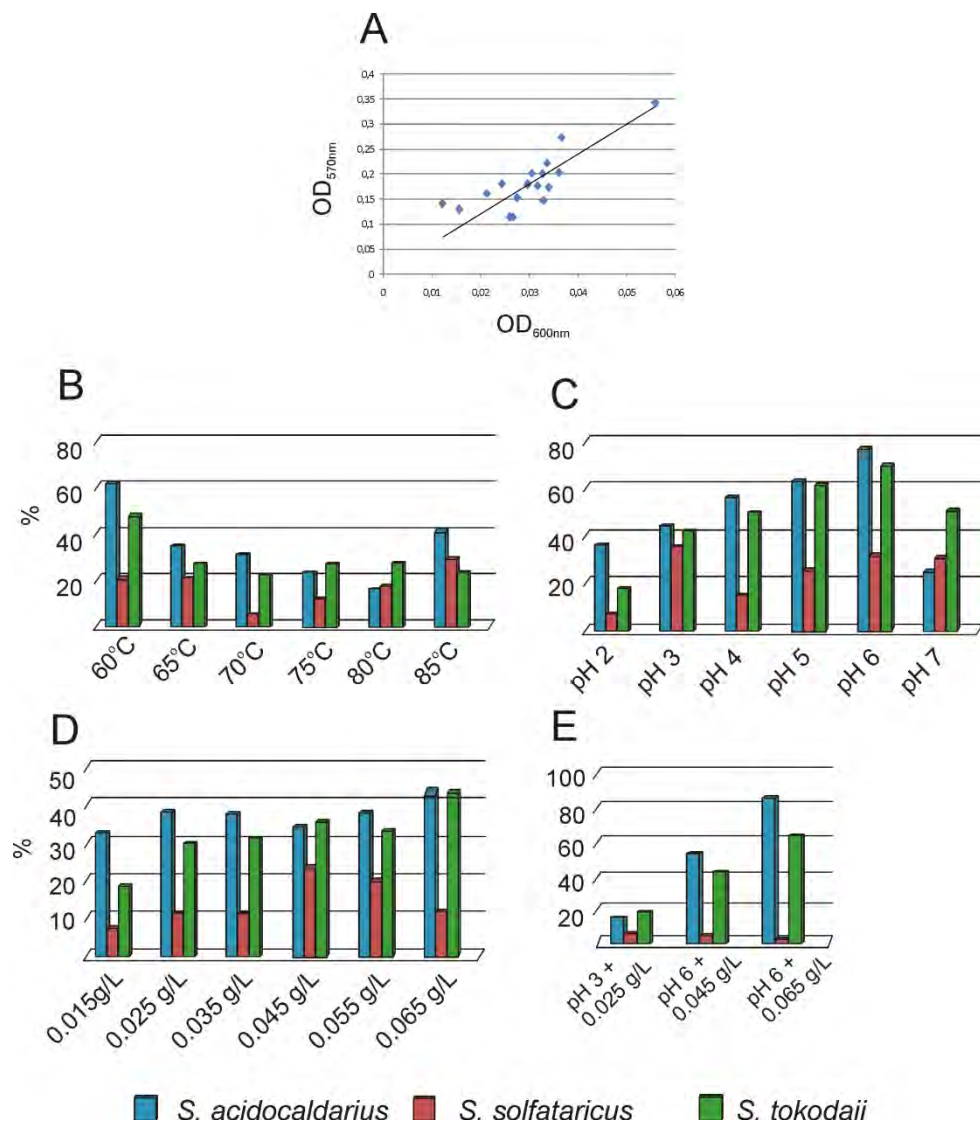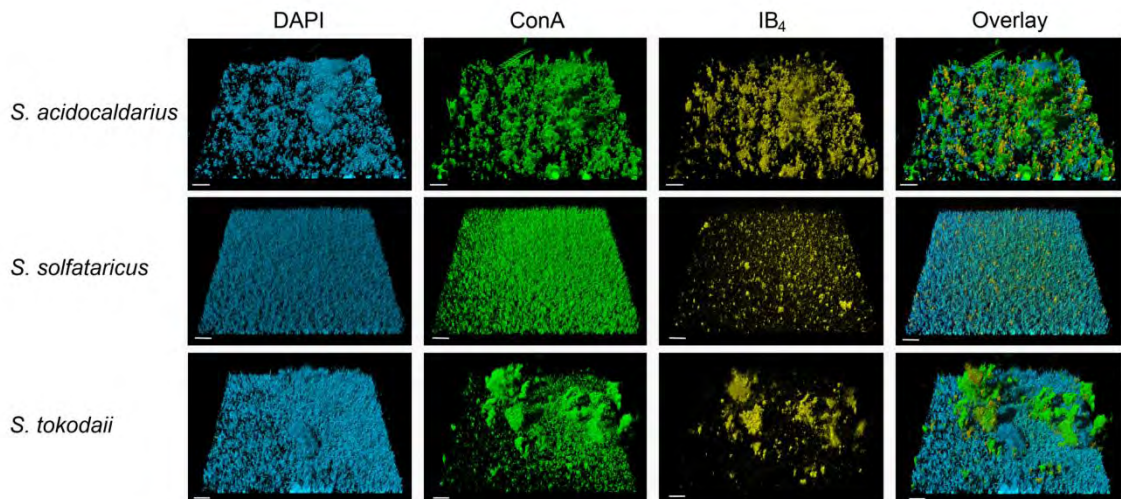

Figure S2

Figure S3

Figure S4

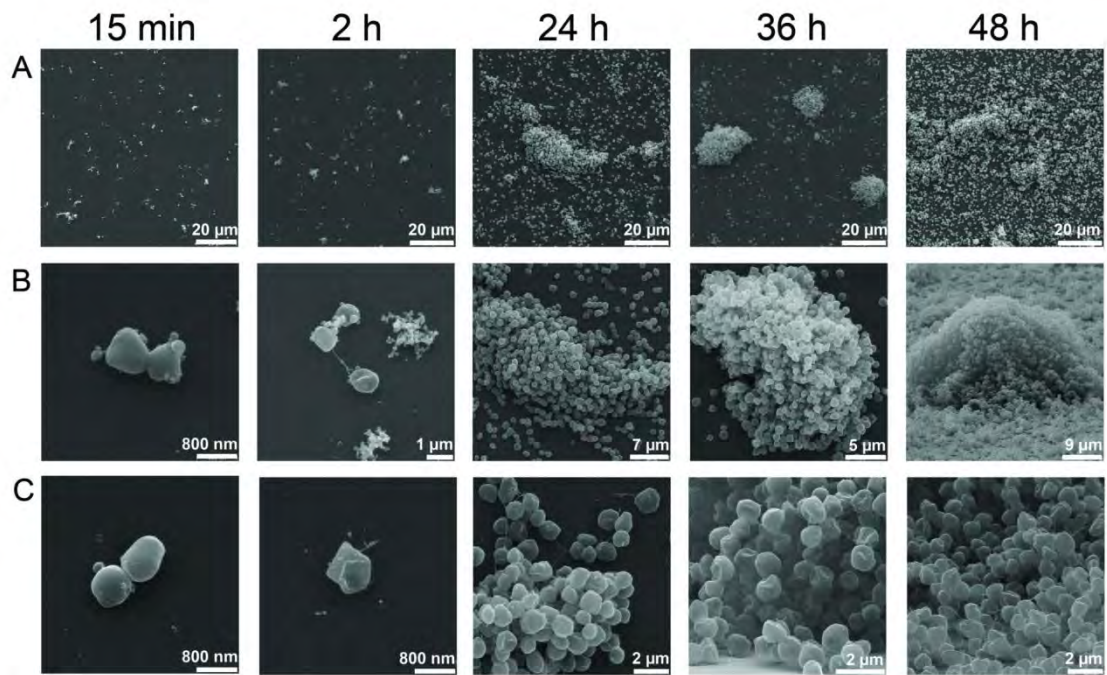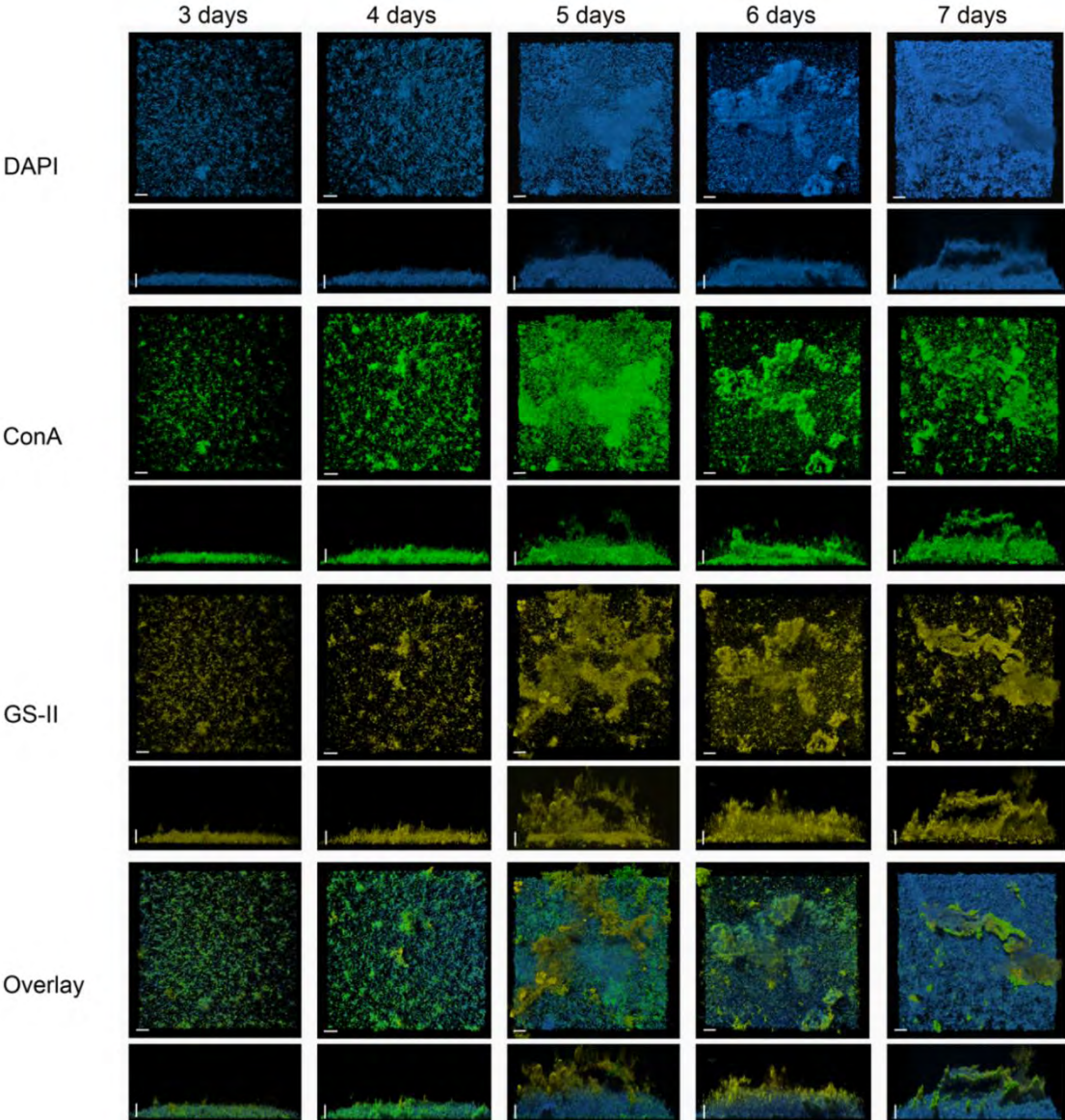**Figure S4**

3.3 Proteomic and transcriptomic of *Sulfolobus ssp.* biofilm

A. Koerdt[#], A. Orell[#], TK. Pham, J. Mukherjee, A. Wlodkowski, E. Karunakaran, CA. Biggs, PC. Wright, and SV. Albers. 2011. **Macromolecular fingerprinting of *Sulfolobus* species in biofilm: a transcriptomic and proteomic approach combined with spectroscopic analysis**

The biofilm lifestyle can be distinguished from the planktonic lifestyle by several features such as, cell-cell connections and cell-cell communication, a higher resistance against environmental stress or toxic agents, the EPS production etc. Usually, in bacteria differential gene expression and protein synthesis, ranging between 1-15% can be observed by comparing both the lifestyles. In the present work we have carried out a comparative study of three *Sulfolobus* strains (*S. acidocaldarius, S. solfataricus and S. tokodaii*) to gain insights into the physiological adjustments that may take place when these archaea are grown as biofilms. We used a combination of spectroscopic, proteomic and transcriptomic approaches to describe physiological and regulatory features involved in the biofilm lifestyle for each strain. Furthermore, we present the data as a comparative analysis to highlight common features in biofilm formation among the three *Sulfolobus* strains under study. Indeed, the obtained results convincingly showed the distinctive differences in the carbohydrate composition in these two lifestyles for each strain. Moreover, the three related *Sulfolobu*s strains show distinct phenotypic differences during the biofilm formation (carpet-, and tower-structures). For the detection of proteins or genes which might cause the differences between the species as well as between both the lifestyles, proteomic and transcriptomic analysis were performed. For all three strains the transcriptome (*S. acidocaldarius* 15%, *S. solfataricus* 3.4% and *S. tokodaii* 1%) and the proteome patterns were found to show unique features. The metabolic processes that were found to be highly regulated from our analysis include processes involved in energy production and conversion, amino acid-, lipid- and carbohydrate- metabolism, transport and binding, stress and adaptation to environmental changes, cell surface appendages and regulatory functions. Commonly regulated genes/proteins in all the three strains lead to the assumption that they might be important for development and maintenance of the biofilm lifestyle

The cell cultures for biofilm and planktonic grown cells for the proteomic and the transcriptomic analysis were carried out by Andrea Koerdt. Andrea Koerdt performed the RNA-isolation, cDNA-synthesis and all experiments related to the q-PCR. The microarrays were performed by the company Febit. The proteomic analysis was

performed by Trong Khoa Pham (Supervisor Phillip C. Wright). The spectroscopic analysis and the FTIR were performed by Catherine A. Biggs, E. Karunakaran and Joy Mukherjee. The analysis for proteomics and transcriptomics data was performed by Alexander Wlodkowski. The analysis of the final proteomic data was carried out by Alvaro Orell, Alexander Wlodkowski and Andrea Koerdt while the transcriptomics related data analysis was performed by Alvaro Orell and Alexander Wlodkowski. The manuscript was written by Alvaro Orell and Sonja Verena Albers and revised by all authors.

Macromolecular Fingerprinting of *Sulfolobus* Species in Biofilm: A Transcriptomic and Proteomic Approach Combined with Spectroscopic Analysis

Andrea Koerdt,[†,‡] Alvaro Orell,[†,‡] Trong Khoa Pham,[§] Joy Mukherjee,[§] Alexander Wlodkowski,[†] Esther Karunakaran,[§] Catherine A. Biggs,[§] Phillip C. Wright,[§] and Sonja-Verena Albers*,[†]

[†]Molecular Biology of Archaea, Max Planck Institute for Terrestrial Microbiology, Karl-von-Frisch-Strasse, 35043 Marburg, Germany

[§]ChELSI Institute, Department of Chemical and Biological Engineering, The University of Sheffield, Mappin Street, Sheffield, S1 3JD, United Kingdom

S *Supporting Information*

ABSTRACT: Microorganisms in nature often live in surface-associated sessile communities, encased in a self-produced matrix, referred to as biofilms. Biofilms have been well studied in bacteria but in a limited way for archaea. We have recently characterized biofilm formation in three closely related hyperthermophilic crenarchaeotes: *Sulfolobus acidocaldarius*, *S. solfataricus*, and *S. tokodaii*. These strains form different communities ranging from simple carpet structures in *S. solfataricus* to high density tower-like structures in *S. acidocaldarius* under static condition. Here, we combine spectroscopic, proteomic, and transcriptomic analyses to describe physiological and regulatory features associated with biofilms. Spectroscopic analysis reveals that in comparison to planktonic life-style, biofilm life-style has distinctive influence on the physiology of each *Sulfolobus* spp. Proteomic and transcriptomic data show that biofilm-forming life-style is strain specific (eg ca. 15% of the *S. acidocaldarius* genes were differently expressed, *S. solfataricus* and *S. tokodaii* had ~3.4 and ~1%, respectively). The -omic data showed that regulated ORFs were widely distributed in basic cellular functions, including surface modifications. Several regulated genes are common to biofilm-forming cells in all three species. One of the most striking common response genes include putative Lrs14-like transcriptional regulators, indicating their possible roles as a key regulatory factor in biofilm development.

KEYWORDS: archaea, sulfolobus, biofilm, proteomics, transcriptomics, FTIR, thermophilic, acidophilic
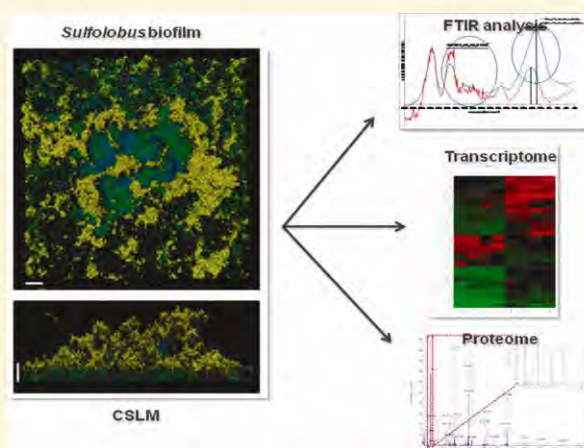
■ INTRODUCTION

It is now broadly recognized that microorganisms in their natural environments are most often found in surface-associated sessile communities, known as biofilms. This multicellular behavior offers the community members benefits, particularly with regard to increased resistance against environmental fluctuations such as temperature, pH and nutrient availability.[1] The underlying mechanisms behind biofilm formation and its importance for microbial survival in natural habitats have attracted increasing interest. Bacterial model biofilm studies have identified many phenotypes and have provided information on numerous of factors that are important during biofilm development and could be of widespread relevance beyond their importance in model systems. Among these factors are cell-to-cell communication, cell attachment mechanisms, cell-to-cell interconnecting components, surface-associated spreading mechanisms, dispersion mechanisms and genetic elements related to the regulation of biofilm development.

Although archaea are frequently detected in biofilm communities in a wide variety of environments,[2,3] limited information is available describing biofilm formation in this domain of life. The first archaeal biofilm was described for the hyperthermophilic euryarchaeon *Thermococcus litoralis*. The *T. litoralis* biofilm developed in rich media on hydrophilic surfaces, for example, polycarbonate filters, and was accompanied by mannose-type extracellular polysaccharides production.[4] The hyperthermophile *Pyrococcus furiosus* was shown to attach to surfaces of mica and carbon coated electron microscopy grids. During this process, the flagella of the cells formed cablelike structures.[5] Additionally, *P. furiosus* adherence to glass was only possible by cocolonization with *Methanopyrus kandlerii* by using its flagella and establishing cell-to-cell contacts.[6] For *Archaeoglobus fulgidus*,

biofilm formation increased in response to unfavorable environmental conditions, including high metal concentrations, pH, and temperature changes.[7] Recently, biofilm characterization was carried out in the mesoacidophilic archaeon *Ferroplasma acidarmanus*. This euryarchaeon is predominantly found in biofilm-associated structures in the environment, and two distinct biofilm morphologies were described: a multilayer film that formed on both an inert glass as well as pyrite that acts as energy source and 5 mm-long filaments that formed on the sintered glass spargers in a gas lift bioreactor. Proteomic studies on these biofilms showed that 6 out of the 10 up-regulated proteins were involved in the adaptation to anaerobic growth indicating anaerobic zones in the multilayered *Ferroplasma* biofilms.[8]

We have chosen the crenarchaeal model organism *Sulfolobus spp.* to initiate comprehensive studies on archaeal biofilms. *Sulfolobus* species are hyperthermoacidophiles growing optimally at 70–85 °C and pH 2–3 that are found worldwide in geothermically active environments such as solfataric fields. Our previous work has provided evidence that cell surface structures such as flagella and pili are essential for the initial attachment of *Sulfolobus solfataricus* to abiotic surfaces from shaking cultures.[9] Furthermore, by means of a microtiter plate assay adapted to high temperatures, we established that biofilm formation occurs more broadly in *S. acidocaldarius*, *S. solfataricus* and *S. tokodaii*. Additionally, it was determined that *S. acidocaldarius* most readily engaged in biofilm formation in comparison to the other investigated *Sulfolobus* strains. Confocal laser scanning microscopy showed that the three strains form very different community morphologies, ranging from simple carpet structures in *S. solfataricus* to high density tower-like forming structures in *S. acidocaldarius*. Lectin staining indicated that all three strains produced extracellular polysaccharides containing glucose, galactose, mannose and *N*-acetylglucosamine once biofilm formation was initiated. Whereas flagella mutants showed no phenotype in three day old static biofilms of *S. solfataricus*, a UV induced pili deletion mutant showed biofilm impairment.[10]

Bacterial biofilms have previously been examined using transcriptomic, proteomic and *in vivo* expression approaches for *Escherichia coli* and *Pseudomonas* spp.[11−13] To date, it has been demonstrated that the transition from a planktonic lifestyle to a sedentary biofilm lifestyle requires the coordinated regulation of genes involved in the development of biofilms. These functional genomics analyses have revealed that hundred genes, most of which are uncharacterized, are differentially expressed during sessile lifestyle.[12,14,15] However, after comparison of the differentially expressed gene sets identified in several recent DNA microarray studies, a common expression pattern for biofilms has yet to emerge, highlighting the particularity of biofilm physiology among the different studied models.[11,14,16] Proteomics has also supplied a broader perspective on gene expression and has been used successfully to study biofilms.[17−20] Recently, a combined approach including proteomic and Fourier transform infrared (FT-IR) spectroscopy analysis immensely assisted the investigation of the distinctiveness of biofilm formation in *Bordetella pertussis*[21] and *E. coli*.[20] These studies have both demonstrated that biofilm formation is a rather complex but distinct process and that deep insights into the biofilm physiology can be provided by the combined use of whole cell metabolic fingerprinting by FT-IR, multivariate statistical analysis, and proteomics.[20,21]

Here, we have carried out a comparative study of three *Sulfolobus* strains (*S. acidocaldarius*, *S. solfataricus* and *S. tokodaii*) to gain insights into the physiological adjustments that may take place when these archaeons are grown as biofilms. We used a combination of spectroscopic, proteomic and transcriptomic approaches to describe physiological and regulatory features involved in the biofilm lifestyle for each strain. Furthermore, we present the data as a comparative analysis, to highlight common features in biofilm formation among the three *Sulfolobus* strains under study.

■ EXPERIMENTAL PROCEDURES

Strains and Growth Conditions

The shaking precultures of *Sulfolobus* strains *Sulfolobus solfataricus* P2 (DSM1617), *Sulfolobus acidocaldarius* (DSM639) and *Sulfolobus tokodaii* (DSM16993) were grown for two days aerobically at 76 °C. The media described by Brock et al. (1972) were adjusted with sulphuric acid to a pH of 3 and supplemented with 0.1% w/v tryptone.

Biofilm Growth and Cell Harvesting

Biofilms of the *Sulfolobus* strains were grown in large Petri dishes (150/20 mm gamma-sterile with Ventilation Cams, Sarstedt, Nümbrecht) for two days in Brock media as a standing culture. Four biological replicates were performed for each of the three strains. For all three strains, as was determined by Koerdt et al. (2010), different OD_{600} inoculations were used: for *S. solfataricus* an OD of 0.03, for *S. acidocaldarius* an OD of 0.01, and for *S. tokodaii* an OD of 0.06. The Petri dishes were put in a specially designed metal box (25 cm L × 20 cm W × 20 cm D) with ~500 mL of water in the bottom to minimize evaporation of the media, as described by Koerdt et al. (2010).

After 48 h the planktonic and the biofilm cells were harvested. The supernatant of the Petri dishes containing the planktonic cells was carefully removed. The biofilm was washed with 50 mL of Brock media. Then, 15 mL Brock media was added and the biofilm was harvested with a cell scraper (Cell Scraper, 28 cm length, Greiner bio-one, Frickenhausen). The biofilm and planktonic cells were spun down for 20 min at 4 °C and 2000× g. The liquid supernatant was removed and the pellets were frozen in liquid nitrogen and stored at −80 °C.

Fourier Transformation Infrared Spectroscopy

Fourier transformation infrared spectroscopy (FTIR) spectroscopy was conducted using a diamond Attenuated Total Reflectance (ATR) apparatus (Pike Technologies, Madison, WI) attached to a Shimadzu IRPrestige-21 Fourier Transformation Infrared Spectrophotometer (Shimadzu, U.K). A blank spectrum, using the ATR without any biological samples, was run as a background and the baseline shift of the spectra was corrected using the IR solution software provided with the Shimadzu instrument. For each biological sample (biofilm or planktonic), a small amount of the cell biomass was mounted on the ATR, covering the entire diamond surface, and allowed to dry at room temperature before analysis. At least 64 scans, with resolution of 4 cm^{-1} using the Happ-Genzel apodization function, were collected for all samples.

As biological macromolecules show characteristic peak absorbance between 800 and 1800 cm^{-1},[22] further spectral processing, including atmospheric correction was focused in this region. Spectral processing was carried out using IR solution software and each significant peak was interpreted using the software "Knowitall" (http://www.knowitall.com/academic/welcome.asp) and corresponding absorption band assignments for functional groups of macromolecules previously reported for bacteria.

Statistical analysis was carried out for all three strains grown planktonically and as a biofilm using Principal Component Analysis (PCA), using the XLSTAT software (http://www.xlstat.com/). Each biological sample was analyzed 5 times to assess technical variations.

X-ray Photoelectron Spectroscopy (XPS) Analysis

XPS analysis was performed as described elsewhere.[23] *Sulfolobus* cells grown planktonically or as a biofilm, were washed twice by centrifugation at $5000 \times g$ for 10 min with demineralised water. The pellets were resuspended in water, freeze-dried under sterile conditions and then mounted onto glass coverslips. The samples with the coverslips were mounted on standard sample studs (sample holder) for analysis. The XPS measurements were carried out on a KRATOS AXIS 165 Ultra Photoelectron spectrometer at 10 kV and 20 mA using the Al Kα X-ray source (1486.6 eV). The takeoff angle was adjusted at 90° and data was collected for each sample at three random selected locations (technical replicates). The area corresponding to each acquisition was 400 μm in diameter. A survey scan was initially carried out (pass energy 20 eV, 1.0 eV step size) for C, O and N, followed by a high resolution scan (pass energy 20 eV, 0.1 eV step size) for C and O. Deconvolution of the high resolution scan enables the local chemical bond environments between C and O to be investigated. The binding energies of the peaks were determined using the C1s peak at 284.5 eV. CasaXPS 2.3.12 software was used to carry out the spectral integration.[23] Elemental composition was expressed as atomic concentration. All measurements were conducted in triplicate.

Protein Extraction and iTRAQ Labeling

Independent biological duplicate cells from three different species harvested as described above were washed twice with cold water before being resuspended in 0.5 M TEAB iTRAQ buffer containing 0.1% SDS. Cells were then lysed using ultrasonication (Sonifier 450, Branson) 4 times (alternatively 1 min on ice) at 70% duty cycle, as described in detail elsewhere[24] before centrifugation first at $3000 \times g$ for 5 min at 4 °C and then at 21,000g at 4 °C for 15 min. Supernatants were subsequently collected as extracted proteins. Total protein concentrations were determined using the RC-DC protein quantification assay (Bio-Rad, U.K.). 100 μg protein (for each phenotype) was used for iTRAQ 4-plex analysis. Proteins were reduced, alkylated, digested and labeled with iTRAQ reagents as described elsewhere.[24] Biological duplicates were used for all three *Sulfolobus* species, and for each phenotype (biofilm and planktonic). The iTRAQ labeling of all samples is shown in Table S2 (Supporting Information). Labeled peptides (for each species) were subsequently combined before being dried in a vacuum concentrator.

Labeled Peptides Separation, Mass Spectrometry and Data Analyses

All dried labeled peptide samples were cleaned and fractionated using strong cation exchange on a BioLC HPLC system (Dionex, UK) as detailed elsewhere.[24] Labeled iTRAQ peptides were collected every minute, and then dried under vacuum. Selected dried labeled peptides were resuspended in 50 μL of buffer A containing 0.1% formic acid and 3% acetonitrile before submission to a QStar XL Hybrid ESI Quadrupole time-of-flight tandem mass spectrometer, ESI-qQ-TOF−MS/MS (Applied Biosystems/MDS Sciex, Canada), coupled with a nano-LC system (LC Packings Ultimate 3000, Dionex, U.K.). Mass

spectrometry was performed as described previously.[24] The sample was separated on a PepMap C-18 revered phase capillary column (LC Packings) at a flow rate of 3 μL/min, and a gradient was generated by variation of the percentage of buffer B (0.1% formic acid and 97% acetonitrile). The mass detector range was set to 350 to 1800 m/z and operated in the positive ion mode. Peptides with +2, +3, and +4 charge states were selected for fragmentation.

All raw mass spectrometry data were converted into MGF format using the mascot.dll script (V1.6) coupled with Analyst QS 2.0 (Applied Biosystems), before submission to an in-house search algorithm Phenyx V 2.6 (Genebio, Geneva) (see Pham et al.,[25] for more detail) with the *Sulfolobus solfataricus* P2, *Sulfolobus acidocaldarius*, *Sulfolobus tokodaii* databases downloaded from NCBI (http://www.ncbi.nlm.nih.gov/Ftp/) in Jan 2009. The search parameters were set as follows: peptide tolerance 0.4 Da, charge +2,+3 and +4, min peptide length, z-score, max p-value and AC score were 5, 5.5, 10^{-6} and 5.5 respectively, and enzymes used for searching were trypsin, with up to two missed cleavages. Modifications were analyzed as follows: 4-plex iTRAQ mass shifts (+144 Da, K and N-term), methylthiol (+46 Da) and oxidation of methionine (+16 Da). Data were then exported to Excel (Microsoft 2008, Redmond, WA) for further analysis. Furthermore, the false positive rates (FPR) were also performed by searching data with the reversed databases of these *Sulfolobus* spp., and calculated as the following equation: $FPR = (2 \times decoy\_hits * 100\%)/(decoy\_hits + true\_hits)$.

The quantification of identified proteins was performed based on methods described previously by Pham, et al. (2010), and a rigorous statistical method, including multiple test correction, was also applied to choose significantly regulated proteins for biological discussions (see also Pham, et al.[25] for full details of methods). First, protein quantification was calculated by the geometric means of the ion reporters' intensities (at least 2 peptides for each protein) before a t test comparison (with α = 0.05) between the reporter ions' intensities was performed, followed by a Bonferroni correction. Furthermore, proteins were considered as regulated ones when all t tests of these proteins were less than a value of α/P (Onferroni corection) (P: number of quantified proteins).

RNA-Isolation

The cell pellet was resuspended in 1 mL ice-cold AE-buffer (20 mM sodium-acetate, pH 5.5; 1 mM EDTA) and then centrifuged for 5 min at 4 °C. The pellet was resuspended in 600 μL AE-buffer. Subsequently, 900 μL of hot phenol-chloroform-isoamyl alcohol (25:24:1, 60 °C) and 10 μL 25% SDS (w/v) were added. The suspension was incubated for 15 min at 60 °C and every 2−3 min the tube was inverted. The tube was incubated for 20−30 min on ice and then centrifuged at $15\,700 \times g$ for 30 min at 4 °C. In a new phase lock tube (Phase Lock Gel Light 2 mL, 5 PRIME, Hamburg), one volume of phenol-chloroform-isoamyl alcohol and 62.5 μL 2 M sodium-acetate were added to the supernatant. After centrifugation $15\,700 \times g$ for 15 min at 4 °C the supernatant was transferred in a new 2 mL tube, 2.5 volumes of 96% ethanol was added and incubated for 1−2 days at −80 °C. The samples were thawed on ice and centrifuged for 30 min at 4 °C. After washing the pellet twice with 500 μL of 70% ethanol, the pellet was air-dried at room temperature. Finally the pellet was resuspended in 100 μL RNase free water (Qiagen, Hilden). The RNA isolation was

controlled via Nanodrop (NanoDrop ND-1000 Peqlab, Erlangen) and analytical gel electrophoresis. To remove all DNA, the samples were digested with DNase (TURBO DNA-*free*, Ambion Applied Biosystems, Darmstadt) according to the manual. Additionally RNase Inhibitor (RNasin Plus RNase Inhibitor, Promega, Mannheim) was added to inhibit the digestion of RNA. The purity of the RNA was tested via PCR with primers for a very small product before and after DNA digestion.

Microarrays Experiments and Statistical Analysis

Four biological replicates per strain were measured both for biofilm and nonbiofilm grown cells. Geniom Biochips containing 4 arrays were used for the analysis. Each array on the chip had 15 000 spots with 50mer probes. For each gene, five to six different probes were computed. The probe computation relies on freely available information of the DoE Joint Genome Institute. For background correction single "T" nucleotide probes were used. For further verifications, additional hybridization controls were added to the array template. Blank, labeling control and hybridization control probes are not included in the data.

Febit (company, Heidelberg) used the MessageAmpII-Bacteria Prokaryotic RNA Kit from Ambion for the labeling of RNA for mRNA expression analysis. The kit provides a transcription of RNA in cDNA, following a transcription in cRNA while enrichment of all nucleic acid molecules is included. For each array, 1 μg of total RNA was labeled according to the manufacturers instructions. After labeling, samples were dried in a vacuum concentrator and fragmented with a fragmentation buffer (see Febit protocol 20). Finally, Febit's proprietary standard Hybridization Buffer (20 μL per array) was added. Hybridization was done automatically overnight (16 h) at 45 °C using the Geniom RT analyzer. After hybridization, the Geniom Biochip was washed automatically. For maximum sensitivity, Febit used biotin and its detection with strptavidin-phycoerythrin (SAPE), in combination with Febit's Consecutive Signal Enhancement (CSE) procedure. For a more detailed description please read Febit protocol 010. The feature recognition (using Cy3 filter set) and signal calculation were done automatically within milliseconds. Accurate detection of mRNA profiles correlates well with the qPCR data. There was no photo bleaching, thus enabling repeated measurements and multiple detection of each Biochip.

The basis of the analysis was Febit's background corrected data sets. In these data sets, all negative values were replaced by 0. To reduce influences of sample binding problems, only the three spots with the highest intensities were used per gene in the following calculations. For each array the sum of all intensities was calculated. Subsequently all intensities of each array were multiplied with a factor to level the total sum to the highest. Afterward, the three intensities of each gene were reduced to the median, followed by quantile normalization. The following calculations were done in Microsoft Excel.

The medians of the four biological replicates for biofilm and planktonic cells were calculated and their logarithmic fold change calculated to the base 2. The significance was computed by a statistical heteroscedastic t test with a two-tailed distribution. Regulated genes were chosen by a specific threshold value for each strain. For *S. acidocaldarius*, the standard threshold value of 0.05 was selected. For the two other strains, the values were adapted by the average of the calculated significances (*S. solfataricus* 0.0631, *S. tokodaii* 0.0747). The resulting significantly regulated genes were split in two groups (up-, down-regulated).

To find homologues for both groups, databases containing the amino acid sequences were created. Afterward, for each gene, a BLAST search in the specific database was performed with a cutoff value of e^{-10}.

Quantitative RT-PCR (qRT-PCR)

The cDNA Synthesis was performed with the iScript cDNA Synthesis Kit (Bio-Rad, Munich) according to the manual. qPCR was performed using SYBR Green qPCR Master Mix (Fermentas, St. Leon-Rot). Two-step cycling qPCR was carried out in 25 μL final volume reaction according to the provider indications. A 20 times diluted cDNA of four biological replicates per strain were assayed both for biofilm and nonbiofilm grown cells. Reactions were set up in a 7300/7500 Real Time PCR Systems Cycler (Applied Biosystems, Darmstadt Germany). Primers were designed to amplify a specific product of a length range of 90−120 bp (oligonucleotide sequences are listed in Table S4 in the Supporting Information section). All primers were used at the final concentration of 0.3 μM. The cycling program used for each primer pair was as follows: 10 min at 95 °C, 40 cycles of 15 s at 95 °C and 60 s at 60 °C (annealing and extension in one step). Saci_0269, SSO0007 and ST2326 genes were used as standards for the relative quantification. The Ct values were calculated automatically using software core application version 1.2.3 (Applied Biosystems).

■ RESULTS

Spectroscopic Analysis of Biofilm versus Planktonic Cells

Fourier Transform Infrared Spectroscopy (FT-IR) and X-ray Photoelectron Spectroscopy (XPS) Analysis. FT-IR spectroscopy has been successfully used as a rapid nondestructive technique to characterize the molecular composition of many different microbial systems,[26−29] including environmental isolates[30] and biofilms.[20,30,31] ATR-FTIR can detect both surface and cytoplasmic constituents of a biological sample. Furthermore, Jiang et al.[29] established that variations in the ATR-IR spectrum essentially arose due to modifications on the cell surface. Therefore, it is proposed that any variations observed in the ATR-IR spectra conducted in this study, can be related to surface specific changes in functional groups.

FT-IR spectra between 800 and 1800 cm^{-1} were recorded from *S. acidocaldarius*, *S. solfataricus* and *S. tokodaii* cell samples grown either in the biofilm or planktonic mode, respectively (Figure 1). Principal component analysis (PCA) of the FT-IR spectra was applied to interpret the variations among the three strains in both lifestyles (biofilm v/s planktonic). PCA analysis showed that cells associated with biofilms clustered separately from their respective planktonic counterparts for each investigated strain (see Figure S1 in Supporting Information). These findings suggest that the FT-IR data provides spectroscopic evidence to support the premise that *Sulofolobus spp.* biofilm population has characteristics that distinguish it from the planktonic cells population.

To further investigate the potential chemical functional groups within the FT-IR spectrum that may have contributed to the observed differences in the PCA analysis, chemical functional groups were assigned to the FT-IR spectra (Figure 1) according to definitions from Eboigbodin and Biggs,[26] Naumann[22] and Bosch et al.[32] Comparative analysis of normalized spectral data (Figure 1) mainly revealed a significant increase in the intensity of absorption bands assigned to carbohydrate functional groups
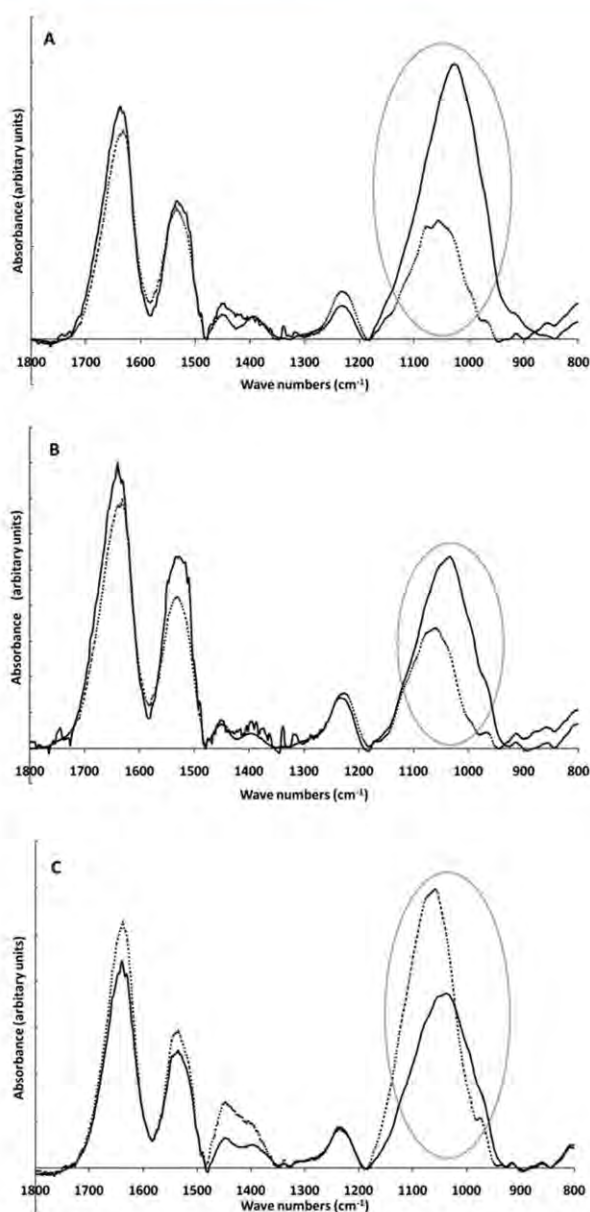
Figure 1. Overlay of normalized spectra FTIR data of (A) *S. acidocaldarius*, (B) *S. solfataricus* and (C) *S. tokodaii* grown either as biofilm (solid line) or planktonically (dotted line). Spectra are baseline corrected and normalized to 2930 cm^{-1}.

(spectral region: 900 to 1200 cm^{-1}) in biofilm cells of both *S. acidocaldarius* (Figure 1A) and *S. solfataricus* (Figure 1B) strains in comparison to their planktonic counterparts. However, despite the same normalization across all strains, the significant increase in absorption band intensity in carbohydrate region of *S. tokodaii* biofilm cells compared to planktonic cells was not found (Figure 1C). Moreover, additional specific banding assignment for chemical function groups was difficult in this region (1200 and 900 cm^{-1}), as it is made up of vibrations corresponding to the stretching of diverse polysaccharides groups.[23]

Additionally, XPS analysis was performed to further describe the cell surface chemical composition in all three *Sulfolobus spp.*

XPS analysis allows for the quantification of the elemental surface composition and to assess the local chemical environment of carbon, oxygen and nitrogen atoms on the cell surface. XPS wide scan data (see Figure S2 and Table S1 in the Supporting Information) showed that the cell surface (approximately 1–10 nm in depth) was mainly comprised of C, N, O.

The abundance of C, N, O was therefore estimated for each *Sulfolobus* strains and in comparison between biofilm-associated cells and planktonic cells samples. N/C and O/C atomic concentration ratios indicate the fraction of carbon linked to either nitrogen or oxygen atoms on the cell surface, respectively (Table 1). The results indicated an excess of O/C linkages on the cell surface of all three strains (Table 1). Furthermore, when compared to planktonic cell samples, an increase in the O/C ratios was determined for biofilm-associated cells of *S. acidocaldarius* and *S. solfataricus*. The opposite was found in the *S. tokodaii* biofilm cell surface (Table 1). Since polysaccharides predominantly contain O/C linkages in their structures, this ratio might be attributed to an increase in polysaccharide moieties. Morever, O/C ratios were found to be higher than N/C ratios, indicating that O/C ratios might arise from polysaccharide moieties rather than from the amide linkages (C-NHCO-C) on the protein moieties (Table 1), as a 1:1 ratio (approx.) between O/C and N/C values is expected for a proteinaceous cell surface.

Thus, the XPS analysis correlated with the FT-IR spectra in that a statistically significant increase was determined in the polysaccharide moieties on the *S. acidocaldarius* and *S. solfataricus* biofilm cell surfaces. The opposite trend was determined in the *S. tokodaii* biofilm cell surface (Table 1). Using both FTIR and XPS, differences between biofilm and planktonic modes of growth in all three *Sulfolobus* species were noted, which is most likely due to changes in the carbohydrate composition.

Comparative Proteomic Analysis of Biofilm versus Planktonic Cells

Taking the spectroscopic evidence that *Sulfolobus* biofilm population shows distinctive features in comparison to the free-living cells, we further assessed the impact of this mode of growth on the proteome of *Sulfolobus* species. Total protein extracts of *S. acidocaldarius*, *S. solfataricus* and *S. tokodaii* from biofilm-associated and planktonic populations were comparatively analyzed using iTRAQ. Planktonic and biofilm cell samples of each strain at the same time (2 days of growth) were used in the proteomic experiments. Using the Phenyx program for searching within correlated databases, 11063, 10122, and 11419 peptides corresponding to 481, 463, and 542 quantified proteins (≥ 2 peptides) were identified for *S. solfataricus*, *S. acidocaldarius*, and *S. tokodaii*, respectively (see sheet 1 for details of peptides lists and sheet 2 for details of quantified proteins lists in proteomics Supporting Information section, Excel files 1, 2, and 3). Furthermore, false positive rates of 0.25%, 0.18% and 0.31% were also estimated for *S. solfataricus*, *S. acidocaldarius*, and *S. tokodaii*, respectively, as described in Experimental procedures section. The numbers of all significantly regulated proteins are summarized in Table S3 (Supporting Information section). Since two biological replicates for each condition (biofilm (iTRAQ labels 116 and 117) and planktonic (iTRAQ labels 114 and 115) for each *Sulfolobus* strain) were carried out, four *t* tests were calculated for each *Sulfolobus* species. To pick up regulated proteins, we required all *t* test values of these proteins to be less than a value of α/P (Bonferroni correction) (where $\alpha = 0.05$ and

Table 1. Quantification of the Elemental Surface Composition (C, O and N) of S. acidocaldarius (S.aci), S. solfataricus (S.so) and S. tokodaii (S.to) Grown Planktonically and as Biofilm[a]

	planktonic cells			biofilm cells		
	S. aci	S. so	S. to	S. aci	S. so	S. to
C	62.23 ± 1.36	63.73 ± 1.10	52.97 ± 1.42	57.42 ± 0.74	59.53 ± 0.56	56.22 ± 2.41
O	29.90 ± 0.17	28.38 ± 1.49	40.81 ± 2.81	34.50 ± 1.04	31.36 ± 0.40	35.49 ± 2.43
N	7.88 ± 1.20	7.90 ± 0.40	6.23 ± 1.39	8.09 ± 0.30	9.12 ± 0.16	8.29 ± 0.03
N/C	0.13 ± 0.02	$0.120 \pm 0.004^{\Delta}$	0.12 ± 0.02	0.140 ± 0.003	$0.150 \pm 0.004^{\Delta}$	0.15 ± 0.01
O/C	$0.48 \pm 0.01^{\epsilon}$	$0.45 \pm 0.03^{\beta}$	$0.77 \pm 0.07^{\gamma}$	$0.60 \pm 0.03^{\alpha}$	$0.53 \pm 0.01^{\beta}$	$0.63 \pm 0.07^{\gamma}$

[a] Numbers with similar Greek symbols are statistically significant (90% confidence interval; Students' t test, $p < 0.1$). Outliers were detected and removed in the data by calculating the interquartile range and also by using Grubbs' test at 99% confidence interval.

P is number of quantified proteins). As a result, values of 1.04×10^{-4}, 1.08×10^{-4} and 9.24×10^{-5} were calculated for S. solfataricus P2, S. acidocaldarius, S. tokodaii, respectively. However, we also considered proteins with p-values ≤ 0.05 regulated proteins for a confirmatory test. Lists of significantly regulated proteins are summarized in sheet 3 in proteomics Supporting Information, Excel files 1, 2, and 3 for S. solfataricus, S. acidocaldarius, S. tokodaii, respectively. In order to get a wider view for understanding the behavior of cells in biofilm versus planktonic conditions, proteins with p-values less than $\alpha = 0.05$ (without correction) (known as lists of potentially regulated proteins) were also used for further discussion. The lists of these potentially regulated proteins are shown in the sheet 4 in proteomics Supporting Information, Excel files 1, 2 and 3.

In terms of identifying proteins that were differentially changed during the biofilm mode of life versus the planktonic counterparts, a protein comparison was performed. S. acidocaldarius had 30 biofilm-regulated proteins (19 up- and 11 down-regulated), S. solfataricus displayed 36 protein changes (17 up- and 19 down-regulated) and for S. tokodaii 67 proteins changed their relative abundances in the biofilm lifestyle (41 up- and 26 down-regulated). All the statistically significant changes are tabulated in Table S3 in the Supporting Information section. The most noteworthy findings are listed in Tables 2 and 3 and discussed in the next section. Additionally, a BLASTp analysis was carried out in order to identify common biofilm-regulated proteins between the three Sulfolobus species (biofilm core response). Amino acid sequences as queries of both significantly up-regulated proteins and down-regulated proteins were used in this analysis, respectively. This analysis yielded three different proteins which were commonly up-regulated, while four proteins were found to be down-regulated in all three Sulfolobus species (Figure 2, Table 2). Furthermore, the BLASTp analysis also yielded homologous proteins that were commonly regulated in at least two strains (Figure 2, Table 3).

Identification of Differentially Expressed Proteins in Biofilm-Grown Sulfolobus Strains

Identified proteins were categorized in functional groups using the assigned COG numbers. By means of this analysis, we were able to find that Sulfolobus spp. biofilm mode of growth altered not only the expression of proteins involved predominantly in cellular functions like energy production, energy conversion, adaptation to environmental changes and stress, and substrate transport/binding activities but also the expression of proteins implicated in cellular processes and regulatory events (Table 3).

Table 2. Common Biofilm-Regulated Proteins and Genes within S. acidocaldarius, S. solfataricus and S. tokodaii Strains

Up-regulated in biofilm		
proteomic analysis annotation	ORF number	fold change ($\log_2$)
transcriptional regulator	Saci_1223	0.85
Lrs14-like protein	SSO1101	1.48
	ST0837	0.82
DNA-binding protein	Saci_0064	1.02
	SSO10610	1.0
	STS077	0.26
Chaperone	Saci_1665	0.79
Small heat shock protein	SSO2427	0.88
hsp20	ST0555	0.58
RNA microarray analysis		
ABC transporter ATP-binding	Saci_2305	0.91
protein	SSO0053	0.74
	ST0535	0.22

Down-regulated in biofilm		
proteomic analysis annotation	ORF number	fold change
Thermosome		
-alpha subunit (thsA)	Saci_1401	−0.24
	SSO0862	−0.67
	ST1253	−0.14
-beta subunit (thsB)	Saci_0666	−0.4
	SSO0282	−0.43
	ST0321	−0.16
-gamma subunit	Saci_1203	−0.63
	SSO3000	−0.43
	ST0820	−0.37
V-type ATPase	Saci_1548	−0.55
	SSO0563	−1.03
	ST1436	−0.47
RNA microarray analysis		
3-oxoacyl-(acyl carrier	Saci_1792	−1.72
protein) reductase (fabG-1)	SSO0975	−0.64
	ST1299	−0.21

Proteomic data showed that adjustments in energetic metabolism are made during growth in a biofilm. Putative cytochrome oxidase subunits were identified as up-regulated in S. solfataricus

Table 3. Selected Up- and Down-regulated Genes and Proteins between *S. acidocaldarius*, *S. solfataricus* and *S. tokodaii* during Biofilm Mode of Growth[a]

functional group	ORF	fold change (log$_2$)		p-value
		proteomic	microarray	microarray
Energy production and conversion				
Cytochrome c oxidase polypeptide I	Saci_0097	n.d.	1.31	0.006
	ST2595	n.s.	0.9	0.017
Cytochrome b558/566, subunit A	SSO2801	1.41	n.d	
Cytochrome *b*	ST0137	0.43	n.s.	
Rieske iron—sulfur protein (SoxL)	Saci_1860	n.d.	2.57	0.001
Quinol oxidase-2, sulfocyanin (SoxE)	SSO2972	n.d.	0.59	0.034
V-type ATP synthase subunit B	Saci_1549	−0.35	−0.5	0.006
V-type ATPase, alpha subunit	Saci_1548	−0.55	n.s.	
	SSO0563	−1.03	n.s.	
	ST1436	−0.47	n.s.	
ATP synthase subunit E	SSO0561	1.01	n.s.	
Acetyl-coenzyme A synthetase	Saci_2062	n.d.	0.94	0.025
	ST1803	n.s.	0.76	0.044
Lactate/malate dehydrogenase	Saci_0246	−1.03	n.s.	
Succinyl- CoAsynthetase betasubunit	ST0963	0.54	n.d.	
NADP dependent glyceraldehyde-3-phosphate dehydrogenase	ST2477	−0.61	n.s.	
Phosphoenolpyruvate synthase	Saci_1417	0.56	n.s.	
Acyl-CoA dehydrogenase related protein (acd-like2)	SSO2497	n.d.	0.27	0.051
	ST0085	n.s.	0.69	0.075
Carbon monoxide dehydrogenase subunit G	SSO2430	n.d.	−1.19	0.029
Sulfurtransferase enoyl-CoA hydratase	ST0048	2.01	n.s.	
Carbon monoxide dehydrogenase large chain	Saci_2117	n.s.	−0.51	0.002
	SSO3009	n.d.	−0.3	0.046
Oxidoreductase	SSO2794	n.d.	−0.32	0.021
Thiosulfate reductase electron transport protein (PhsB)	ST1839	n.d.	−0.67	0.022
Pyridine nucleotide-disulfide oxidoreductase	Saci_0331	−1.16	n.s.	
	ST0615	−0.71	n.s.	
Formate dehydrogenase subunit alpha	ST0081	−0.3	n.s.	
Indolepyruvate oxidoreductase, subunit A	ST0732	−0.62	n.s.	
Anaerobic glycerol-3-phosphate dehydrogenase subunit C	ST2369	−0.65	n.s.	
Diphosphomevalonate decarboxylase	Saci_1245	1.08	n.s.	
	ST0977	1.02	n.d.	
Dehydrogenase (flavoprotein)	Saci_0292	0.61	n.s	
3-hydroxybutyryl-CoA Dehydrogenase	Saci_1109	0.5	n.s.	
Inorganic pyrophosphatase	SSO2390	1.16	n.s.	
Anaerobic dimethylsulfoxide reductase	ST1789	1.06	n.s.	
Putative thiosulfate sulfurtransferase	ST2564	1.22	n.s.	
Sulfurtransferase enoyl-CoA hydratase	ST0048	2.01	n.s.	
Carbohydrate transport and metabolism				
Sugar-related transporter	Saci_1782	n.d.	−0.59	0.381
	SSO2057	n.d.	−0.93	0.023
Sugar transporter	Saci_2111	n.d.	−0.71	0.006
	SSO2716	n.d.	−0.66	0.012
proline/betaine transporter	SSO2938	n.d.	−0.31	0.056
Maltose-binding protein	ST1103	0.44	n.s.	
Lipid transport and metabolism				
3-oxoacyl-(acyl carrier protein) reductase (fabG-1)	Saci_1792	n.d.	−1.72	0.003
	SSO0975	n.d.	−0.64	0.012
	ST1299	n.d.	−0.21	0.032

Table 3. Continued

| functional group | ORF | fold change (log$_2$) | | p-value |
		proteomic	microarray	microarray
4-coumarate-CoA ligase 1	Saci_2207	n.d.	0.79	0.015
	ST1388	n.d.	0.29	0.041
Transport-related proteins				
	SSO2619	0.79	n.s.	
Oligopeptide-binding protein	ST2539	0.28	n.s.	
Permease, major facilitator Superfamily	SSO2701	1.58	n.s.	
Inorganic ion transport and metabolism				
ABC transporter ATP-binding protein	Saci_2305	n.d.	0.91	0.032
	SSO0053	n.d.	0.74	0.031
	ST0535	n.s.	0.22	0.015
ABC transporter, ATP binding subunit	SSO1078	n.s.	0.26	0.61
	ST1577	n.d.	0.2	0.016
Copper transport ATP-binding protein	Saci_2305	n.d.	0.91	0.032
	SSO0053	n.d.	0.74	0.031
	ST0535	n.s.	0.22	0.015
Cation efflux integral membrane protein	Saci_0242	n.d.	0.76	0.022
	ST2110	n.d.	0.28	0.048
Predicted solute binding protein	SSO1273	0.94	0.58	0.033
Transcriptional regulators				
Lrs14 like protein	Saci_1223	0.85	n.d.	
	SSO1101	1.48	n.d.	
	ST0837	0.82	n.s.	
Lrs14 like protein	SSO1108	0.91	n.d.	
Sugar-specific transcriptional regulator	SSO0048	1.24	n.s.	
	ST2050	0.25	n.d.	
Stress-related proteins and chaperones				
Small heat shock protein, hsp20	Saci_1665	0.79	n.s.	
	SSO2427	0.88	n.d.	
	ST0555	0.58	n.s.	
Thermosome Hsp60, alpha subunit	Saci_1401	−0.24	n.s.	
	SSO0862	−0.67	n.d.	
	ST1253	−0.14	n.s.	
Thermosome Hsp60, beta subunit	Saci_0666	−0.4	n.s.	
	SSO0282	−0.43	n.s.	
	ST0321	−0.16	n.s.	
Thermosome (gamma subunit)	Saci_1203	−0.55	−0.68	0.041
	SSO3000	−1.03	−0.15	0.072
	ST0820	−0.47	n.s.	
Thioredoxin	Saci_1823	n.d.	0.88	0.002
	SSO2232	n.d.	0.4	0.039
Peroxiredoxin	Saci_2227	n.d.	0.47	0.05
	SSO2613	n.s.	0.38	0.063
FKBP-type peptidyl-prolyl cis−transisomerase	SSO0758	−0.36	n.s.	
Bacterioferritin comigratory protein	ST1785	0.33	n.s.	
Universal stress protein	SSO1865	0.74	n.s.	
Cell motility/surface appendages				
Flagella accessory protein J (flaJ)	Saci_1172	n.d.	0.84	0.005
Flagellar accessory protein FlaH	Saci_1174	n.d.	1.42	0.003
Flagellar protein F	Saci_1175	n.d.	0.75	0.001
Hypothetical protein	Saci_1173	n.d.	0.73	0.002
	SSO0119	n.d.	0.54	0.06

Table 3. Continued

| functional group | ORF | fold change (log₂) | | p-value |
		proteomic	microarray	microarray
UV induced pili system (upsF)	SSO0119	n.d.	0.54	0.06
Surface layer glycoprotein; Flags: Precursor	SSO0389	0.6	n.d.	
Cell wall/membrane/envelope biogenesis				
hypothetical protein	ST2425	n.d.	0.8	0.001
hypothetical protein	SSO2829	n.d.	0,78	0.001
hypothetical protein	Saci_0134	n.d.	0,68	0,001
DNA binding proteins				
Similarity with Sso10 (hypothetical proteins)	Saci_0882	1.11	−0.94	
DNA-binding protein 7 (Sul7d)	Saci_0064	1.02	n.d.	
	SSO10610	1	n.d.	
	STS077	0.26	n.d.	
DNA-binding protein 7	Saci_0362	0.73	n.s.	
	SSO9180	1.02	n.d.	
Chromatin protein Cren7	Saci_1307	0.78	n.d.	
	SSO6901	1.2	n.d.	
Chromatin protein Alba	Saci_1322	0.74	n.s.	
	STS141	0.36	n.d.	
Transcription and translation components				
Methylation guide ribonucleoprotein complex	Saci_1347	0.27	n.s.	
50S ribosomal protein L7Ae	Saci_1520	0.45	n.s.	
	Cell cycle			
ATP-dependent Zn Protease	Saci_0838	0.54	n.s.	
Replication				
Replication factor C small subunit	ST0475	−1	n.s.	
Conserved/hypothetical protein	Saci_0134	n.d.	0.7	0.001
	SSO2829	n.d.	0.78	0
	ST2425	n.d.	0.8	0.002
	Saci_0139	n.d.	−0.75	0.001
	SSO0550	n.d.	−0.56	0.034
Similarity with Sso10	Saci_0882	1.11	n.s.	
	ST0658	0.43	n.d.	
Mn-dependent transcriptional regulator	SSO3242	0.85	n.d.	
Superfamily I DNA and RNA helicases	SSO1456	1.05	n.d.	
Endobeta-mannanase	SSO3007	1.24	n.s.	
Aconitate hydratase	ST0833	0.44	n.s.	
Undecaprenyl pyrophosphate	ST1813	0.53	n.s.	
CRISPR-associated autoregulator, DevR- family	ST0029	−0.42	n.s	

[a] Fold changes correspond to the ratio of biofilm v/s planktonic. Result confidentiality was estimated by p-values calculation. $p \leq 0.05$ was used for all 3 strains in the proteomic analysis f. p-values of ≤ 0.05, ≤ 0.0631 and ≤ 0.0747 were used for S. acidocaldarius, S. solfataricus and S. tokodaii respectively, in the transcriptomic analysis. n.d., not determined; n.s., not significant; −, down-regulated in biofilm.

(SSO2801) and S. tokodaii (ST0137) biofilm cells (Table 3). In addition, while V-type ATPase subunit B levels were decreased in S. acidocaldarius biofilm cells, V-type ATPase alpha subunit was found to be down-regulated in all three Sulfolobus strains biofilm cells (Table 2).

Levels of proteins related to transport functions were altered in biofilm-associated cells of S. solfataricus and S. tokodaii. A homologous oligopeptide-binding protein (SSO2619 and ST2539) was up-regulated in both strains and a maltose-binding protein levels (ST1103) were greater in S. tokodaii biofilm-associated cells. Moreover, a putative permease (SSO2701) was biofilm-up-regulated in S. solfataricus (Table 3). Furthermore, molecular chaperones were regulated during biofilm growth. A small heat shock protein (Hsp20) was found to be commonly biofilm-up-regulated among the three Sulfolobus species (Saci_1665 and SSO2447). Additionally, the three thermosome subunits were down-regulated in biofilm-associated cells from each species (Table 2). S. acidocaldarius and S. solfataricus also displayed up-regulation of two other
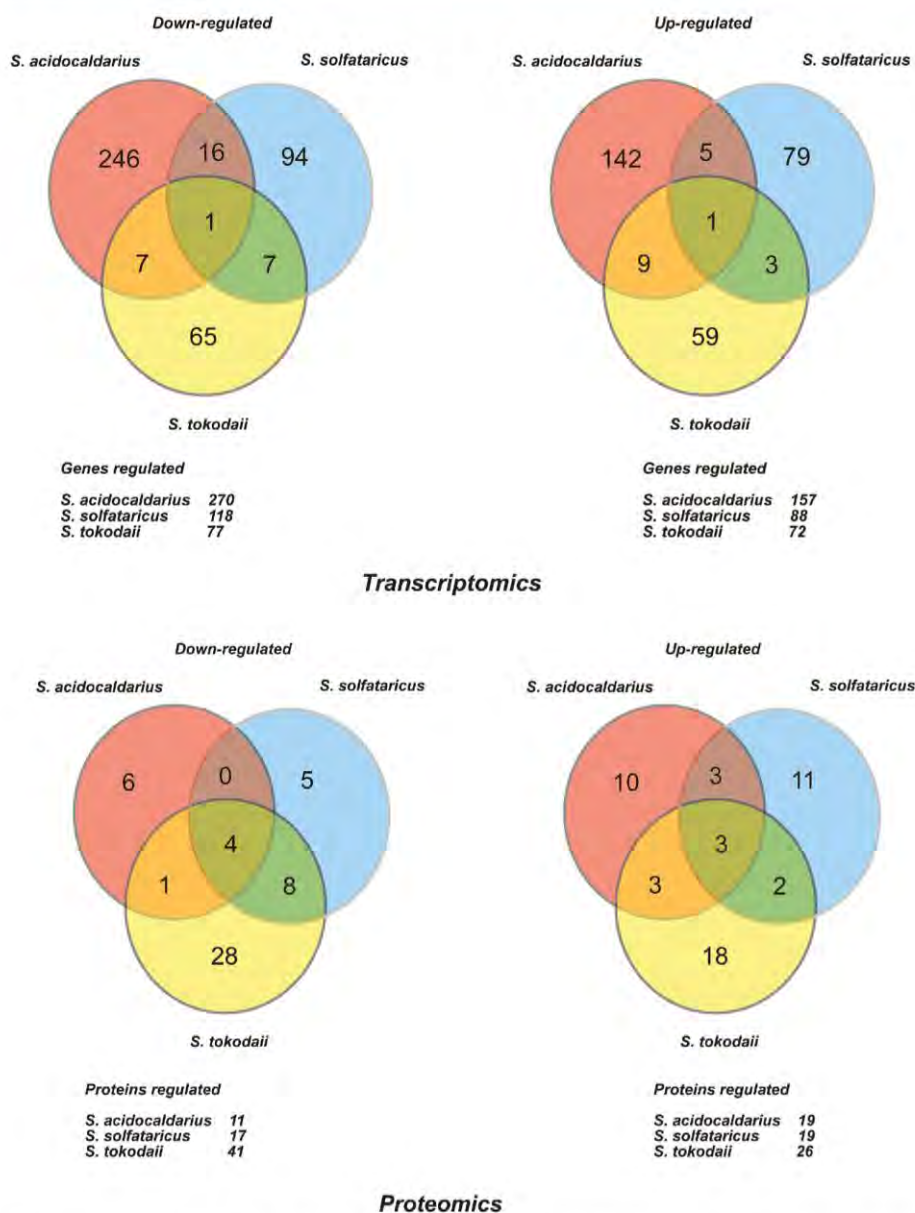
ARTICLE

Figure 2. Venn-diagram of (A) transcriptomic and (B) proteomic profiling biofilm response between *Sulfolobus* strains. Up- and down regulated genes and proteins were analyzed by BLASTp in order to identify common biofilm-regulated changes at the transcriptomic and proteomic level. The number of homologous genes and protein between the *Sulfolobus* species are indicated by numbers.

stress-related proteins, that is, a thioredoxin (Saci_1823 and SSO2232) and a peroxiredoxin (Saci_2227 and SSO2613), while *S. tokodaii* showed increased levels of a bacterioferritin comigratory protein-like, belonging to the peroxiredoxins family proteins.[33] As is well-known, peroxiredoxins are ubiquitous proteins that catalyze the reduction of hydroperoxides, which undertake the thiol-dependent reduction of peroxide substrates, thus conferring resistance to oxidative stress.[33]

The DNA-binding protein Sul7d (Saci_0064, SSO10610 and STS007) also exhibited altered expression patterns in all three *Sulfolobus* species in biofilm-grown populations. Sul7d has been intensely studied in *S. acidocaldarius* and *S. solfataricus*,

and it is described as an archaeal histone-like protein that binds nonspecifically to DNA inducing negative supercoiling (Baumeister et al.[34]).

From our BLASTp analyses, we identified a putative transcriptional regulator Lrs14-like that was upregulated in biofilms of all three species (Saci_1223, SSO1101 and ST0837) (Table 2). These putative proteins are homologous to the Lrs14 protein (SSO1108) of *S. solfataricus*, the protein levels of which were also increased during the biofilm lifestyle (Table 3). Thus, the expression of these homologous transcriptional regulators might constitute a key regulatory factor involved in *Sulfolobus* biofilm development. Additionally, the expression of some other genes
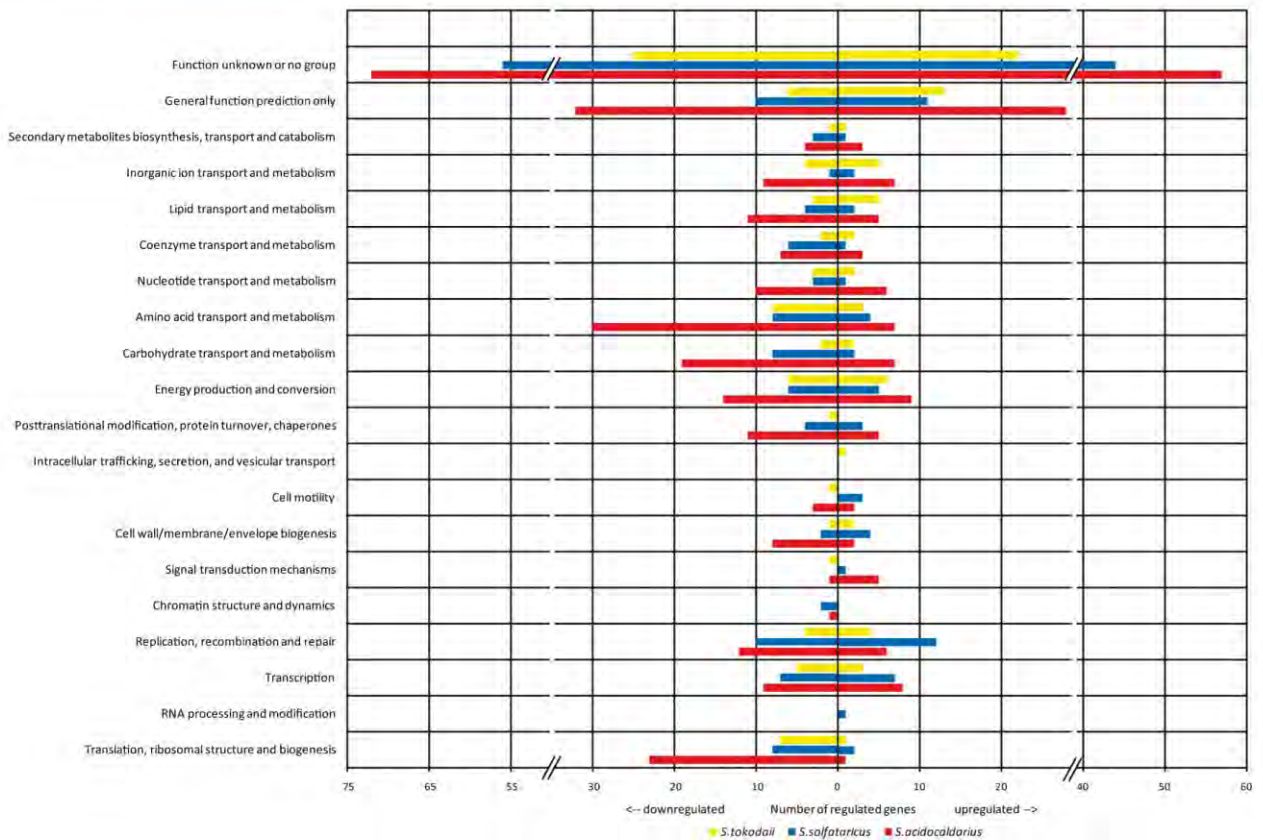
Figure 3. Whole genome expression profiling of *S. acidocaldarius*, *S. solfataricus* and *S. tokodaii* biofilms compared to planktonic cells after 2 days of growth. Genes whose expression levels significantly changed were categorized into functional groups in terms of their COG assigned numbers. The bars show the numbers of genes belonging to each group that were altered in expression (up- and down-regulated).

encoding for homologous Lrs14 proteins were also altered during the biofilm mode of growth, as revealed by qRT-PCR experiments (Table S4, Supporting Information).

Transcriptional Response of Biofilm-Grown *Sulfolobus* Strains

To broaden our analysis from proteomics to include transcriptomics to identify biofilm-regulated genes, the transcriptional profile of *S. acidocaldarius*, *S. solfataricus* and *S. tokodaii* biofilm-associated cells was compared to that of their planktonic counterparts using microarray analysis. Results from the microarrays indicates that the expression of 437, 244, and 152 transcripts changed significantly for *S. acidocaldarius*, *S. solfataricus* and *S. tokodaii*, respectively, during the establishment of a two day old biofilm (Supporting Information, Excel file "Transcriptomic significant data.xlsx"). *S. acidocaldarius* transcriptomic data showed that 335 genes (~15% of the *S. acidocaldarius* genome) displayed a 1.5-fold ($\log_2 0.5$) or more change in expression. These included 103 genes that were up-regulated in the biofilm and 206 down-regulated genes. For *S. solfataricus*, 103 genes had an altered expression level of 1.5-fold or more (~3.4% of the *S. solfataricus* genome), the majority of which (60) were down-regulated, while 43 were up-regulated. *S. tokodaii* transcriptomic data showed that the change in expression levels was lower than those from *S. acidolcaldarius* and *S. solfataricus*. Up to 32 genes were differentially regulated 1.5-fold or more in *S. tokodaii* (~1% of the genome), 15 of which that were up-regulated in biofilm and 17 of which were down-regulated.

It was determined that 51%, 59% and 66% of the differentially expressed genes corresponded to those annotated as having hypothetical or unknown function for *S. acidocaldarius*, *S. solfataricus* and *S. tokodaii*, respectively. All biofilm-regulated genes were catalogued into functional groups according to their COG category. The analysis yielded genes predominantly involved in energy production, energy conversion, amino acid metabolism, lipid and carbohydrate metabolism, transport related functions, and cell surface appendages (Figure 3). The key findings are discussed below (Table 3) and the complete data set is presented in the Supporting Information, Excel file: "Transcriptomic significant data.xlsx".

RNA microarray experiments displayed biofilm-regulated genes encoding terminal oxidases in *Sulfolobus* spp. cells. More specifically, the data show up-regulation of the gene encoding for the polypeptide I of the cytochrome c oxidase complex *ba3* in both *S. acidocaldarius* (Saci_0097) and *S. tokodaii* (ST2595) biofilm-associated cells. In addition, a quinol oxidase-2 gene (*sox*E) was also up-regulated in *S. solfataricus* (SSO2972). In *S. acidocaldarius*, SoxE forms part of the *bb3* terminal oxidase complex SoxM (SoxEFGHIM).[35] In general, the findings from proteomic analyses revealed no noteworthy correlation at the transcriptomic level, and only the down-regulation of V-type ATPase subunit B encoding gene (Saci_1549) correlated on both in transcriptomic and proteomic analyses (Table 3).

As performed for the proteomic data, a BLASTp analysis was performed for each transcript using the encoded amino acid

sequences for queries of both significantly up-regulated genes and significantly down-regulated genes. By doing so, we were able to cluster biofilm-regulated genes common to all three *Sulfolobus* species (Figure 3, Table 2). From the up-regulated data set, only one gene was determined to be overexpressed in all three *Sulfolobus* species in biofilm-associated cells (Figure 2, Table 2). This change corresponds to an ATP-binding transporter (Saci_2305, SSO0053 and ST0535), most likely involved in cation detoxification. Further ORFs annotated as inorganic substrates transporters were found to be up-regulated in at least two *Sulfolobus* strains (SSO1078 and ST1577).

On the other hand, the single common biofilm down-regulated gene, or alternatively, up-regulated in planktonic cells, corresponded to a 3-oxoacyl-(acyl-carrier-protein) reductase (Saci_1792, SSO0975 and ST1299) (Table 3). Interestingly, this enzyme is involved in the production of the quorum sensing autoinducer 3-oxo-C12-HSL in *P. aeuruginosa*.[36]

Some of the genes proposed to be required for flagella biosynthesis and assembly were up-regulated in *S. acidocaldarius* biofilm-associated cells, as revealed by RNA microarrays (Table 3). The UV-inducible type IV pili related gene *ups*F (SSO0119) was up-regulated. *ups*F encodes a putative transmembrane protein proposed to form part of the membrane platform of the pili structure (Table 3).

The expression of some genes catalogued into the cell wall/membrane/envelope biogenesis functional group was also altered in *Sulfolobus* biofilm cells (Table 3). *S. acidocaldarius* displayed the overexpression of ORFs Saci_0134, which encodes a hypothetical protein sharing significant sequence similarity to an annotated NAD-dependent epimerase/dehydratase of *Metallosphaera sedula* (Msed_0434). This enzyme is potentially involved in extracellular polysaccharides (EPS) production.[37]

■ DISCUSSION

General Overview

We previously described that *S. acidocaldarius*, *S. solfataricus*, and *S. tokodaii* form very different biofilm morphologies, ranging from simple carpet structures in *S. solfataricus* to high-density tower-like forming structures in *S. acidocaldarius*.[10] In this study, we have further characterized the process of *Sulfolobus* biofilm formation by integrating spectroscopic analysis, transcriptomics and proteomics in order to determine how each of the three species is adapted to growth in biofilms.

As we showed through FTIR analysis, spectral data sets from biofilm cells within *Sulfolobus* biofilms differed substantially from their planktonic counterparts. In addition, we were able to show that a biofilm-associated lifestyle displayed distinct expression transcriptomic and proteomic profiles in all *Sulfolobus* species. These results resonate with those from studies of bacteria, in which proteomics and FT-IR spectroscopy with multivariate statistical analysis were combined to show a distinct, species-specific differences between the physiology of biofilm-associated and planktonic bacterial cells.[20,21,38,39]

In addition, the expression profile as per microarray analysis showed that the biofilm lifestyle affects each strain differently. While ca. 15% of the *S. acidocaldarius* genes' expression was altered by a factor of 1.5 or more, the change in genes expression patterns represented only ~3.4 and ~1% in *S. solfataricus* and *S. tokodaii*, respectively. The percentage differences in biofilm-regulated genes between the *Sulfolobus* species are consistent with what has been reported in transcriptomes from biofilm-grown

bacteria. For example, in *E. coli*, 5.5% of ORFs were determined to have different expression patterns in biofilm-associated cells, while 14% of genes in biofilm-associated *B. subtilis* cells had a different expression pattern when compared to planktonic cells.[40,41] Furthermore, the numbers of biofilm-regulated genes in other bacterial systems are even smaller, as *P. aeruginosa* transcriptomic experiments showed that only 1% of genes are differentially expressed in biofilms.[42]

The difference in gene expression levels between *Sulfolobus* biofilm-associated and planktonic cells were found to be less than that of eubacteria. Thus, it is tempting to suggest that lifestyle transition from planktonic to biofilm does not radically alter the regulated transcript abundance in *Sulfolobus* biofilms. However, even slight changes in gene expression may potentially have a profound effect on cellular physiology, as has been described by analyses of transcriptomes from biofilm-associated bacteria.[14]

Discrepancies observed between transcriptome and proteome profiling underscores the putative role that post-transcriptional and post-translational regulation mechanisms might play in *Sulfolobus* biofilm formation. In this regard, the reduced regulation at the transcriptional level observed in *S. tokodaii* in comparison to the remarkable proteomic changes obtained suggests that the physiological effect might correspond to intense post-transcriptional regulation. Moreover, in the future we expect to gain further understanding of the role of regulatory noncoding RNAs in biofilm-associated *Sulfolobus* cells.

Energetic Adjustments during the Biofilm Mode of Life

Genes and proteins involve in energetic metabolism were highly altered in *Sulfolobus* spp. biofilm-associated population. These changes included mainly genes related to respiratory complexes, Tricarboxylic acid cycle (TCA) enzymes and V-ATPases subunits (Table 3, Figure 3). Genes encoding cytochrome o ubiquinol oxidase subunits have been also described as up-regulated in both *Salmonella enterica* serovar Tiphymurium and *E. coli* K-12 biofilm-associated cells, suggesting that the environment of these biofilms was aerobic,[13,15] which might also be the case for *Sulfolobus* biofilms. On the other hand, previous studies have shown that terminal respiratory complexes work as proton pumps for maintaining the intracellular pH and generating proton motive force in certain *Sulfolobales*.[43] Moreover, it has been proposed that the SoxM complex might serve as a pH sensor and it would assume its highest activity when the pH rises to values greater than 5 in the extracellular medium.[35] As we previously observed, the pH in the extracellular medium during biofilm development progressively raises above 5 in *Sulfolobus* spp. cells (Koerdt et al., unpublished results). Consequently, the overexpression of Sox complex-related genes might be a response to keep the ambient pH down.

Furthermore, several genes playing a role in TCA cycle were also altered, being most of them down-regulated in biofilm-associated cells, suggesting a decreased metabolic activity in this cell population in comparison to the planktonic counterparts. V-ATPases subunits were also down-regulated in *S. acidocaldarius* biofilm-associated cells (Table 3). Conversely, the ATP synthase subunit E was found up-regulated in *S. solfataricus* biofilm-associated cells (Table 3).

Cell Surface Modifications

As we have previously described, *S. acidocaldarius* more readily engages in community formation than other *Sulfolobus* species.[10] This descriptive observation is conducive with and complementary to our spectroscopic analysis. *S. acidocaldarius* showed the

most radical spectral change in comparisons of biofilm-associated versus planktonic samples. In line with this premise, XPS analysis also showed that *S. acidocaldarius* biofilm-associated cells experienced an increase of polysacharide-containing molecules on their cell surfaces (Table 1). Interestingly, a putative glycosyl tranferase-encoding gene were regulated in *S. acidocaldarius* (Table 3). Glycosyltransferases (GTs) play an important role modifying both lipid and protein components of biological membranes by the covalent addition of polysaccharides. In addition, the specific function of GTs in biosynthesis of high-molecular-weight sugar-rich heteropolymeric EPS molecules has been described in bacterial systems.[44] Moreover, GT encoding genes have been found to be overexpressed in bacterial biofilms, and their disruption alters the ability to synthesize the EPS matrix.[45] The increased expression of EPS production related genes observed in *S. acidocaldarius* biofilm cells might be correlated to its particular cell surface chemical composition. Future analyses will focus on determining their involvement in the EPS biosynthetic pathway, which is expected to involve further enzymatic activities.

Commonly Biofilm-Regulated Genes among the Three Strains

The description of biofilm-regulated genes and proteins common to all three examined *Sulfolobus* species yielded some interesting findings. All three displayed increased levels of a putative transcriptional regulator belonging to the Lrs14-like proteins (Saci_1223, SSO1101 and ST0837) (Table 2). These putative proteins are homologous to the Lrs14 protein (SSO1108) of *S. solfataricus*, the protein levels of which were also increased during the biofilm lifestyle (Table 3). It has been described that *S. solfataricus* Lrs14 (SSO1108) is autoregulated in a negative manner and accumulates in the midexponential and late growth phases.[46] Archaeal Lrs14-like regulators are thought to be related to the Lrp-AsnC bacterial transcriptional regulator family (leucine-responsive regulatory protein).[46] The Lrp *E. coli* regulon includes genes involved in amino acid biosynthesis (*ilvIH*, *serA*), in the biosynthesis of cell surface structures such as pili (*pap*, *fan*, *fim*), and in the assimilation of ammonia (*glnA*, gltBD).[47] However, Lrp-like regulators have not been yet directly identified as being involved in biofilms. In biofilm-associated bacteria, several global gene regulators are known to control a wide range of adaptive physiological and regulatory circuits within sessile community and to be up-regulated as a response to environmental conditions, that is, nutrient limitation, oxygen availability and osmotic stress.[15] Thus, the expression of these homologous transcriptional regulators might constitute a master regulatory factor involved in *Sulfolobus* biofilm development. The functional role of Lrs14-like proteins in *Sulfolobus* biofilms is being currently investigated.

One gene, 3-oxoacyl-(acyl-carrier-protein) reductase (FabG) (Table 3), was found to be down-regulated in biofilm-associated cells (and up-regulated in planktonic cells) in all three *Sulfolobus* strains. FabG enzymatic activity is involved in the production of the Quorum Sensing (QS) autoinducer (AI) 3-oxo-dodecanoyl-HSL (3-oxo-C12-HSL) in *P. aeruginosa*.[36] In bacteria, QS phenomena is known to be closely interrelated to biofilm formation. QS provides the means to coordinate the activities of cells so that they function as a multicellular community. Interestingly, FabG levels were also found to be heightened in *P. aeuruginosa* planktonic cells in comparison to their biofilm counterparts.[17] Although, it seems that *Sulfolobus* genomes do not encode

LasI-homologous proteins, an utterly different mechanism employed by an unknown activity might be involved in tandem with FabG to produce putative archaeal AI molecules. In this regard, studies in biofilms of the archaeon *F. acidarmanus* Fer1 showed no evidence for quorum sensing or signaling molecules.[8] However, the production of AI molecules by *Sulfolobus* cells still has to be proven. Furthermore, in the future, it will be of interest to determine the potential occurrence of cell signaling and communication within *Sulfolobus* biofilm-associated communities.

■ ASSOCIATED CONTENT

ⓢ Supporting Information

DNA microarrays significant data of each *Sulfolobus* strains is listed in the exel file "Transcriptomic significant data.xlsx". Proteomic data analysis of each *Sulfolobus* strains is listed in the exel files: "Proteomic suplementary-1.xlsx" for *S. solfataricus* P2, "Proteomic suplementary-2.xlsx" for *S. acidocaldarius* and "Proteomic suplementary-3.xlsx" for *S. tokodaii*. Sheet 1 shows details of peptides lists and Sheet 2 shows details of quantified proteins lists. Table S1 shows binding energies, assignments and composition (%) of XPS spectral bands of *Sulfolobus acidocaldarius, solfataricus* and *tokodaii* grown planktonically and as biofilm. Table S2, iTRAQ labeling of samples. Table S3 shows all significant result obtained from iTRAQ proteomic analysis. Table S4, determination of gene expression by qRT-PCR. Table S5 lists qPCR oligonucleotides. This material is available free of charge via the Internet at http://pubs.acs.org.

■ AUTHOR INFORMATION

Corresponding Author
*S.-V. Albers, e-mail: albers@mpi-marburg.mpg.de. Tel.: +496421178426. Fax: +496421178429.

Author Contributions
[‡]These authors contributed equally to this manuscript

■ ACKNOWLEDGMENT

■ REFERENCES

(1) Lopez, D.; Vlamakis, H.; Kolter, R. Biofilms. *Cold Spring Harb. Perspect. Biol.* **2010**, *2* (7), a000398.

(2) Kruger, M.; Blumenberg, M.; Kasten, S.; Wieland, A.; Kanel, L.; Klock, J. H.; Michaelis, W.; Seifert, R. A novel, multi-layered methanotrophic microbial mat system growing on the sediment of the Black Sea. *Environ. Microbiol.* **2008**, *10* (8), 1934–47.

(3) Zhang, C. L.; Ye, Q.; Huang, Z.; Li, W.; Chen, J.; Song, Z.; Zhao, W.; Bagwell, C.; Inskeep, W. P.; Ross, C.; Gao, L.; Wiegel, J.; Romanek, C. S.; Shock, E. L.; Hedlund, B. P. Global occurrence of archaeal amoA genes in terrestrial hot springs. *Appl. Environ. Microbiol.* **2008**, *74* (20), 6417–26.

(4) Rinker, K. D.; Kelly, R. M. Growth Physiology of the Hyperthermophilic Archaeon *Thermococcus litoralis*: Development of a Sulfur-Free Defined Medium, Characterization of an Exopolysaccharide, and Evidence of Biofilm Formation. *Appl. Environ. Microbiol.* **1996**, *62* (12), 4478–85.

(5) Näther, D. J.; Rachel, R.; Wanner, G.; Wirth, R. Flagella of *Pyrococcus furiosus*: multifunctional organelles, made for swimming, adhesion to various surfaces, and cell-cell contacts. *J. Bacteriol.* **2006**, *188* (19), 6915–6923.

(6) Schopf, S.; Wanner, G.; Rachel, R.; Wirth, R. An archaeal bi-species biofilm formed by *Pyrococcus furiosus* and *Methanopyrus kandleri*. *Arch. Microbiol.* **2008**, *190* (3), 371–7.

(7) Lapaglia, C.; Hartzell, P. L. Stress-Induced Production of Biofilm in the Hyperthermophile Archaeoglobus fulgidus. *Appl. Environ. Microbiol.* **1997**, *63* (8), 3158–63.

(8) Baker-Austin, C.; Potrykus, J.; Wexler, M.; Bond, P. L.; Dopson, M. Biofilm development in the extremely acidophilic archaeon 'Ferroplasma acidarmanus' Fer1. *Extremophiles* **2010**, *14* (6), 485–491.

(9) Zolghadr, B.; Klingl, A.; Koerdt, A.; Driessen, A. J.; Rachel, R.; Albers, S. V. Appendage-mediated surface adherence of *Sulfolobus solfataricus*. *J. Bacteriol.* **2010**, *192* (1), 104–10.

(10) Koerdt, A.; Gödeke, J.; Berger, J.; Thormann, K. M.; Albers, S. V. Crenarchael biofilm formation under extreme conditions. *PLoS One* **2010**, *5* (11), e14104.

(11) Sauer, K. The genomics and proteomics of biofilm formation. *Genome Biol.* **2003**, *4* (6), 219.

(12) Beloin, C.; Valle, J.; Latour-Lambert, P.; Faure, P.; Kzreminski, M.; Balestrino, D.; Haagensen, J. A.; Molin, S.; Prensier, G.; Arbeille, B.; Ghigo, J. M. Global impact of mature biofilm lifestyle on *Escherichia coli* K-12 gene expression. *Mol. Microbiol.* **2004**, *51* (3), 659–74.

(13) Beloin, C.; Ghigo, J. M. Finding gene-expression patterns in bacterial biofilms. *Trends Microbiol* **2005**, *13* (1), 16–9.

(14) Schembri, M. A.; Kjaergaard, K.; Klemm, P. Global gene expression in *Escherichia coli* biofilms. *Mol. Microbiol.* **2003**, *48* (1), 253–67.

(15) Hamilton, S.; Bongaerts, R. J. M.; Mulholland, F.; Cochrane, B.; Porter, J.; Lucchini, S.; Lappin-Scott, H. M.; Hinton, J. C. D. The transcriptional programme of Salmonella enterica serovar Typhimurium reveals a key role for tryptophan metabolism in biofilms. *BMC Genomics* **2009**, *10*, 599–620.

(16) Wen, Z. T.; Burne, R. A. Functional genomics approach to identifying genes required for biofilm development by *Streptococcus mutans*. *Appl. Environ. Microbiol.* **2002**, *68* (3), 1196–203.

(17) Nigaud, Y.; Cosette, P.; Collet, A.; Song, P. C.; Vaudry, D.; Vaudry, H.; Junter, G. A.; Jouenne, T. Biofilm-induced modifications in the proteome of *Pseudomonas aeruginosa* planktonic cells. *Biochim. Biophys. Acta* **2010**, *1804* (4), 957–66.

(18) Oosthuizen, M. C.; Steyn, B.; Lindsay, D.; Brozel, V. S.; von Holy, A. Novel method for the proteomic investigation of a dairy-associated *Bacillus cereus* biofilm. *FEMS Microbiol. Lett.* **2001**, *194* (1), 47–51.

(19) Steyn, B.; Oosthuizen, M. C.; MacDonald, R.; Theron, J.; Brozel, V. S. The use of glass wool as an attachment surface for studying phenotypic changes in *Pseudomonas aeruginosa* biofilms by two-dimensional gel electrophoresis. *Proteomics* **2001**, *1* (7), 871–9.

(20) Mukherjee, J.; Ow, S. Y.; Noirel, J.; Biggs, C. A. Quantitative protein expression and cell surface characteristics of *Escherichia coli* MG1655 biofilm. *Proteomics* **2010**, *11* (3), 339–351.

(21) Serra, D. O.; Lücking, G.; Weiland, F.; Schulz, S.; Görg, A.; Yantorno, O. M.; Ehling-Schulz, M. Proteome approaches combined with Fourier transform infrared spectroscopy revealed a distinctive biofilm physiology in *Bordetella pertussis*. *Proteomics* **2008**, *8* (23–24), 4995–5010.

(22) Naumann, D., Infrared spectroscopy in microbiology. *Encyclopedia of analytical chemistry*; John Wiley and Sons ltd.: Chichester, 2000.

(23) Ojeda, J. J.; Romero-Gonzalez, M. E.; Bachmann, R. T.; Edyvean, R. G.; Banwart, S. A. Characterization of the cell surface and cell wall chemistry of drinking water bacteria by combining XPS, FTIR spectroscopy, modeling, and potentiometric titrations. *Langmuir* **2008**, *24* (8), 4032–40.

(24) Zaparty, M.; Esser, D.; Gertig, S.; Haferkamp, P.; Kouril, T.; Manica, A.; Pham, T. K.; Reimann, J.; Schreiber, K.; Sierocinski, P.; Teichmann, D.; van Wolferen, M.; von Jan, M.; Wieloch, P.;

Albers, S. V.; Driessen, A. J.; Klenk, H. P.; Schleper, C.; Schomburg, D.; van der Oost, J.; Wright, P. C.; Siebers, B. "Hot standards" for the thermoacidophilic archaeon *Sulfolobus solfataricus*. *Extremophiles* **2009**, *14* (1), 119–42.

(25) Pham, T. K.; Roy, S.; Noirel, J.; Douglas, I.; Wright, P. C.; Stafford, G. P. A quantitative proteomic analysis of biofilm adaptation by the periodontal pathogen *Tannerella forsythia*. *Proteomics* **2010**, *10* (17), 3130–41.

(26) Eboigbodin, K. E.; Biggs, C. A. Characterization of the extracellular polymeric substances produced by *Escherichia coli* using infrared spectroscopic, proteomic, and aggregation studies. *Biomacromolecules* **2008**, *9* (2), 686–95.

(27) Piatek, R.; Bruździak, P.; Zalewska-Piatek, B.; Kur, J.; Stangret, J. Preclusion of irreversible destruction of Dr adhesin structures by a high activation barrier for the unfolding stage of the fimbrial DraE subunit. *Biochemistry* **2009**, *48* (49), 11807–16.

(28) Helm, D.; Labischinski, H.; Schallehn, G.; Naumann, D. Classification and identification of bacteria by Fourier-transform infrared spectroscopy. *J. Gen. Microbiol.* **1991**, *137* (1), 69–79.

(29) Jiang, W.; Saxena, A.; Song, B.; Ward, B. B.; Beveridge, T. J.; Myneni, S. C. Elucidation of functional groups on gram-positive and gram-negative bacterial surfaces using infrared spectroscopy. *Langmuir* **2004**, *20* (26), 11433–42.

(30) Geoghegan, M.; Andrews, J. S.; Biggs, C. A.; Eboigbodin, K. E.; Elliott, D. R.; Rolfe, S.; Scholes, J.; Ojeda, J. J.; Romero-Gonzalez, M. E.; Edyvean, R. G.; Swanson, L.; Rutkaite, R.; Fernando, R.; Pen, Y.; Zhang, Z.; Banwart, S. A. The polymer physics and chemistry of microbial cell attachment and adhesion. *Faraday Discuss.* **2008**, *139*, 85–103. discussion105–28. 419–20.

(31) Serra, D. O.; Lucking, G.; Weiland, F.; Schulz, S.; Gorg, A.; Yantorno, O. M.; Ehling-Schulz, M. Proteome approaches combined with Fourier transform infrared spectroscopy revealed a distinctive biofilm physiology in *Bordetella pertussis*. *Proteomics* **2008**, *8* (23–24), 4995–5010.

(32) Bosch, A.; Serra, D.; Prieto, C.; Schmitt, J.; Naumann, D.; Yantorno, O. Characterization of Bordetella pertussis growing as biofilm by chemical analysis and FT-IR spectroscopy. *Appl. Microbiol. Biotechnol.* **2006**, *71* (5), 736–47.

(33) Clarke, D. J.; Ortega, X. P.; Mackay, C. L.; Valvano, M. A.; Govan, J. R.; Campopiano, D. J.; Langridge-Smith, P.; Brown, A. R. Subdivision of the bacterioferritin comigratory protein family of bacterial peroxiredoxins based on catalytic activity. *Biochemistry* **2010**, *49* (6), 1319–30.

(34) Guagliardi, A.; Napoli, A.; Rossi, M.; Ciaramella, M. Annealing of complementary DNA strands above the melting point of the duplex promoted by an archaeal protein. *J. Mol. Biol.* **1997**, *267* (4), 841–8.

(35) Komorowski, L.; Verheyen, W.; Schafer, G. The archaeal respiratory supercomplex SoxM from *S. acidocaldarius* combines features of quinole and cytochrome c oxidases. *Biol. Chem.* **2002**, *383* (11), 1791–9.

(36) Hoang, T. T.; Sullivan, S. A.; Cusick, J. K.; Schweizer, H. P. Beta-ketoacyl acyl carrier protein reductase (FabG) activity of the fatty acid biosynthetic pathway is a determining factor of 3-oxo-homoserine lactone acyl chain lengths. *Microbiology* **2002**, *148* (Pt 12), 3849–56.

(37) Auernik, K. S.; Maezato, Y.; Blum, P. H.; Kelly, R. M. The genome sequence of the metal-mobilizing, extremely thermoacidophilic archaeon *Metallosphaera sedula* provides insights into bioleaching-associated metabolism. *Appl. Environ. Microbiol.* **2008**, *74* (3), 682–92.

(38) Vilain, S.; Brozel, V. S. Multivariate approach to comparing whole-cell proteomes of *Bacillus cereus* indicates a biofilm-specific proteome. *J. Proteome Res.* **2006**, *5* (8), 1924–30.

(39) Vilain, S.; Cosette, P.; Hubert, M.; Lange, C.; Junter, G. A.; Jouenne, T. Comparative proteomic analysis of planktonic and immobilized *Pseudomonas aeruginosa* cells: a multivariate statistical approach. *Anal. Biochem.* **2004**, *329* (1), 120–30.

(40) Ren, D.; Bedzyk, L. A.; Setlow, P.; Thomas, S. M.; Ye, R. W.; Wood, T. K. Gene expression in *Bacillus subtilis* surface biofilms with and without sporulation and the importance of yveR for biofilm maintenance. *Biotechnol. Bioeng.* **2004**, *86* (3), 344–64.

(41) Ren, D.; Bedzyk, L. A.; Thomas, S. M.; Ye, R. W.; Wood, T. K. Gene expression in *Escherichia coli* biofilms. *Appl. Microbiol. Biotechnol.* **2004**, *64* (4), 515–24.

(42) Whiteley, M.; Bangera, M. G.; Bumgarner, R. E.; Parsek, M. R.; Teitzel, G. M.; Lory, S.; Greenberg, E. P. Gene expression in *Pseudomonas aeruginosa* biofilms. *Nature* **2001**, *413* (6858), 860–4.

(43) Lubben, M.; Arnaud, S.; Castresana, J.; Warne, A.; Albracht, S. P.; Saraste, M. A second terminal oxidase in Sulfolobus acidocaldarius. *Eur. J. Biochem.* **1994**, *224* (1), 151–9.

(44) Lebeer, S.; Verhoeven, T. L.; Francius, G.; Schoofs, G.; Lambrichts, I.; Dufrene, Y.; Vanderleyden, J.; De Keersmaecker, S. C. Identification of a Gene Cluster for the Biosynthesis of a Long, Galactose-Rich Exopolysaccharide in *Lactobacillus rhamnosus* GG and Functional Analysis of the Priming Glycosyltransferase. *Appl. Environ. Microbiol.* **2009**, *75* (11), 3554–63.

(45) Koo, H.; Xiao, J.; Klein, M. I.; Jeon, J. G. Exopolysaccharides produced by *Streptococcus mutans* glucosyltransferases modulate the establishment of microcolonies within multispecies biofilms. *J. Bacteriol.* **2010**, *192* (12), 3024–32.

(46) Napoli, A.; van der Oost, J.; Sensen, C. W.; Charlebois, R. L.; Rossi, M.; Ciaramella, M. An Lrp-like protein of the hyperthermophilic archaeon *Sulfolobus solfataricus* which binds to its own promoter. *J. Bacteriol.* **1999**, *181* (5), 1474–80.

(47) Calvo, J. M.; Matthews, R. G. The leucine-responsive regulatory protein, a global regulator of metabolism in *Escherichia coli*. *Microbiol. Rev.* **1994**, *58* (3), 466–90.

3.3.1 Supplemented material

Online available data which is not shown here:

http://pubs.acs.org/doi/suppl/10.1021/pr2003006

MS Exel

- pr2003006_si_002.xls (3.78 MB)
- pr2003006_si_003.xls (3.64 MB)
- pr2003006_si_004.xls (4.14 MB)
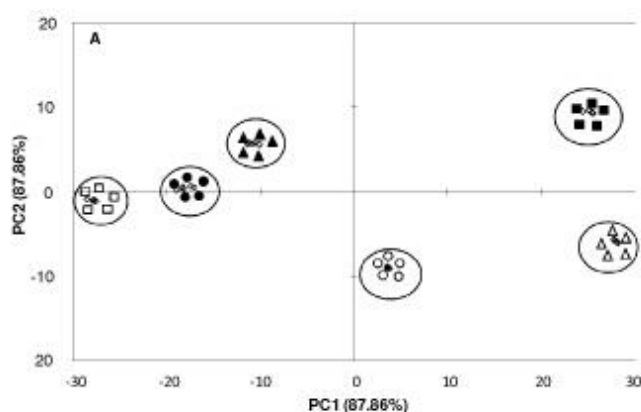- pr2003006_si_005.xls (241 KB)

Figure S1. Principal components analysis (PCA) for FTIR spectra of *S. acidocaldarius* (■□), *S. solfataricus* (●○) and *S. tokodaii* (▲△) samples grown either as biofilm (filled symbols) or planktonically (open symbols). PCA plot of first and second principal component for the FTIR spectra is shown. Five replicates for strain and growth conditions were performed.
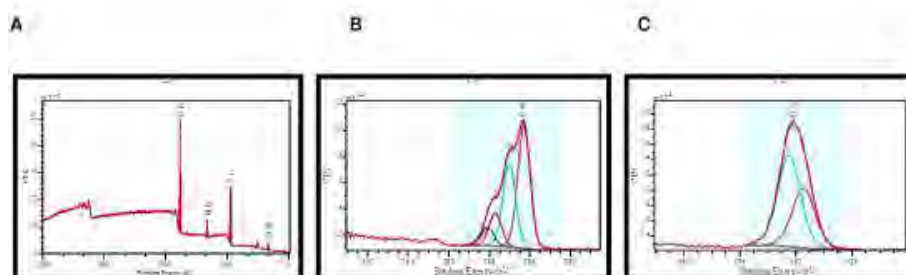

Figure S2. A wide scan of the XPS survey spectrum of *Sulfolobus acidocaldarius* grown planktonically as an example to shown the distribution of the binding energies of different elements (A). Plots (B) and (C) show the high resolution scan deconvoluted peaks related to C_{1s} and O_{1s} respectively for *Sulfolobus acidocaldarius* grown planktonically. For the deconvolution of the carbon peaks (B) the peak at position 284.6eV coloured pink corresponds to C-(C,H), peak at position 286.05eV coloured light blue corresponds to C-(O,N), peak at position 287.36eV coloured red corresponds to C=O, O-C-O and peak at position 288.61eV coloured deep blue corresponds to COOR. For the deconvoluted oxygen peaks (C) the peak at position 531.38eV coloured pink corresponds to C=O, P=O, whereas the peak at position 532.44eV coloured light blue corresponds to C-OH, C-O-C, P-OH. In plot A, the Si peak is likely to be derived from the glassware used in the sample preparation, as similar found by Ojeda et al [23]

Table S1. Binding energies, assignments and composition (%) of XPS spectral bands of *Sulfolobus acidocaldarius, solfataricus* and *tokodaii* grown planktonically and as biofilm.

Sulfolobus acidocaldarius planktonic				*Sulfolobus acidocaldarius* Biofilm			
Element	Peak (eV)	Conc (%)	assignment	Element	Peak (eV)	Conc (%)	assignment
Total C	282.66	59.41±1.30		Total C	283.5	51.25±4.31	
Total O	529.66	26.55±1.49		Total O	530	30.21±1.02*	
Total N	397.33	7.35±0.49		Total N	398	6.50±2.74	
C_{1s}	284.6	41.84±7.67	C-(C,H)	C_{1s}	284.6	43.72±1.01*	C-(C,H)
C_{1s}	286.05	36.43±5.02	C-(O,N)	C_{1s}	286.05	36.06±0.68*	C-(O,N)
C_{1s}	287.36	13.34±0.78*	C=O, O-C-O	C_{1s}	287.36	16.21±1.00*	C=O, O-C-O
C_{1s}	288.61	8.4±1.87	COOR	C_{1s}	288.61	4.02±0.66	COOR
O_{1s}	531.38	36.1±4.86*	C=O, P=O	O_{1s}	531.38	45.44±1.13*	C=O, P=O
O_{1s}	532.44	60.46*[†]	C-OH, C-O-C, P-OH	O_{1s}	532.44	54.56±1.13*	C-OH, C-O-C, P-OH

NB: *sign against the values implies that they are statistically different as found by carrying "t-test".
[†]Only one replicate could be resolved

Sulfolobus solfataricus planktonic				*Sulfolobus solfataricus* biofilm			
Element	Peak (eV)	Conc (%)	assignment	Element	Peak (eV)	Conc (%)	assignment
Total C	282.33	53.16±5.3		Total C	282	53.74±0.92	
Total O	529.33	30.6±3.68		Total O	529	30.55±0.11	
Total N	397.33	7.37±1.22		Total N	397	6.6±1.14	
C_{1s}	284.6	50.51±1.10	C-(C,H)	C_{1s}	284.6	51.72±1.36*	C-(C,H)
C_{1s}	286.05	31.46±1.03	C-(O,N)	C_{1s}	286.05	30.99±1.07*	C-(O,N)
C_{1s}	287.36	14.98±1.99	C=O, O-C-O	C_{1s}	287.36	15.81±0.04	C=O, O-C-O
C_{1s}	288.61	3.06±2.05	COOR	C_{1s}	288.61	1.5±0.33	COOR
O_{1s}	531.38	40.1±3.97*	C=O, P=O	O_{1s}	531.38	36.77±2.56*	C=O, P=O
O_{1s}	532.44	59.9±3.97*	C-OH, C-O-C, P-OH	O_{1s}	532.44	63.23±2.56*	C-OH, C-O-C, P-OH

NB: *sign against the values implies that they are statistically different as found by carrying "t-test".

Sulfolobus tokodaii planktonic				*Sulfolobus tokodaii* biofilm,			
Element	Peak (eV)	Conc (%)	assignment	Element	Peak (eV)	Conc (%)	assignment
Total C	282	57.70±0.49		Total C	283	50.32±0.85	
Total O	529	27.08±0.96		Total O	529.33	32.89±1.71*	
Total N	397	7.22±1.24		Total N	397.33	6.73±0.40	
C_{1s}	284.6	48.59±5.31	C-(C,H)	C_{1s}	284.6	46.53±0.20	C-(C,H)
C_{1s}	286.05	32.74±1.54	C-(O,N)	C_{1s}	286.05	35.26±0.76*	C-(O,N)
C_{1s}	287.36	15.47±2.16	C=O, O-C-O	C_{1s}	287.36	16.17±0.7	C=O, O-C-O
C_{1s}	288.61	3.2±1.6	COOR	C_{1s}	288.61	2.05±1.26	COOR
O_{1s}	531.38	45.795±8.38	C=O, P=O	O_{1s}	531.38	36.31±0.07*	C=O, P=O
O_{1s}	532.44	54.205±8.38	C-OH, C-O-C, P-OH	O_{1s}	532.44	63.69±0.07*	C-OH, C-O-C, P-OH

NB: *sign against the values implies that they are statistically different as found by carrying "t-test".

3.4 The role of surface appendages in *Sulfolobus acidocaldarius*

A. Koerdt[#], AL. Henche[#], A. Ghosh and SV Albers. 2011. **Influence of cell surface structures on crenarchaeal biofilm formation** (Submitted to Environmental Microbiology)

The impact of surface appendages in surface attachment and biofilm formation was extensively studied in bacteria while in archaea only a few studies have been demonstrated that some of these extracellular appendages are involved in attachment. The first insight of the requirement of flagella or pili for surface attachment of *Sulfolobus ssp.* was provided by the results obtained from our previous study on *S. solfataricus*. Interestingly, analysis of the biofilm developed under static condition for either of flagella or Ups-Pili mutants of *S. solfataricus* revealed only very little effect in comparison to wild type cells. Therefore, the intention of this work was to figure out if *S. acidocaldarius* MW001 which expresses App-pili besides flagella and Ups-pli, behaves in a similar fashion under biofilm growth like for *S. solfataricus* PBL2025. A detailed analysis of a combination of double and triple appendage mutants (flagella, Ups-, and Aap-pili) of *S. acidocaldarius* was performed in the present study where the main goal was to find out whether they can influence biofilm formation independently or in a combination. Our analysis revealed that for *S. acidocaldarius* MW001 some of these appendages are important in the maintenance of the typical architecture. Different numbers of cells were found to attach to the surface for different double and triple mutants; however the single mutants exhibited only slight differences compared to wild type strain. In general, the deletion of two or all the surface appendages resulted in dramatic decrease in the attachment with only one exception where the double mutant (Δ*upsE*Δ*flaJ*) expressing only the Aap-Pili on the surface, showed an increase of 150% in comparison to MW001. Furthermore, a regulation involving the *aapF* seems to be occurred where an increased expression of flagella has been evident. The hyper-flagellated Δ*aapF*-mutant attaches as clustered cells indicating precise interplay between the Aap-pili with the flagella. Furthermore, we observed three distinct phenotypes of the biofilm formed by the mutant strains indicating a distinct role for each filament in initial attachment and biofilm development. The dominant Aap-phenotype (high cell density) and the Ups-phenotype (tower-structure with high EPS production) were assigned separately from the wild type phenotype.

All biofilm or surface attachment related analyses were performed or supervised by Andrea Koerdt. The analysis of the CLSM data, the pixel calculation and the construction of GFP and the adaptation for the use in biofilm was done by Andrea

Koerdt. The construction of the deletion mutants, the motility assay, the calculation of the results of the surface attachment and support for the biofilm assay were performed by Anna Lena Henche. The electron microscopy was performed by Anna Lena Henche and Abhrajyoti Ghosh. The manuscript was written by Sonja-Verena Albers and revised by all authors.

Influence of cell surface structures on crenarchaeal biofilm formation using a thermostable green fluorescent protein

Henche; AL#[1], Koerdt, A#[1], Ghosh. A.[1], Albers, S.-V.[1*]

Abstract   The thermoacidophilic crenarchaeote *Sulfolobus acidocaldarius* displays three distinct type IV pili structures on its surface, (i) the flagellum, (ii) the UV induced pili and (iii) the adhesive pili. In bacteria surface appendages play an important role in the spatial organization from initial surface attachment to the development of a mature community structure. To investigate the influence of a diverse set of type IV pili in *S. acidocaldarius*, single, double and triple mutants lacking the cell surface structures were constructed and analyzed for their behavior in attachment assays and during biofilm formation using confocal laser scanning microscopy. The triple mutant was strongly reduced in attachment; however, the aap pili were most important for adherence to glass from a shaking culture. The deletion of the flagella only led to an attachment defect in the presence of the two other pili. Using a heat stable green fluorescent protein, mixed biofilms of different strains could be analyzed for a deeper understanding of the interplay of the surface structures during biofilm formation. During this process the deletion of the aap pili and ups pili led to the most pronounced effects, either an increase in cell density or increased cluster formation as in comparison to the wild type, respectively. All three cell surface appendages therefore seem to play a role in the colonization of surfaces and only the interplay of all three appendages leads to the observed wild type biofilm phenotype.

[1]Molecular Biology of Archaea, Max Planck Institute for terrestrial Microbiology, Karl-von-Frisch-Strasse, 35043 Marburg, Germany

[#]both authors contributed equally

[*]Correspondence to S.V. Albers, e-mail: albers@mpi-marburg.mpg.de, tel.: +496421178426, fax: +496421178429

Introduction

Like bacteria archaea posses a variety of different surface structures like flagella, different kinds of pili, hami and cannulae that are involved in a multitude of functions including surface attachment, mediation of cell aggregation, surface and swimming motility (Albers and Meyer, 2011). Whereas the hami and cannulae seem to be specialized surface structures that have so far been only found in the euryarchaeon SM1 and *Pyrodictium* species (Stetter et al., 1983; Rudolph et al., 2001; Moissl et al., 2005), respectively, most archaea possess flagella and/or pili.

The only archaeal pilus that has not been grouped as a type IV pilus is the appendage formed by the Mth60 pilin from *Methanothermobacter thermoautotrophicus* (Thoma et al., 2008). All other so far characterized archaeal surface structures can be classified as type IV pili (Albers and Pohlschroder, 2009; Pohlschroder et al., 2011). Their structural subunits possess type IV prepilin signal peptides that are processed by a signal peptidase (PibD/FlaK) homologous to the bacterial PilD (Strom and Lory, 1992) and the archaeal homologues were identified in methanogens, halophiles and Sulfolobales (Bardy and Jarrell, 2002; Albers et al., 2003; Tripepi et al., 2010). Moreover, the archaeal pili and flagella assembly systems contain an ATPase and an integral membrane protein that resemble the assembly ATPase and the central membrane protein of bacterial type IV pili assembly systems and therefore these systems seem to be evolutionary linked (Pohlschroder et al., 2011).

Some archaeal type IV pili seem to play a role in adhesion as a PibD deletion mutant in *Haloferax*

volcanii lost its ability to adhere to glass surfaces (Tripepi et al., 2010) and also in *Methanococcus maripaludis* the pili in concert with the flagella proved to be a prerequisite for successful binding of the cells to a variety of abiotic surfaces (Jarrell *et al.*, 2011). The rather thick (15 nm) and very abundant pili of *Ignicoccus hospitalis* were very brittle, therefore it is unlikely that they are involved in attachment, but their function still has to be elucidated (Muller *et al.*, 2009). UV induced (ups) pili have been observed after UV treatment of *S. solfataricus* and *S. acidocaldarius* cells (Frols *et al.*, 2008)(Ajon et al, submitted), respectively. The assembly of the ups pili led to cell aggregation and DNA exchange (Ajon et al. unpublished). Archaeal flagella, which structurally resemble type IV pili, have been implicated in swimming in *Hbt. salinarum* (Marwan *et al.*, 1991) and surface motility in *H. volcanii*, *M. maripaludis* and *S. solfataricus* (Szabo et al., 2007; VanDyke et al., 2009; Tripepi et al., 2010). Moreover, they are important in the initial attachment to surfaces in *S. solfataricus* (Zolghadr *et al.*, 2010) and persistence on surfaces in *M. maripaludis*, *M. villosus* and *Pyrococcus furiosus* (Näther et al., 2006; Bellack et al., 2011; Jarrell et al., 2011). In *S. solfataricus* it was demonstrated that flagella do not seem to play a role in static biofilm formation whereas surprisingly the deletion of the ups pili led to fewer cells adhered at the bottom of the biofilm and cluster formation occurred (Koerdt *et al.*, 2010). Although, the ups pili were first thought to only be involved in cell-cell-aggregation, the biofilm defect of the ups pili deletion mutant confirmed the observation that this mutant also was unable to attach from shaking cultures to abiotic surfaces similar to the non-flagellated cells (Zolghadr *et al.*, 2010). This implied that the ups pili might be involved in the establishment of cell-cell and cell-surface connections under different conditions.

In bacteria the role that type IV pili and flagella play during initial attachment, micro colony formation and biofilm maturation is species dependent. In some bacteria the flagellum is essential for initial attachment as e.g. for *Caulobacter crescentus* (Entcheva-Dimitrov and Spormann, 2004), whereas in *Pseudomonas aeruginosa* the flagellum plays a more vital role in the cap formation of the tower-like structures (Barken *et al.*, 2008). However, an interplay of the type IV pili with the flagella is important to obtain the typical mushroom-like structures known for *P. aeruginosa* biofilms (Klausen et al., 2003; Barken et al., 2008). In the fruit pathogen *Acidovorax citrulli* type IV pili were mainly involved in attachment and biofilm formation whereas the deletion of flagella had no impact on these processes, but was shown essential for the penetration of host tissues (Bahar *et al.*, 2010; Bahar *et al.*, 2011). Therefore the functions that the different surface appendages play during attachment and biofilm formation has to be evaluated in each species separately.

The thermoacidophilic crenarchaeote *S. acidocaldarius* exhibits three type IV pili like appendages at its cell surface (see for image: (Albers and Meyer, 2011)). During exponential growth phase the cells are surrounded by very abundant pili that are termed archaeal adhesive (aap) pili due to their ability to promote attachment to glass surfaces (Henche et al, unpublished). During stationary growth the expression of the flagella is induced (Lassak et al., submitted) and as described earlier the ups pili are formed upon UV light damage (Ajon et al, submitted). In this study we wanted to investigate the role these different cell appendages play in attachment to surface and formation and maturation of *S. acidocaldarius* biofilms. Therefore single, double and the triple mutants lacking either one, two or all three the cell surface appendages have been constructed and tested for their ability to adhere to a glass surface and for the formation of static biofilms for three, six and eight days. Whereas the aap pilus was most important for adhesion, the ups pili had a major effect on the structure of the biofilm and the flagella were involved in release of cells at later time points of biofilm maturation.

Material and Methods

Strains and growth conditions

Sulfolobus acidocaldarius MW001 (Wagner et al, unpublished) and all constructed deletion mutants were aerobically grown in Brock media (Brock *et al.*, 1972) with a pH of 3 at 76°C. The media were supplemented with 0.1% (w/v) tryptone or with 0.1% (w/v) N-Z-Amine or 0.2% maltose for the induction of the expression of eCGP123 (see

below). The growth of the cells was monitored by measurement of the optical density at 600 nm.

Construction of deletion mutant plasmids and complementation plasmids

For the construction of the deletion mutant plasmids the respective up- and downstream flanking regions of *aapF* (saci_2318) and *flaJ* (saci_1172) were PCR amplified from *S. acidocaldarius* genomic DNA. The primer pairs for the *aapF* flanking regions were 606/640 and 607/642 for the up and downstream flanking region, respectively. For the *flaJ* flanking regions primers 600/638 and 602/641 were used. By overlap extension PCR the up and downstream flanking were joined by using the outward bound primer of the respective primer pair. The overlap extension PCR products were restricted with Pst1 and BamHI and subsequently ligated into the plasmid Δ2pyrEF, which contained the pyrEF cassette from *S. solfataricus* (Wagner *et al.*, 2009). This ligation yielded the *aapF* deletion plasmid pSVA179 and the *flaJ* deletion plasmid pSVA180. The deletion mutant construct for *upsE* (saci_1493) was constructed in another study and will be described there (van Wolferen and Albers, in preparation).

Plasmids for the complementation of the Δ*aapF* and Δ*upsE* strain were constructed in the plasmid pSVA406, which contains the *S. solfataricus* pyrEF for selection in *S. acidocaldarius*. The aapF region was amplified using the primer pair 3506/3507 and the upsE region was amplified using primers 3508/3509. Both PCR products were restricted with *Nco*I and *Bam*HI and ligated into pSVA406 yielding plasmids pSVA223 and pSVA224, the *aapF* and *upsE* complementation plasmid, respectively. All constructs were sequenced to confirm their identity. All primer sequences are given in Supplementary Table 1.

Construction of deletion mutants

Methylated deletion mutant of complementation plasmids were transformed into MW001 or any of the mutants via electroporation as described

essentially in Berkner et al., 2007. Integrants were selected on uracil selective gelrite plates for 5 days at 75°C.

All deletion mutants were confirmed by sequencing PCR products that were obtained using primers that bound at least 100 bp up or downstream of the respective primers used for the construction of the flanking regions for the deletion mutant plasmids. Primer pairs for sequencing PCRs of an *aapF* deletion were 583/584, for a *flaJ* deletion were 581/582 and for a *upsE* deletion were 2010/2015, respectively.

Construction of the eCGP123 expression plasmid

A highly heat stable adapted consensus green fluorescent protein was recently published by (Kiss et al., 2009) termed eCGP123. The sequence of eCGP123 was codon adjusted to the S. acidocaldarius codon usage by Genescript (USA) and synthesized. The synthetic gene was delivered blunt end ligated into pUC57 and this construct was termed pSVA634. The gene was excised from pSVA634 using BamHI/ ApaI and ligated into pMZ1 yielding pSVA612 thereby adding 6 amino acids to the N-terminus of the eCGP123 which originate from the multiple cloning site of pMZ1. pMZ1 contains an expression cassette for *Sulfolobus* species including a terminator region (Zolghadr et al., 2007). The eCGP123 gene was then excised with the terminator region from pSVA612 by using NcoI/ EagI and ligated into the *S. acidocaldarius* expression vector pSVA1450 (Wlodkowski and Albers, unpublished) which is based on pCmalLacS (Berkner et al., 2010) and is allowing for maltose inducible expression of proteins. This construct was termed pSVA629 and used for the expression of eCGP123 in different *S. acidocaldarius* strains. The plasmid was methylated as described above and then transformed by electroporation. Plasmid containing colonies were selected on gelrite plates without uracil. Obtained colonies were grown in liquid Brock medium and used for the inoculation of biofilms.

Motility assay in soft gelrite

100 ml laboratory bottles were filled with 40 ml Brock medium pH3.5 supplemented with 0.1% NZ-Amine, 10 µg/ml uracil, 3 mM $CaCl_2$, 10 mM $MgCl_2$ and 0.1% gel-rite. After polymerization the medium was inoculated by carefully releasing 10 µl of a grown culture OD_{600nm} 0,6-0,7 using a 100 µl syringe. The bottles were closed to avoid evaporation of the medium and incubated at 76°C for 2 days. The specific pattern of movement of each strain was documented with a camera.

Attachment assays and light microscopy

S. acidocaldarius MW001 and all described deletion mutants were grown one day as shaking culture in 0.1% NZ-Amine medium in the presence of a glass slide in 100 ml Schott flasks. After cooling down the cultures the glass slides were first washed with Brock, pH 5 containing 2.5% formaldehyde and the cells were fixed with 5% formaldehyde for 30 min. Cells on the lower side of the glass slides were removed with EtOH. The samples were analyzed by light microscopy using a Zeiss Image MI (Oberkochen, Germany) equipped with Cascade 1K camera (Visitron Systems, Puchheim, Germany) and a Zeiss Plan Apochro-mat 100x/1.4 differential interference contrast (DIC) objective. Image processing was carried out using Metamorph 7.1.2. To evaluate the amount of cells bound to the glass slides 12 images at different places of the glass slides were taken and all present cells were counted. The attachment assays were repeated three times for each strain.

Growth of biofilms and confocal laser scanning microscopy (CLSM)

Biofilms of the *Sulfolobus* strains were grown in small Petri dishes (µ-dishes, 35 mm, Ibidi, Martinsried) in Brock media as a standing culture. 2 biological replicates were performed for each of the 8 strains and grown for three, six and eight days. For all strains the inoculation OD was 0.01. The Petri dishes were put in a specially designed metal box (25 cm L x 20 cm W x 20 cm D) with ~ 500 ml of

water in the bottom to minimize evaporation of the media, as described by Koerdt et al. (2010). To visualize the biofilms by CLSM different fluorescent probes were employed and was essentially performed as described in Koerdt et al. (2010). In brief, DAPI (4',6-Diamidino-2-phenylindol) was used to stain the cells of the biofilm and images were taken at an excitation wavelength of 345 nm and an emission wavelength of 455 nm. Fluorescently labelled lectins were employed to visualize the EPS (extracellular polymeric secretions) of the biofilms. Before adding lectins to the biofilm, the growth medium was replaced with medium adjusted to pH 5 to ensure that binding of lectins was not inhibited by low pH. Fluorescein conjugated concanvalin A (ConA) (5 mg/ml; Invitrogen, Karlsruhe, Germany) binds to α-mannopyranosyl and α-glucopyranosyl residues and its signal was recorded at an excitation wavelength of 494 nm and an emission wavelength of 518 nm. Alexa Fluor® 594 conjugated IB_4 recognizes specifically α-D-galactosyl residues (isolectin GS-IB4 from *Griffonia simplicifolia* 1mg/ml; Invitrogen, Karlsruhe, Germany) and images were taken at an excitation wavelength of 591 nm and an emission wavelength of 618 nm. The lectin biofilm mixtures were incubated at room temperature for 20-30 minutes, in the absence of light. After incubation, the biofilm was washed with Brock media (pH 5) to remove excess label and images were taken with CSLM. For biofilms grown with cells containing eCGP123 expressing plasmids cells were grown in medium containing 0.1% NZ-amine and 0.2% maltose for the induction of protein expression. The medium was exchanged every 24 hrs. After three days the biofilms were washed ones with Brock medium, if needed stained with DAPI and then analyzed by CLSM. Image data obtained were processed by using the IMARIS software package (Bitplane AG, Zürich, Switzerland).

Electron microscopy of deletion mutants

Cells on carbon-coated nickel grids were negatively stained with 2% uranyl acetate and analyzed by transmission electron microscopy on a JEOL 3010,

300 kV high-performance transmission electron microscope (JEOL, Eching, Germany).

Gene expression analysis

MW001 and all the deletion mutants were grown as static biofilms for three, six and eight days. The cells from the biofilms were harvested and total RNA isolation and cDNA synthesis were performed as described previously (Zolghadr et al., 2010). Gene specific primer sets (Supplementary Table 1)

The quantitative PCR analysis was carried out according to the protocol and chemicals provided by the genomic region. PCR products were analyzed on were used to detect the presence of selected genes in

0.8 % agarose gels. Applied Biosystem. For each gene of interest, a duplicate setup of 25 μl PCR mixture was prepared from 12.5 μl SYBR green master mix, 2 μl of 0.3 μM primer pair stock solution, 1 μl cDNA and 9.5 μl nucleotide-free water. The negative control assays were done with RNA mixtures that were prepared for cDNA synthesis. Primer efficiencies were calculated from the average slope of the linear regression curves according to the calculation model advised by Applied Biosystem. The fluorescence quantities of the reactions were measured with ABI 7500 instrument (Applied Biosystems, Foster City, CA).

Table 1: List of archaeal strains used in this study

Strain no.	Genotype	Source/derivation
MW001	Δ *pyrEF (91-412 bp)*	Wagner and Albers, unpublished
MW156	Δ *aapF* (*Saci2318*) (1-1836 bp)	MW001, this study
MW155	Δ *flaJ* (*Saci1172*) (18-1437 bp)	MW001, Lassak and Albers, unpublished
MW109	Δ *upsE* (*Saci1494*) (1-1410 bp)	MW001, van Wolferen and Albers, unpublished
MW157	Δ *aapF* Δ *upsE*	MW001,this study
MW151	Δ *aapF* Δ *flaJ*	MW001,this study
MW158	Δ *flaJ* Δ *upsE*	MW001,this study
MW152	Δ *aapF* Δ *flaJ* Δ *upsE*	MW001,this study
MW163	Δ *aapF::aapF*	MW156, this study
MW164	Δ *upsE::upsE*	MW109, this study
MW001-CGP	MW001 carrying pSVA629	MW001, this study
Δ *aapF* -CGP	Δ *aapF* carrying pSVA629	Δ *aapF*, this study
Δ *upsE* -CGP	Δ *upsE* carrying pSVA629	Δ *upsE*, this study

Table 2: List of plasmids used in this study

Plasmid no.	Description	Source/reference
Δ2pyrEF	Plasmid used for inframe deletion in *S. acidocaldarius*, contains *pyrEF* of *S. solfataricus*	pBluescript, (Wagner et al., 2009)
pSVA406	Plasmid used for inframe deletion in *S. acidocaldarius*, contains *pyrEF* of *S. solfataricus*	pBluescript, Michaela Wagner and Albers, unpublished
pSVA179	Deletion plasmid for *ΔflaJ* (Δ*saci1172*)	Δ2pyrEF, Lassak and Albers, unpublished
pSVA180	Deletion plasmid for *ΔaapF* (Δ*saci2318*)	Δ2pyrEF, this study
pSVA1804	Deletion plasmid for *ΔupsE* (Δ*saci1494*)	pSVA406, van Wolferen and Albers, unpublished
pSVA223	complementation plasmid for *ΔaapF::aapF* (Δ*saci2318*)	pSVA406, this study
pSVA224	Deletion plasmid for *ΔupsE::upsE* (Δ*saci1494*)	pSVA406, this study
pSVA634	eCGP123 codon adjusted gene inserted into pUC57	pUC57
pSVA612	Codon adjusted eCGP123 from pSVA634 inserted into pMZ1 using ApaI/BamHI	pMZ1 (Zolghadr et al., 2007)
pSVA629	Codon adjusted eCGP123 transferred from pSVA612 into the S. acidocaldarius expression vector pSVA1450	pSVA1450 (Wlodkowski and Albers, unpublished), expression vector based on pCmalLacs (Berkner et al., 2010)

Results

Single, double and triple deletion mutants of all surface structures of *S. acidocaldarius*

Each of the pili operons contain three components in common that are essential for assembly: the pilin subunit(s)(AapA/B, UpsA/B and FlaB), an ATPase (AapE, UpsE and FlaI) and an integral membrane protein (AapF, UpsF and FlaJ)(see Figure 1)(Szabo et al., 2007; Frols et al., 2008). In frame deletion mutants of one essential gene of each pili operon was constructed by a markerless-inframe deletion mutant method using the uracil auxotrophic mutant MW001 as wild type (Wagner and Albers, unpublished). The construction of the deletion plasmids and the strains is described in the Material and Method section. The single mutants of the membrane protein of the aap pili, *aapF*, the membrane protein of the flagella assembly system, *flaJ*, and the ATPase of the ups system, *upsE*, were constructed first. These were used to obtain the double mutants Δ*aapF*Δ*upsE*, Δ*aapF*Δ*flaJ* and Δ*flaJ*Δ*upsE* and finally the triple deletion mutant Δ*aapF*Δ*upsE*Δ*flaJ*. The identity of all strains was verified by sequencing of the appropriate part of the genome. None of the deletion strains showed a difference in growth rates in comparison to the MW001 wild type strain. Electron microscopic analysis of the deletion strains confirmed that the strains were only exhibiting the cell surface appendages of which no components had been deleted (Fig. S1). Therefore the triple mutant was devoid of any type IV pili structures on its cell surface. The only surface structure that remained was the very thin filaments, dubbed threads. These seem not be formed by type IV pilins since a deletion mutant of the type IV prepilin signal peptidase PibD still contained these filaments, but not any of the other three filaments (van Wolferen and Albers, unpublished). Interestingly, the Δ*aapF* deletion mutant exhibited a large amount of flagella.

Motility assay in soft gelrite

To test the different cell surface structure deletion mutants for motility, 100 µl cell suspensions were inoculated using 100 µl tips into 100 ml Schott flasks that were filled with soft gelrite (0.1 %) in Brock medium supplemented with 0.1% NZ-amine and uracil. After two days at 76°C the flasks were analyzed and photographed. A typical result is shown in Fig. 2. MW001 cells were able to swim from the inoculation channel, whereas all mutants that were devoid of flagella were non-motile and only grew along the inoculation channel. On the other hand the Δ*aapF*Δ*upsE* deletion mutant seemed hypermotile, which can be explained by the increased expression of flagella in the Δ*aapF* background (see below). However, the single *aapF* deletion mutant showed motility similar to wild type levels.

Attachment assay

In *S. solfataricus* the flagella and ups pili deletion mutant could not adhere to glass, mica or carbon coated gold grids (Zolghadr et al., 2010). To test whether these surface structures fulfill the same role in *S. acidocaldarius*, MW001 and all deletion mutants were grown in shaking cultures in 100 ml Schott flasks in which an objective glass was inserted. After 24 hrs cells were removed from the lower side of the glass side and attached cells were counted from 12 frames taken by a light microscope. The experiments were repeated three times and the data are presented in Fig. 3 including the standard deviations. The triple deletion mutant that is devoid of flagella and the two different pili showed only 25% of the wild type cells attachment implying that the threads at the cell surface are not involved in attachment. Interestingly, the Δ*aapF*Δ*flaJ* mutant attached as low as the triple mutant. Therefore the ups pili seem not to contribute to initial attachment to surfaces in the absence of the other cell surface structures. The highest amount of attached cells was counted in the cells that only exhibit the aap pili with an increase of more than 100 % in comparison to the wild type. An increase was visible already in
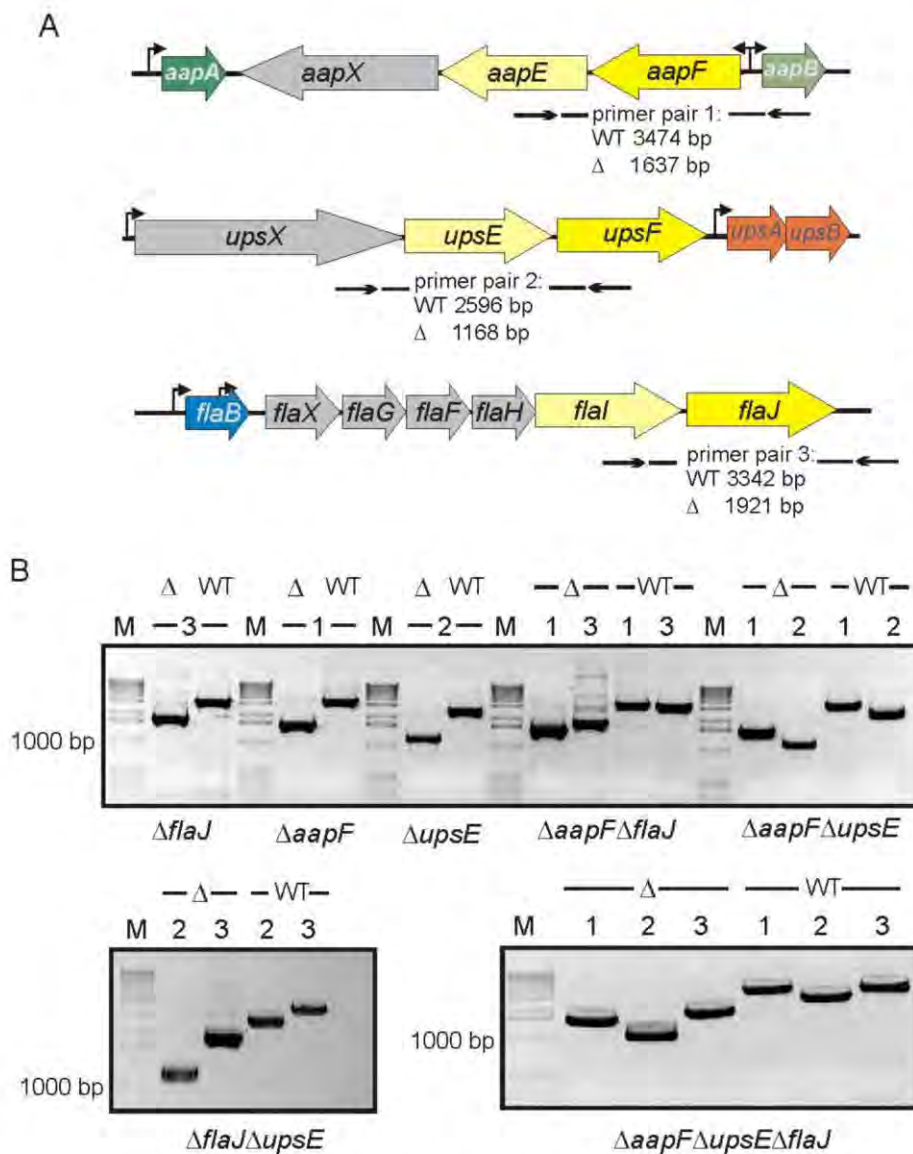
Figure 1: Deletion mutant analysis. (A) Operon structure of the three systems encoding the aap pilus, the UV inducible pili (ups) and the flagellum. The assembly ATPases (AapE, UpsE and FlaI) are indicated in light yellow, whereas the central membrane protein (AapF, UpsF and FlaJ) are depicted in yellow. The structural subunits (AapA/B, UpsA/B, and FlaB) are colored in green, orange and blue, respectively. Arrows indicate putative transcription start sites. The arrows below the arrows indicate the position of the primers that were used for PCR to confirm the deletion of the specific gene. The expected sizes for wild type and deletion mutant PCR products are given. (B) PCR reactions were performed using the primer pairs 1 (for *aapF*), 2 (for *upsE*), and 3 (for *flaJ*), respectively. The respective tested deletion mutant is indicated below the gel image. Δ, deletion mutant; WT, wild type.

the ΔupsE mutant, but clearly when also the flagella operon was deleted this led to a large amount of attached cells by the aap pili. The Δ*aapF* deletion mutant was hyperflagellated (see below), which might explain the slightly higher amount of attached cells in comparison to the wild type. However, flagella seem to play only a minor role in attachment from shaking culture as the deletion mutant attached only slightly less than the wild type.

Biofilm formation

As in bacterial biofilm formation cell surface appendages play an important role in shaping the structure and appearance of the community (Pratt and Kolter, 1998; Barken et al., 2008), MW001 and all the cell surface structures mutants were grown as

static biofilms for three, six and eight days. Whereas the cells in the biofilms were visualized using DAPI, the presence of extracellular polysaccharides were detected by fluorescently labeled lectins that specifically bind mannose/glucose (ConA) and galactosyl sugar residues (IB$_4$). In Figure 4 the overlay of the three fluorescent signals is depicted. The development of the MW001 biofilm resembles

the one from *S. acidocaldarius* DSM 639 described before (Koerdt et al., 2010). The cell density of the community increases strongly from the third day to the sixth, but then decreases slightly towards the eights day. The EPS production detected by the lectins increases steadily and led to the formation of clouds of EPS on top of the biofilm. Interestingly, at the sixth day primarily ConA signal is visible

The Figure 2: Motility assay in soft gelrite. The wild type and deletion mutant strains were inoculated by a syringe into the soft gelrite and incubated for two days
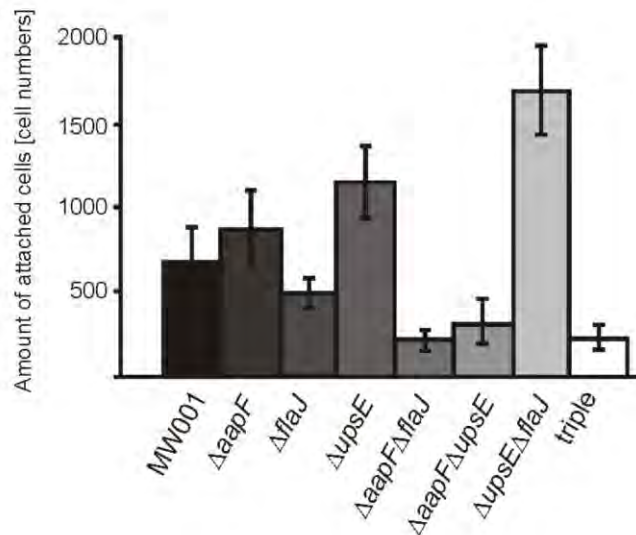

Figure 3:. Attachment assay of the different cell surface appendage mutants. Strains were grown in 100 ml Schott flask in which an objective slide was inserted. After 24 hours of growth the cells attached to the glass slides were fixed and counted. The error bars represent the standard deviation of three biological replicates. Triple indicates the triple mutant $\Delta aapF\Delta upsE\Delta flaJ$.
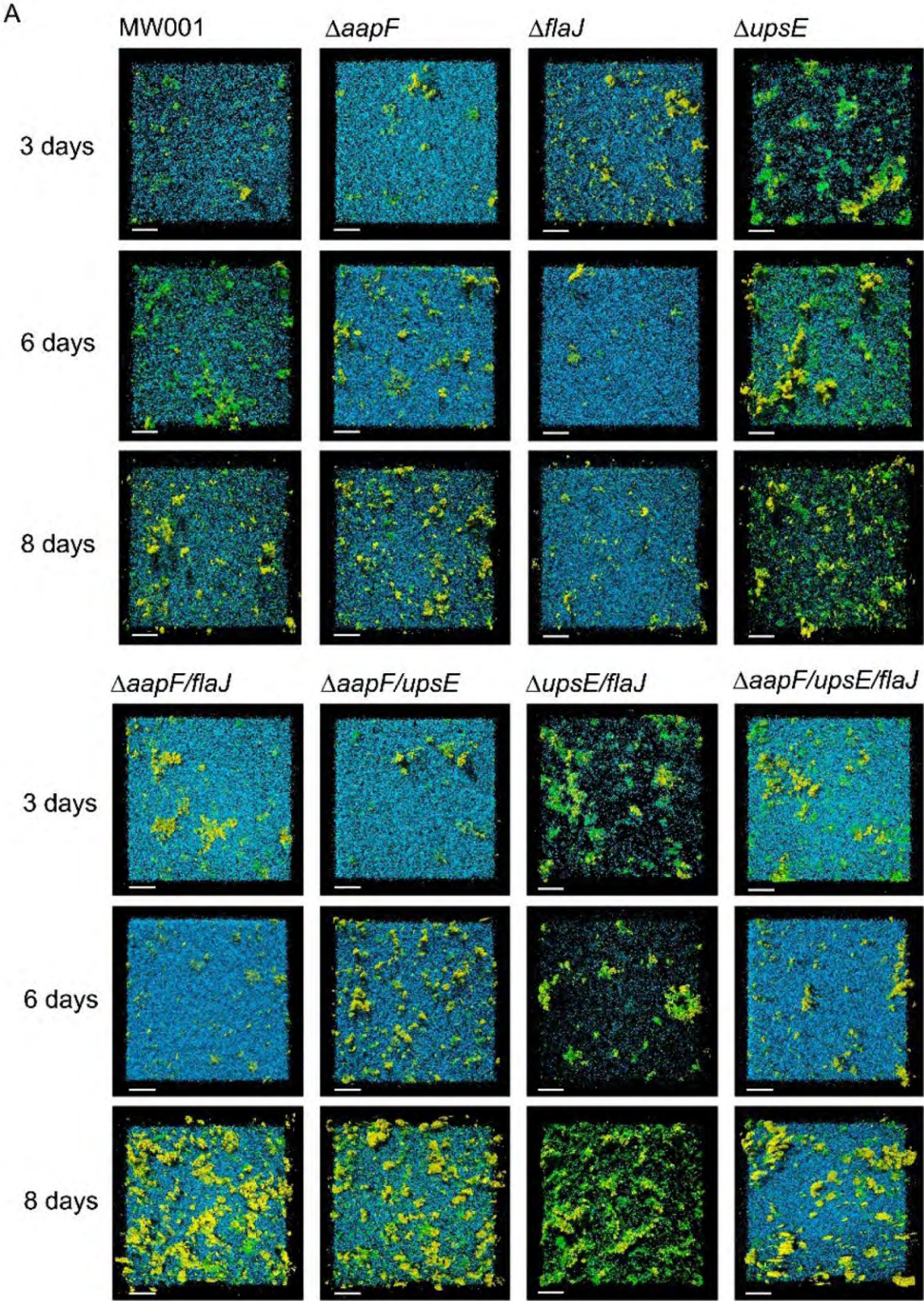
slightly decreased in comparison to MW001. Biofilm formed by the $\Delta upsE$ deletion strain showed an opposed phenotype: here the cell density in general was much lower than in any $\Delta aapF$ deletion mutant and clearly lower than in the MW001. In contrast to the $\Delta aapF$ biofilms the $\Delta upsE$ cells formed large loose aggregates that resulted in a higher biofilms than the wild type biofilm of MW001. Moreover, the production of EPS that reacts with the employed lectins is strongly increased at all stages of the maturation of the biofilm. Interestingly, the production of glucose/mannose containing EPS is higher in the $\Delta upsE$ strain in relation to the IB$_4$ signal than in the other strains. The phenotype of the $upsE$ deletion was dominant also in the $\Delta upsE\Delta flaJ$ deletion strain. Only the aapF mutation was epistatic to the $upsE$ deletion. Therefore the biofilm phenotypes of the different surface structure mutants can be arranged in three major groups: (A) the biofilm of the of the wildtype and the $\Delta flaJ$ mutant that appeared very similar in cell density and height, with the only difference that the cell release at the eight day was less in the $\Delta flaJ$ mutant; (B) the biofilm phenotype by mutants that carried an aapF deletion resulted in a very high density and therefore diminished height of the biofilms, whereas in the third biofilm phenotype (C) the cells were only loosely connected in the biofilm which led to strong aggregate formation and high tower-like structures. Moreover, the production of EPS was highly induced in $\Delta upsE$ deletion mutants.

The surface coverage of the biofilms formed by MW001 and all deletion mutants at three, six and eight days of maturation was determined. The light microscopy picture of the bottom layer of the biofilms was taken and converted into a black and white picture with white representing the attached cells. The ratio of white and black pixels was determined. MW001 had the lowest surface coverage after three days, but then showed the highest increase in cell density in the bottom layer of the forming community (Fig. 5D). All deletion mutant biofilms showed a higher surface coverage

whereas in the later stage the IB$_4$ signal was much more prominent. Whereas the biofilm of the $\Delta flaJ$ mutant was comparable to the MW001 biofilm development, the absence of the aap pili in the $\Delta aapF$ strain resulted in a very high density of cells in the biofilm. This feature was apparent at all growth stages of the $\Delta aapF$ biofilm. This effect was dominant in all mutants which were devoid of the aap pili ($\Delta aapF\Delta flaJ$, $\Delta aapF\Delta upsE$ and the triple deletion mutant $\Delta aapF\Delta upsE\Delta flaJ$, respectively). Biofilms formed by these deletion mutants exhibited a high cell density, but the height of the biofilm was
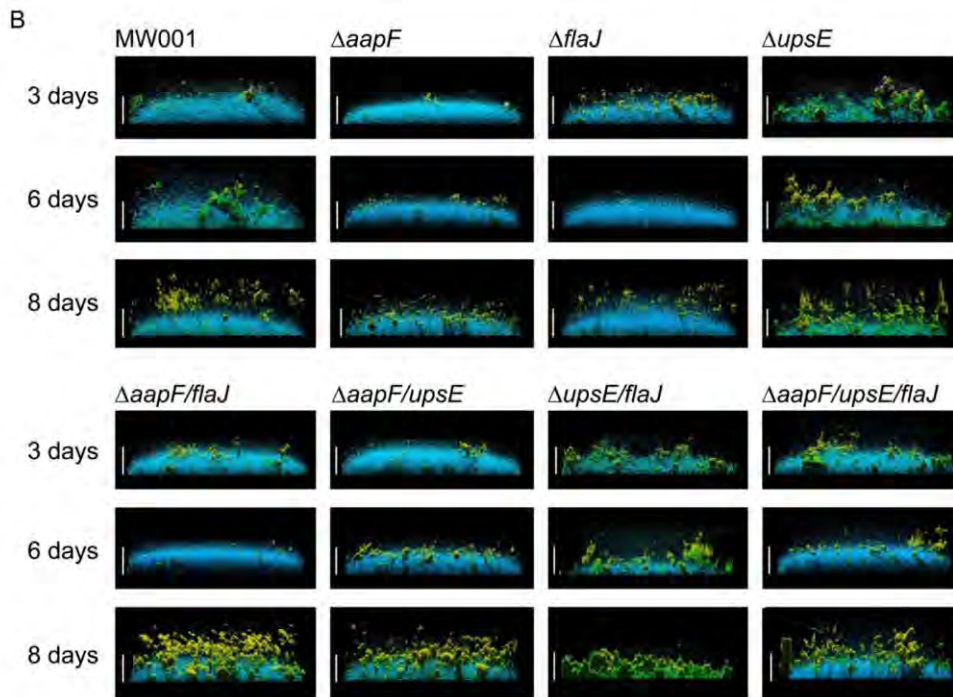
A

Figure 4: CLSM of the development of biofilms at 3,6 and 8 days of the wild type and the various cell appendage deletion mutants. (A) represents the top view of all examined communities, whereas (B) shows the side view of the biofilms. The blue channel is the DAPI-staining. The green channel represents the fluorescently labeld lectin ConA which binds to glucose and mannose residues. The lectin IB4 able to bind to a-galactosyl-residues and is shown in yellow. Scale bar = 40 µm.

after three days than the wild type. Of these consistent with the CLSM images all biofilms formed by a deletion mutant carrying the $\Delta aapF$ deletion had the highest surface coverage during all time points of biofilm formation. The $\Delta flaJ$, the $\Delta upsE$ and the $\Delta flaJ\Delta upsE$ mutants showed the lowest surface coverage off all deletion mutants, whereas the triple mutant phenocopied the surface coverage of the $\Delta aapF$ deletion mutant.

Both, the single mutant $\Delta aapF$ and $\Delta upsE$, were complemented and analyzed during biofilm formation in comparison to the wild type. The complemented strains behaved like the wild type cells indicating that the observed phenotypes are related exclusively to the deleted surface structure and that no polar effects played a role (Supplemantary. The $\Delta flaJ$ was also complemented, but will be published elsewhere (Lassak et al, submitted).

Concluding it was evident that the presence or absence of the different surface structures had a clear impact on the structure and spatial organization of the *S. acidocaldarius* biofilm community.

Differential regulation of the pili and flagellum operons during biofilm maturation

MW001 and all deletion mutants except for the triple deletion mutant were grown in static biofilm conditions for three, six and eight days and the cell mass was then used for the isolation of mRNA to perform qRT-PCR. The qRT-PCR results are depicted in Fig. 6 and show the fold induction in comparison to the wild type MW001. As mentioned before it was evident that in all $\Delta aapF$ deletion strains transcription of the flagella operon (measured by *flaB* and *flaJ* expression levels) was highly induced (up to 256 fold in the $\Delta aapF$ deletion strain) leading to hyperflagellation. This might explain the high cell density and decreased height of the biofilm as the flagella are used not only for adhesion, but also to establish cell-cell connections. The ups pili system was only upregulated 4-8 fold in all strains measured, but that did not markedly influence the phenotypes of the formed biofilms (Fig.4). Interestingly, in the $\Delta upsE$ deletion strain the *aapA*, one of the pilins of the aap pilus, was highly induced (128 fold), whereas the *aapB* and *aapF* were down regulated like in the $\Delta upsE\Delta flaJ$ deletion strain. This could be the reason that the $\Delta upsE$ deletion strain
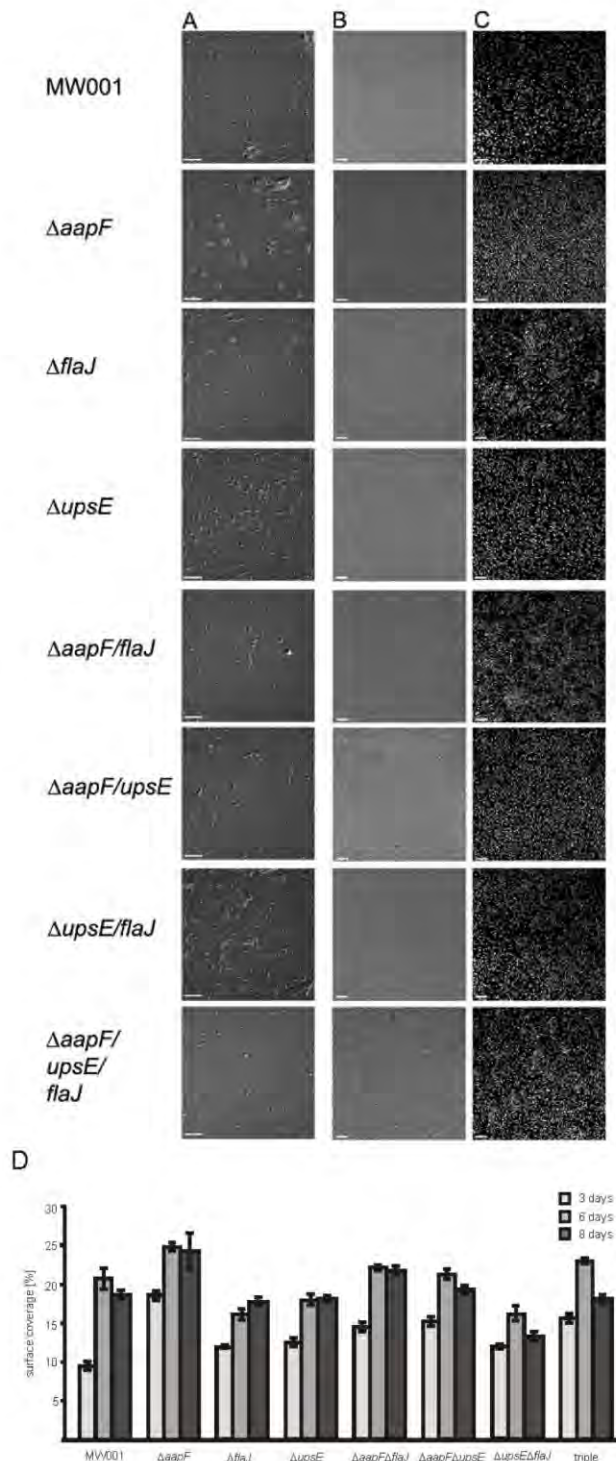
D

Figure 5: Surface coverage in the bottom layer of biofilms formed by the wild type and the various mutant strains. MW001 and the different cell surface appendages. Column (A) presents the DIC pictures from glass slide attached cells for comparison. Scale bar = 40 μm. (B) and (C) show the bottom layer from 3 day grown biofilms of the different mutants as DIC and black/white representation, respectively. The black/white pictures were used for the calculations of the surface coverage. (D) Development of surface coverage during 3, 6 and 8 days of community formation of MW001 and all the deletion mutants.

had a higher surface coverage (Fig 5D) and a denser appearance in the CLSM analysis (Fig. 4) than the $\Delta upsE\Delta flaJ$ deletion strain.

Visualizing *Sulfolobus* biofilms using a heat stable fluorescent protein

In studies on bacterial biofilm formation the influence of different mutants on each other during this process can quite easily be addressed by using strains that express different fluorescent proteins. For hyperthermophilic species so far these studies were not possible as no heat stable fluorescent protein was available that would withstand the growth conditions of these organisms. We expressed codon adjusted eCGP123, a very heat stable green fluorescent protein (Kiss et al., 2009), in MW001 using pSVA629 and obtained green fluorescing cells that could be used for direct detection by fluorescent microscopy. Three days old static biofilms of eCGP123 expressing MW001 cells (Fig 8, D-F) appeared similar to DAPI stained biofilms of MW001 (Fig. 4A). *Sulfolobus* cells possessed a green auto fluorescence (Fig 8, A-C), however, compared to the signal obtained from the eCGP123 expressing cells, that signal was negligible. The overlay of the DIC image and the GFP-channel image of a bottom-layer of the eCGP123 expressing MW001 showed that most of the cells were indeed fluorescent (Fig 8, G-I). Therefore, we used pSVA629 for the expression of eCGP123 in different mutants to be able to visualize formation of biofilms by mixing two different strains.

As the $\Delta upsE$ and $\Delta aapF$ strains showed the most pronounced phenotypes in the previous experiments, these two strains were transformed with pSVA629 and allowed to form biofilm in static conditions for three days. Both strains were also stained with DAPI before analysis by CLSM, so that the DAPI signal could be compared to the CGP derived signal. Both the biofilms formed by the $\Delta upsE$ and $\Delta aapF$ strains showed the same phenotype as before confirming that the expression of the eCGP123 had no negative impact on cell growth (Fig 9, first and third row). However, when the $\Delta aapF$ -CGP strain was mixed
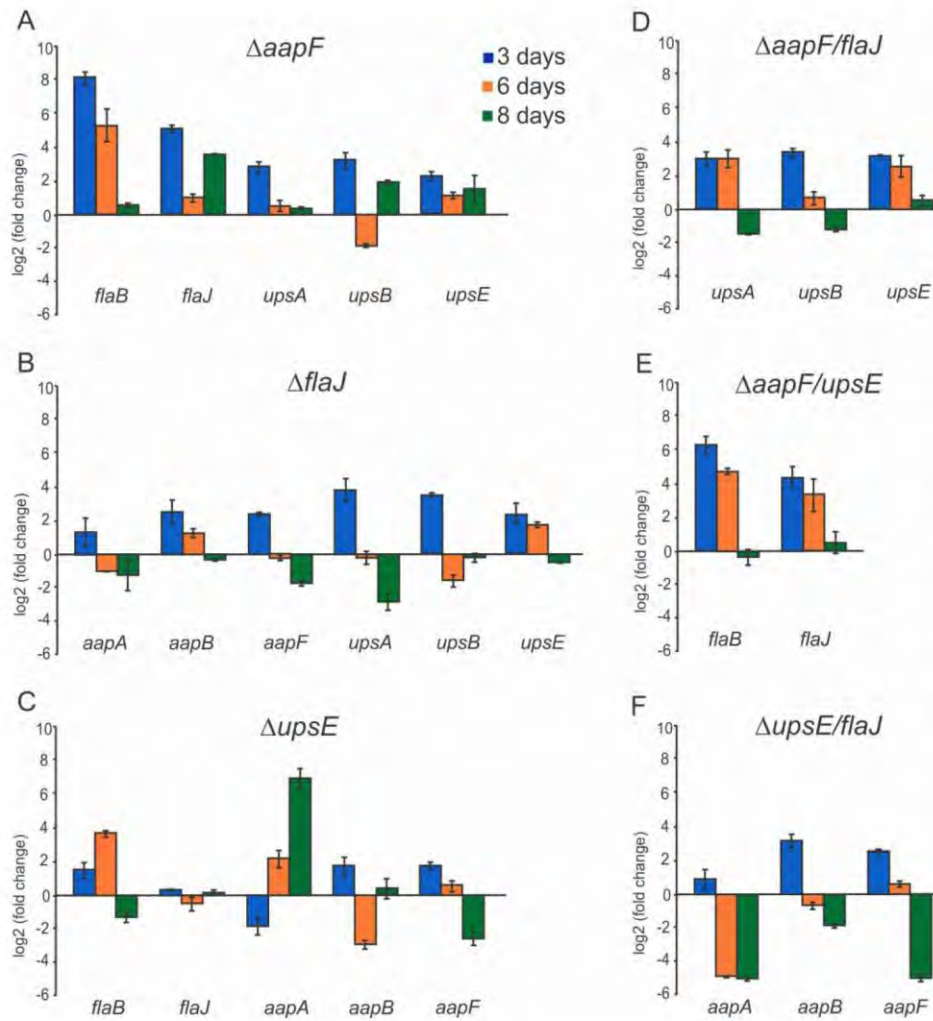
11

Figure 6: Differential expression of pili and flagellum operons in MW001 and all deletion strains during biofilm maturation. qRT-PCRs were performed on biofilms matured for three, six and eight days from MW001 and all the deletion strains (A-F) except for the triple mutant. Tested targets are indicated below the graph, the respective strain is given above the graph. Relative transcript expression levels of each target were normalized to an internal control gene *secY*. The values reflect the fold change in expression compared to MW001, which is designated as baseline. The means and SDs of biological replicates are shown.
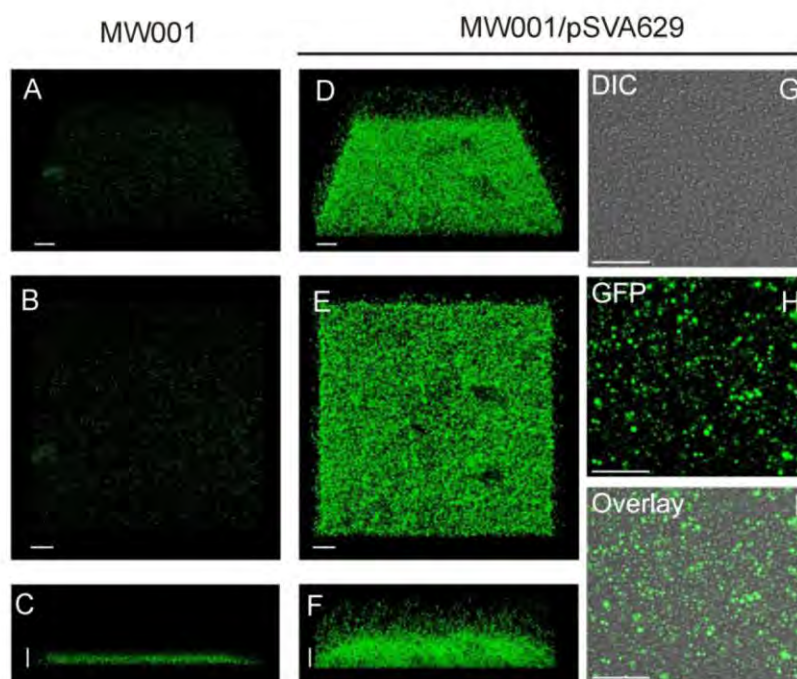

Figure 7. CSLM of MW001 and MW001 expressing eCGP123 three days old static biofilms. Only the GFP-channel was used for the visualization of two days old biofilms of MW001 (A-C) and MW001 expressing eCGP123 (D-I). (A-D) represent different top views, whereas C and F show the corresponding side views. In (G-I) the bottom layer of the MW001(pSVA629) biofilm is shown in DIC (G), in the GFP channel (H) and as an overlay of the DIC and the GFP channel signal (I). Scale bar = 40 μm.
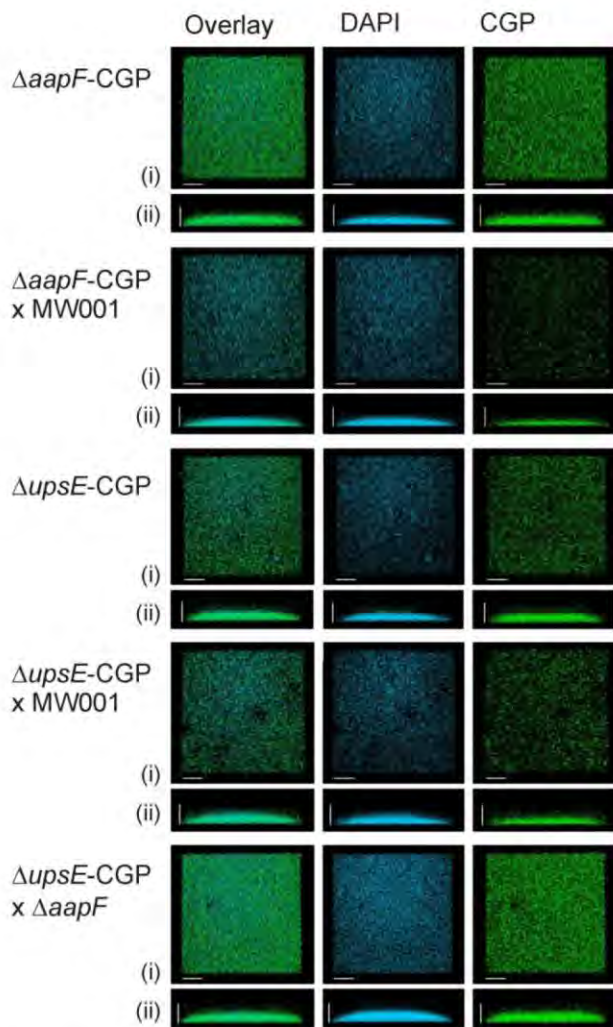
Figure 8: CSLM of three days old biofilms by strains expressing eCGP123 and mixtures of these with other deletion strains. Each strain and mixture of strains is indicated at the left. The biofilms were stained with DAPI to discriminate between the eCGP123 expressing strain and the prospective other strain. IN each case the top views (i) and the side views (ii) are depicted. Scale bar = 40 μm.
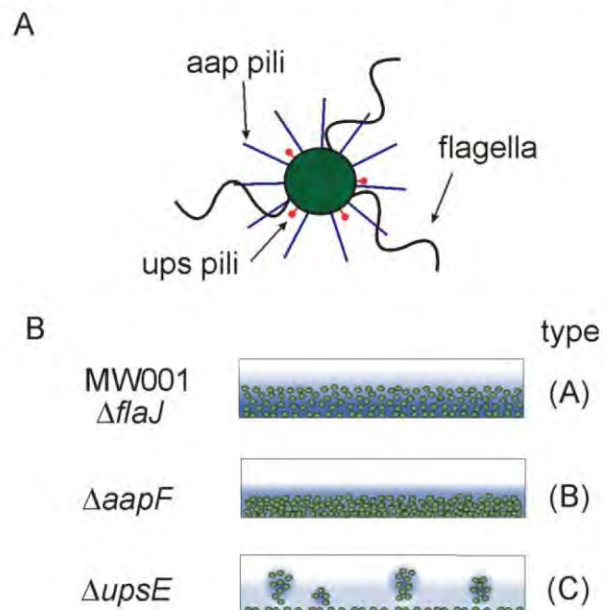

Figure 9. Model of a *S. acidocaldarius* cell and the different types of formed biofilms. (A) A *S. acidocaldarius* cell showing all the discussed cell surface structures: (i) the flagella with a curved appearance which are up to several μm long, (ii) the aap pili which are mostly straight and (iii) the ups pili that are the shortest pili. (B) The three different types of biofilm formation observed by the wild type and the various mutants: type (B) exhibits a largely increased cell density throughout the whole formed community in comparison to the wild type biofilm and in type (C) biofilms the density at the bottom is dense, but the higher layers of the biofilms mainly large clusters of cells were formed.

with MW001, it was evident that the GFP signal was thinned out in comparison to the overall DAPI signal implying that the MW001 was growing much better than the Δ*aapF* -CGP strain (Fig. 9, second row). Also, the high cell density usually seen in the Δ*aapF* deletion strains was not observed here. In the co-culture of MW001 and the Δ*upsE*-CGP strain the typical loose phenotype of the upsE mutation was dominant showing holes in the biofilm that reached down to the bottom of the biofilm (Fig. 9, fourth row). When finally both mutants were grown together (Δ*upsE*-CGP and Δ*aapF*), a high cell density which was reminiscent of the Δ*aapF* strain phenotype was observed. However, it seemed that the CGP signal was very strong and therefore due to

increased growth of the Δ*upsE*-CGP strain (Fig. 9, last row).This implicated that the presence of the Δ*aapF* strain dominated the Δ*upsE* phenotype, but led to a better growth of the Δ*upsE*-CGP strain.

Discussion

Although an increasing number of archaeal appendages are being identified the function of only a few have been studied in detail. In this study we have tried to understand which role the three surface structures, the aap pili, the ups pili and the flagella of *S. acidocaldarius* play during attachment to surfaces in shaking cultures and static biofilm formation of this organism.

Attachment assays with the three double mutants which carry only one of the surface structures showed that the aap pili are indeed important for adhesion to surfaces whereas the flagella and ups pili need to have one other surface structure present

to be involved in adhesion as the level of attachment of the mutants only expressing either the flagella or ups pili is similar to the triple deletion mutant, which is devoid of appendages. This is in agreement with data obtained in *S. solfataricus* in which the deletion of either the ups pili or the flagella led to an inability to attach to surfaces from shaking cultures (Zolghadr et al., 2010). However, as *S. acidocaldarius* has the additional aap pili in comparison to S. solfataricus, this effect could only be demonstrated in the double deletion mutants as in the single flagella or ups pili mutants only a minor attachment effect or even an increase in attachment was observed, respectively. Such a prominent role in adhesion as for the aap pili was also observed for the pili of *M. thermoautrophicus* which could only be detached by the addition of antibodies from grids (Thoma et al., 2008). However, an interplay of pili and flagella was necessary for the attachment of *M. maripaludis* cells to a variety of surfaces which in turn resembles the situation between the *S. acidocaldarius* ups pili and flagella (Jarrell et al., 2011). The cable like structures formed by bundles of flagella that were observed in *P. furiosus*, *M. maripaludis* and *M. villosus* (Näther et al., 2006; Bellack et al., 2011; Jarrell et al., 2011), were so far not demonstrated in *Sulfolobales* and might explain why in *Sulfolobus* species the flagella seem to primarily be important for motility and only initial attachment, but not the persistence on surfaces. This was also confirmed in this study as the flagella mutant showed no phenotype in comparison to the wild type in biofilm formation as described also for *S. solfataricus* (Koerdt et al., 2010).

In contrast to the flagellum the ups and aap pili deletions had a profound effect on the structure and development of the static biofilms development of *S. acidocaldarius*. Although the ups pili were only thought to have a role in UV induced cell aggregation and DNA transfer (Frols et al., 2008), experiments in *S. solfataricus* showed earlier that they are not only essential for surface attachment from shaking culture, but might also be involved in biofilm maturation (Koerdt et al., 2010; Zolghadr et

al., 2010). The deletion of the ups pili led to an organization in the biofilms that resembles type C in Fig. 9. In this organization a dense monolayer of cells is present at the bottom of the biofilm attaching to the substratum, but above that large clusters are formed. Moreover the ups deletion mutants also seem to secrete larger amounts of EPS during the biofilm development than the wild type cells.

In biofilms of aap deletion mutants cells were packed very densely. Therefore it seemed that the aap pili, although they are used for adhesion, keep the cells within a biofilm in a certain distance to each other, possibly to ensure optimal fluid exchange and therefore nutrient access for the biofilm embedded cells. qPCRs demonstrated that the deletion of the *aapF* gene led to an upregulation of the flagella operon causing the cells to be hyperflagellated. Therefore the increased abundance of flagella might also cause the observed phenotype. However, that is unlikely as the Δ*aapF*Δ*flaJ* showed the same phenotype (Fig. 9B) during biofilm formation as the Δ*aapF* and Δ*aapF*Δ*upsE* deletion mutants.

For the first time we employed a heat stable green fluorescent protein in a hyperthermophilic archaeon. An optimized expression vector for *S. acidocaldarius* was the base for the stable and high expression of codon adjusted eCGP123 (Wagner and Albers, unpublished). Using eCGP123 allowed us to study the effect of the different cell surface deletion mutants on biofilm growth in co-cultures and showed that the Δ*upsE* phenotype was dominant in co-culture with the wild type MW001 whereas the Δ*aapF* deletion strain was overgrown by MW001. This again showed that the aap pili fulfill an important role by keeping the cells within a biofilm at a certain distance to each other. When both mutants were co-incubated, it seemed that the Δ*aapF* phenotype dominated above the Δ*upsE* phenotype, although the green signal in this case resembling the Δ*upsE* strain was very strong. However, it seemed that the presence of the Δ*aapF* strain led to the "complementation" of the Δ*upsE*

phenotype and is favored during the establishment of the biofilms.

Concluding we showed that the three *S. acidocaldarius* cell appendages fulfill important, but different functions during surface attachment and biofilm formation. As a regulatory link seems to exist between at least the aap pili and the flagella operon, it will be interesting to unravel which system is regulating the expression of these two appendages. The influence the pili and the flagellum have on biofilm maturation in crenarchaea seems to be as complex as in bacteria and will have to be analyzed for each biological system separately.

References

Albers, S.V., and Pohlschroder, M. (2009) Diversity of archaeal type IV pilin-like structures. *Extremophiles* **13**: 403-410.

Albers, S.V., and Meyer, B.H. (2011) The archaeal cell envelope. *Nat Rev Microbiol* **9**: 414-426.

Albers, S.V., Szabo, Z., and Driessen, A.J. (2003) Archaeal homolog of bacterial type IV prepilin signal peptidases with broad substrate specificity. *J Bacteriol* **185**: 3918-3925.

Bahar, O., De La Fuente, L., and Burdman, S. (2010) Assessing adhesion, biofilm formation and motility of Acidovorax citrulli using microfluidic flow chambers. *FEMS Microbiol Lett* **312**: 33-39.

Bahar, O., Levi, N., and Burdman, S. (2011) The cucurbit pathogenic bacterium Acidovorax citrulli requires a polar flagellum for full virulence before and after host tissue penetration. *Mol Plant Microbe Interact*.

Bardy, S.L., and Jarrell, K.F. (2002) FlaK of the archaeon Methanococcus maripaludis possesses preflagellin peptidase activity. *FEMS Microbiology Letters* **208**: 53-59.

Barken, K.B., Pamp, S.J., Yang, L., Gjermansen, M., Bertrand, J.J., Klausen, M. et al. (2008) Roles of type IV pili, flagellum-mediated motility and extracellular DNA in the formation of mature multicellular structures in Pseudomonas aeruginosa biofilms. *Environ Microbiol* **10**: 2331-2343.

Bellack, A., Huber, H., Rachel, R., Wanner, G., and Wirth, R. (2011) Methanocaldococcus villosus sp. nov., a heavily flagellated archaeon that adheres to surfaces and forms cell-cell contacts. *Int J Syst Evol Microbiol* **61**: 1239-1245.

Berkner, S., Wlodkowski, A., Albers, S.V., and Lipps, G. (2010) Inducible and constitutive promoters for genetic systems in *Sulfolobus acidocaldarius*. *Extremophiles*.

Brock, T.D., Brock, K.M., Belly, R.T., and Weiss, R.L. (1972) *Sulfolobus*: a new genus of sulfur-oxidizing bacteria living at low pH and high temperature. *Arch Mikrobiol* **84**: 54-68.

Entcheva-Dimitrov, P., and Spormann, A.M. (2004) Dynamics and control of biofilms of the oligotrophic bacterium Caulobacter crescentus. *J Bacteriol* **186**: 8254-8266.

Frols, S., Ajon, M., Wagner, M., Teichmann, D., Zolghadr, B., Folea, M. et al. (2008) UV-inducible cellular aggregation

of the hyperthermophilic archaeon *Sulfolobus solfataricus* is mediated by pili formation. *Mol Microbiol* **70**: 938-952.

Jarrell, K.F., Stark, M., Nair, D.B., and Chong, J.P. (2011) Flagella and pili are both necessary for efficient attachment of Methanococcus maripaludis to surfaces. *FEMS Microbiol Lett* **319**: 44-50.

Kiss, C., Temirov, J., Chasteen, L., Waldo, G.S., and Bradbury, A.R. (2009) Directed evolution of an extremely stable fluorescent protein. *Protein Eng Des Sel* **22**: 313-323.

Klausen, M., Heydorn, A., Ragas, P., Lambertsen, L., Aaes-Jorgensen, A., Molin, S., and Tolker-Nielsen, T. (2003) Biofilm formation by Pseudomonas aeruginosa wild type, flagella and type IV pili mutants. *Mol Microbiol* **48**: 1511-1524.

Koerdt, A., Godeke, J., Berger, J., Thormann, K.M., and Albers, S.V. (2010) Crenarchaeal biofilm formation under extreme conditions. *PLoS One* **5**: e14104.

Marwan, W., Alam, M., and Oesterhelt, D. (1991) Rotation and switching of the flagellar motor assembly in Halobacterium halobium. *J Bacteriol* **173**: 1971-1977.

Moissl, C., Rachel, R., Briegel, A., Engelhardt, H., and Huber, R. (2005) The unique structure of archaeal 'hami', highly complex cell appendages with nano-grappling hooks. *Mol Microbiol* **56**: 361-370.

Muller, D.W., Meyer, C., Gurster, S., Kuper, U., Huber, H., Rachel, R. et al. (2009) The Iho670 fibers of Ignicoccus hospitalis: a new type of archaeal cell surface appendage. *J Bacteriol* **191**: 6465-6468.

Näther, D.J., Rachel, R., Wanner, G., and Wirth, R. (2006) Flagella of *Pyrococcus furiosus*: multifunctional organelles, made for swimming, adhesion to various surfaces, and cell-cell contacts. *Journal of Bacteriology* **188**: 6915-6923.

Pohlschroder, M., Ghosh, A., Tripepi, M., and Albers, S.V. (2011) Archaeal type IV pilus-like structures-evolutionarily conserved prokaryotic surface organelles. *Curr Opin Microbiol*.

Pratt, L.A., and Kolter, R. (1998) Genetic analysis of *Escherichia coli* biofilm formation: roles of flagella, motility, chemotaxis and type I pili. *Mol Microbiol* **30**: 285-293.

Rudolph, C., Wanner, G., and Huber, R. (2001) Natural communities of novel archaea and bacteria growing in cold sulfurous springs with a string-of-pearls-like morphology. *Appl Environ Microbiol* **67**: 2336-2344.

Stetter, K.O., Konig, H., and Stackebrandt, E. (1983) Pyrodictium Gen-Nov, a New Genus of Submarine Disc-Shaped Sulfur Reducing Archaebacteria Growing Optimally at 105-Degrees-C. *Systematic and Applied Microbiology* **4**: 535-551.

Strom, M.S., and Lory, S. (1992) Kinetics and sequence specificity of processing of prepilin by PilD, the type IV leader peptidase of Pseudomonas aeruginosa *J Bacteriol* **174**: 7345-7351.

Szabo, Z., Sani, M., Groeneveld, M., Zolghadr, B., Schelert, J., Albers, S.V. et al. (2007) Flagellar motility and structure in the hyperthermoacidophilic archaeon Sulfolobus solfataricus. *J Bacteriol* **189**: 4305-4309.

Thoma, C., Frank, M., Rachel, R., Schmid, S., Nather, D., Wanner, G., and Wirth, R. (2008) The Mth60 fimbriae of *Methanothermobacter thermoautotrophicus* are functional adhesins. *Environ Microbiol* **10**: 2785-2795.

Tripepi, M., Imam, S., and Pohlschroder, M. (2010) Haloferax volcanii flagella are required for motility but are not involved in PibD-dependent surface adhesion. *J Bacteriol* **192**: 3093-3102.

VanDyke, D.J., Wu, J., Logan, S.M., Kelly, J.F., Mizuno, S., Aizawa, S., and Jarrell, K.F. (2009) Identification of genes involved in the assembly and attachment of a novel flagellin N-linked tetrasaccharide important for motility in the archaeon Methanococcus maripaludis. *Mol Microbiol* **72**: 633-644.

Wagner, M., Berkner, S., Ajon, M., Driessen, A.J., Lipps, G., and Albers, S.V. (2009) Expanding and understanding the genetic toolbox of the hyperthermophilic genus Sulfolobus. *Biochem Soc Trans* **37**: 97-101.

Zolghadr, B., Weber, S., Szabo, Z., Driessen, A.J., and Albers, S.V. (2007) Identification of a system required for the functional surface localization of sugar binding proteins with class III signal peptides in *Sulfolobus solfataricus*. *Mol Microbiol* **64**: 795-806.

Zolghadr, B., Klingl, A., Koerdt, A., Driessen, A.J., Rachel, R., and Albers, S.V. (2010) Appendage-mediated surface adherence of *Sulfolobus solfataricus*. *J Bacteriol* **192**: 104-110.

3.4.1 Supplementary material

Table 1: List of primers used in this study

Primer no.	sequence	description
638	5'-GCGCTGCAGAAACCGCATCTGG-3'	Forward primer for upstream region Δ*flaJ* with *Pst*I restriction site
600	5'-GGTCCTTTCAAAATAAGTACCTTTGGTCATATATTTTCATCAAATATTACTGACATATTTTATCGCCTCCTCC-3'	Reverse primer for upstream region Δ*flaJ*, overlapping region
602	5'TCAAATATTACTGACATATTTTATCGCCTCCTCCTGAA AATATATGACCAAAGGTACTTATTTTGAAAGGACC-3'	Forward primer for downstream region Δ*flaJ*, overlapping region
640	5'-GCGGGATCCGAGTGTTTGACATACTTAGAG-3'	Reverse primer for downstream region Δ*flaJ* with BamHI restriction site
581	5'-GAGTCTGCCTGACGGTTCT-3'	Forward sequencing primer Δ*flaJ*
582	5'-GGAGAGTTAAGCTTTCGGCC-3'	reverse sequencing primer Δ*flaJ*
605	5'-GGATCCGGGACATTTAGTCCATTCAC-3'	Forward primer for upstream region Δ*aapF* with *Apa*I restriction site
606	5'AATTTATATACTTTTACTGTGTGAATATACACAACTAG ATAAAGTTAAATATTTTTTATA-3'	Reverse primer for upstream region Δ*aapF*, overlapping region
607	5'-TATAAAAAATATTTAACTTTATCTAGTTGTGTATATTCA CACAGTAAAAGTATATAAATT-3'	Forward primer for downstream region Δ*aapF*, overlapping region
642	5'-GCGGGATCCTCTACCGGCAGGGATAGAAG-3'	Reverse primer for downstream region Δ*aapF* with BamHI restriction site
583	5'-CTGCTATTCTATCTCCTGCAGG-3'	Forward sequencing primer Δ*aapF*
584	5'-CAGTGTTGCTGGAGCTC-3'	reverse sequencing primer Δ*aapF*
2010	5'-GTAGGGCCCGTGTATAATGATGACCTATTTAGCTG-3'	Forward primer for upstream region Δ*upsE* with *Apa*I restriction site
2011	5'-CTAATATTTTCAAGCCATAAGAAGGAAATATTAAAAG-3'	Reverse primer for upstream region Δ*upsE*, overlapping region
2012	5'-CTTCTTATGGCTTGAAAATATTAGCATGTGATATATTC-3'	Forward primer for downstream region Δ*upsE*, overlapping region
2013	5'-GTCGGATCCCTTAATCTATCCTTAAGCGAAACGC-3'	Reverse primer for downstream region Δ*upsE* with BamHI restriction site
2015	5'-GTAAACTGGAAGCCTATAAGG-3'	reverse sequencing primer Δ*upsE*
3506	5'-CATTCCATGGCAACCTCTTCATTCAATACG-3'	Forward primer Δ*aapF*::*aapF* with *Nco*I restriction site
3507	5'-CATTGGATCCCTCCCTGTCCGTTAGAGAAG-3'	Reverse primer Δ*aapF*::*aapF* with *Bam*HI restriction site
666	5'-CTCTGTCTAAAGCCATAAAGATGAG-3'	Forward sequencing primer Δ*aapF*::*aapF*
667	5'-ATATCCACCTCATACTCAGACG-3'	reverse sequencing primer Δ*aapF*::*aapF*
3508	5'-CATTCCATGGCCGTCCTTACTAAGGAAGTC-3'	Forward primer Δ*upsE*::*upsE* with *Nco*I restriction site
3509	5'-CATTGGATCCCTGAATTAGGCTGCATAATTG-3'	reverse primer Δ*upsE*::*upsE* with *Bam*HI restriction site
720	5'-CCCCGAGCTCTCACATGCTAATATTTTCAACC-3'	reverse sequencing primer Δ*upsE*::*upsE*
724	5' -CCCCCGGATCCGATGGATCAGGTATTAGCAGAG-3'	Forward sequencing primer Δ*upsE*::*upsE*
1424	5'-ACT GCG TCT ACT GCG TTA TCT TTA TC-3'	*flaB*-qRT-PCR-fw
1425	5'-GGA GAT AAG TCT ACA CTA GAT ACA CCA GAA-3'	*flaB*-qRT-PCR-rev
1436	5'-CCA GAA AGG AGC AGA ACG GTA GG-3'	*flaJ*-qRT-PCR-fw
1437	5'-GCT ATT ACC GAA GCC AAT TCA CCA ATC-3'	*flaJ*-qRT-PCR-rev
696	5'-CTCTAATTTTAACGTCTCAGTAACTAGC-3'	*aapA*-qRT-PCR-rev
697	5'-CCTACTTGTTCCATAGGATTGTTAGG-3'	*aapA*-qRT-PCR-rev
3504	5'-CTTCTATCCCTGCCGGTAGAAC-3'	*aapB*-qRT-PCR-rev
3505	5'-CTGTGTATGATGCACCTGGAGAG-3'	*aapB*-qRT-PCR-rev
3512	5'-CTCCTGACTACCAACTGACTATTTATC-3'	*aapF*-qRT-PCR-rev
3513	5'-GTTCACCAGTAGAATAGCTCTTTACAC-3'	*aapF*-qRT-PCR-rev
2079	5'-TAGCCAGGGTATGTTCAGTAATC-3'	*upsA*-qRT-PCR-rev
2080	5'-ACCTAAGTTCCCGTTATTGAC-3'	*upsA*-qRT-PCR-rev
2081	5'-GACCAATTCGCTATCCAACTC-3'	*upsB*-qRT-PCR-rev
2082	5'-CTGCATGTCTGATTTCCTACC-3'	*upsB*-qRT-PCR-rev
2075	5'-GCTAGTAAAGCCAACAAGAGTG-3'	*upsE*-qRT-PCR-rev
2075	5'-ATATAGTCGCTGCTACCCTATG-3'	*upsE*-qRT-PCR-rev
1480	5'-CCT GCA ACA TCT ATC CAT AAC ATA CCG A-3'	*secY*-housekeep-qRT-PCR-fw
1481	5'-CCT CAT AGT GTA TAT GCT TTA GTA GTA G-3'	*secY*-housekeep-qRT-PCR-rev
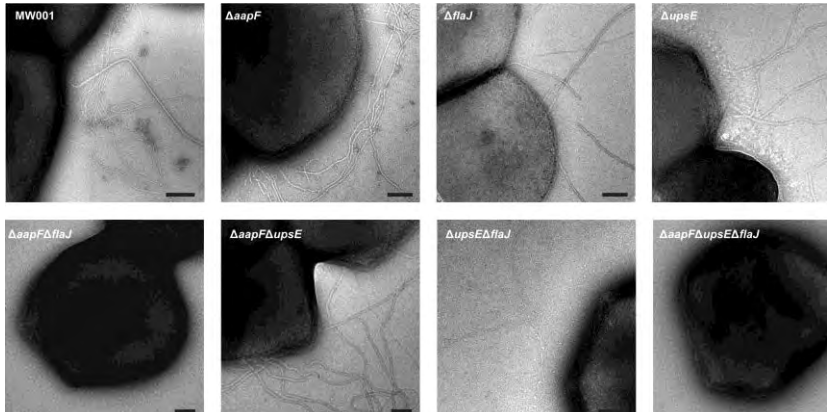
Figure. S1. Electronmicroscopic analyses of all constructed deletion mutants in comparison to the wild type MW001.
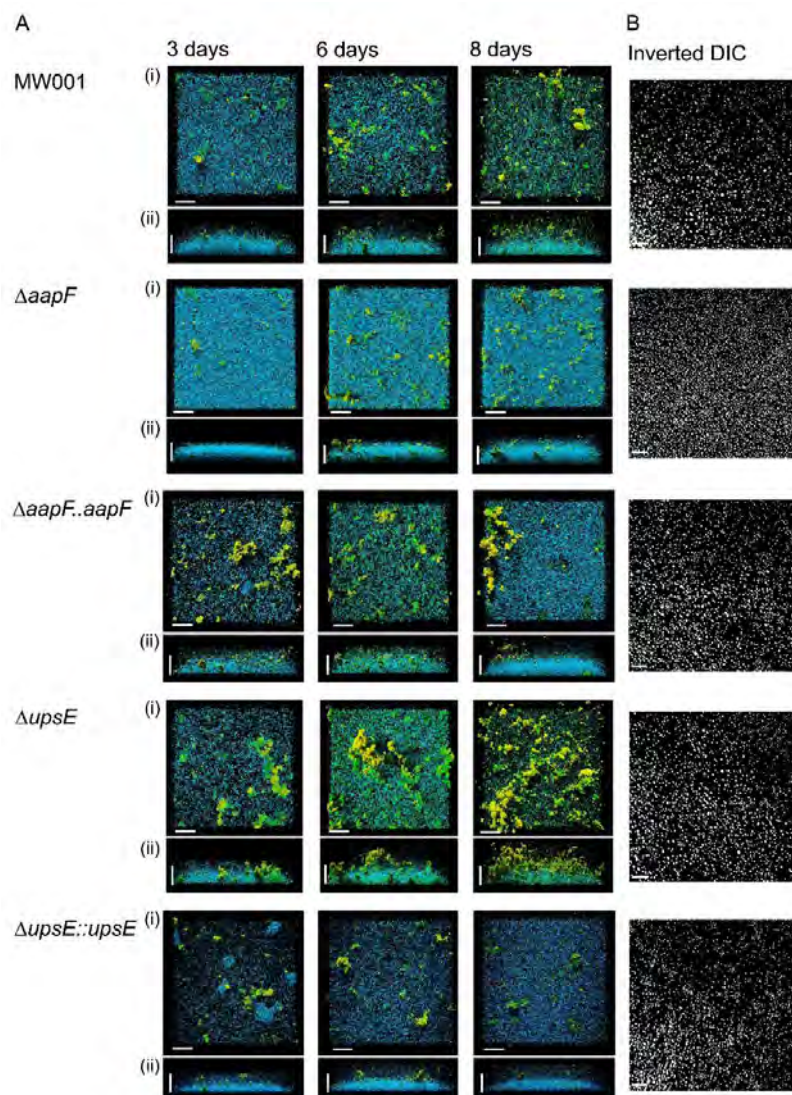
Figure S2. CLSM analysis of complemented upsE and aapF deletion strains. (A) CLSM images of 3, 6, and 8 days grown biofilms of the wild type, the Daapf, and the DupsE strain in comparison to the complemented DaapF::aapF and DupsE::upsE strains. The blue channel depicts the DAPI stain, the green channel the ConA lectin and in yellow the IB4 lectin is given. (B) The black/ white image of the surface coverage of the bottom layer of all the strains shown in (A). The length of the bar is 40 µm

3.5   In vivo analysis of Ssα-man in *S. solfataricus* PBL2025

Koerdt A., Jachlewski S., Ghosh A., Wingender J., Siebers B., Albers SV. 2011.
**Complementation of *Sulfolobus solfataricus* PBL2025 with an α-mannosidase:
effects on surface attachment and biofilm formation** (Submitted to Extremophiles)

N-glycosylation is a protein modification which occurs in all three domains of life and
usually occurs, so far, in all identified archaeal proteins which are exposed to the
environment. Compared to *S. solfataricus* P2, the *S. solfataricus* spontaneous mutant
PBL2025 misses 50 genes (SSO3004-3050), including genes coding for a multitude of
enzymes possibly involved in sugar degradation or metabolism. Furthermore, PBL2025
possesses altered EPS structure with higher amount of sugars (increased mannose
and/or glucose) especially during surface attachment and within biofilm in comparison
to *S. solfataricus* P2. Therefore, the aim of this study was to find out the prospective
candidate gene amongst the 50 lacking genes which might be responsible for the
observed phenotypic differences with respect to the higher production of EPS. We
complemented PBL2025 with two characterized proteins encoded in this genomic
region: the α-mannosidase (SSO3006, Ssα-man) and the β-galactosidase LacS
(SSO3019), and performed comparative fluorescence microscopy and confocal laser
scanning microscopy to analyze the recombinant strains. In our attempt we could
express both these proteins in PBL2025 using the virus vector pSVA9 and also could
successfully purify the expressed proteins. SDS-Page and Western Blot analyzes
demonstrated a high and specific expression of Ssα-man. Fluorescence (surface
attached cells) and confocal laser scanning microscopy (biofilm) of PBL2025
complemented with Ssα-man revealed a change in the EPS production, especially in
respect to biofilm. The change was clearly related to Ssα-man as no changes observed
either for the control or LacS. Analysis of the amount of protein and carbohydrates
within biofilm of all tested strains showed that the complemented strain (Ssα-man)
resembles the P2. The ConA signal of the complemented (Ssα-man) PBL2025 cell
envelope (S-Layer) exhibited a strong reduction indicating its possible role in archaeal
glycosylation.

All experiments of this study were performed by Andrea Koerdt. Abhrajyoti Ghosh
helped in the purification of the Ssα-man. The measurement of the protein- and
carbohydrate amount of the different strains were performed by Silke Jachlewski
(Supervisor Bettina Siebers), and supported by Jost Wingender. The manuscript was
written by Sonja Verena Albers and Andrea Koerdt, and revised by all authors.

Complementation of *Sulfolobus solfataricus* PBL2025 with an α-mannosidase: effects on surface attachment and biofilm formation

Koerdt, A.[1], Jachlewski S.[2], Ghosh. A.[1], Wingender, J.[3] , Siebers, B.[2], Albers, S.-V.[1*]

Abstract Compared to Sulfolobus solfataricus P2, the *Sulfolobus solfataricus* spontaneous mutant PBL2025 misses 50 genes (SSO3004-3050), including genes coding for a multitude of enzymes possibly involved in sugar degradation or metabolism. We complemented PBL2025 with two characterized proteins encoded in this genomic region: the α-mannosidase (SSO3006, Ssα-man) and the β-galactosidase LacS (SSO3019), and performed comparative fluorescence microscopy and confocal laser scanning microscopy to analyze the recombinant strains. We demonstrated that the Ssα-man complemented strain resembled indeed the *S. solfataricus* P2 behavior in respect to attachment of shaking culture cells to glass and growth of cells in the biofilm mode of life. During expression of the Ssα-man, but not LacS, glucose and mannose-containing EPS levels changed in the recombinant strains during surface attachment and biofilm formation. Therefore, the Ssα-man might be involved in the modulation of the EPS composition or in the de-mannosylation of the glycan tree which is attached to extracellular glycosylated proteins in *S. solfataricus*. However, LacS expression in PBL2025 reduced the carbohydrate part of the isolated total EPS implying a role in the modulation of the produced EPS during static biofilm formation. These are the first enzymes identified to play a role in archaeal EPS formation.

[1]Molecular Biology of Archaea, Max Planck Institute for terrestrial Microbiology, Karl-von-Frisch-Strasse, 35043 Marburg, Germany

[2]Molecular Enzyme Technology and Biochemistry (MEB), Biofilm Centre, Faculty of Chemistry, University of Duisburg-Essen, Universitätsstr. 5, 45141 Essen, Germany

[3]Aquatische Mikrobiologie, Biofilm Centre, Faculty of Chemistry, University of Duisburg-Essen, Universitätsstr. 5, 45141 Essen, Germany

[*]Correspondence to S.V. Albers, e-mail: albers@mpi-marburg.mpg.de, tel.: +496421178426, fax: +496421178429

Introduction

Although only few of the so far characterized archaea possess peptidoglycan in their cell envelope, they have been shown to produce and secrete extracelluar polysaccharides (4). While *Thermococcus litoralis* only produces mannose-containing carbohydrates (30-31), haloarchaea and Sulfolobales secrete sulphated exopolysaccharides containing the sugar residues glucose, galactose and rhamnose (5, 26-27).

Most of the extracellular proteins of archaea have been shown to be N- and/or O- glycosylated. O-linked glycans, which are linked via hydroxyl oxygens to Ser or Thr residues have been found in the S-layer proteins of *Halobacterium salinarum* and *Haloferax volcanii* (23, 34). However, detailed studies have only been performed on the N-glycosylation pathway in archaea and demonstrated that the pathway resembles that of Eukarya. Archaeal N-glycans, which are covalently linked to the nitrogen of Asn residues, show an impressive diversity of glycans ranging from linear glycans that encompass even amino acids in methanogens to tri-branched eukarya-like chitibiose bearing glycans in Sulfolobales (1, 20, 29, 36).

Recently, an α-mannosidase (SSO3006, Ssα-man) of *S. solfataricus* belonging to the glycoside hydrolase family 38 (GH38), was shown to catalyze the degradation of α(1,2), α(1,3), and α(1,6)-D-mannobiose *in vitro*, thus exhibiting a broad substrate specificity. In addition the enzyme has been shown to demannosylate high-mannose oligosaccharides (e.g. Man3GlcNAc2, Man7GlcNAc2) commonly found in glycoproteins (11). Most importantly, also the demannosylatation of N-glycosylated proteins (RnaseB) was demonstrated and, therefore, an involvement in protein glycosylation has been postulated (11). While in bacteria GH38 mannosidases are involved in diverse catabolic and metabolic reactions (22, 25, 32), in Eukarya they have been proven to be involved in the trimming of the glycan tree in the endoplasmatic reticulum (18).

The thermoacidophilic crenarchaea *Sulfolobus* spp. contain a high number of N-glycosylated extracellular proteins such as substrate binding proteins, the S-layer protein and flagellins (2). For *Sulfolobus acidocaldarius* it was shown that the tri-branched glycan tree of the S-layer protein contains three mannose sugar residues (29). Moreover, *S. solfataricus* cells attached to a glass surface produced EPS that contained glucose, mannose, galactose and N-acetylglucosamine (37). Similarly, other Sulfolobales strains secreted clouds of EPS during static biofilm formation (21).

Interestingly, it was observed that in contrast to *S. solfataricus* P2, PBL2025, a spontaneous mutant, which is derived from *S. solfataricus* 98/2 (33), formed microcolonies, which secreted a higher amount of EPS (37). Among the 50 genes that are absent in PBL2025 compared to P2 are many sugar degrading, modulating and transporting proteins (33) including the Ssα-man. RT-PCR studies revealed that the Ssα-man was significantly induced in glass-attached cells compared to planktonic cells (37) leading to the hypothesis that the Ssα-man might also be involved in the modulation of EPS (37). LacS (SSO3019), a well described β-glycosidase of P2 (13, 24), is also one of the sugar degrading enzymes that are missing in PBL2025.

This enzyme has a broad spectrum of activity towards substrates including β-galactosides and their chemical analogs. Therefore, addition of X-Gal leads to a blue coloration of LacS-containing cells and it has been demonstrated that LacS is essential for growth of P2 in lactose minimal media (8). Like the Ssα-man, LacS was upregulated during attachment of *S. solfataricus* cells to glass surfaces (37).

In this study we have expressed the Ssα-man and LacS from P2 in PBL2025 and compared the recombinant strains to P2 regarding their behavior during surface attachment, biofilm and EPS formation. Comparative confocal laser scanning microscopy and the isolation and quantitative analysis of EPS of these strains demonstrated the possible function of the Ssα-man in the modulation of the EPS or the intracellular de-mannosylation of the glycan tree prior to transfer to the extracellular glycoproteins.

Material and Methods

Strains and media

Sulfolobus solfataricus P2, PBL2025 (33), PBL2025-ABCE1, PBL2025-LacS (3) and PBL2025- Ssα-man were aerobically grown in liquid Brock medium (10) with a pH of 3 at 76°C. The medium was supplemented either with 0.1% (w/v) tryptone or with 0.1% (w/v) N-Z-Amine, 0.2% (w/v) glucose and 0.2% (w/v) D-arabinose for expression purposes. The growth of the cells was monitored by measurement of the optical density at 600 nm.

Expression of Ssα-man, LacS and ABCE1 in PBL2025

The α-mannosidase gene (*SSO3006*) was amplified from the genomic DNA of P2. The restriction sites *Bam*HI and *Nco*I were incorporated into the PCR product using the primers 5′-TTCCCATGGGAAGAAACATAAACGAGC-3' and 5′-TTCGGATCCACCCCTCACACTTATTG-3', respectively. Cloning of the *Nco*I/*Bam*HI

digested PCR product into pMZ1 resulted in plasmid pSVA620 (38), expressing SSO3006 with a C-terminal tandem tag (Strep-10xHis-tag). The expression construct pSVA621 was generated by digesting pSVA620 with *Eag*I/*Bln*I, followed by ligation of the digested insert to pre-digested pSVA9, thereby replacing *lacS* in the multiple cloning site of pSVA9. For homologous expression of the β-galactosidase LacS (SSO3019) (9) in PBL2025 we used the virus-based vector pSVA9, which contains the β-galactosidase *lacS* under control of the arabinose-inducible promoter *paraS* (3). The control expression plasmid pSVA31 contained ABCE1 (SSO0287), a cytoplasmic protein involved in ribosome recycling (6), under the control of the *paraS* promoter with a C-terminal tandem tag (3). The constructs pSVA621, pSVA9 and pSVA31 were electroporated into PBL2025, which was grown in medium containing 0.1% N-Z-amine, 0.2% glucose and 0.2% D-arabinose as previously described (38). The expression of either α-mannosidase (pSVA621) or ABCE1 (pSVA31) was verified by SDS-PAGE followed by Western blotting. Expression of LacS was tested by a colorimetric assay as described in Albers *et al.* (2006). All constructed plasmids were verified by sequencing.

Attachment assay, fluorescence and differential interference contrast (DIC) microscopy

Microscopy was performed as described in Zolghadr *et al.* (37). Briefly, the cells were grown for 24 h in 40 mL medium containing 0.1% N-Z-amine, 0.2% glucose and 0.2% D-arabinose in the presence of an objective glass slide in 100 mL Schott flasks as shaking cultures at $76^{o}C$ (RPM, Abmessung Glas). The inoculation OD_{600} was 0.01. After 24 h the glass slides were removed from the Schott flasks, washed with Brock medium and then incubated in 5% formaldehyde containing Brock medium with a pH of 5. Light microscopy was performed with fixed cells on the glass slides. For lectin staining, the glass slides were incubated with 15 μl concanvalin A (ConA, 5 mg/mL, Invitrogen, Karlsruhe, Germany).

After lectin staining glass slides were incubated in the dark for 20 min. Prior to microscopy analysis the glass slides were washed once more with Brock medium (pH 5).

Biofilm growth and confocal laser scanning microscopy (CLSM)

CLSM was performed as described in Koerdt *et al.* (21). Briefly, the cells were inoculated to grow static biofilms with an OD_{600} of 0.03 in hydrophobic microscopy plastic dishes (μ-Dishes, 35 mm high; Ibidi, Martinsried). The biofilms were either cultivated in 3 mL Brock medium supplemented with 0.1% tryptone or medium containing 0.1% N-Z-amine, 0.2% glucose and 0.2% D-arabinose for expression under static conditions at 75°C for 3 days, with an exchange of the media (see above) after every 24 h. The biofilm was stained with 6 μl DAPI (4',6-diamidino-2-phenylindole, 300 μg/mL), 15 μl fluorescein-conjugated ConA (5 mg/mL; Invitrogen, Karlsruhe, Germany), specific for α-mannopyranosyl and α-glucopyranosyl residues and 8 μl Alexa Fluor® 594 conjugated isolectin GS-IB$_4$ (IB$_4$) (*Griffonia simplicifolia* 1 mg/mL; Invitrogen, Karlsruhe, Germany), binding to α-D-galactosyl residues. The staining solutions were incubated for at least 20 min at room temperature. Before the CLSM images were taken with an inverted TCS-SP5 confocal microscope (Leica, Bensheim, Germany), unbound lectins were removed by washing of the biofilm with Brock medium (pH 5). The obtained data were analyzed using the program IMARIS (Bitplane AG, Zürich, Switzerland).

Overexpression of Ssα-man (SSO3006), LacS (SSO3019) and ABCE1 (SSO0287) in PBL2025

Twenty milliliters of an overnight culture of PBL2025 cells harboring either the pSVA9, pSVA31 or pSVA621 over-expression plasmids were used to inoculate 300 mL of Brock medium containing 0.1 % NZ-amine and 0.2 % D-arabinose. Cells were grown at 76°C until an $OD600_{nm}$ of 0.8 was reached. The cells were collected by centrifugation, resuspended in lysis buffer [50 mM

HEPES-NaOH, pH 7.5, 150 mM NaCl, 10% (v/v) glycerol] containing the complete EDTA-free protease inhibitor cocktail (1 tablet/ 50 mL of lysate; Roche, Manheim, Germany), frozen in liquid nitrogen and stored at -80°C.

Purification of recombinant proteins

Prior to purification, frozen resuspended cell pellets were thawed on ice. Cells were lysed by sonication with a Sonoplus HD3100 sonicator (Bandelin Sonorex Biotechnique,Germany) using probe HD3100 (60%, 1 minute on, 1 minute off for 20 minutes). Cell debris was removed by centrifugation at 6,000 x g for 15 min followed by centrifugation at 150,000 x g for 30 min at 4^0C in an OptimaTM MAX-XP ultracentrifuge (rotor MLA 55) (Beckman Coulter, USA) to remove membranes. The supernatant was used for histidine affinity chromatography using the ProfiniaTM protein purification system (BioRad Laboratories, Inc, USA) following the manufacturer's protocol. Briefly, for the purification of His-tagged proteins, supernatant was applied to a Ni^{2+}-affinity column (Native IMAC) on the ProfiniaTM protein purification system. Bound protein was eluted in lysis buffer containing 500 mM imidazole. Protein purity was monitored by sodium dodecyl sulphate-polyacrylamide gel electrophoresis (SDS-PAGE). Gels were stained with Biosafe (BioRad Laboratories, Inc, USA) protein stain. Protein concentration was determined with the BioRad protein assay dye-dependent reagent (BioRad Laboratories, Inc, USA). To further check the expression and purification, Western blot analysis was performed using both anti-His (Sigma) and anti-Strep antibodies (BioRad Laboratories, Inc, USA).

EPS extraction and characterization

For EPS extraction S. solfataricus P2, PBL2025, PBL2025- Ssα-man, PBL2025 -LacS and PBL2025-ABCE1 shaking cultures were grown aerobically in Brock medium supplemented with 0.1% (w/v) N-Z-Amine, 0.2% (w/v) glucose and 0.2% (w/v) D-arabinose at 76°C. After two days of incubation,

cultures were streaked on gellan gum-solidified Brock medium (6 g/L gellan gum; Gelzan^{TM} CM Sigma-Aldrich, Munich, Germany) using an inoculation loop. The plates were sealed in plastic bags and incubated at 76°C for 4 days. The biomass was carefully scraped from the surface of the solid medium, using a spatula, weighed and suspended in 6 mM phosphate buffer (pH 7; 0.1 g of wet biomass per 10 mL). Total cell number was determined by DAPI staining (5 µg/mL, 20 min) and enumeration using an epi-fluorescence microscope at 1000-fold magnification

The biofilm suspensions were transferred into 50 mL centrifuge tubes in 10 mL aliquots. To each tube, 2 g of a hydrated cation exchange resin (Dowex® Marathon® C sodium form, Sigma-Aldrich, Munich, Germany), that had been washed twice with phosphate buffer (pH 7, 15 min; 10 mL/g Dowex), were added. The samples were shaken at highest capacity for 20 min on a shaker (VortexGenie®2, Scientific Industries, New York, USA). Afterwards samples were centrifuged (20 min; 20,000 x g; 4°C) and the supernatants (EPS and low molecular weight substances) were filter-sterilized (pore size 0.22 µm) (Rotilabo®, Roth, Karlsruhe, Germany) and dialyzed against deionized water using a dialysis membrane of 12-14 kDa MWCO. The dialyzed supernatant corresponded to the cell-free EPS solution. All extractions were performed in triplicates.

Protein and carbohydrate concentration were determined using photometric methods. Carbohydrate concentrations were measured with the phenol sulfuric acid method (16) using D-glucose as standard. For determination of protein concentrations a modified Lowry assay was applied using bovine serum albumin as standard (28).

Results

Recently, it was demonstrated that surface attached cells of a natural mutant of S. solfataricus 98/2, PBL2025, lacking 50 genes mainly involved in sugar metabolism and transport (33), showed a

highly increased production of EPS and a different structural appearance than P2 (37). To determine whether this difference was also apparent during biofilm formation, P2 and PBL2025 biofilms were grown for 3 days under aerobic static biofilm conditions in small Petri dishes at 76°C in Brock medium supplemented with 0.1% tryptone as described in Koerdt *et al.* (21). To ensure optimal growth, the medium was exchanged every 24 h. The biofilms growing on the bottom of the Petri dishes were washed and stained with DAPI as well as fluorescently labeled lectins (ConA and IB$_4$). While DAPI binds to DNA, ConA binds to mannose and glucose residues and IB$_4$ to galactosyl residues. Previously, it was shown that extracellular proteins of Sulfolobus are N-glycosylated and contain sugars like glucose, galactose, mannose and N-acetylglucosamine (2). Moreover, the glycan structure of the *S. acidocaldarius* S-layer protein has been determined and contained mannose, N-acteylglucosamine, glucose and the sugar sulfoquinovose (29). Additionally, biofilms of *S. tokodaii*, *S. acidocaldarius* and *S.solfataricus* were shown to produce EPS which reacted with ConA, IB4 and GSII (21). Therefore, ConA and IB4 were chosen to analyze the established biofilms. The biofilms formed by P2 and PBL2025 were similar with respect to cell density and thickness of the biofilms as observed by the DAPI signal (Figure 1). Moreover, secretion of galactosyl containing EPS was comparable as demonstrated by staining with IB$_4$ lectin (Data not shown). However, there was a tremendous difference in the observed ConA signal (Figure 1). In PBL2025 a confluent staining with ConA was observed while in P2 exhibited an uneven, very low ConA signal indicating a higher production of glucose- and/or mannose-containing EPS or glycosylated cell surface proteins.

Expression of Ssα-man, LacS and ABCE1 in PBL2025

The lack of 50 genes in the genome of PBL2025 compared to P2 and the previously shown induction of 8 of 18 tested genes of these 50 genes upon
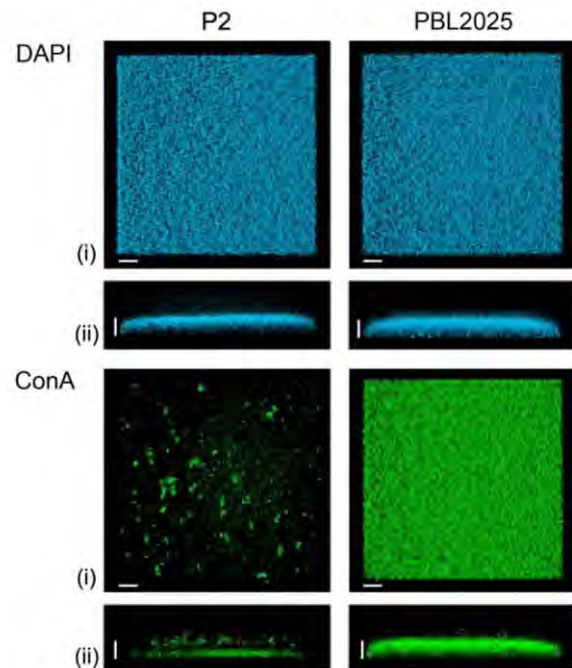
Figure 1: CLSM analysis of three days old P2 and PBL2025 biofilm in Petri dishes. The three days old biofilms of P2 (left) and PBL2025 (right) were stained with DAPI (blue signal) and ConA (green signal) and analyzed by CLSM. Bars are 20 μm in length. (i) represents the top view and (ii) the side view of the biofilms, respectively.
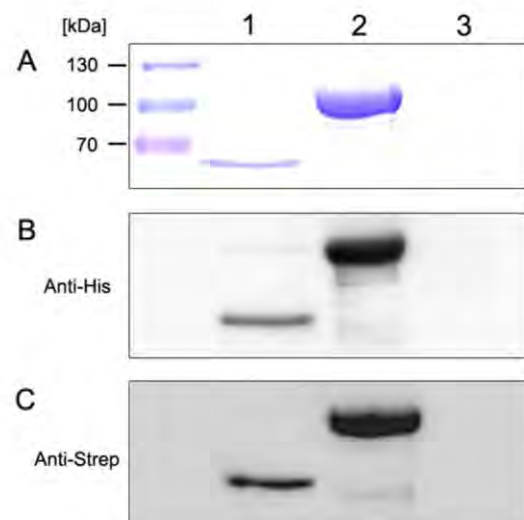
Figure 2: Over-expression and His-tag purification of, PBL2025-Ssα-man, PBL2025-LacS and PBL2025-ABCE1. (A) Coomassie blue-stained SDS-PAGE gel of the Ni affinity chromatography of cytoplasm, Western Blot with (B) anti-His antibody and (C) anti-Strep antibody of PBL2025-ABCE1(1), PBL2025-Ssα-man (2) and PBL2025-LacS (3).

surface attachment suggested a possible function of these enzymes in production and modulation of the EPS and/or S-layer glycoproteins (37). Interestingly,
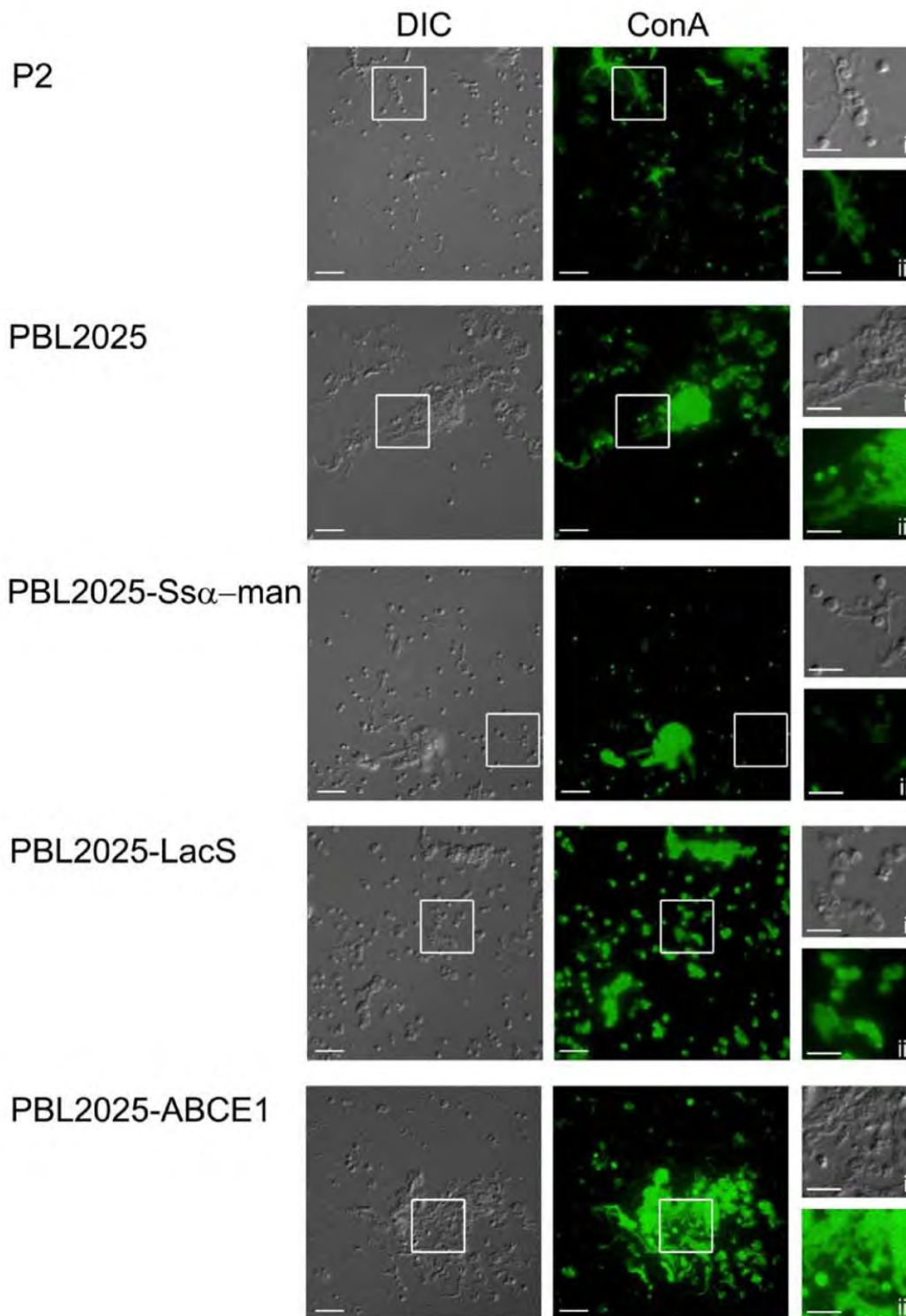
Figure 3: 24 hr Attachment to glass Fluorescence microscopy of ConA stained *S. solfataricus* cells. Surface attached P2, PBL2025, PBL2025 PBL2025-Ssα-man, PBL2025-LacS and PBL2025-ABCE1 were fixed and stained with ConA. In the first column the DIC pictures are illustrated, in the second column the ConA stain and in the third column the overlay of the DIC and ConA stain (bars, 10 μm). The last column displays a detailed view of the grey boxes indicated in the overlay images as DIC (i) and ConA (ii) pictures with higher magnification (bars, 5 μm), respectively.

the previously characterized enzymes α-mannosidase (11) and LacS (13) were among the induced genes.

A recent study by Cobucci-Ponzano *et al.* (2010) demonstrated that the recombinant α-mannosidase from *S. solfataricus* de-mannosylates oligosaccharides, which were frequently found in glycosylated proteins and a possible role in the N-glycosylation pathway was suggested (11). Therefore, we used the available homologous *Sulfolobus* virus based expression system (3, 19) to complement PBL2025 with the α-mannosidase and *lacS* of P2 in order to unravel their role in surface attachment, biofilm and EPS formation.

Five different strains P2, PBL2025 and PBL2025-complemented with either pSVA621 (PBL2025-Ssα-man), pSVA9 (PBL2025-LacS), or pSVA31 (PBL2025-ABCE1 were constructed. ABCE1, a cytosolic protein involved in ribosome recycling was used as control in all experiments (6-7). To confirm that transformation of the plasmids into PBL2025 and expression of the proteins was successful, the recombinant ABCE1 and Ssα-man with C-terminal His- and Strep tag were purified via Ni^{2+} affinity chromatography. Analysis via SDS-PAGE of elution fractions revealed two dominant proteins of the expected molecular mass of 68 kDa for ABCE1 and 110 kDa for Ssα-man (Figure 2A). To further confirm the identity of both proteins, immunoblotting with anti-His- and anti-Strep antibodies was performed (Figure 2C). Recombinant LacS was expressed without any affinity tag. Therefore, its expression was tested via a colorimetric assay, in which the colorless X-GAL was hydrolyzed by LacS resulting in blue coloration of the cells (data not shown).

Attachment of P2, PBL2025 and recombinant strains to glass

To determine whether alterations of EPS production of PBL2025 could be observed when Ssα-man or LacS are overexpressed in this strain, we analyzed the surface attachment from shaking culture in comparison to P2 and PBL2025-ABCE1 after 24 h. P2 (Figure 3, first row) and PBL2025 (Figure 3, second row) showed a phenotype as described before (37): P2 attached with a thin layer of ConA stained material and single cells were visible, which were connected to each other or to the surface by thin filament-like structures (Figure 3, first row (i)). In contrast to this, PBL2025 forms microcolonies surrounded by ConA-stained extracellular material with cells embedded in it (Figure 3, second row (i)). PBL2025-LacS and PBL2025-ABCE1 displayed the same biofilm phenotype as PBL2025. The EPS is voluminous and thin connections are not apparent (Figure 3, third and fourth row). However, EPS of PBL2025-Ssα-man is less voluminous in comparison to PBL2025, but still exhibits a higher amount of EPS than P2 (Figure 3, third row). Considering the fact that still a number of genes are missing in PBL2025-Ssα-man, it was not unexpected that the phenotype could not completely be reversed by the expression of Ssα-man. However, P2 exhibited a weak ConA signal (Figure 3, first row (ii)) whereas PBL2025 gave a strong ConA signal (Figure 3, second row (ii)). The ConA signals for PBL2025-LacS and PBL2025-ABCE1 were comparable to PBL2025 (Figure 3, third and fourth row) and only in the Ssα-man expressing strain the detected ConA signal was greatly diminished in comparison to PBL2025 (Figure 3 third row (ii). Interestingly, the levels of the ConA signal of PBL2025-Ssα-man were comparable to P2 (Figure 3, third row). Therefore, we concluded that the EPS production of PBL2025-Ssα-man is still higher than that of the P2, but the composition changed, i.e. the amount of mannose/glucose is reduced. This is documented by the ConA signal of the cells, which is reduced in the Ssα-man overexpressing strain with respect to all other strains (Figure 3, third row (ii)) tested in this study, implying a change in the S-layer glycan or the EPS of this strain.

Biofilm formation of P2, PBL2025 and the recombinant strains

To further explore this phenomenon we analyzed biofilm formation of all transformed strains. Due to the fact that the α-mannosidase gene was under control of an arabinose inducible promoter in the virus vector (3), these biofilms were grown in the presence of 0.1% N-Z-amine, 0.2% glucose and 0.2% D-arabinose. The biofilms of P2 and PBL2025 showed the same morphology: both exhibited a confluent appearance and the cell density was comparable (Figure 4, row 1 and 2). Importantly, the infection with the virus vector did not influence or
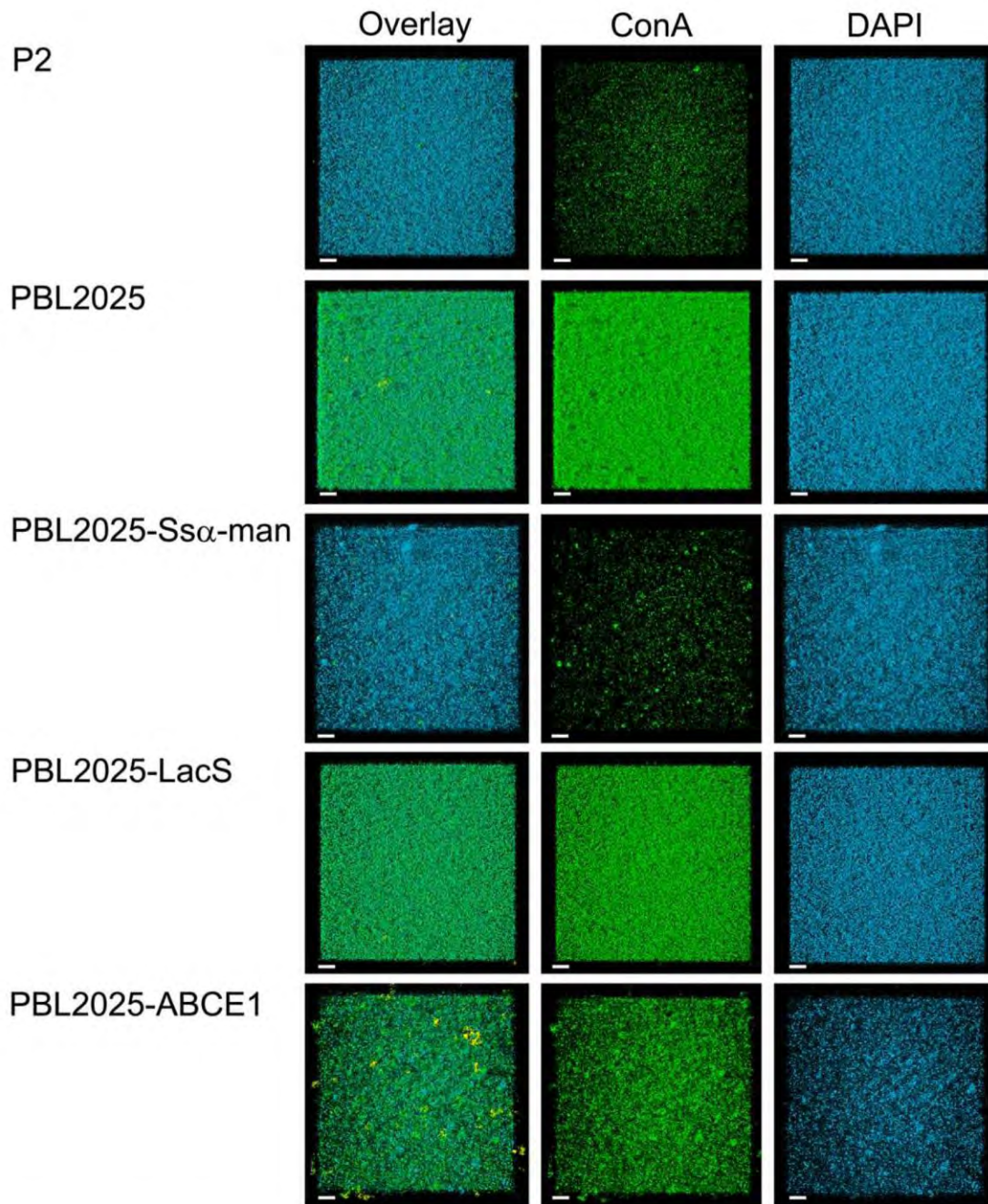
Figure 4: CLSM-analysis of stained *Sulfolobus* biofilm. The 3 days old biofilm of *Sulfolobus solfataricus* P2, PBL2025, PBL2025-Ssα-man, PBL2025-LacS and PBL2025-ABCE1 were stained with DAPI (blue), ConA (green) and IB$_4$ (yellow). In the first column the overlay of all three channels is shown; the second column shows the ConA stain and the third column the DAPI stain. IB$_4$ signal is only shown in the overlay. Bars are 20 μm in length.

change the phenotype of the PBL2025 biofilm, in contrast to what has been observed in bacteria (12, 14-15, 35). PBL2025 and PBL2025-LacS showed the same phenotype with respect to cell density and lectin staining (Figure 4, line 2 and 34). In the PBL2025-ABCE1 biofilm the cell density was lower, which possibly indicated an effect of the overexpression of ABCE1 influencing the cell growth under these conditions (Figure 4, row 5). In contrast to this the biofilm of PBL2025-Ssα-man was comparable with the P2 biofilm (Figure 4, row 3). The ConA signal was strongly reduced and resembled P2 levels (Figure 4, row 3). The ConA signal of the biofilm of PBL2025 and the control strains, PBL2025-LacS and PBL2025-ABCE1 (Figure 4, row 4 and 5) had a similar intensity, like that of surface attached cells (Figure 3). Therefore, all these strains exhibited more EPS or S-layer proteins containing glucose or mannose than P2. Moreover, the complementation of PBL2025 with α-mannosidase led to a phenotype, which is comparable to P2, with respect to the ConA signal.

EPS characterization

In order to determine differences in the composition and quantity of EPS components during biofilm formation P2, PBL2025 and PBL2025-Ssα-man,-LacS and -ABCE1 were grown as biofilms on gellan gum-solidified Brock medium. After EPS extraction using a cation exchange resin (Dowex) the protein and carbohydrate content of the non-dialyzed cell-free supernatant (i.e. total amount of extracellular carbohydrates and proteins including low molecular weight substances) and the dialyzed cell-free supernatant (EPS) in respect to total cell number was determined (Fig. 5, 6).

For P2 the analyses revealed a rather low total carbohydrate concentration of 12.78 fg/cell (Fig. 5). The vast majority of the measured carbohydrates in P2 was of low molecular weight (< 14 kDa) and, thus, was removed by dialysis leading to a concentration of EPS carbohydrates of 4.82 fg/cell. For PBL2025, PBL2025-LacS and PBL2025-ABCE1 a significantly increased carbohydrate

Figure 5: Carbohydrate concentration in the non-dialyzed and dialyzed the cell-free supernatants of biofilms of P2, PBL2025, PBL2025-LacS PBL2025-ABCE1 and PBL2025-Ssα-man.
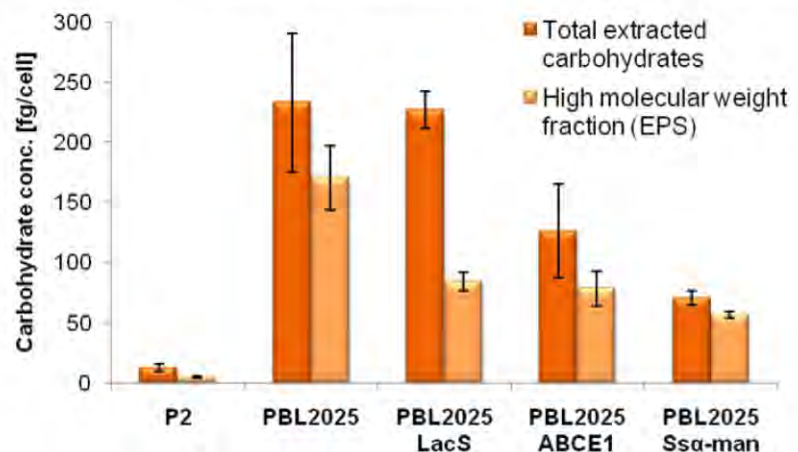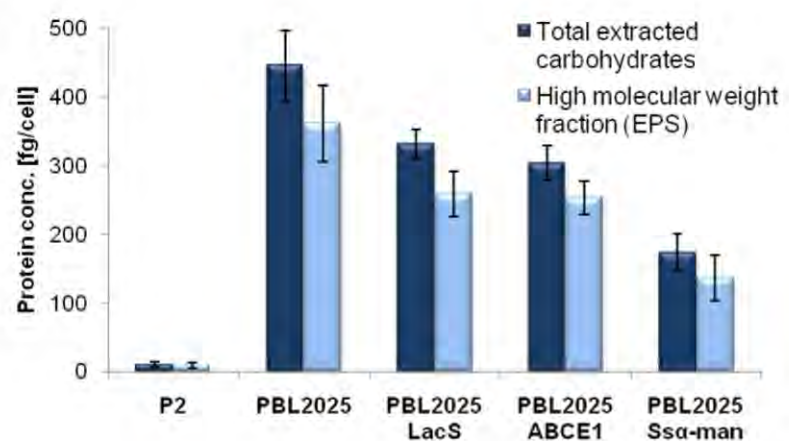

Figure 6: Protein concentration in the non-dialyzed and dialyzed cell-free supernatants of biofilms of P2, PBL2025, PBL2025-LacS PBL2025-ABCE1 and PBL2025-Ssα-man.

production per cell was observed, which contained a significantly higher percentage of high molecular weight compounds. PBL2025 and PBL2025-LacS revealed a 17-fold higher carbohydrate concentration compared to P2 of which 73% and 37% were of high molecular weight, respectively. PBL2025-ABCE1 showed only a slightly higher concentration of total carbohydrates compared to P2. However, the EPS carbohydrate content made up 62% and, therefore, by far exceeded the EPS carbohydrate content in P2. PBL2025-Ssα-man showed a significantly reduced total carbohydrate concentration similar to P2 with 80% being EPS carbohydrates.

Protein quantification revealed a similar trend as observed for carbohydrates (Fig. 6). All strains exhibited protein concentrations of 11 to 445 fg/cell with 78-83% being EPS proteins. P2 showed the lowest production (11 fg/cell) of EPS proteins followed by PBL2025- Ssα-man (136 fg/cell). The highest concentration of proteins was found in the natural mutant PBL2025. Determination of total proteins of this mutant led to a concentration of 445 fg/cell, with 81% being EPS proteins.

Discussion

Previously, we observed that *S. solfataricus* P2 and PBL2025 exhibit different phenotypes upon adhesion to surfaces (37). PBL2025 produced more extracellular material during surface attachment, which contained high levels of sugars including glucose, mannose, galactose and N-acetyl-D-glucosamine. In contrast to P2 PBL2025 lacks 50 genes that are presumably involved in sugar metabolism, degradation and synthesis (33). Therefore, we expressed the two only characterized enzymes of this gene region, LacS (13) and the Ssα-man (11), in PBL2025 to monitor their effect on EPS production and and surface protein glycosylation during attachment and biofilm formation.

Although biofilm formation of PBL2025 on plastic surfaces (Petri dishes) appeared similar to the one of P2 in respect to cell density and biofilm thickness, detection of Glc/Man residues by fluorescently labeled ConA revealed that similar as in microcolonies on glass slides PBL2025 produced either more exopolysaccharide containing Glc/Man residues and/or exhibited a significant change in the glycosylation of its cell surface-associated or extracellular proteins (Fig. 1). Strikingly, the expression of the Ssα-man in PBL2025 resulted in a similar phenotype as P2 with respect to EPS production and surface protein glycosylation in surface attachment and biofilm formation assays. In contrast the expression of LacS as well as ABCE1 did not alter the appearance of the biofilm with respect to the ConA signal. Only for the ABCE1 expressing strain a decrease in cell density of the biofilm was observed compared to the other strains (Fig 4, row 5). ABCE1 is a cytoplasmic protein involved in ribosome recycling and its overexpression might have an effect on cells, however, this effect was not observed during growth curves (data not shown) or surface attachment (Figure 3, row 5). Important is that, although the cell density of the PBL2025-ABCE1 was lower during biofilm formation than in P2, the ConA signal was comparable to the one of PBL2025.

In order to address if the expression of the Ssα-man in PBL2025 has a major effect on EPS formation the amount and overall carbohydrate and protein composition of EPS of all strains was analyzed biochemically. Strains P2 and PBL2025 clearly showed an increased production of EPS, which was reflected in the elevated carbohydrate as well as in the protein content of the extracellular material of strain PBL2025. This further confirmed the hypothesis that the 50 genes lacking in PBL2025 compared to P2 might be involved in the modulation of the EPS. The identity of the extracellular carbohydrates and proteins is still to be investigated. Potential components of extracellular material may be exopolysaccharides (25), S-layer derived glycosylated proteins, membrane vesicles coated

with S-layer proteins (17) as well as flagella and pili (37) released from the biofilm cells.

Although the expression of LacS and ABCE1 had no effect on the ConA binding to biofilms visualized by CLSM, the quantitative EPS analysis showed a decrease in protein and carbohydrate content of the EPS, which was a bit more pronounced in the Ssα- man complemented strain. The reduced formation of EPS by the ABCE1 expression strain was rather unexpected, however, as already indicated by the decreased cell density of the biofilm a major effect is observed, which did, however, not influence ConA binding.

Therefore the expression of the Ssα-man in PBL2025 seemed to have a significant effect, which resulted in a phenotype of biofilm formation and EPS production resembling that of strain P2. As ConA binds preferably to mannose or glucose residues and the Ssα-man hydrolyses high-mannose oligosaccharides as well as demannosylates N-glycosylated proteins (Rnase B) (11), it is most likely that the amount of mannose as a component of glycoproteins changed depending on the absence or presence of Ssα-man. This raised the question whether the Ssα-man expression may affect the glycan tree of glycosylated proteins.

According to the current understanding the archaeal N-glycosylation pathway resembles the eukaryal one, in which ER located α-mannosidases play a crucial role in the trimming of the glycan tree or might also be involved in the degradation and catabolism of glycoproteins (18, 25). A main function of the intracellularly localized Ssα-man in N-glycan processing was proposed previously from *in vitro studies* (11); as the glycan tree is assembled at the cytoplasmic side of the membrane and an overexpression of the cytoplasmic Ssα-man might lead to the de-mannosylation of the glycan tree before transfer of the mature glycoprotein to the extracellular side of the membrane. This would result in a reduced mannosylation of cell surface-associated proteins and –as observed in our experiments– a reduction of the ConA binding to

biofilm cells in CLSM analysis. Therefore, these studies offer first evidence for an *in vivo* function of the cytoplasmic Ssα-man of *S. solfataricus* in trimming of the glycan tree.

Taken together, our study has yielded the following observations, (1) the lack of 50 genes in PBL2025 leads to a change of the sugar content of the EPS/surface proteins in biofilms, and (2) the complementation of PBL2025 with cytoplasmic α-mannosidase (SSO3306), partially recovered the phenotype of P2 during surface attachment and biofilm formation and supports an *in vivo* function of the enzyme in trimming of the glucan tree. Moreover a method was developed to isolate EPS from *Sulfolobus* biofilms, which will enable further studies on the composition, secretion and function of EPS synthesis during *Sulfolobus* biofilm formation.

References

1. **Abu-Qarn, M., S. Yurist-Doutsch, A. Giordano, A. Trauner, H. R. Morris, P. Hitchen, O. Medalia, A. Dell, and J. Eichler.** 2007. Haloferax volcanii AglB and AglD are involved in N-glycosylation of the S-layer glycoprotein and proper assembly of the surface layer. J Mol Biol **374:**1224-36.
2. **Albers, S. V., M. G. Elferink, R. L. Charlebois, C. W. Sensen, A. J. Driessen, and W. N. Konings.** 1999. Glucose transport in the extremely thermoacidophilic Sulfolobus solfataricus involves a high-affinity membrane-integrated binding protein. J Bacteriol **181:**4285-4291.
3. **Albers, S. V., M. Jonuscheit, S. Dinkelaker, T. Urich, A. Kletzin, R. Tampe, A. J. Driessen, and C. Schleper.** 2006. Production of recombinant and tagged proteins in the hyperthermophilic archaeon *Sulfolobus solfataricus*. Appl Environ Microbiol **72:**102-11.
4. **Albers, S. V., and B. H. Meyer.** 2011. The archaeal cell envelope. Nat Rev Microbiol **9:**414-26.
5. **Antón, J., I. Meseguer, and F. Rodríguez-Valera.** 1988. Production of an Extracellular Polysaccharide by Haloferax mediterranei. Applied and Environmental Microbiology **54:**2381-2386.
6. **Barthelme, D., S. Dinkelaker, S. V. Albers, P. Londei, U. Ermler, and R. Tampe.** 2011. Ribosome recycling depends on a mechanistic link between the FeS cluster domain and a conformational switch of the twin-ATPase ABCE1. Proc Natl Acad Sci U S A **108:**3228-33.
7. **Barthelme, D., U. Scheele, S. Dinkelaker, A. Janoschka, F. Macmillan, S. V. Albers, A. J. Driessen, M. S. Stagni, E. Bill, W. Meyer-Klaucke, V. Schunemann, and R. Tampe.** 2007. Structural organization of essential iron-sulfur clusters in the evolutionarily highly conserved ATP-

binding cassette protein ABCE1. J Biol Chem **282**:14598-607.

8. **Bartolucci, S., M. Rossi, and R. Cannio.** 2003. Characterization and functional complementation of a nonlethal deletion in the chromosome of a beta-glycosidase mutant of Sulfolobus solfataricus Journal of Bacteriology **185**:3948-3957.

9. **Bartolucci, S., M. Rossi, and R. Cannio.** 2003. Characterization and functional complementation of a nonlethal deletion in the chromosome of a beta-glycosidase mutant of *Sulfolobus solfataricus*. J Bacteriol **185**:3948-57.

10. **Brock, T. D., K. M. Brock, R. T. Belly, and R. L. Weiss.** 1972. *Sulfolobus*: a new genus of sulfur-oxidizing bacteria living at low pH and high temperature. Arch Mikrobiol **84**:54-68.

11. **Cobucci-Ponzano, B., F. Conte, A. Strazzulli, C. Capasso, I. Fiume, G. Pocsfalvi, M. Rossi, and M. Moracci.** 2010. The molecular characterization of a novel GH38 alpha-mannosidase from the crenarchaeon *Sulfolobus solfataricus* revealed its ability in de-mannosylating glycoproteins. Biochimie **92**:1895-907.

12. **Corbin, B. D., R. J. McLean, and G. M. Aron.** 2001. Bacteriophage T4 multiplication in a glucose-limited *Escherichia coli* biofilm. Can J Microbiol **47**:680-4.

13. **Cubellis, M. V., C. Rozzo, P. Montecucchi, and M. Rossi.** 1990. Isolation and sequencing of a new á-galactosidase-encoding Archaebacterial gene. Gene **94**:89-94.

14. **Doolittle, M. M., J. J. Cooney, and D. E. Caldwell.** 1995. Lytic infection of *Escherichia coli* biofilms by bacteriophage T4. Can J Microbiol **41**:12-8.

15. **Doolittle, M. M., J. J. Cooney, and D. E. Caldwell.** 1996. Tracing the interaction of bacteriophage with bacterial biofilms using fluorescent and chromogenic probes. J Ind Microbiol **16**:331-41.

16. **Dubois, M., K. A. Gilles, J. K. Hamilton, P. A. Rebers, and F. Smith.** 1956. Colorimetric method for determination of sugars and related substances. Anal Chem **28**:350-356.

17. **Ellen, A. F., S. V. Albers, W. Huibers, A. Pitcher, C. F. V. Hobel, H. Schwarz, M. Folea, S. Schouten, E. J. Boekema, B. Poolman, and A. J. M. Driessen.** 2009. Proteomic analysis of secreted membrane vesicles of archaeal Sulfolobus species reveals the presence of endosome sorting complex components. Extremophiles **13**:67-79.

18. **Herscovics, A.** 1999. Importance of glycosidases in mammalian glycoprotein biosynthesis. Biochim Biophys Acta **1473**:96-107.

19. **Jonuscheit, M., E. Martusewitsch, K. M. Stedman, and C. Schleper.** 2003. A reporter gene system for the hyperthermophilic archaeon Sulfolobus solfataricus based on a selectable and integrative shuttle vector. Molecular Microbiology **48**:1241-1252.

20. **Kelly, J., S. M. Logan, K. F. Jarrell, D. J. VanDyke, and E. Vinogradov.** 2009. A novel N-linked flagellar glycan from Methanococcus maripaludis. Carbohydr Res **344**:648-53.

21. **Koerdt, A., J. Gödeke, J. Berger, K. M. Thormann, and S. V. Albers.** 2010. Crenarchael biofilm formation under extreme conditions. PlosOne *in press*.

22. **Maruyama, Y., T. Nakajima, and E. Ichishima.** 1994. A 1,2-alpha-D-mannosidase from a *Bacillus sp.*: purification, characterization, and mode of action. Carbohydr Res **251**:89-98.

23. **Mescher, M. F., and J. L. Strominger.** 1976. Purification and characterization of a prokaryotic glucoprotein from the cell envelope of *Halobacterium salinarium*. J Biol Chem **251**:2005-14.

24. **Moracci, M., M. Ciaramella, and M. Rossi.** 2001. Beta-glycosidase from Sulfolobus solfataricus. Methods Enzymol **330**:201-15.

25. **Nakajima, M., H. Imamura, H. Shoun, and T. Wakagi.** 2003. Unique metal dependency of cytosolic alpha-mannosidase from Thermotoga maritima, a hyperthermophilic bacterium. Arch Biochem Biophys **415**:87-93.

26. **Nicolaus, B., M. C. Manca, I. Ramano, and L. Lama.** 1993. Production of an exopolysaccharide from two thermophilic archaea belonging to the genus *Sulfolobus*. FEMS microbiology letters **109**:203-206.

27. **Paramonov, N. A., L. A. Parolis, H. Parolis, I. F. Boán, J. Antón, and F. Rodríguez-Valera.** 1998. The structure of the exocellular polysaccharide produced by the Archaeon Haloferax gibbonsii (ATCC 33959). Carbohydrate research **309**:89-94.

28. **Petersen, G. L.** 1977. A simplification of the protein assay of Lowry which is more generally applicable. Anal Chem **83**:346-353.

29. **Peyfoon, E., B. Meyer, P. G. Hitchen, M. Panico, H. R. Morris, S. M. Haslam, S. V. Albers, and A. Dell.** 2010. The S-layer glycoprotein of the crenarchaeote *Sulfolobus acidocaldarius* is glycosylated at multiple sites with chitobiose-linked N-glycans. Archaea **2010**.

30. **Rinker, K. D., and R. M. Kelly.** 2000. Effect of carbon and nitrogen sources on growth dynamics and exopolysaccharide production for the hyperthermophilic archaeon Thermococcus litoralis and bacterium Thermotoga maritima. Biotechnol Bioeng **69**:537-47.

31. **Rinker, K. D., and R. M. Kelly.** 1996. Growth Physiology of the Hyperthermophilic Archaeon Thermococcus litoralis: Development of a Sulfur-Free Defined Medium, Characterization of an Exopolysaccharide, and Evidence of Biofilm Formation. Appl Environ Microbiol **62**:4478-85.

32. **Sampaio, M. M., F. Chevance, R. Dippel, T. Eppler, A. Schlegel, W. Boos, Y. J. Lu, and C. O. Rock.** 2004. Phosphotransferase-mediated transport of the osmolyte 2-O-alpha-mannosyl-D-glycerate in *Escherichia coli* occurs by the product of the mngA (hrsA) gene and is regulated by the mngR (farR) gene product acting as repressor. J Biol Chem **279**:5537-48.

33. **Schelert, J., V. Dixit, V. Hoang, J. Simbahan, M. Drozda, and P. Blum.** 2004. Occurrence and characterization of mercury resistance in the hyperthermophilic archaeon *Sulfolobus solfataricus* by use of gene disruption. J Bacteriol **186**:427-37.

34. **Sumper, M., E. Berg, R. Mengele, and I. Strobel.** 1990. Primary structure and glycosylation of the S-layer protein of *Haloferax volcanii*. J Bacteriol **172**:7111-8.

35. **Sutherland, I. W., K. A. Hughes, L. C. Skillman, and K. Tait.** 2004. The interaction of phage and biofilms. FEMS Microbiol Lett **232**:1-6.

36. **Voisin, S., R. S. Houliston, J. Kelly, J. R. Brisson, D. Watson, S. L. Bardy, K. F. Jarrell, and S. M. Logan.** 2005. Identification and characterization of the unique N-linked glycan common to the flagellins and S-layer

glycoprotein of Methanococcus voltae. Journal of Biological Chemistry **280:**16586-16593.

37. **Zolghadr, B., A. Klingl, A. Koerdt, A. J. Driessen, R. Rachel, and S. V. Albers.** 2010. Appendage-mediated surface adherence of *Sulfolobus solfataricus*. J Bacteriol **192:**104-10.

38. **Zolghadr, B., S. Weber, Z. Szabo, A. J. Driessen, and S. V. Albers.** 2007. Identification of a system required for the functional surface localization of sugar binding proteins with class III signal peptides in *Sulfolobus solfataricus*. Mol Microbiol **64:**795-806.

4   Discussion

Organisms struggle for their existence and those who can adopt better to subtle changes in the environment survive. Each living organism follows different strategies to adapt to different environmental conditions and one such strategy is biofilm formation. Cells which are part of a biofilm community survive better under adverse conditions in comparison to the planktonic living cells (169, 288). In spite of considerable effort to understand and analyse this life style, our understanding is mostly restricted to the domain bacteria.

The idea of the third domain of life, archaea, was developed during the 80s from groundbreaking studies by Woese and co-workers (311-312). Since then, research on this domain demonstrated mainly that archaea are virtually detected in all known habitats (not all archaea are extremophiles) (53, 71, 139). It has also been shown that archaea exhibit both unique (69, 134) and shared features of bacteria and eukarya (45). It has recently been shown that like bacteria, archaea can also form biofilms to thrive under different environmental conditions. In the present study the biofilm of the *Sulfolobus spp*. was analysed. This is the first detailed analysis of an archaeal biofilm showing the ability of archaea to switch between different lifestyles, e.g., planktonic and biofilm, respectively, depending on the environmental conditions (temperature, pH, iron-concentrations etc). Three related species were analyzed that belong to the genus *Sulfolobus* for their comparative ability to form biofilm. We aimed to analyze mostly the similarities and differences between these strains in their biofilm lifestyle. Owing to the fact that *Sulfolobus* is a thermoacidophile, the primary initiative was to adopt and develop biofilm-methods for the analysis at 75°C and pH 2. Subsequently experiments, e.g., a method for developing biofilm, microtiter assay, confocal laser scanning microscopy (CLSM), surface attachment, staining of biofilm and harvesting of biofilm cells (146-147, 327) were successfully designed and will be discussed at the appropriate chapter.

4.1   The phenotypical comparison of *Sulfolobus spp*. biofilm

The first and foremost question in biofilm research is how the biofilm looks like for a given organism. Furthermore the next important aspect is to know how physical conditions influence the biofilm (262). To answer these questions researchers use different biochemical and microscopic methods to analyze biofilms. A commonly used method to visualize biofilm is on one hand electron microscopy or CLSM. Both

methods have advantages as well as disadvantages with respect to biofilm analysis and are dependent largely on the purpose of the analysis. While the electron microscopy shows the structure of the cell, appendages and the clusters at a very high resolution, this method includes steps which dehydrate structures and could change the matrix of the biofilm which contains, according to estimates, 97% water (268). In comparison, CLSM is an option to display the biofilm in 3 dimensions in a non-destructive and real-time manner in which a fluorescent signal is required to probe the cells and/or the extra-cellular structures and the resolution is low (154, 223, 298). However, both strategies have been used to reveal the architecture of the *Sulfolobus spp.* biofilms (Figure 4-1).

Many different biofilm phenotypes have been described for bacterial biofilm considering the shape, distribution and also the height of biofilms. However, depending on the species under study and also the nature of the biofilm (static or dynamic) these features have been shown to differ even for the same species. With respect to shape, biofilm can be classified in two types; one with the irregular topology which reflects a tower-like structure with some voids and low coverage of the surface whereas in case of the other type a carpet-structure is evident and is correlated to a generally higher surface coverage (136). It is noteworthy to mention at this stage that several factors must be taken into account while discussing the architecture of biofilm. It is assumed that at least four different biophysical parameters can influence the structure of the biofilm and these are the surface or interface properties, hydrodynamics, the nutrients and finally the biofilm consortia (262). For example *Pseudomonas aeruginosa* PAO1 can form carpet-like biofilm when grown in presence of citrate, benzoate and casamino acids, however the same species forms tower-like biofilm structure when grown on glucose as a sole carbon source (114, 144, 261).

For *Sulfolobus spp.* a similar phenomena was observed although they grew under the same conditions, in respect to temperature, pH and media. The major differences with respect to the architecture was observed after three days of growth under static biofilm condition at which *S. acidocaldarius* formed a biofilm with tower-like structure, *S. solfataricus* a carpet-like structure while *S. tokodaii* exhibited a structure with characteristics of the before mentioned phenotypes (Figure 4-1; Chapter 3.2; (146). Indeed, these differences between the species were observed over a time range of three to eight days (Figure 4-1; 6 days old *Sulfolobus spp.* biofilm). *S. acidocaldarius* was found to produce the most stable biofilm throughout this time range compared to other *Sulfolobus* species. The higher stability might be correlated with the high amount of extracellular materials (EPS) as evident from the lectin staining (yellow and green

fluorescence signal) in the figure 4-1 (A). The differences regarding the EPS will be discussed in depth elsewhere in this chapter.
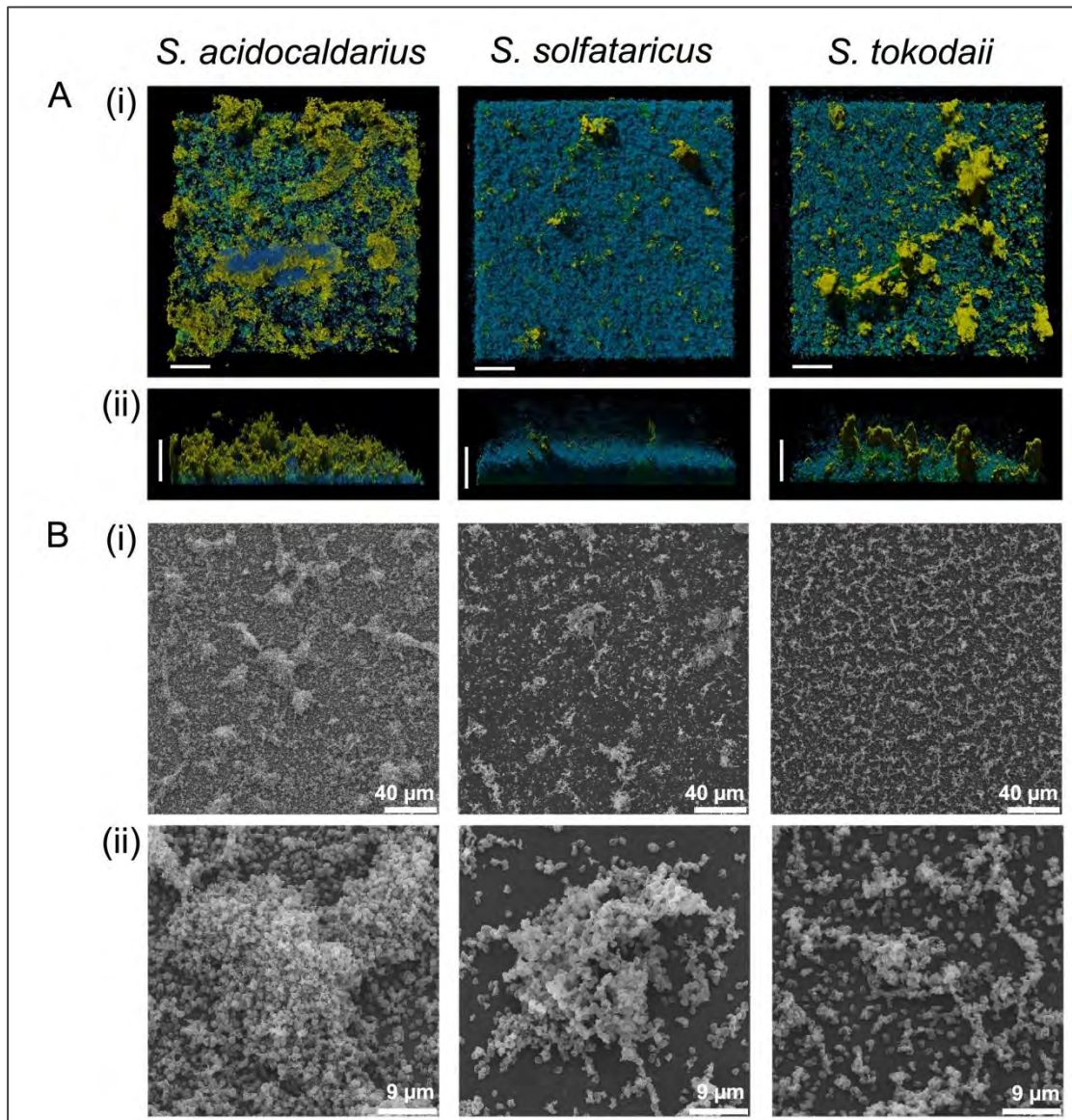
Figure 4-1: Architecture of 6 days old biofilms of *Sulfolobus ssp.*: (A) Confocal laser scanning microscopy of the *S. acidocaldarius*, *S. solfataricus* and *S. tokodaii* biofilm. In the first line the overview (i) and in the second line the sideview (ii) of the biofilm stained with DAPI (blue) and the lectins, ConA (green) and IB$_4$ (yellow) is depicted. Bars are 40 µm in length. (B) Scanning electron microscopy of *S. acidocaldarius*, *S. solfataricus* and *S. tokodaii* biofilm. The third line shows an overview of the biofilm (i) while the fourth line demonstrates parts of the biofilm with higher resolution (ii). Bars are 40 µm (i) or 9 µm (ii) in length.

Besides the structural aspects also the transcriptomic and proteomic data showed next to some similarities clear differences between the three strains. A detailed analysis is required for the understanding how *Sulfolobus* biofilm develops to reveal some possible reasons for the differences. However, the following part will further compare the three species while in the last part of this comparison a conclusive hypothesis will

be introduced which connects the so far obtained results and brings them in correlation to the native habitat of *Sulfolobus spp.*

4.2   The matrix of the biofilm

The matrix, the extracellular substances (EPS), of the biofilm is a key component of this lifestyle and required for several benefits. It is assumed that the EPS sustains the structure and is used as a glue to connect the cells and additionally for protection for instance against shearing forces (264). Therefore, the analysis of the matrix is an issue of major importance. Regrettably, the biofilm matrix of archaea has not been studied in detail so far, while just for *Archeoglobus fulgidus* it is known that the EPS produced in biofilm contains protein, polysaccharide, and metals (152). However, this study did not provide any data about the biochemical composition of the matrix. It was postulated that the EPS of archaea might be similar to those of bacteria; however, lack of evidence further hindered the progress in the field. The matrix of bacterial biofilm is composed of proteins, glycoproteins, glycolipid, polysaccharides or eDNA (83, 267). The determination of the proportion of each of these components is difficult to evaluate due to the challenge that in the process of purification of the EPS often contamination by the cell or macromolecules occur, which are tightly associated with the EPS (83). Additionally, the growth conditions govern the composite of the matrix leading to changes in dependency of the nutrients, temperature or pH (87, 141-142, 145, 293, 300, 313). In spite of these problems the current knowledge, considering the bacterial EPS, increases continuously. So far several components of the matrix have been identified and the functional support for the biofilm formation and stability is proven. Major components of the bacterial biofilm are exopolysaccharides while one of the best studied one is the alginate of the mucoid *P. aeruginosa*. Beside alginate two other exopolysacchrides contribute the biofilm formation, the polysaccharides Psl and Pel (43, 234). Owing to the advanced knowledge, especially to bacterial biofilm, the operon which codes for the exopolysaccarides as well as the sugar composition is known (86-87, 167). An induction of expression levels or the deletion of the exopolysacchride production leads to increased attachment, change of the architecture, or in the case of the deletion to strains with to a defect in biofilm formation (167). Indeed, the deletion of genes which codes for enzymes involved in polysaccharide production of the biofilm matrix result in a defect in biofilm formation for other species as well; for instance the *vps* locus of *Vibrio cholerae* (305) or colonic acid operon of *Escherichia coli* (65).

Although there exists no information on the archaeal biofilm matrix, there is some information available for the exopolysacchride synthesis in archaea. *Haloferax*

mediterranei possess a polymer which is composed of the sugars like mannose, glucose, amino sugars, uronic acids and large amounts of sulphate (16, 231). Other examples are *Natronococcus occultis* which produces a polysaccharide containing L-glutamat (197) or *Natrialba aegyptiaca* which produces poly-γ-D-(glutamtat) (PGA) (115). A study of exopolysaccharides of *Thermococcus litoralis* showed the presence of a sulfated, mannan-like sugar while it was assumed it might be involved in biofilm.

In *Sulfolobus spp*. the operons encoding the exopolysaccaride (glucose, mannose, glucosamine and galactose; (196)) biosynthesis genes are unknown. Using lectin based staining (mannose or glucose (ConA), N-acetyl-D-glucosamine (GS-II) and α-D-galactosyl (IB$_4$)) of the biofilm matrix as it is usual for bacteria (155, 166, 191) we could successfully demonstrate the presence of sugars that were identified previously as part of exopolysaccharides in *Sulfolobus*. The most of the secreted proteins of archaea are glycosylated, e.g., flagellins (192), pilins (193) or S-Layer proteins (179, 213, 266) and for *S. acidocaldarius* is known that the branched glycan tree of the S-Layer contains two mannose residues and a glucose residue (213) to which ConA could bind. It could be argued that the obtained ConA signal stems from the stained S-Layer but there are some facts against this argumentation. First of all, direct cell to cell connection were visualized by ConA (Chapter 3.2; (146)) which definitely do not contain S-Layer and secondly there were also EPS clouds in the top of biofilm stained which do not contain cells (Chapter 3.2; (146)). Furthermore, another indication for the staining of secreted proteins to which the lectins bind is given by the comparison of the ConA signal of *S. solfataricus* and PBL2025. PBL2025 lacks 50 genes involved in sugar metabolism and transport (240). Interestingly, with respect to the ConA signal the intensity of wildtype is recovered by complementation of PBL2025 with SSO3006 which codes for the α-mannosidase (Ssα-man). Ssα-man is involved in the degradation of α(1,2), α(1,3), and α(1,6)-D-mannobiose as well as the demannosylation of glycosylated protein (61). In eukarya a homolog of the α-mannosidase is involved in glycan trimming (112). Therefore the Ssα-man might serve a similar function in *S. solfataricus*. If this is the case, it can be concluded that the obtained ConA signal of *Sulfolobus ssp* biofilm stems also from glycosylated proteins beside to exopolysaccharides.

Nevertheless, *S. acidocaldarius* in comparison to the other species was found to produce a high amount of extracellular substances after three days of biofilm development at which these substances were located at the top of the biofilm. In contrast, *S. solfataricus* showed no comparable structures in the upper part of biofilm and *S. tokodaii* was found to produce comparatively less EPS in these areas (Chapter 3.2, (146)). Another common observation in *Sulfolobus ssp*. biofilm was related to the eDNA which support in bacteria the stability of several biofilms (136). A negligible

amount of eDNA was detected by staining *Sulfolobales spp* biofilm with DAPI (binds to extra- and intracellular DNA) and DDAO (bind to extracellular DNA). In *Sulfolobus ssp.* biofilm the DNAse treatment exhibit a reduction of the little amount of eDNA but the stability and the structure remained undisturbed (Chapter 3.2, (146)). We therefore concluded that eDNA plays no role in stabilizing the biofilm architecture in *Sulfolobus spp.*.

4.3   Transcriptional and proteomic profile of *Sulfolobus* biofilm

It can be expected that the transition from the planktonic to the biofilm lifestyle is associated with a significant change in the expression of genes as well as the synthesized proteins. Such differences were previously analyzed and demonstrated in several bacterial species, in which the results indicated that, the amount or percentage of differences is dependent on fluctuation of physiochemical parameters. In bacteria, the comparison of planktonic cells to biofilm cells revealed that in general 1-15% of the genes were differentially expressed (30, 225, 241, 257, 310). The regulated genes mostly are coding for proteins responsible for the development of matrix, involved in stress condition or anaerobic growth (14, 28, 136). A common responsive expression pattern within bacteria however was not evident from these studies indicating that different bacterial species behave differently during the transition from planktonic to biofilm lifestyle.

Among *Sulfolobus spp.* we expected to find a common response in the proteome and transcriptome between the planktonic and biofilm style of life. However, to our surprise, only very few genes or proteins were in either of the approaches commonly regulated. In general the expression pattern of biofilm cells, in comparison to the planktonic cells, showed significant alteration across all the three species (Chapter 3.3, (147) (transcriptom: *S. acidocaldarius* 15%, *S. solfataricus* 3.4% and *S. tokodaii* 1%). These obtained transcriptional differences were found to be comparable with the results of bacterial biofilm (*E. coli* 5.5% (225) or *Bacillus subtilis* of 14% (224)). Transcriptional analysis of *P. aeruginosa* biofilm showed conversely a broad range of percentage, ranging from 1% (310) up to ~12% (301). Obviously, fluctuations are expected depending on the culture conditions used in the respective studies (301, 310).

In *Sulfolobus spp.* biofilm, most of the differentially regulated gene or proteins were found to be associated with functions related to energy production and conversion, adaptation to environmental changes or stress-responses, substrate transfer, amino acid-, lipid-, carbohydrate- metabolism and motility (surface appendages). Additionally, some regulated proteins were possibly involved in the regulatory network or involved in

other cellular processes (Chapter 3.3, (147)). It should be noted that the received data reflected the situation of a two days old biofilm which is regarding to the current knowledge, a young biofilm and corresponds to the stage of the maturation I.

However, the most striking observation was a common up-regulation of a Lrs14-like protein and the down-regulation of 3-oxoacyl-(acyl-carrier-protein) reductase (FabG) in all the three species used in our study.

In *P. aeruginosa* the FabG protein is participating in the production of the quorum sensing autoinducer (AI) (116). In reference to the cell to cell communication, quorum sensing molecules attracted immense attention in recent years (13, 95). In *Sulfolobus spp.* commonly down-regulated gene 3-oxoacyl-(acyl-carrier-protein) reductase (FabG) is a first indication of the possible existence of cell to cell communication in this organism. However, further research needs to be performed to unravel whether quorum sensing plays a role during the development of the biofilm in *Sulfolobus spp.*.

Lrs14-like proteins, present in both bacteria and archaea, are transcriptional regulators and members of Lrp-AsnC bacterial transcriptional regulator family (leucine-responsive regulatory protein) (189). In in *E. coli* Lrs14-like transcription factors were shown to regulate approximately 75 genes (52). In *Sulfolobus spp.* several Lrp14-like protein homologs are present and the corresponding genes are dispersed across the whole genome. *S. solfataricus* has seven Lrp-like proteins among which five of them have been characterized (LysM (44), Ss-Lrp (58), Ss-LrpB (211), Lrs14 (189) and Sta1 (2)) while for *S. acidocaldarius* only one Lrp-like protein, Sa-Lrp (80) (orthology to Ss-Lrp) was characterized. With exception of Sta1, the expression of Lrp-like proteins is auto-regulated. Interestingly, the Lrs14 (SSO1108) of *S. solfataricus* exhibits, at first, high homology to the common regulated Lrs14-like proteins of the *Sulfolobus ssp.* (SSO1101, ST0837 and Saci_1223) and secondly, is up-regulated in biofilm as well. This indicates that the function of Lrs14 is similar to these homologs, especially because Lrs14 accumulates in the midexponential and late growth phase (189), which would again underline the persistent character of biofilm. Nevertheless, the Lrs14-like protein is very promising regarding to the regulation of some or several genes during biofilm formation and is currently an important subject of research. It might be interesting to figure out if they regulate more than one gene; if they exhibit, as it is known for *E. coli,* a more global regulation pattern; and lastly if they recognize along the three species promoters of different genes and therefore the dissimilarity between the three species occurs in biofilm maturation.

4.4   Development of *S. acidocaldarius* biofilm

As the project progressed, it became clear that the biofilm formation of *S. acidocaldarius* showed the most interesting features. In general, this organism formed the strongest biofilms and produced the highest amount of EPS. Furthermore, this strain was the most attractive in our study as the genetic tools are available (marker less deletion and inducible expression). Therefore, a detailed analysis of biofilm formation in *S. acidocaldarius* was initiated.

Hence, a time course up to seven days was performed (Figure 4-2) to figure out how the structure of the biofilm changes and whether this process resembles the stages known from bacterial biofilm maturation. Naturally, similar experiments were performed for the other two *Sulfolobus ssp.* strains as well (Figure 4-1), for which significant differences or similarities will be mentioned is this section as well.

The analyses demonstrated that the cell density (Figures 4-2; A (i)) and the height of the *S. acidocaldarius* biofilm increased from 20-25 µm up to 40-60 µm after 7 days (Figures 4-2; A, C (ii)) while this increase was also observed for *S. solfataricus* and *S. tokodaii* (Figure 4-1; A (ii))) (Chapter 3.2, (146)). The extracellular material could be visualized in two locations; firstly between the cells for the anchorage to each other and to the surface as it is known for bacteria (63, 136, 187); secondly in areas in the top of the biofilm, while there were no cells detected. It seems that the cells within biofilm secreted a high amount of these substances (which might be exopolysaccharides and/or glycosylated proteins) and over time covered the cells, possibly acting as a protective shield (Figure 4-2; B; D). Similar, but in a reduced form, was the situation in *S. tokodaii* while *S. solfataricus* did not produce this layer on the top of the biofilm (Figure 4-1). However, during the maturation the composition of the matrix was found to be changed in all three tested species with time which was evident from the time (time curve) dependent lectin staining.

The Figure 4-2 E illustrates the biofilm formation of *S. acidocaldarius*. At the third and fourth day the green ConA (glucose and mannose) signal exhibited the strongest intensity, while at the fourth day the yellow signals for IB$_4$ (α-Dgalactosyl) and GS-II (N-acetyl-D-glucosamine) became gradually stronger (Figure 4-2; B, D, E). At the fifth and seventh days the yellow signal by IB$_4$ as well as GS-II signal was predominant and the green ConA signal reduced gradually and disappeared almost completely at the seventh day. A comparable situation occurred for *S. tokodaii* and *S. solfataricus*. *S. acidocaldarius* displayed a decrease in cell numbers towards the seventh day (Figure 4-2; A (ii), C). The cells started to invade into the higher levels of the community while they were embedded or connected to a substance to which the lectins

could bind (Figure 4-2; B (ii), D, E). It is important to underline that the cells which grew in this manner were not stably connected to the lower section of the biofilm.
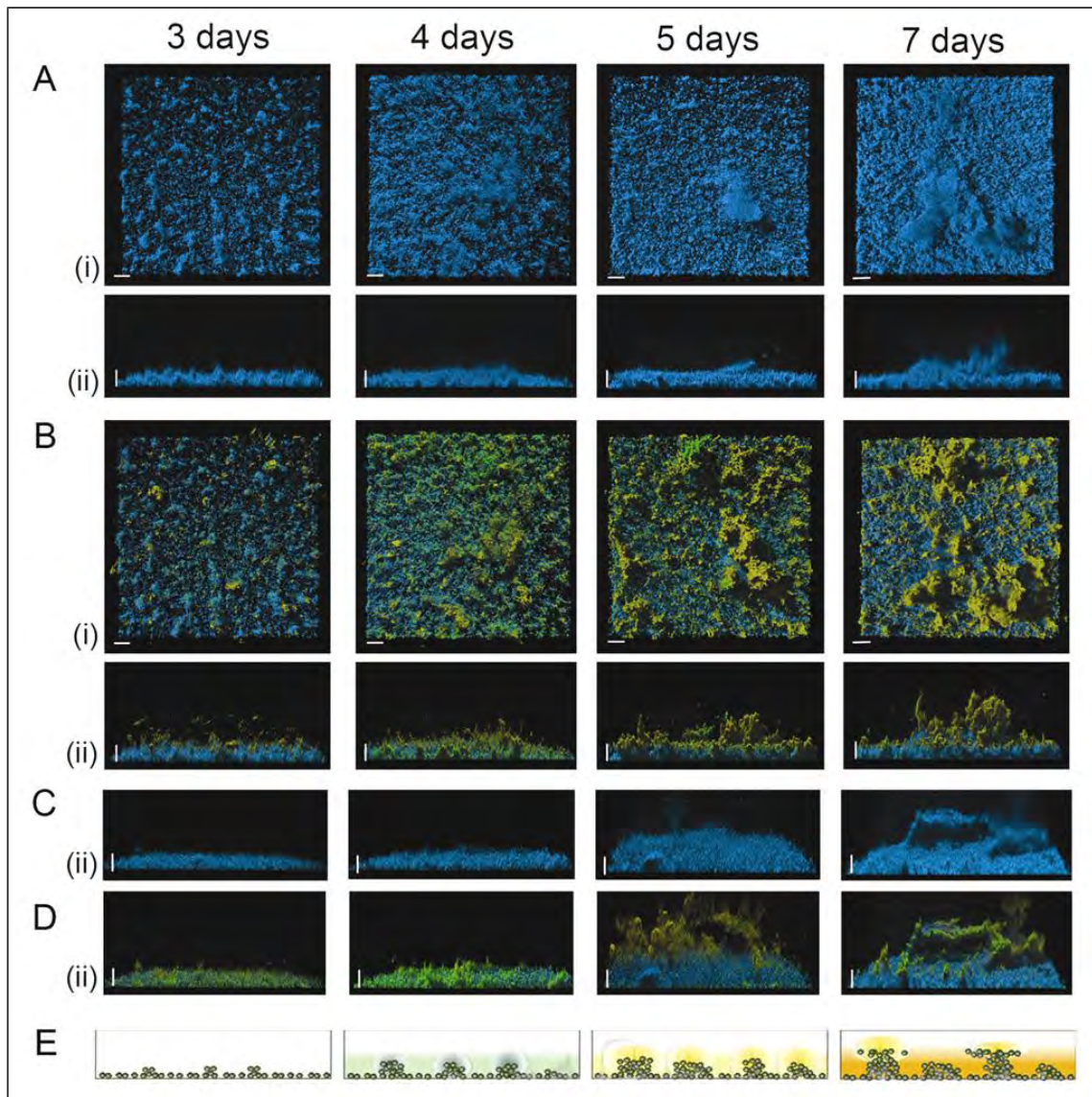
Figure 4-2: Development of *S. acidocaldarius* biofilm. The biofilm formation of *S. acidocaldarius* analyzed over a time range from three to the seventh day (the sixth days datapoint gave no additional supporting information) and stained with DAPI and the lectins ConA (green), IB$_4$ (B, yellow) and GS-II (D, yellow). In A and B is demonstrated one of the replicates stained with DAPI (A), IB$_4$ and ConA (B; overlay of all three signals) while C and D are the second replicate stained with DAPI (C) GS-II and ConA (D; overlay of all three signals). For A and B the overview (i) and the sideview (ii) is shown and for C and D just the sideview (ii). E is the illustrating, in a model-like manner, the sideview of the biofilm development of *S. acidocaldarius*.

Clearly, in the development of bacterial biofilm a similar behaviour can be observed. Based on the current model of bacterial biofilm, the start of the EPS production is important for the transition from attachment to the stage of maturation I (63, 186-187, 199). This can be also observed in the early stage of the *Sulfolobus spp.* biofilm (Chapter 3.2; (146)) (three days). In the transcriptomic analysis two genes were

identified as up-regulated and were correlated to higher EPS production. However, further analysis needs to be performed in order to confirm their exact role in the EPS production. One of these genes shows homology to the NAD-dependent epimerase/dehydratase of *Metallosphaera sedula*, where its participation in exopolysaccharides synthesis is highly suggested (19). The other gene codes for a glycosyl transferase, which in bacteria was found to be involved in the synthesis of heteropolymeric EPS structures (156). The over expression of these genes in bacterial biofilm have been demonstrated, while the deletion led to changes in EPS production (149). In particular, the higher EPS production in *S. acidocaldarius* possibly indicates the higher stability of the biofilm in comparison with *S. solfataricus* and *S. tokodaii* and most likely is responsible for it. It is obvious that additional research needs to be done to confirm or refute this hypothesis.

Nevertheless, the growth or/and motility of *S. acidocaldarius* at the seventh day can be compared to bacterial behaviour which also release cells at this stage from the biofilm into the planktonic phase. This might be caused by two reasons or most possible by a combination of these two: At first, in the later stages of bacterial biofilm the cells can form tower-like structure, parted by channels and void (10, 154) which leads to a better access to nutrients. Beside this higher share forces in hydrodynamic systems at the higher positions of the towers can cause some of the cell clusters to fall down that in turn enables these to colonize new substrates which results in a decrease of cell mass in the biofilm (107, 185, 263). This strategy could be used by *S. acidocaldarius* as well, such that the seventh day of the development represents the later stage leading to dispersal of the cell clusters.

Secondly, another interesting possibility exists regarding the motility of the cells. Motility is indeed evident in the later stages of some bacterial biofilms. For example the fruiting bodies of *Myxococcus xanthus* also show motility which is type-IV pili dependent (164). In some bacteria like *P. aeruginosa* and *Serratia marcescens* (39, 74, 170), mature biofilms contain two distinct subpopulations within the biofilm. In order to demonstrate two sub-populations, *P. aeruginosa* biofilm was treated with antimicrobial peptide colistin that showed the higher sensitivity of the cells located at the stalks (sessile) compared to those located at the cup (motile) of the biofilm. (105). Additionally, the stalk and cup cells exhibit also differences related to the production and secretion of distinct substances. One is for instance eDNA, acting as matrix component; the biosurfactant rhamnolipid is another substance involved in processes of dispersal while both are produced by subpopulations of the stalk (10, 160). Considering the motility, the eDNA produced by the stalk plays an important role, because *P. aeruginosa* form tower-structured biofilms by the use of eDNA. In other

words, cells located at the stalk use the secreted eDNA to climb to the top of the biofilm by the uptake of these mentioned eDNA by type-IV pili (10, 292).

In view of *S. acidocaldarius* and the increased tower-like structures at the seventh day, which are completely embedded in EPS (IB$_4$) or in contact to the cells (GS-II), it might be interesting to explore if this more separate located cells arrived at this position by active moving/sliding along the EPS or if this happened by simple growing. Further experiments are necessary to shed light on this postulate.

4.5   The role of surface appendages in *Sulfolobus* biofilm

Many organisms use their surface appendages for attachment and the development of biofilm (40, 176, 182, 216). However, for other organisms surface appendages play a minor role in these events (145, 217, 238, 257, 281). The influence of flagella or pili for attachment to a surface was demonstrated for members in the domain of archaea. *Pyrococcus furiosus* can attach to different abiotic surfaces using its flagella. However, the attachment was abolished when the cells were treated with flagella specific antibodies (190). Comparatively, by the use of antibodies against the Mth60 fimbriae of *Methanothermobacter thermoautotrophi* the attachment is decreased. Furthermore the deletion of either the flagella or pili, as well as the double knock out, in *Methanococcus maripaludis* leads to the loss of the attachment phenotype (128). While flagella are increasingly shown to be essential in attachment for many archaeal species, it was found to be dispensable in *H. volcanii* (281). Rather the study of Tripepi and Coworkers (281) reported a type IV pili-like structure which might be essential for attachment and is found to be processed by the same peptidase (PibD) as the flagellins.

In *S. solfataricus* the Ups-pili and the flagella are found to be essential for attachment while they play a minor role in biofilm development (Chapter 3.2; (146)). In fact, bacterial flagella mutants can exhibit a similar behaviour: they are unable to attach but can still form directly multi-layered micro colonies (153, 209). *S. acidocaldarius* exhibits, next to Ups-pili and flagella, an additional appendage called the Aap-pili (archaeal adherence pili), which was studied in more detail in this work. For the construction of surface appendages deletion mutants a *S. acidocaldarius* wildtype derived strain, MW001 was used (uracil auxotrophic *pyrE*-deletion strain; Wagner et al, unpublished).

The MW001 biofilms exhibit small differences in the architecture of the biofilm in comparison to the wild type strain DSM639, possibly because of the change in the uridine monophosphate (UMP) synthesis pathway. In general the phenotype reflects

the wild type phenotype, but in an attenuated form, implicating that the clusters are smaller and the EPS production is reduced. A similar situation occurs in an UMP synthesis mutants of *P. aeruginosa*, while as this mutant showed reduced biofilm formation as well (282). Therefore, a complementation on the genomic level of MW001 was performed to restore the wild type situation. Surprisingly, although several different clones were tested for biofilm formation and even though the gene sequence corresponded to the wild type, the MW001 phenotype was maintained for an unknown reason. However, the deletions of the surface appendages were performed using MW001 as background strain. All possible single, double and triple deletion mutants were constructed for a detailed analysis of attachment and biofilm formation. In general electron microscopic analysis revealed that the MW001 possesses usually 3-4 flagella and a high amount of Aap-pili, while the visualization of the Ups-pili are difficult under the tested conditions (Figure 4-3 B (i)). The Ups-pili are smaller in size and normally highly induced after UV light stress (89). Interestingly, the Δ*aapF* (*aapF* encodes for central membrane protein in Aap-pili assembly system) mutant exhibits as expected no Aap-pili, but a very high amount of flagella on its cell surface (Figure 4-3 B (ii)).

In contrast to *S. solfataricus* all single knock outs of the appendages, derived from MW001, were still able to attach to a glass surface. However, the number of attached cells was changed; for the Δ*aapF* deletion mutant attachment increased up to 30%, whereas for Δ*flaJ* a decrease of approximately 30% was observed, while for the Δ*upsE* mutant attachment increased to around 80% (Chapter 3.4). A change in attachment was more predominant in deletion strains that lack two or three appendages. With only the exception of the Δ*upsE*/Δ*flaJ* mutant*,* in which the attachment increased more than 150%, all the double and triple mutants exhibited a reduced attachment of approximately 60-70% (Chapter 3.4). Furthermore, it was also observed that the Δ*aapF*-mutant, which is highly flagellated, attached as cell clusters rather than as single cells which holds true for MW001 (Figure 4-3; B, C). Therefore the appendages were found to be important for attachment in *S. acidocaldarius*, but deletions did not lead to immediate loss off the ability to attach as observed in *S. solfataricus* (Chapter 3.1; (327)). The situation in MW001 reflects a possible cross-talk between the surface appendages with respect to attachment to different surfaces. Further experiments might shed light on their precise role in each of the above mentioned events. Nevertheless, the biofilm formation of the deletion mutants unravelled the influence of these appendages. Three distinct phenotypes are evident in the studied mutants as described in the appropriate section and for remembrance depicted in figure 4-3 A (Chapter 3.4).

Briefly, the first phenotype, termed as wild type phenotype (MW001 and the Δ*flaJ* deletion mutant); and characterized by the layer of cells covering the bottom of the structured biofilm and connected to each other (averages height after 3 days is around 25 μm). The next phenotype is the Ups-phenotype (Δ*upsE* and Δ*upsE*/.Δ*flaJ* deletion mutant), which displays similar bottom coverage as for the MW001 strain, but at higher level the cell density decreases and almost no cells are detectable (Chapter 3.4). Large tower-like structures consisting of a high amount of EPS are visible in this case, but only few cells (Figure 4-3; A). Usually, the Ups-pili are not visible by electron microscopy without UV-treatment, but obviously they do influence the biofilm formation. Whereas the requirement for cell aggregation during UV-stress has been demonstrated (89-90), the exact role these appendages play for the architecture of the biofilm is still elusive. The last biofilm phenotype is the Aap-phenotype, which is dominant over all other phenotypes. In other words, all mutants in which the Aap-pili are lacking showed a high surface coverage, very tense cell layers and a slightly reduced height (3 days; 20-22 μm) (Figure 4-3; A) (Chapter 3.4). This phenotype emerged when the *aapF* is deleted resulting in hyper-flagellated cells (Figure 4-3; C). However the deletion of the other genes from *aap*-operon did not exhibit the same effect (Henche et al, unpublished). Therefore AapF seems to be involved in transcriptional regulation that also links to the expression of the flagella genes.

Nevertheless, the first assumption which arises, considering the cell density, is that the flagella are responsible for the closer cell to cell contacts (Figure 4-3; A). Although the deletion of the flagella led to a slight reduction in the attachment, the biofilm formation remains unaltered. This indicates that similar to other organisms the flagella in this case are also involved in surface attachment.

Recently, Díaz and coworkers demonstrated that the flagella of surface attached *P. fluorescens* getting in contact to neighbouring cells, probably driven by attracting forces (72). It might be that the higher amount of flagella in the Δ*aapF* deletion mutant leads to a closer contact of the cells resulting in cluster formation and higher cell density within the biofilm (Figure 4-3 A). Conversely, mutants in which both the flagella and the AapF pili were deleted (Δ*aapF*/Δ*flaJ* and Δ*aapF*/Δ*flaJ*/Δ*upsE*) the cell density within the biofilm remained unaltered. So, this phenotype definitely refutes that only the flagella are responsible for this phenotype. On the other hand the cluster formation during surface attachment is clearly evident in the hyper flagellated Δ*aapF* mutant, but not in either the Δ*aapF*/Δ*flaJ* or the Δ*aapF*/Δ*flaJ*/Δ*upsE* deletion strains.

In bacteria several factors influence the ability to surface attachment and biofilm formation, for instance cell surface hydrophobicity, presence of pili/flagella and the EPS production.
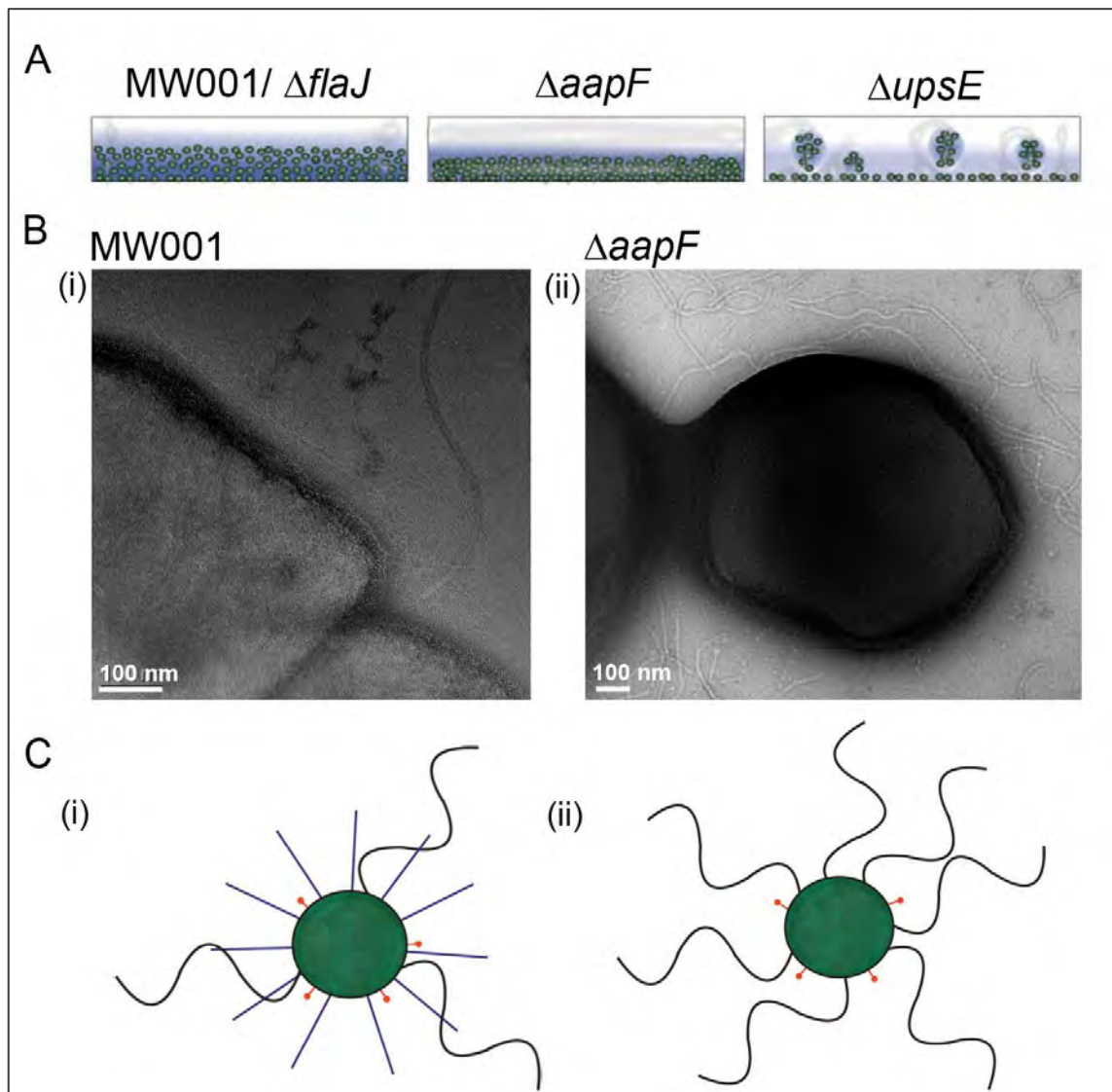
Figure 4-3: Surface appendages mutants of *S. acidocaldarius* MW001. (A) The model like illustration of the three distinct biofilm phenotypes of MW001 and the surface appendages mutants Δ*flaJ*, Δ*aapF* and Δ*upsE*. The phenotype of MW001 and Δ*flaJ* is comparable and therefore depicted as one phenotype. (B) Electron microscopy of MW001- (i) and Δ*aapF* -cells (ii). These pictures illustrate which surface appendage exhibited by each strain and reflects the distribution of those. (C) The Model representation of single cells of MW001 (i) and Δ*aapF* (ii) based on the observation of the electron microscopy. Both cells exhibit flagella and Ups-Pili while the Aap-pili are just present in the MW001 strain. Additionally, the model clarifies the differences regarding to the abundance of the flagella.

The hydrophobicity of the cell surface plays an important role for adhesion to a surface. Usually, bacteria are negatively charged and exhibit surface components with hydrophobic character (73, 289). Surface structures, however, also contribute to the cell surface hydrophobicity. For instance it was shown that fimbriae have no effect on the surface attachment itself, but its component proteins possess a high proportion of hydrophobic amino acids resulting in the hydrophobic nature of the surface (73, 208). This supports the hypothesis that probably this hydrophobicity of the cell surface equips the cells with the ability to overcome the initial electrostatic repulsion barrier between substrate and cell (35, 73). An indication that the hydrophobicity of the cell

surface or the substrate is important for the attachment or the biofilm formation of *Sulfolobus ssp.* is obtained by the fact that *Sulfolobus ssp* form biofilms preferably on hydrophilic surfaces (Chapter 3.2; (146)). Moreover, until recently there was no information available regarding the effect of cell charge or hydrophobicity in either the attachment or the biofilm formation in archaea. The present study, however, strongly suggests the existence of a similar scenario like in bacteria. Further experiments are needed to prove the interpretation of the current observations. In MW001 all three appendages (flagella, Aap- and Ups-Pili) are present leading to the presence of a precisely defined force (cell charge or hydrophobicity) that exists between the cells. Attractive and pushing forces are in balance, keeping the cells in a specific distance to each other and responsible for the distinct way of attachment and the structure of biofilm, which is characteristic for MW001 (Figure 4-4; A; B (i)).
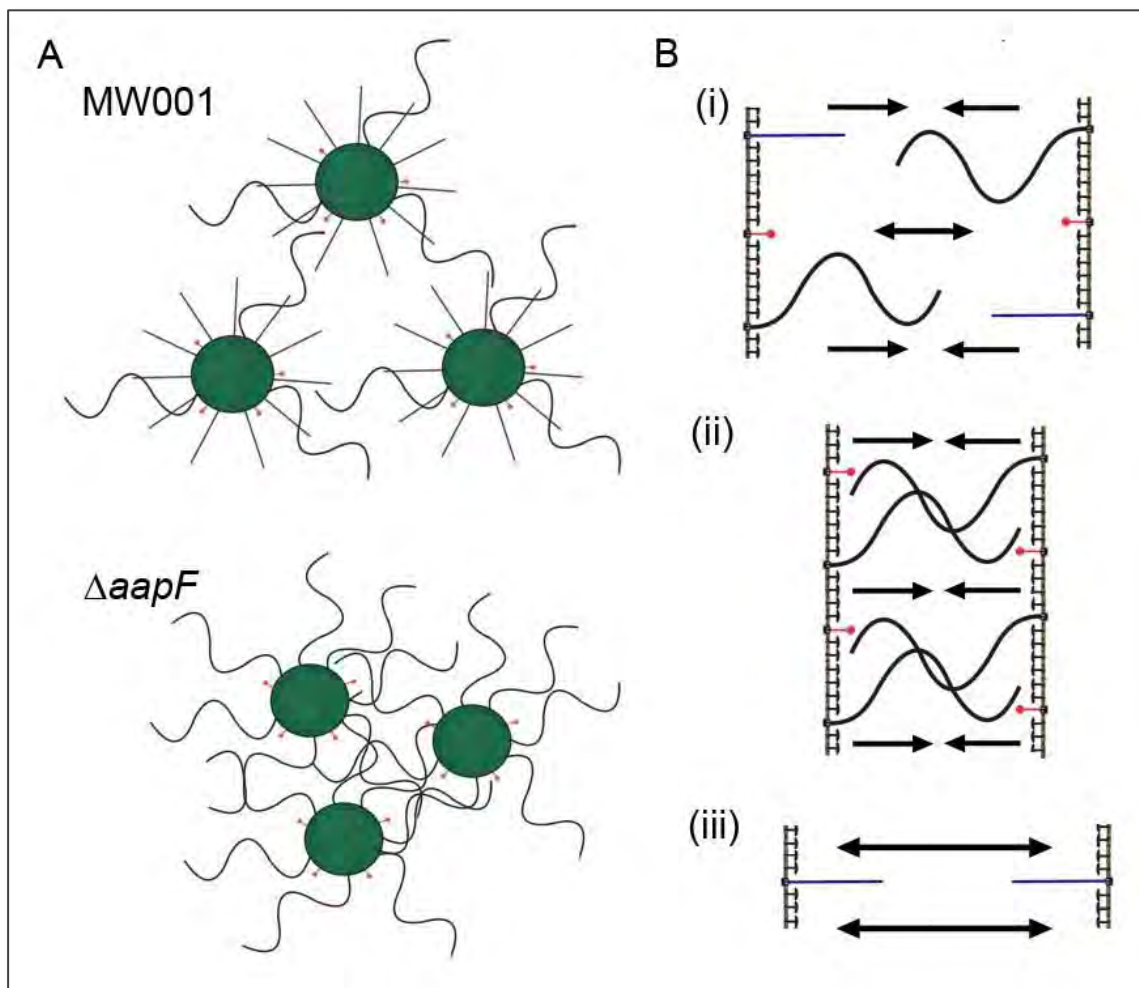
Figure 4-4: Influence of surface appendages and the predicted change in forces between cells. (A) Illustration of the distance between the surface attached and in biofilm of MW001 and Δ*aapF* mutants. The model is based on results of surface attachment, CLSM and the calculation of bottom coverage (Chapter 3.4). (B) Model of the predicted forces between cells in dependency of the abundance of surface appendages. (i) For MW001 is assumed that the attractive and pushing forces in equilibrium. (ii) With higher number of flagella increases the attractive forces while for the Aap-Pili (iii) pushing forces demonstrated.

If *aapF* is deleted the cell express a high number of flagella and form clusters during surface attachment (Figure 4-4; A). Hence, it can be concluded that the level of attracting forces increases (Figure 4-4; B (ii)). In fact, if the flagella and the Aap pili are lacking the cluster formation during surface attachment is abolished, but still the high cell density within biofilm can be observed. This might be explainable by reduction of pushing forces, normally powered by the Aap pili (Figure 4-4, B (iii)). Certainly, this hypothesis needs to be proven by further experiments

5   Conclusive hypothesis

5.1   Biofilm formation in consideration of the native habitat

The tower-like biofilm of *S. acidocaldarius* is the most stable biofilm with the highest resistance against shear forces, in contrast to that of *S. solfataricus* and *S. tokodaii* which are less stable. With respect to the native habitat, it was recently shown that for re-isolation of *Sulfolobus* strains different position within the volcanic spring increases the possibility for selecting a specific *Sulfolobus ssp.*. In other words, if a sample is taken from the crusts around the volcanic spring the most abundant species is *S. acidocaldarius* (Karl-Otto Stetter, personal communication), whereas if it is taken from the middle of the spring (were the "liquid" flow and the share forces are higher) it is mostly *S. tokodaii* and *S. solfataricus* (Christa Schleper, personal communication).

The native habitats of the *Sulfolobales* are hot volcanic spring and they grow under laboratory condition optimally at 75°C and pH around 2. Volcanic habitats can be found under marine conditions (which will not be discussed here) or continental locations (solfataras), from which the *Sulfolobus ssp.* have been isolated. Solfataras are boiling springs, mudholes, and heated soils which contain a high amount of sulfur and a pH that can vary between highly acidic and almost neutral (also slightly alkaline in some cases) (48).

Volcanic springs exhibit a gradient of different physical and chemical properties like carbon sources, iron concentration, oxygen, pH, temperature and sulfate-derivates (85, 122, 244, 303, 321). In figure 5-1 the gradient of some traits are demonstrated; on one hand temperature and pH from the middle of the spring vary to the edges and on the other hand the temperature, pH, ferric iron and oxygen concentrations vary from the surface layer to deeper regions. In the centre of the hot spring is the source of the volcanic stream located and is therefore associated with a very high temperature and acidic pH (Figure 5-1, A). With respect to the depth the upper part (around 30 cm) is highly acidic (pH 0.5-4), aerobic and rich in ferric iron (122, 259-260), whereas the lower part the environment is anaerobic and the pH is higher (259-260) (Figure 5-1, B). In general both zones (upper and lower part) contain high concentrations of sulfur (244).

Based on the results of this work and the conditions in the native habitat a hypothesis is proposed regarding the preferred area for optimal colonization by the different *Sulfolobus ssp.*. However, the three related species developed over the time (evolution) and became specialized and favour distinct conditions and can be found in

delimited areas (Figure 5-1). This statement can be supported by the analysis of biofilm under different stress conditions and the different areas within the native habitat from which a certain strain can be isolated with higher possibility. *S. acidocaldarius* prefers to stay in biofilm at the crusts near to the edges of the springs (Figure 5-1, A; yellow circle). This work confirmed this observation on the basis of result that the efficiency of biofilm formation increased at lower temperatures (60°C) and a pH around 5-6 for *S. acidocaldarius* (Chapter 3.2; (146)). These conditions can be found at the edges of the spring. Additionally, it was detected that the biofilm of *S. acidocaldarius* was the most stable one. Although *S. tokodaii,* as well as *S. solfataricus* stay preferably in the middle of the hot spring, *S. solfataricus* seems to tolerate temperatures above 80°C. While for *S. solfataricus* the most efficient biofilm is formed at 85°C, for *S. tokodaii* the biofilm formation starts to decrease at this temperature (Chapter 3.2; (146)).
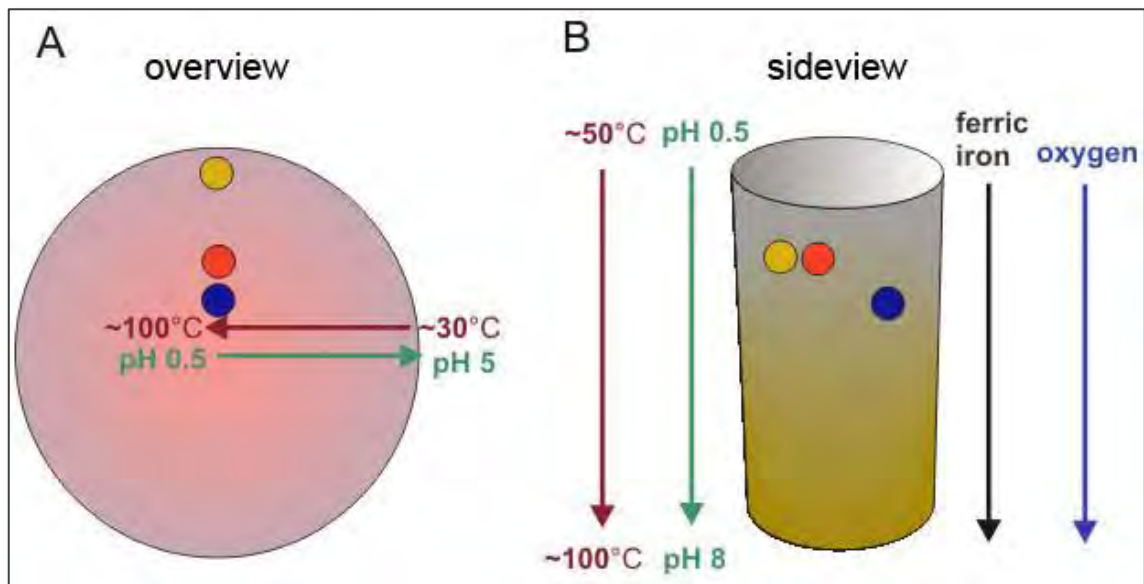
Figure 5-1: Illustration of the physically and chemical gradient of the solfataras. (A) Overview of a mudhole: the middle of the big circle demonstrates in a scheme the center of a mudhole with the higher "liquid" flow; while (B) reflects the sideview of the hole. The arrows indicate if the temperature (red), pH (green) ferric iron concentration (black) or oxygen (blue) concentration is increasing or decreasing along the habitat. The small colored circles shows the preferred location in the habitat of *S. acidocaldarius* (yellow), *S. tokodaii* (orange) and *S. solfataricus* (blue).

The figure 5-1 showed that *S. solfataricus* (Figure 5-1, A; blue circle) is located more close to the middle of the hot springs than *S. tokodaii* (Figure 5-1, A; orange circle). Furthermore, it was also shown that the combination of high iron concentrations and high pH led to a dramatically increased formation of biofilm for *S. tokodaii* and *S. acidocaldarius,* whereas *S. solfataricus* cannot tolerate these combined stresses (Chapter 3.2; (146)). Therefore, it could be concluded that *S. solfataricus* (Figure 5-1, B: blue circle) is located in positions with lower iron concentration, higher temperatures and high pH. On the contrary, *S. acidocaldarius* and *S. tokodaii* can form biofilm more

efficiently if the pH is around 5, the iron concentration is high, and the temperature is 65°C for (*S. tokodaii*; orange circle) or 60°C (*S. acidocaldarius*; yellow circle) (Figure 5-1 B). Indeed, under these conditions it can be generalized that *S. acidocaldarius* and *S. tokodaii* are closer to the surface (higher iron concentration, lower temperature), whereas *S. solfataricus* is in the deeper regions (lower iron concentration, higher temperature). The experiments which were performed during this study strongly support this hypothesis, but surely do not reflect the real situation in which several other aspects like other species, nutrients, the oxygen level, other heavy metals or chemical compounds influence the growth of the strains.

5.2   The role of oxygen in *Sulfolobus* biofilm

The concentration of oxygen is an important feature for biofilm formation and was a matter of interest in the past for bacterial biofilm research. With the use of microelectrodes it was demonstrated for instance for *Klebsiella pneumoniae* and *P. aeruginosa* that the concentration of oxygen decreases in the lower parts of the biofilm when the thickness of biofilm increases (15, 302). The cells in the upper part consume the oxygen resulting in the reduction of both oxygen and nutrients in the biofilm. Thus, cells at the lowest point may exhibit an anaerobic metabolism (136). Furthermore, for some bacterial species it has been shown that the depletion of oxygen and the accumulation of anaerobic metabolic products can lead to the dispersal of the biofilm. For instance, the abrupt decrease of the oxygen level in the *Shewanella oneidensis* biofilm leads to the dissolving of the cell assemblies (278). Apart from this, *P. aeruginosa* exhibits the dispersal of biofilm during nitrosative stress induced by the synthesis of reactive nitrogen intermediates, which are side products of anaerobic respiration (22). Often the poor supply of required nutrients and oxygen correlates with forced or induced cell lyses and cell dead (177, 306). The induced cell lyses appears to be part of the program of the development for the release of eDNA as part of the matrix, which is for some species required for the stability of the biofilm (34, 174, 221, 277, 309) and was discussed in detail above.

Members of *Sulfolobales* are strict aerobes. On this account, it might be a problem for the cells with respect to the fact that within the biofilm clusters the oxygen concentration is low. Furthermore, in lower areas of the native habitat the concentration of oxygen drops down and conditions become anaerobic (259-260). Precisely, this led to the assumption that oxygen depletion is one of the major reasons for the reduction in *Sulfolobus ssp.* biofilm formation in the native habitat that can eventually lead to forced

cell death. Interestingly, it was demonstrated via Life-Dead staining that around 90% of the cells in the three days old biofilm are alive, which implies that no stress conditions are present (Chapter 3.2; (146)). Additionally, transcriptomic and proteomic results of two days old *Sulfolobus ssp.* biofilm indicate that the conditions are aerobic as the genes for respiratory pathways were found to be up-regulated (Chapter 3.3; (147)). Indeed, a similar phenomenon was evident in both *E. coli* K-12 and *Salmonella enterica* serovar Typhimurium biofilm in which the cytochrome o ubiquinol oxidase subunits were found up-regulated (28, 109).

During the study of the *Sulfolobus ssp.* biofilm, Simon and Coworkers published that *S. solfataricus* growth is unaltered at a O_2 range between 1.5%- 24% (252). They also suggested that under low oxygen condition the energy transduction becomes more efficient reflected by the rate of glucose consumption which did not change, but nevertheless a change in the transcriptional pattern was observed (252). Indeed, also in *Sulfolobus ssp.* biofilm changes in the RNA and protein levels of the genes involved in energy metabolism were evident (Chapter 3.3; (147)). Under these circumstances and assuming that *S. acidocaldarius* and *S. tokodaii* also grow under micro-aerophilic condition it is drawing following conclusion. The three *Sulfolobus* species form biofilm and prefer to stay in certain location within the habitat. The cells most likely exhibit a stationary growth phase character. This is supported by the up-regulation of the transcriptional regulators Lrs14 (SSO1108) in *S. solfataricus* and the common regulation of homologs in the three species (Chapter 3.3 (147); Lrs14-like: Saci_1223, SSO1101 and ST0837) while for Lrs14 is demonstrated that it is accumulating in the midexponential and late growth stages (189). Furthermore, similar to what was already demonstrated for bacterial biofilm (18, 274), the metabolism of *Sulfolobus spp.* biofilm showed down regulation of the genes encoding enzymes involved in to the tricarboxylic acid cycle at RNA-level reflecting lower metabolic activities (Chapter 3.3 (147)).Indeed, this persistent lifestyle is common in bacteria as well and one of the reason for the higher resistance of biofilm against toxic components (161). That means that the cells within the biofilm show, because of the limitation of nutrient and oxygen, a behaviour which is comparable with cells in the stationary growth phase (18, 256, 274). The oxygen depletion within *Sulfolobus* biofilm within the native habitat might not influence the growth. Therefore it can be assumed that the limited nutrient supply is responsible for the stationary growth character. However, in contrast to bacteria, *Sulfolobus ssp.* biofilm exhibit more living cells, at least after three days, which leads to the assumption that *Sulfolobus ssp.* is well adapted to biofilm and developed mechanisms which support this life style.

6   Outlook

It is obvious that the knowledge in the field of archaeal biofilm is far behind the bacteria and eukarya. Therefore, several open questions remained unanswered and the results of the present work display the first detailed study of biofilm formation in archaea.

For a profound understanding of archaeal biofilm formation or to be precise *Sulfolobus spp*. biofilm the establishment of a hydrodynamic system is important. It is to be expected that the architecture would reveal stronger differences then statically grown biofilms. Furthermore the analysis of mutants which showed just slight phenotypes grown as static culture probably will show more pronounced phenotypes in a hydrodynamic system. An important advantage for the future will be the expression of GFP in the biofilm grown cells. Currently ongoing optimization of the expression of GFP will be useful to better understand the biofilm formation as well as studies on fusion proteins.

With respect to the analysis of mutants it is still an open question why the MW001 shows difference to the *S. acidocaldarius* wild type. Although, some experiments were performed to figure out if the deletion of *pyrE* is responsible, however the complementation did not lead to a change in phenotype. Available data from deep sequencing analysis indicates the high abundance of anti-sense RNAs in the *S. acidocaldarius* genome which might be involved in so far unknown regulatory processes and therefore secondary mutations might have caused differential regulation of genes in biofilm formation in MW001 in contrast to the *S. acidocaldarius* wild type. Actually, the current state of research is not sufficient to shed light on this phenotypic difference in MW001.

We used MW001 in this study and interestingly found that the deletion of surface appendages resulted in strong phenotypes. The influence of the appendages for attachment as well as biofilm is evident and needs to be further analyzed to understand the role flagella, Ups pili and Aap pili play during the establishment and maturation of the biofilm. It is important to figure out whether the cell charge or the hydrophobicity change in mutants compared to the wild type are the reason for the phenotypic differences and also how a possible cross talk between the appendages is regulated. It is possible that the expression levels of AapF act as negative regulator for the transcription of the flagella. In this respect the role of the Lrs14 regulators is crucial and is currently carried out in our laboratory, It is important to find out whether the Lrs14-like regulators are responsible or involved in the biofilm formation. It is necessary to uncover the binding sites for these transcription factors to better understand their precise role in regulation during the transition from plancktonic to biofilm cells. Ongoing

research of a transcriptional analysis over different time points (1, 3, 4, 6 and 8 days) for *S solfataricus* P2 and *S solfataricus* PBL2025 biofilms showed that the transcriptional regulator and homologues of Lrs14-like proteins are differentially expressed at distinct time points. Therefore, it is important to reveal the genes which might be regulated by these regulator(s).

Next to intracellular regulation, also extracellular regulation is an important aspect for biofilm formation and demonstrated in bacteria. The first indication that this might be true for *Sulfolobus spp* was the common down-regulation of FabG, which might be involved in the production of secreted auto-inducers involved in quorum sensing as known from bacteria. The first results leading to the assumption that such signals are present came from experiments in which the growth of biofilm was strongly inhibited by the addition of supernatant of 6 days old biofilm (Orell et al., unpublished). The identification of small molecules and the possible involvement of FabG in biofilm formation are just in the beginning and need several additional experiments before a conclusion can be drawn.

However, the research of archaeal biofilm is just at a premature state and further research is necessary to understand biofilm formation and its molecules in details.

7   Summary

In this study, the first analysis of crenarchaeal biofilm was performed. Furthermore, this work represents the first in-depth investigation of archaeal biofilm at all. Methods for the analysis of hyperthermophilic biofilm were developed, for instance, microtiter assay, CLSM, and detection of biofilm by fluorescent probes. Furthermore, it was shown that the three related strains *S. solfataricus*, *S. acidocaldarius* and *S. tokodaii* exhibit a high number of differences related to the architecture (carpet-like ranging to tower-like structures), protein and expression pattern, and the requirement of surface appendages.

It was revealed that the matrix of biofilm contains a high amount of sugars (mannose, glucose, N-acetyl-D-glucosamine and galactosyl residues), while it is still unclear if these sugars are present in the exopolysaccharides, glycosylated proteins or both. Furthermore, the matrix included low levels eDNA which are not important for the stability and structure of the biofilm. Remarkable was the fact that the strains showed different reactions when they were exposed to stressful conditions (temperature, pH, and iron).

Commonly required genes/proteins in all three *Sulfolobus ssp.* included Lrs14-like transcriptional regulators and FabG, which could be involved in a novel-archaea quorum sensing system. Another interesting aspect considered the impact of surface appendages to attachment and biofilm formation. *S. solfataricus* requires the flagella and the Ups-pili for surface attachment, but they seemed to be less important for biofilm formation. In contrast, *S. acidocaldarius* exhibited differences in surface attachment dependent on the presence of surface structures, while at least two appendages needed to be deleted before a significant reduction of attachment could be observed. The exception was the mutant which exhibited just the Aap-pili and had a higher affinity to the surface (150% increased). Additionally, the architecture of the biofilm changed in dependency on the appendages as well (three distinct phenotypes were observed).

Furthermore, it was also possible to adapt a GFP usable for the study of biofilm formation in *S. acidocaldarius*. Finally, *in vivo* analyses of the expression of Ssα-man discovered the involvement in the sugar modification of the EPS in *S. solfataricus*. The result of this study indicated the possibility that glycan trimming might be existent in *Sulfolobus spp.*

8 Zusammenfassung

In dieser Studie wurden Biofilmanalysen an Crenarchaeota durchgeführt, welche die ersten tiefergehenden Untersuchungen an archaealen Biofilm überhaupt sind. Es wurden Methoden für die Analyse von Biofilm entwickelt, wie zum Beispiel der Mikrotiter Assay, CLSM und das Färben zur Detektion von Biofilm. Die verwandten Stämme *S. solfataricus*, *S. acidocaldarius* und *S. tokodaii* zeigten erhebliche Unterschiede in ihrer Biofilmarchitektur (von teppich- bis zu turmartigen Strukturen), im Protein- und Transkriptionsmuster, als auch im Bedarf von Zellanhängen für die Biofilmentwicklung.

In der Biofilmmatrix konnten hohe Anteile an Zuckern (Mannose-, Glucose-, N-acetyl-D-glucosamin- und Galactosylreste) detektiert werden, wobei derzeit noch unklar ist, ob diese Zucker auf Exopolysaccharide, glykosylierte Proteine oder beides zurückzuführen sind. Zusätzlich wurden in der Biofilmmatrix geringe Mengen an eDNA nachgewiesen, die allerdings nicht für die Stabilität und Struktur des Biofilms benötigt werden. Auffällig war, dass alle Stämme unterschiedliche Reaktionen im Biofilm unter Stressbedingungen zeigten (Temperatur, pH und Eisen).

Gene, die möglicherweise in Archaea generell eine Rolle in der Biofilmbildung spielen sind der Transkriptionsregulator Lrs14 und FabG, welches möglicherweise an einem neuartigen „quorum sensing system" von Archaeen beteiligt ist. Weitere interessante Beobachtungen wurden bei der Analyse von Mutanten und dem Einfluss von Oberflächenstrukturen auf Biofilm Formation und Anheftung gemacht. Während *S. solfataricus* sowohl die Flagelle als auch den Ups-Pilus für die Anheftung an Oberflächen benötigt, sind diese für die weitere Biofilmformation weniger essentiell. Ein anderes Ergebnis wurde bei *S. acidocaldarius* erzielt, wo die Deletion von mindestens zwei Anhängen zu einer reduzierten Anheftung führte. Eine Ausnahme war hier das Anheften das bei Mutanten beobachtet wurde, die nur noch den Aap-Pilus besaßen (Steigerung um 150%). Die einzelnen Deletion von Oberflächenstrukturen hatte zudem auch Einfluss auf die Biofilmarchitekturen (drei verschiedene Phänotypen).

Ein GFP wurde adaptiert und bietet nun die Möglichkeit für Biofilm Analysen von *S. acidocaldarius*. Abschließend hat eine *in vivo* Analyse der Ssα-man einen Einfluss auf die Zuckerzusammensetzung des EPS in *S. solfataricus* ergeben. Wobei aufgrund der erzielten Ergebnisse, nicht auszuschließen ist, dass dieses Protein in *Sulfolobus spp.* an einer möglichen Prozessierung des Glycan beteiligt ist.

References

1.   **Aas, J. A., B. J. Paster, L. N. Stokes, I. Olsen, and F. E. Dewhirst.** 2005. Defining the normal bacterial flora of the oral cavity. J Clin Microbiol **43:**5721-5732.

2.   **Abella, M., S. Rodriguez, S. Paytubi, S. Campoy, M. F. White, and J. Barbe.** 2007. The *Sulfolobus solfataricus* radA paralogue sso0777 is DNA damage inducible and positively regulated by the Sta1 protein. Nucleic Acids Res **35:**6788-6797.

3.   **Abu-Qarn, M., and J. Eichler.** 2007. An analysis of amino acid sequences surrounding archaeal glycoprotein sequons. Archaea **2:**73-81.

4.   **Abu-Qarn, M., S. Yurist-Doutsch, A. Giordano, A. Trauner, H. R. Morris, P. Hitchen, O. Medalia, A. Dell, and J. Eichler.** 2007. *Haloferax volcanii* AglB and AglD are involved in N-glycosylation of the S-layer glycoprotein and proper assembly of the surface layer. J Mol Biol **374:**1224-1236.

5.   **Albers, S. V., and A. J. Driessen.** 2008. Conditions for gene disruption by homologous recombination of exogenous DNA into the *Sulfolobus solfataricus* genome. Archaea **2:**145-149.

6.   **Albers, S. V., M. G. Elferink, R. L. Charlebois, C. W. Sensen, A. J. Driessen, and W. N. Konings.** 1999. Glucose transport in the extremely thermoacidophilic *Sulfolobus solfataricus* involves a high-affinity membrane-integrated binding protein. J Bacteriol **181:**4285-4291.

7.   **Albers, S. V., S. M. Koning, W. N. Konings, and A. J. Driessen.** 2004. Insights into ABC transport in archaea. J Bioenerg Biomembr **36:**5-15.

8.   **Albers, S. V., and M. Pohlschroder.** 2009. Diversity of archaeal type IV pilin-like structures. Extremophiles **13:**403-410.

9.   **Albers, S. V., Z. Szabo, and A. J. Driessen.** 2003. Archaeal homolog of bacterial type IV prepilin signal peptidases with broad substrate specificity. J Bacteriol **185:**3918-3925.

10.   **Allesen-Holm, M., K. B. Barken, L. Yang, M. Klausen, J. S. Webb, S. Kjelleberg, S. Molin, M. Givskov, and T. Tolker-Nielsen.** 2006. A characterization of DNA release in *Pseudomonas aeruginosa* cultures and biofilms. Mol Microbiol **59:**1114-1128.

11.   **Allison, D. G., and I. W. Sutherland.** 1987. The role of exopolysaccharides in adhesion of freshwater bacteria. Microbiology **133:**1319.

12.   **Amano, A.** 2010. Bacterial adhesins to host components in periodontitis. Periodontol 2000 **52:**12-37.

13.   **An, D., T. Danhorn, C. Fuqua, and M. R. Parsek.** 2006. Quorum sensing and motility mediate interactions between *Pseudomonas aeruginosa* and *Agrobacterium tumefaciens* in biofilm cocultures. Proc Natl Acad Sci U S A **103:**3828-3833.

14.   **An, D., and M. R. Parsek.** 2007. The promise and peril of transcriptional profiling in biofilm communities. Curr Opin Microbiol **10:**292-296.

15.   **Anderl, J. N., J. Zahller, F. Roe, and P. S. Stewart.** 2003. Role of nutrient limitation and stationary-phase existence in *Klebsiella pneumoniae* biofilm resistance to ampicillin and ciprofloxacin. Antimicrob Agents Chemother **47:**1251-1256.

16.   **Anton, J., I. Meseguer, and F. Rodriguez-Valera.** 1988. Production of an Extracellular Polysaccharide by *Haloferax mediterranei*. Appl Environ Microbiol **54:**2381-2386.

17.   **Arsene, F., T. Tomoyasu, and B. Bukau.** 2000. The heat shock response of *Escherichia coli*. Int J Food Microbiol **55:**3-9.

18.   **Ashby, M. J., J. E. Neale, S. J. Knott, and I. A. Critchley.** 1994. Effect of antibiotics on non-growing planktonic cells and biofilms of *Escherichia coli*. J Antimicrob Chemother **33:**443-452.

19.   **Auernik, K. S., Y. Maezato, P. H. Blum, and R. M. Kelly.** 2008. The genome sequence of the metal-mobilizing, extremely thermoacidophilic archaeon *Metallosphaera sedula*

provides insights into bioleaching-associated metabolism. Appl Environ Microbiol **74:**682-692.

20. **Baker-Austin, C., J. Potrykus, M. Wexler, P. L. Bond, and M. Dopson.** 2010. Biofilm development in the extremely acidophilic archaeon '*Ferroplasma acidarmanus*' Fer1. Extremophiles.

21. **Bardy, S. L., T. Mori, K. Komoriya, S. Aizawa, and K. F. Jarrell.** 2002. Identification and localization of flagellins FlaA and FlaB3 within flagella of *Methanococcus voltae*. J Bacteriol **184:**5223-5233.

22. **Barraud, N., D. J. Hassett, S. H. Hwang, S. A. Rice, S. Kjelleberg, and J. S. Webb.** 2006. Involvement of nitric oxide in biofilm dispersal of *Pseudomonas aeruginosa*. J Bacteriol **188:**7344-7353.

23. **Bassler, B. L., and R. Losick.** 2006. Bacterially speaking. Cell **125:**237-246.

24. **Baumeister, W., I. Wildhaber, and B. M. Phipps.** 1989. Principles of organization in eubacterial and archaebacterial surface proteins. Can J Microbiol **35:**215-227.

25. **Bayley, D. P., and K. F. Jarrell.** 1998. Further evidence to suggest that archaeal flagella are related to bacterial type IV pili. J Mol Evol **46:**370-373.

26. **Bechet, M., and R. Blondeau.** 2003. Factors associated with the adherence and biofilm formation by *Aeromonas caviae* on glass surfaces. J Appl Microbiol **94:**1072-1078.

27. **Bellack, A., H. Huber, R. Rachel, G. Wanner, and R. Wirth.** 2011. *Methanocaldococcus villosus* sp. nov., a heavily flagellated archaeon that adheres to surfaces and forms cell-cell contacts. Int J Syst Evol Microbiol **61:**1239-1245.

28. **Beloin, C., and J. M. Ghigo.** 2005. Finding gene-expression patterns in bacterial biofilms. Trends Microbiol **13:**16-19.

29. **Beloin, C., A. Roux, and J. M. Ghigo.** 2008. *Escherichia coli* biofilms. Curr Top Microbiol Immunol **322:**249-289.

30. **Beloin, C., J. Valle, P. Latour-Lambert, P. Faure, M. Kzreminski, D. Balestrino, J. A. Haagensen, S. Molin, G. Prensier, B. Arbeille, and J. M. Ghigo.** 2004. Global impact of mature biofilm lifestyle on *Escherichia coli* K-12 gene expression. Mol Microbiol **51:**659-674.

31. **Berg, H. C., and R. A. Anderson.** 1973. Bacteria swim by rotating their flagellar filaments. Nature **245:**380-382.

32. **Beveridge, T.** 2005. Bacterial surface structure, physicochemistry and geo-reactivity. Geochimica et Cosmochimica Acta Supplement **69:**668.

33. **Beveridge, T. J., P. H. Pouwels, M. Sara, A. Kotiranta, K. Lounatmaa, K. Kari, E. Kerosuo, M. Haapasalo, E. M. Egelseer, I. Schocher, U. B. Sleytr, L. Morelli, M. L. Callegari, J. F. Nomellini, W. H. Bingle, J. Smit, E. Leibovitz, M. Lemaire, I. Miras, S. Salamitou, P. Beguin, H. Ohayon, P. Gounon, M. Matuschek, and S. F. Koval.** 1997. Functions of S-layers. FEMS Microbiol Rev **20:**99-149.

34. **Biswas, R., L. Voggu, U. K. Simon, P. Hentschel, G. Thumm, and F. Gotz.** 2006. Activity of the major staphylococcal autolysin Atl. FEMS Microbiol Lett **259:**260-268.

35. **Bitton, G., and K. C. Marshall.** 1980. Adsorption of microorganisms to surfaces. John Wiley and Sons, Inc.

36. **Blattner, F. R., G. Plunkett, 3rd, C. A. Bloch, N. T. Perna, V. Burland, M. Riley, J. Collado-Vides, J. D. Glasner, C. K. Rode, G. F. Mayhew, J. Gregor, N. W. Davis, H. A. Kirkpatrick, M. A. Goeden, D. J. Rose, B. Mau, and Y. Shao.** 1997. The complete genome sequence of *Escherichia coli* K-12. Science **277:**1453-1462.

37. **Bodenmiller, D., E. Toh, and Y. V. Brun.** 2004. Development of surface adhesion in *Caulobacter crescentus*. J Bacteriol **186:**1438-1447.

38. **Boles, B. R., and A. R. Horswill.** 2008. Agr-mediated dispersal of *Staphylococcus aureus* biofilms. PLoS Pathog **4:**e1000052.

39. **Boles, B. R., M. Thoendel, and P. K. Singh.** 2004. Self-generated diversity produces "insurance effects" in biofilm communities. Proc Natl Acad Sci U S A **101:**16630-16635.

40.   **Bouttier, S., C. Linxe, C. Ntsama, G. Morgant, M. N. Bellon-Fontaine, and J. Fourniat.** 1997. Attachment of Salmonella choleraesuis choleraesuis to beef muscle and adipose tissues. J Food Prot **60:**16-22.

41.   **Boyd, A., and A. M. Chakrabarty.** 1994. Role of alginate lyase in cell detachment of *Pseudomonas aeruginosa*. Appl Environ Microbiol **60:**2355-2359.

42.   **Boyer, R. R., S. S. Sumner, R. C. Williams, M. D. Pierson, D. L. Popham, and K. E. Kniel.** 2007. Influence of curli expression by *Escherichia coli* 0157:H7 on the cell's overall hydrophobicity, charge, and ability to attach to lettuce. J Food Prot **70:**1339-1345.

43.   **Branda, S. S., S. Vik, L. Friedman, and R. Kolter.** 2005. Biofilms: the matrix revisited. Trends Microbiol **13:**20-26.

44.   **Brinkman, A. B., S. D. Bell, R. J. Lebbink, W. M. de Vos, and J. van der Oost.** 2002. The *Sulfolobus solfataricus* Lrp-like protein LysM regulates lysine biosynthesis in response to lysine availability. J Biol Chem **277:**29537-29549.

45.   **Briones, C., S. C. Manrubia, E. Lazaro, A. Lazcano, and R. Amils.** 2005. Reconstructing evolutionary relationships from functional data: a consistent classification of organisms based on translation inhibition response. Mol Phylogenet Evol **34:**371-381.

46.   **Brochier-Armanet, C., B. Boussau, S. Gribaldo, and P. Forterre.** 2008. Mesophilic Crenarchaeota: proposal for a third archaeal phylum, the Thaumarchaeota. Nat Rev Microbiol **6:**245-252.

47.   **Brock, T. D., K. M. Brock, R. T. Belly, and R. L. Weiss.** 1972. *Sulfolobus*: a new genus of sulfur-oxidizing bacteria living at low pH and high temperature. Arch Mikrobiol **84:**54-68.

48.   **Brock, T. D., and M. P. Starr.** 1978. Thermophilic microorganisms and life at high temperatures. Springer-Verlag New York.

49.   **Bu, S., Y. Li, M. Zhou, P. Azadin, M. Zeng, P. Fives-Taylor, and H. Wu.** 2008. Interaction between two putative glycosyltransferases is required for glycosylation of a serine-rich streptococcal adhesin. J Bacteriol **190:**1256-1266.

50.   **Caiazza, N. C., J. H. Merritt, K. M. Brothers, and G. A. O'Toole.** 2007. Inverse regulation of biofilm formation and swarming motility by *Pseudomonas aeruginosa* PA14. J Bacteriol **189:**3603-3612.

51.   **Calo, D., L. Kaminski, and J. Eichler.** 2010. Protein glycosylation in Archaea: sweet and extreme. Glycobiology **20:**1065.

52.   **Calvo, J. M., and R. G. Matthews.** 1994. The leucine-responsive regulatory protein, a global regulator of metabolism in *Escherichia coli*. Microbiol Rev **58:**466-490.

53.   **Cavicchioli, R.** 2011. Archaea--timeline of the third domain. Nat Rev Microbiol **9:**51-61.

54.   **Chaban, B., S. M. Logan, J. F. Kelly, and K. F. Jarrell.** 2009. AglC and AglK are involved in biosynthesis and attachment of diacetylated glucuronic acid to the N-glycan in *Methanococcus voltae*. J Bacteriol **191:**187-195.

55.   **Chaban, B., S. Y. M. Ng, M. Kanbe, I. Saltzman, G. Nimmo, S. I. Aizawa, and K. F. Jarrell.** 2007. Systematic deletion analyses of the fla genes in the flagella operon identify several genes essential for proper assembly and function of flagella in the archaeon, *Methanococcus maripaludis*. Molecular microbiology **66:**596-609.

56.   **Chaban, B., S. Voisin, J. Kelly, S. M. Logan, and K. F. Jarrell.** 2006. Identification of genes involved in the biosynthesis and attachment of *Methanococcus voltae* N-linked glycans: insight into N-linked glycosylation pathways in Archaea. Mol Microbiol **61:**259-268.

57.   **Chandra, J., D. M. Kuhn, P. K. Mukherjee, L. L. Hoyer, T. McCormick, and M. A. Ghannoum.** 2001. Biofilm formation by the fungal pathogen Candida albicans: development, architecture, and drug resistance. J Bacteriol **183:**5385-5394.

58.   **Charlier, D., M. Roovers, T. L. Thia-Toong, V. Durbecq, and N. Glansdorff.** 1997. Cloning and identification of the *Sulfolobus solfataricus* lrp gene encoding an archaeal

homologue of the eubacterial leucine-responsive global transcriptional regulator Lrp. Gene **201:**63-68.

59.   **Chen, L., K. Brugger, M. Skovgaard, P. Redder, Q. She, E. Torarinsson, B. Greve, M. Awayez, A. Zibat, H. P. Klenk, and R. A. Garrett.** 2005. The genome of *Sulfolobus acidocaldarius*, a model organism of the Crenarchaeota. J Bacteriol **187:**4992-4999.

60.   **Chen, Q., H. Wu, and P. M. Fives-Taylor.** 2004. Investigating the role of secA2 in secretion and glycosylation of a fimbrial adhesin in *Streptococcus parasanguis* FW213. Mol Microbiol **53:**843-856.

61.   **Cobucci-Ponzano, B., F. Conte, A. Strazzulli, C. Capasso, I. Fiume, G. Pocsfalvi, M. Rossi, and M. Moracci.** 2010. The molecular characterization of a novel GH38 alpha-mannosidase from the crenarchaeon *Sulfolobus solfataricus* revealed its ability in de-mannosylating glycoproteins. Biochimie **92:**1895-1907.

62.   **Cookson, A. L., W. A. Cooley, and M. J. Woodward.** 2002. The role of type 1 and curli fimbriae of Shiga toxin-producing *Escherichia coli* in adherence to abiotic surfaces. Int J Med Microbiol **292:**195-205.

63.   **Costerton, J. W., Z. Lewandowski, D. E. Caldwell, D. R. Korber, and H. M. Lappin-Scott.** 1995. Microbial biofilms. Annu Rev Microbiol **49:**711-745.

64.   **Danese, P. N., L. A. Pratt, S. L. Dove, and R. Kolter.** 2000. The outer membrane protein, antigen 43, mediates cell-to-cell interactions within *Escherichia coli* biofilms. Mol Microbiol **37:**424-432.

65.   **Danese, P. N., L. A. Pratt, and R. Kolter.** 2000. Exopolysaccharide production is required for development of *Escherichia coli* K-12 biofilm architecture. J Bacteriol **182:**3593-3596.

66.   **Davey, M. E., and A. O'Toole G.** 2000. Microbial biofilms: from ecology to molecular genetics. Microbiol Mol Biol Rev **64:**847-867.

67.   **Davies, D. G., A. M. Chakrabarty, and G. G. Geesey.** 1993. Exopolysaccharide production in biofilms: substratum activation of alginate gene expression by *Pseudomonas aeruginosa*. Appl Environ Microbiol **59:**1181-1186.

68.   **de Carvalho, C. C.** 2007. Biofilms: recent developments on an old battle. Recent Pat Biotechnol **1:**49-57.

69.   **De Rosa, M., A. Trincone, B. Nicolaus, and A. Gambacorta.** 1991. Archaebacteria: lipids, membrane structures, and adaptations to environmental stresses. Berlin Heidelberg: Springer-Verlag.

70.   **Dell, A., A. Galadari, F. Sastre, and P. Hitchen.** 2010. Similarities and differences in the glycosylation mechanisms in prokaryotes and eukaryotes. Int J Microbiol **2010:**148178.

71.   **DeLong, E. F.** 1998. Everything in moderation: archaea as 'non-extremophiles'. Curr Opin Genet Dev **8:**649-654.

72.   **Díaz, C., P. Schilardi, R. Salvarezza, and M. Mele.** 2010. Have flagella a preferred orientation during early stages of biofilm formation?: AFM study using patterned substrates. Colloids and Surfaces B: Biointerfaces.

73.   **Donlan, R. M.** 2002. Biofilms: microbial life on surfaces. Emerg Infect Dis **8:**881-890.

74.   **Drenkard, E., and F. M. Ausubel.** 2002. *Pseudomonas* biofilm formation and antibiotic resistance are linked to phenotypic variation. Nature **416:**740-743.

75.   **Elferink, M. G., S. V. Albers, W. N. Konings, and A. J. Driessen.** 2001. Sugar transport in *Sulfolobus solfataricus* is mediated by two families of binding protein-dependent ABC transporters. Mol Microbiol **39:**1494-1503.

76.   **Elkins, J. G., M. Podar, D. E. Graham, K. S. Makarova, Y. Wolf, L. Randau, B. P. Hedlund, C. Brochier-Armanet, V. Kunin, I. Anderson, A. Lapidus, E. Goltsman, K. Barry, E. V. Koonin, P. Hugenholtz, N. Kyrpides, G. Wanner, P. Richardson, M. Keller, and K. O. Stetter.** 2008. A korarchaeal genome reveals insights into the evolution of the Archaea. Proc Natl Acad Sci U S A **105:**8102-8107.

77.   **Emerson, S. U., K. Tokuyasu, and M. I. Simon.** 1970. Bacterial flagella: polarity of elongation. Science **169:**190-192.

78.   **Engelhardt, H.** 2007. Are S-layers exoskeletons? The basic function of protein surface layers revisited. J Struct Biol **160:**115-124.

79.   **Engelhardt, H., and J. Peters.** 1998. Structural research on surface layers: a focus on stability, surface layer homology domains, and surface layer-cell wall interactions. J Struct Biol **124:**276-302.

80.   **Enoru-Eta, J., D. Gigot, T. L. Thia-Toong, N. Glansdorff, and D. Charlier.** 2000. Purification and characterization of Sa-lrp, a DNA-binding protein from the extreme thermoacidophilic archaeon *Sulfolobus acidocaldarius* homologous to the bacterial global transcriptional regulator Lrp. J Bacteriol **182:**3661-3672.

81.   **Faille, C., C. Jullien, F. Fontaine, M. N. Bellon-Fontaine, C. Slomianny, and T. Benezech.** 2002. Adhesion of Bacillus spores and Escherichia coli cells to inert surfaces: role of surface hydrophobicity. Can J Microbiol **48:**728-738.

82.   **Fiala, G., and K. O. Stetter.** 1986. *Pyrococcus furiosus* sp. nov. represents a novel genus of marine heterotrophic archaebacteria growing optimally at 100 C. Archives of Microbiology **145:**56-61.

83.   **Flemming, H. C., T. R. Neu, and D. J. Wozniak.** 2007. The EPS matrix: the "house of biofilm cells". J Bacteriol **189:**7945-7947.

84.   **Flemming, H. C., and J. Wingender.** 2010. The biofilm matrix. Nat Rev Microbiol **8:**623-633.

85.   **Fliermans, C. B., and T. D. Brock.** 1972. Ecology of sulfur-oxidizing bacteria in hot acid soils. J Bacteriol **111:**343-350.

86.   **Friedman, L., and R. Kolter.** 2004. Genes involved in matrix formation in *Pseudomonas aeruginosa* PA14 biofilms. Mol Microbiol **51:**675-690.

87.   **Friedman, L., and R. Kolter.** 2004. Two genetic loci produce distinct carbohydrate-rich structural components of the *Pseudomonas aeruginosa* biofilm matrix. J Bacteriol **186:**4457-4465.

88.   **Froeliger, E. H., and P. Fives-Taylor.** 2001. *Streptococcus parasanguis* fimbria-associated adhesin fap1 is required for biofilm formation. Infect Immun **69:**2512-2519.

89.   **Frols, S., M. Ajon, M. Wagner, D. Teichmann, B. Zolghadr, M. Folea, E. J. Boekema, A. J. Driessen, C. Schleper, and S. V. Albers.** 2008. UV-inducible cellular aggregation of the hyperthermophilic archaeon *Sulfolobus solfataricus* is mediated by pili formation. Mol Microbiol **70:**938-952.

90.   **Frols, S., P. M. Gordon, M. A. Panlilio, I. G. Duggin, S. D. Bell, C. W. Sensen, and C. Schleper.** 2007. Response of the hyperthermophilic archaeon *Sulfolobus solfataricus* to UV damage. J Bacteriol **189:**8708-8718.

91.   **Frye, J., J. E. Karlinsey, H. R. Felise, B. Marzolf, N. Dowidar, M. McClelland, and K. T. Hughes.** 2006. Identification of new flagellar genes of *Salmonella enterica serovar* Typhimurium. J Bacteriol **188:**2233-2243.

92.   **Garrett, E. S., D. Perlegas, and D. J. Wozniak.** 1999. Negative control of flagellum synthesis in *Pseudomonas aeruginosa* is modulated by the alternative sigma factor AlgT (AlgU). J Bacteriol **181:**7401-7404.

93.   **Gerstel, U., and U. Romling.** 2001. Oxygen tension and nutrient starvation are major signals that regulate agfD promoter activity and expression of the multicellular morphotype in *Salmonella typhimurium*. Environ Microbiol **3:**638-648.

94.   **Giron, J. A., A. G. Torres, E. Freer, and J. B. Kaper.** 2002. The flagella of enteropathogenic *Escherichia coli* mediate adherence to epithelial cells. Mol Microbiol **44:**361-379.

95.   **Gonzalez Barrios, A. F., R. Zuo, Y. Hashimoto, L. Yang, W. E. Bentley, and T. K. Wood.** 2006. Autoinducer 2 controls biofilm formation in *Escherichia coli* through a novel motility quorum-sensing regulator (MqsR, B3022). J Bacteriol **188:**305-316.

96. **Gonzalez, D. S., K. Karaveg, A. S. Vandersall-Nairn, A. Lal, and K. W. Moremen.** 1999. Identification, expression, and characterization of a cDNA encoding human endoplasmic reticulum mannosidase I, the enzyme that catalyzes the first mannose trimming step in mammalian Asn-linked oligosaccharide biosynthesis. J Biol Chem **274:**21375-21386.

97. **Goon, S., J. F. Kelly, S. M. Logan, C. P. Ewing, and P. Guerry.** 2003. Pseudaminic acid, the major modification on *Campylobacter* flagellin, is synthesized via the Cj1293 gene. Mol Microbiol **50:**659-671.

98. **Gotz, D., S. Paytubi, S. Munro, M. Lundgren, R. Bernander, and M. F. White.** 2007. Responses of hyperthermophilic crenarchaea to UV irradiation. Genome Biol **8:**R220.

99. **Grass, S., A. Z. Buscher, W. E. Swords, M. A. Apicella, S. J. Barenkamp, N. Ozchlewski, and J. W. St Geme, 3rd.** 2003. The *Haemophilus influenzae* HMW1 adhesin is glycosylated in a process that requires HMW1C and phosphoglucomutase, an enzyme involved in lipooligosaccharide biosynthesis. Mol Microbiol **48:**737-751.

100. **Gristina, A. G., C. D. Hobgood, L. X. Webb, and Q. N. Myrvik.** 1987. Adhesive colonization of biomaterials and antibiotic resistance. Biomaterials **8:**423-426.

101. **Grogan, D. W.** 1996. Isolation and fractionation of cell envelope from the extreme thermo-acidophile *Sulfolobus acidocaldarius*. Journal of microbiological methods **26:**35-43.

102. **Grogan, D. W.** 1996. Organization and interactions of cell envelope proteins of the extreme thermoacidophile *Sulfolobus acidocaldarius*. Canadian journal of microbiology **42:**1163-1171.

103. **Grogan, D. W.** 1989. Phenotypic characterization of the archaebacterial genus *Sulfolobus*: comparison of five wild-type strains. J Bacteriol **171:**6710-6719.

104. **Guggenheim, B., R. Gmur, J. C. Galicia, P. G. Stathopoulou, M. R. Benakanakere, A. Meier, T. Thurnheer, and D. F. Kinane.** 2009. In vitro modeling of host-parasite interactions: the 'subgingival' biofilm challenge of primary human epithelial cells. BMC Microbiol **9:**280.

105. **Haagensen, J. A. J., M. Klausen, R. K. Ernst, S. I. Miller, A. Folkesson, T. Tolker-Nielsen, and S. Molin.** 2006. Differentiation and distribution of colistin/SDS tolerant cells in *Pseudomonas aeruginosa* biofilms. Journal of Bacteriology**:**JB. 00720-00706v00721.

106. **Hall-Stoodley, L., J. W. Costerton, and P. Stoodley.** 2004. Bacterial biofilms: from the natural environment to infectious diseases. Nat Rev Microbiol **2:**95-108.

107. **Hall-Stoodley, L., and P. Stoodley.** 2005. Biofilm formation and dispersal and the transmission of human pathogens. Trends Microbiol **13:**7-10.

108. **Hall-Stoodley, L., and P. Stoodley.** 2009. Evolving concepts in biofilm infections. Cell Microbiol **11:**1034-1043.

109. **Hamilton, S., R. J. M. Bongaerts, F. Mulholland, B. Cochrane, J. Porter, S. Lucchini, H. M. Lappin-Scott, and J. C. D. Hinton.** 2009. The transcriptional programme of *Salmonella enterica* serovar Typhimurium reveals a key role for tryptophan metabolism in biofilms. BMC Genomics **10**599-620.

110. **Hancock, I.** 1991. Microbial cell surface architecture. Microbial cell surface analysis. VCH, Weinheim, Germany**:**21-59.

111. **Herrmann, J. L., P. O'Gaora, A. Gallagher, J. E. Thole, and D. B. Young.** 1996. Bacterial glycoproteins: a link between glycosylation and proteolytic cleavage of a 19 kDa antigen from *Mycobacterium tuberculosis*. EMBO J **15:**3547-3554.

112. **Herscovics, A.** 1999. Importance of glycosidases in mammalian glycoprotein biosynthesis. Biochim Biophys Acta **1473:**96-107.

113. **Heydorn, A., B. Ersboll, J. Kato, M. Hentzer, M. R. Parsek, T. Tolker-Nielsen, M. Givskov, and S. Molin.** 2002. Statistical analysis of *Pseudomonas aeruginosa* biofilm development: impact of mutations in genes involved in twitching motility, cell-to-cell

signaling, and stationary-phase sigma factor expression. Appl Environ Microbiol **68:**2008-2017.

114.   **Heydorn, A., A. T. Nielsen, M. Hentzer, C. Sternberg, M. Givskov, B. K. Ersboll, and S. Molin.** 2000. Quantification of biofilm structures by the novel computer program COMSTAT. Microbiology **146 (Pt 10):**2395-2407.

115.   **Hezayen, F. F., B. H. Rehm, B. J. Tindall, and A. Steinbuchel.** 2001. Transfer of *Natrialba asiatica* B1T to *Natrialba taiwanensis sp.* nov. and description of *Natrialba aegyptiaca sp.* nov., a novel extremely halophilic, aerobic, non-pigmented member of the Archaea from Egypt that produces extracellular poly(glutamic acid). Int J Syst Evol Microbiol **51:**1133-1142.

116.   **Hoang, T. T., S. A. Sullivan, J. K. Cusick, and H. P. Schweizer.** 2002. Beta-ketoacyl acyl carrier protein reductase (FabG) activity of the fatty acid biosynthetic pathway is a determining factor of 3-oxo-homoserine lactone acyl chain lengths. Microbiology **148:**3849-3856.

117.   **Hoffman, L. R., D. A. D'Argenio, M. J. MacCoss, Z. Zhang, R. A. Jones, and S. I. Miller.** 2005. Aminoglycoside antibiotics induce bacterial biofilm formation. Nature **436:**1171-1175.

118.   **Hoiby, N., T. Bjarnsholt, M. Givskov, S. Molin, and O. Ciofu.** 2010. Antibiotic resistance of bacterial biofilms. Int J Antimicrob Agents **35:**322-332.

119.   **Horn, C., B. Paulmann, G. Kerlen, N. Junker, and H. Huber.** 1999. In vivo observation of cell division of anaerobic hyperthermophiles by using a high-intensity dark-field microscope. J Bacteriol **181:**5114-5118.

120.   **Hornef, M. W., M. J. Wick, M. Rhen, and S. Normark.** 2002. Bacterial strategies for overcoming host innate and adaptive immune responses. Nat Immunol **3:**1033-1040.

121.   **Huber, H., M. J. Hohn, R. Rachel, T. Fuchs, V. C. Wimmer, and K. O. Stetter.** 2002. A new phylum of Archaea represented by a nanosized hyperthermophilic symbiont. Nature **417:**63-67.

122.   **Huber, R., H. Huber, and K. O. Stetter.** 2000. Towards the ecology of hyperthermophiles: biotopes, new isolation strategies and novel metabolic properties. FEMS Microbiol Rev **24:**615-623.

123.   **Iino, T.** 1969. Polarity of flagellar growth in *salmonella*. J Gen Microbiol **56:**227-239.

124.   **Itoh, T., K. Suzuki, P. Sanchez, and T. Nakase.** 2003. *Caldisphaera lagunensis* gen. nov., sp. nov., a novel thermoacidophilic crenarchaeote isolated from a hot spring at Mt Maquiling, Philippines. International Journal of Systematic and Evolutionary Microbiology **53:**1149.

125.   **Itoh, Y., J. D. Rice, C. Goller, A. Pannuri, J. Taylor, J. Meisner, T. J. Beveridge, J. F. Preston, 3rd, and T. Romeo.** 2008. Roles of pgaABCD genes in synthesis, modification, and export of the *Escherichia coli* biofilm adhesin poly-beta-1,6-N-acetyl-D-glucosamine. J Bacteriol **190:**3670-3680.

126.   **Jackson, D. W., K. Suzuki, L. Oakford, J. W. Simecka, M. E. Hart, and T. Romeo.** 2002. Biofilm formation and dispersal under the influence of the global regulator CsrA of *Escherichia coli*. J Bacteriol **184:**290-301.

127.   **Jarrell, K. F., and M. J. McBride.** 2008. The surprisingly diverse ways that prokaryotes move. Nat Rev Microbiol **6:**466-476.

128.   **Jarrell, K. F., M. Stark, D. B. Nair, and J. P. Chong.** 2011. Flagella and pili are both necessary for efficient attachment of *Methanococcus maripaludis* to surfaces. FEMS Microbiol Lett **319:**44-50.

129.   **Jenal, U., and J. Malone.** 2006. Mechanisms of cyclic-di-GMP signaling in bacteria. Annu Rev Genet **40:**385-407.

130.   **Jones, G. W., and R. E. Isaacson.** 1983. Proteinaceous bacterial adhesins and their receptors. Crit Rev Microbiol **10:**229-260.

131.   **Kagawa, H. K., J. Osipiuk, N. Maltsev, R. Overbeek, E. Quaite-Randall, A. Joachimiak, and J. D. Trent.** 1995. The 60 kDa heat shock proteins in the hyperthermophilic archaeon *Sulfolobus shibatae*. J Mol Biol **253:**712-725.

132.   **Kalmokoff, M., P. Lanthier, T. L. Tremblay, M. Foss, P. C. Lau, G. Sanders, J. Austin, J. Kelly, and C. M. Szymanski.** 2006. Proteomic analysis of *Campylobacter jejuni* 11168 biofilms reveals a role for the motility complex in biofilm formation. J Bacteriol **188:**4312-4320.

133.   **Kalmokoff, M. L., and K. F. Jarrell.** 1991. Cloning and sequencing of a multigene family encoding the flagellins of *Methanococcus voltae*. J Bacteriol **173:**7113-7125.

134.   **Kandler, O., and H. Konig.** 1978. Chemical composition of the peptidoglycan-free cell walls of methanogenic bacteria. Arch Microbiol **118:**141-152.

135.   **Kang, Y., H. Liu, S. Genin, M. A. Schell, and T. P. Denny.** 2002. *Ralstonia solanacearum* requires type 4 pili to adhere to multiple surfaces and for natural transformation and virulence. Mol Microbiol **46:**427-437.

136.   **Karatan, E., and P. Watnick.** 2009. Signals, regulatory networks, and materials that build and break bacterial biofilms. Microbiol Mol Biol Rev **73:**310-347.

137.   **Karcher, U., H. Schroder, E. Haslinger, G. Allmaier, R. Schreiner, F. Wieland, A. Haselbeck, and H. Konig.** 1993. Primary structure of the heterosaccharide of the surface glycoprotein of *Methanothermus fervidus*. J Biol Chem **268:**26821-26826.

138.   **Karlyshev, A. V., P. Everest, D. Linton, S. Cawthraw, D. G. Newell, and B. W. Wren.** 2004. The *Campylobacter jejuni* general glycosylation system is important for attachment to human epithelial cells and in the colonization of chicks. Microbiology **150:**1957-1964.

139.   **Karner, M. B., E. F. DeLong, and D. M. Karl.** 2001. Archaeal dominance in the mesopelagic zone of the Pacific Ocean. Nature **409:**507-510.

140.   **Kawarabayasi, Y., Y. Hino, H. Horikawa, K. Jin-no, M. Takahashi, M. Sekine, S. Baba, A. Ankai, H. Kosugi, A. Hosoyama, S. Fukui, Y. Nagai, K. Nishijima, R. Otsuka, H. Nakazawa, M. Takamiya, Y. Kato, T. Yoshizawa, T. Tanaka, Y. Kudoh, J. Yamazaki, N. Kushida, A. Oguchi, K. Aoki, S. Masuda, M. Yanagii, M. Nishimura, A. Yamagishi, T. Oshima, and H. Kikuchi.** 2001. Complete genome sequence of an aerobic thermoacidophilic crenarchaeon, *Sulfolobus tokodaii* strain7. DNA Res **8:**123-140.

141.   **Kierek, K., and P. I. Watnick.** 2003. Environmental determinants of *Vibrio cholerae* biofilm development. Appl Environ Microbiol **69:**5079-5088.

142.   **Kierek, K., and P. I. Watnick.** 2003. The *Vibrio cholerae* O139 O-antigen polysaccharide is essential for Ca2+-dependent biofilm development in sea water. Proc Natl Acad Sci U S A **100:**14357-14362.

143.   **Kirov, S. M., M. Castrisios, and J. G. Shaw.** 2004. *Aeromonas* flagella (polar and lateral) are enterocyte adhesins that contribute to biofilm formation on surfaces. Infect Immun **72:**1939-1945.

144.   **Klausen, M., A. Aaes-Jorgensen, S. Molin, and T. Tolker-Nielsen.** 2003. Involvement of bacterial migration in the development of complex multicellular structures in *Pseudomonas aeruginosa* biofilms. Mol Microbiol **50:**61-68.

145.   **Klausen, M., A. Heydorn, P. Ragas, L. Lambertsen, A. Aaes-Jorgensen, S. Molin, and T. Tolker-Nielsen.** 2003. Biofilm formation by *Pseudomonas aeruginosa* wild type, flagella and type IV pili mutants. Mol Microbiol **48:**1511-1524.

146.   **Koerdt, A., J. Godeke, J. Berger, K. M. Thormann, and S. V. Albers.** 2010. Crenarchaeal biofilm formation under extreme conditions. PLoS One **5:**e14104.

147.   **Koerdt, A., A. Orell, T. K. Pham, J. Mukherjee, A. Wlodkowski, E. Karunakaran, C. A. Biggs, P. C. Wright, and S. V. Albers.** 2011. Macromolecular Fingerprinting of *Sulfolobus* Species in Biofilm: A Transcriptomic and Proteomic Approach Combined with Spectroscopic Analysis. J Proteome Res.

148.   **Konig, H.** 1988. Archaeobacterial cell envelopes. Can. J. Microbiol **34:**395-406.

149. **Koo, H., J. Xiao, M. I. Klein, and J. G. Jeon.** 2010. Exopolysaccharides produced by *Streptococcus mutans* glucosyltransferases modulate the establishment of microcolonies within multispecies biofilms. J Bacteriol **192:**3024-3032.

150. **Kuchma, S. L., K. M. Brothers, J. H. Merritt, N. T. Liberati, F. M. Ausubel, and G. A. O'Toole.** 2007. BifA, a cyclic-Di-GMP phosphodiesterase, inversely regulates biofilm formation and swarming motility by *Pseudomonas aeruginosa* PA14. J Bacteriol **189:**8165-8178.

151. **Kuo, C., N. Takahashi, A. F. Swanson, Y. Ozeki, and S. Hakomori.** 1996. An N-linked high-mannose type oligosaccharide, expressed at the major outer membrane protein of *Chlamydia trachomatis*, mediates attachment and infectivity of the microorganism to HeLa cells. J Clin Invest **98:**2813-2818.

152. **Lapaglia, C., and P. L. Hartzell.** 1997. Stress-Induced Production of Biofilm in the Hyperthermophile *Archaeoglobus fulgidus*. Appl Environ Microbiol **63:**3158-3163.

153. **Lauriano, C. M., C. Ghosh, N. E. Correa, and K. E. Klose.** 2004. The sodium-driven flagellar motor controls exopolysaccharide expression in *Vibrio cholerae*. J Bacteriol **186:**4864-4874.

154. **Lawrence, J. R., D. R. Korber, B. D. Hoyle, J. W. Costerton, and D. E. Caldwell.** 1991. Optical sectioning of microbial biofilms. J Bacteriol **173:**6558-6567.

155. **Lawrence, J. R., G. D. Swerhone, U. Kuhlicke, and T. R. Neu.** 2007. In situ evidence for microdomains in the polymer matrix of bacterial microcolonies. Can J Microbiol **53:**450-458.

156. **Lebeer, S., T. L. Verhoeven, G. Francius, G. Schoofs, I. Lambrichts, Y. Dufrene, J. Vanderleyden, and S. C. De Keersmaecker.** 2009. Identification of a Gene Cluster for the Biosynthesis of a Long, Galactose-Rich Exopolysaccharide in *Lactobacillus rhamnosus* GG and Functional Analysis of the Priming Glycosyltransferase. Appl Environ Microbiol **75:**3554-3563.

157. **Leigh, J. A., S. V. Albers, H. Atomi, and T. Allers.** 2011. Model organisms for genetics in the domain Archaea: methanogens, halophiles, *Thermococcales* and *Sulfolobales*. FEMS Microbiol Rev.

158. **Lemon, K. P., A. M. Earl, H. C. Vlamakis, C. Aguilar, and R. Kolter.** 2008. Biofilm development with an emphasis on Bacillus subtilis. Curr Top Microbiol Immunol **322:**1-16.

159. **Lemon, K. P., D. E. Higgins, and R. Kolter.** 2007. Flagellar motility is critical for *Listeria monocytogenes* biofilm formation. J Bacteriol **189:**4418-4424.

160. **Lequette, Y., and E. P. Greenberg.** 2005. Timing and localization of rhamnolipid synthesis gene expression in *Pseudomonas aeruginosa* biofilms. J Bacteriol **187:**37-44.

161. **Lewis, K.** 2007. Persister cells, dormancy and infectious disease. Nat Rev Microbiol **5:**48-56.

162. **Li, Y., Y. Chen, X. Huang, M. Zhou, R. Wu, S. Dong, D. G. Pritchard, P. Fives-Taylor, and H. Wu.** 2008. A conserved domain of previously unknown function in Gap1 mediates protein-protein interaction and is required for biogenesis of a serine-rich streptococcal adhesin. Mol Microbiol **70:**1094-1104.

163. **Lindenthal, C., and E. A. Elsinghorst.** 1999. Identification of a glycoprotein produced by enterotoxigenic *Escherichia coli*. Infect Immun **67:**4084-4091.

164. **Lux, R., Y. Li, A. Lu, and W. Shi.** 2004. Detailed three-dimensional analysis of structural features of *Myxococcus xanthus* fruiting bodies using confocal laser scanning microscopy. Biofilms **1:**293-303.

165. **Lynch, A. S., and G. T. Robertson.** 2008. Bacterial and fungal biofilm infections. Annu Rev Med **59:**415-428.

166. **Ma, L., M. Conover, H. Lu, M. R. Parsek, K. Bayles, and D. J. Wozniak.** 2009. Assembly and development of the *Pseudomonas aeruginosa* biofilm matrix. PLoS Pathog **5:**e1000354.

167. **Ma, L., K. D. Jackson, R. M. Landry, M. R. Parsek, and D. J. Wozniak.** 2006. Analysis of *Pseudomonas aeruginosa* conditional psl variants reveals roles for the psl polysaccharide in adhesion and maintaining biofilm structure postattachment. J Bacteriol **188:**8213-8221.

168. **Magidovich, H., S. Yurist-Doutsch, Z. Konrad, V. V. Ventura, A. Dell, P. G. Hitchen, and J. Eichler.** 2010. AglP is a S-adenosyl-L-methionine-dependent methyltransferase that participates in the N-glycosylation pathway of *Haloferax volcanii*. Mol Microbiol **76:**190-199.

169. **Mah, T. F., and G. A. O'Toole.** 2001. Mechanisms of biofilm resistance to antimicrobial agents. Trends Microbiol **9:**34-39.

170. **Mai-Prochnow, A., J. S. Webb, B. C. Ferrari, and S. Kjelleberg.** 2006. Ecological advantages of autolysis during the development and dispersal of *Pseudoalteromonas tunicata* biofilms. Appl Environ Microbiol **72:**5414-5420.

171. **Maruyama, Y., T. Nakajima, and E. Ichishima.** 1994. A 1,2-alpha-D-mannosidase from a *Bacillus sp.*: purification, characterization, and mode of action. Carbohydr Res **251:**89-98.

172. **Marwan, W., M. Alam, and D. Oesterhelt.** 1991. Rotation and switching of the flagellar motor assembly in *Halobacterium halobium*. J Bacteriol **173:**1971-1977.

173. **Mathee, K., O. Ciofu, C. Sternberg, P. W. Lindum, J. I. Campbell, P. Jensen, A. H. Johnsen, M. Givskov, D. E. Ohman, S. Molin, N. Hoiby, and A. Kharazmi.** 1999. Mucoid conversion of *Pseudomonas aeruginosa* by hydrogen peroxide: a mechanism for virulence activation in the cystic fibrosis lung. Microbiology **145 (Pt 6):**1349-1357.

174. **Matsukawa, M., and E. P. Greenberg.** 2004. Putative exopolysaccharide synthesis genes influence *Pseudomonas aeruginosa* biofilm development. J Bacteriol **186:**4449-4456.

175. **McClaine, J. W., and R. M. Ford.** 2002. Characterizing the adhesion of motile and nonmotile *Escherichia coli* to a glass surface using a parallel-plate flow chamber. Biotechnol Bioeng **78:**179-189.

176. **McClaine, J. W., and R. M. Ford.** 2002. Reversal of flagellar rotation is important in initial attachment of *Escherichia coli* to glass in a dynamic system with high- and low-ionic-strength buffers. Appl Environ Microbiol **68:**1280-1289.

177. **McKenzie, G. J., R. S. Harris, P. L. Lee, and S. M. Rosenberg.** 2000. The SOS response regulates adaptive mutation. Proc Natl Acad Sci U S A **97:**6646-6651.

178. **Meibom, K. L., X. B. Li, A. T. Nielsen, C. Y. Wu, S. Roseman, and G. K. Schoolnik.** 2004. The *Vibrio cholerae* chitin utilization program. Proc Natl Acad Sci U S A **101:**2524-2529.

179. **Mescher, M. F., and J. L. Strominger.** 1976. Purification and characterization of a prokaryotic glucoprotein from the cell envelope of *Halobacterium salinarium*. J Biol Chem **251:**2005-2014.

180. **Mills, E., I. S. Pultz, H. D. Kulasekara, and S. I. Miller.** 2011. The bacterial second messenger c-di-GMP: mechanisms of signalling. Cell Microbiol **13:**1122-1129.

181. **Miron, J., and C. W. Forsberg.** 1999. Characterisation of cellulose-binding proteins that are involved in the adhesion mechanism of *Fibrobacter intestinalis* DR7. Appl Microbiol Biotechnol **51:**491-497.

182. **Mobili, P., E. Gerbino, E. Tymczyszyn, and A. Gómez-Zavaglia.** 2010. S-layers in *lactobacilli*: structural characteristics and putative role in surface and probiotic properties of whole bacteria.

183. **Moissl, C., R. Rachel, A. Briegel, H. Engelhardt, and R. Huber.** 2005. The unique structure of archaeal 'hami', highly complex cell appendages with nano-grappling hooks. Mol Microbiol **56:**361-370.

184. **Monds, R. D., P. D. Newell, R. H. Gross, and G. A. O'Toole.** 2007. Phosphate-dependent modulation of c-di-GMP levels regulates *Pseudomonas fluorescens* Pf0-1

biofilm formation by controlling secretion of the adhesin LapA. Mol Microbiol **63:**656-679.

185.   **Monds, R. D., and G. A. O'Toole.** 2009. The developmental model of microbial biofilms: ten years of a paradigm up for review. Trends Microbiol **17:**73-87.

186.   **Monroe, D.** 2007. Looking for chinks in the armor of bacterial biofilms. PLoS Biol **5:**e307.

187.   **Moorthy, S., and P. I. Watnick.** 2004. Genetic evidence that the *Vibrio cholerae* monolayer is a distinct stage in biofilm development. Mol Microbiol **52:**573-587.

188.   **Nakajima, M., H. Imamura, H. Shoun, and T. Wakagi.** 2003. Unique metal dependency of cytosolic alpha-mannosidase from *Thermotoga maritima*, a hyperthermophilic bacterium. Arch Biochem Biophys **415:**87-93.

189.   **Napoli, A., J. van der Oost, C. W. Sensen, R. L. Charlebois, M. Rossi, and M. Ciaramella.** 1999. An Lrp-like protein of the hyperthermophilic archaeon *Sulfolobus solfataricus* which binds to its own promoter. J Bacteriol **181:**1474-1480.

190.   **Näther, D. J., R. Rachel, G. Wanner, and R. Wirth.** 2006. Flagella of *Pyrococcus furiosus* : multifunctional organelles, made for swimming, adhesion to various surfaces, and cell-cell contacts. Journal of Bacteriology **188:**6915-6923.

191.   **Neu, T. R., and J. R. Lawrence.** 1999. Lectin-binding analysis in biofilm systems. Methods Enzymol **310:**145-152.

192.   **Ng, S. Y., B. Chaban, and K. F. Jarrell.** 2006. Archaeal flagella, bacterial flagella and type IV pili: a comparison of genes and posttranslational modifications. J Mol Microbiol Biotechnol **11:**167-191.

193.   **Ng, S. Y., J. Wu, D. B. Nair, S. M. Logan, A. Robotham, L. Tessier, J. F. Kelly, K. Uchida, S. Aizawa, and K. F. Jarrell.** 2011. Genetic and mass spectrometry analyses of the unusual type IV-like pili of the archaeon *Methanococcus maripaludis*. J Bacteriol **193:**804-814.

194.   **Nickel, J. C., I. Ruseska, J. B. Wright, and J. W. Costerton.** 1985. Tobramycin resistance of *Pseudomonas aeruginosa* cells growing as a biofilm on urinary catheter material. Antimicrob Agents Chemother **27:**619-624.

195.   **Nickell, S., R. Hegerl, W. Baumeister, and R. Rachel.** 2003. *Pyrodictium* cannulae enter the periplasmic space but do not enter the cytoplasm, as revealed by cryo-electron tomography. J Struct Biol **141:**34-42.

196.   **Nicolaus, B., M. C. Manca, I. Ramano, and L. Lama.** 1993. Production of an exopolysaccharide from two thermophilic archaea belonging to the genus *Sulfolobus*. FEMS microbiology letters **109:**203-206.

197.   **Niemetz, R., U. Karcher, O. Kandler, B. J. Tindall, and H. Konig.** 1997. The cell wall polymer of the extremely halophilic archaeon *Natronococcus occultus*. Eur J Biochem **249:**905-911.

198.   **Nigaud, Y., P. Cosette, A. Collet, P. C. Song, D. Vaudry, H. Vaudry, G. A. Junter, and T. Jouenne.** 2010. Biofilm-induced modifications in the proteome of *Pseudomonas aeruginosa* planktonic cells. Biochim Biophys Acta **1804:**957-966.

199.   **Nikolaev Iu, A., and V. K. Plakunov.** 2007. [Biofilm--"City of microbes" or an analogue of multicellular organisms?]. Mikrobiologiia **76:**149-163.

200.   **Nothaft, H., and C. M. Szymanski.** 2010. Protein glycosylation in bacteria: sweeter than ever. Nat Rev Microbiol **8:**765-778.

201.   **Noyce, J. O., H. Michels, and C. W. Keevil.** 2006. Use of copper cast alloys to control *Escherichia coli* O157 cross-contamination during food processing. Appl Environ Microbiol **72:**4239-4244.

202.   **Nutsch, T., W. Marwan, D. Oesterhelt, and E. D. Gilles.** 2003. Signal processing and flagellar motor switching during phototaxis of *Halobacterium salinarum*. Genome Res **13:**2406-2412.

203. **O'Toole, G. A., and R. Kolter.** 1998. Flagellar and twitching motility are necessary for *Pseudomonas aeruginosa* biofilm development. Mol Microbiol **30:**295-304.

204. **O'Toole, G. A., and R. Kolter.** 1998. Initiation of biofilm formation in *Pseudomonas fluorescens* WCS365 proceeds via multiple, convergent signalling pathways: a genetic analysis. Mol Microbiol **28:**449-461.

205. **Ohnishi, K., Y. Ohto, S. Aizawa, R. M. Macnab, and T. Iino.** 1994. FlgD is a scaffolding protein needed for flagellar hook assembly in *Salmonella typhimurium*. J Bacteriol **176:**2272-2281.

206. **Oosthuizen, M. C., B. Steyn, J. Theron, P. Cosette, D. Lindsay, A. Von Holy, and V. S. Brozel.** 2002. Proteomic analysis reveals differential protein expression by *Bacillus cereus* during biofilm formation. Appl Environ Microbiol **68:**2770-2780.

207. **Ortega Morales, B. O., J. Santiago García, M. Chan Bacab, X. Moppert, E. Miranda Tello, M. L. Fardeau, J. Carrero, P. Bartolo Pérez, A. Valadéz González, and J. Guezennec.** 2007. Characterization of extracellular polymers synthesized by tropical intertidal biofilm bacteria. Journal of applied microbiology **102:**254-264.

208. **Otto, K., H. Elwing, and M. Hermansson.** 1999. The role of type 1 fimbriae in adhesion of *Escherichia coli* to hydrophilic and hydrophobic surfaces. Colloids and Surfaces B: Biointerfaces **15:**99-111.

209. **Parise, G., M. Mishra, Y. Itoh, T. Romeo, and R. Deora.** 2007. Role of a putative polysaccharide locus in *Bordetella* biofilm development. J Bacteriol **189:**750-760.

210. **Peabody, C. R., Y. J. Chung, M. R. Yen, D. Vidal-Ingigliardi, A. P. Pugsley, and M. H. Saier, Jr.** 2003. Type II protein secretion and its relationship to bacterial type IV pili and archaeal flagella. Microbiology **149:**3051-3072.

211. **Peeters, E., S. V. Albers, A. Vassart, A. J. Driessen, and D. Charlier.** 2009. Ss-LrpB, a transcriptional regulator from *Sulfolobus solfataricus*, regulates a gene cluster with a pyruvate ferredoxin oxidoreductase-encoding operon and permease genes. Mol Microbiol **71:**972-988.

212. **Peng, Z., H. Wu, T. Ruiz, Q. Chen, M. Zhou, B. Sun, and P. Fives-Taylor.** 2008. Role of gap3 in Fap1 glycosylation, stability, in vitro adhesion, and fimbrial and biofilm formation of *Streptococcus parasanguinis*. Oral Microbiol Immunol **23:**70-78.

213. **Peyfoon, E., B. Meyer, P. G. Hitchen, M. Panico, H. R. Morris, S. M. Haslam, S. V. Albers, and A. Dell.** 2010. The S-layer glycoprotein of the crenarchaeote *Sulfolobus acidocaldarius* is glycosylated at multiple sites with chitobiose-linked N-glycans. Archaea **2010**.

214. **Pohlschroder, M., M. I. Gimenez, and K. F. Jarrell.** 2005. Protein transport in Archaea: Sec and twin arginine translocation pathways. Curr Opin Microbiol **8:**713-719.

215. **Potvin, E., F. Sanschagrin, and R. C. Levesque.** 2008. Sigma factors in *Pseudomonas aeruginosa*. FEMS Microbiol Rev **32:**38-55.

216. **Pratt, L. A., and R. Kolter.** 1998. Genetic analysis of *Escherichia coli* biofilm formation: roles of flagella, motility, chemotaxis and type I pili. Mol Microbiol **30:**285-293.

217. **Prigent-Combaret, C., O. Vidal, C. Dorel, and P. Lejeune.** 1999. Abiotic surface sensing and biofilm-dependent regulation of gene expression in *Escherichia coli*. J Bacteriol **181:**5993-6002.

218. **Prokofeva, M., M. Miroshnichenko, N. Kostrikina, N. Chernyh, B. Kuznetsov, T. Tourova, and E. Bonch-Osmolovskaya.** 2000. *Acidilobus aceticus* gen. nov., sp. nov., a novel anaerobic thermoacidophilic archaeon from continental hot vents in Kamchatka. International Journal of Systematic and Evolutionary Microbiology **50:**2001.

219. **Prosser, B. L., D. Taylor, B. A. Dix, and R. Cleeland.** 1987. Method of evaluating effects of antibiotics on bacterial biofilm. Antimicrob Agents Chemother **31:**1502-1506.

220. **Pruschenk, R., W. Baumeister, and W. Zillig.** 1987. Surface structure variants in different species of Sulfolobus. FEMS microbiology letters **43:**327-330.

221.   **Qin, Z., Y. Ou, L. Yang, Y. Zhu, T. Tolker-Nielsen, S. Molin, and D. Qu.** 2007. Role of autolysin-mediated DNA release in biofilm formation of *Staphylococcus epidermidis*. Microbiology **153:**2083-2092.

222.   **Rachid, S., K. Ohlsen, U. Wallner, J. Hacker, M. Hecker, and W. Ziebuhr.** 2000. Alternative transcription factor sigma(B) is involved in regulation of biofilm expression in a *Staphylococcus aureus* mucosal isolate. J Bacteriol **182:**6824-6826.

223.   **Ramsing, N. B., M. Kuhl, and B. B. Jorgensen.** 1993. Distribution of sulfate-reducing bacteria, O2, and H2S in photosynthetic biofilms determined by oligonucleotide probes and microelectrodes. Appl Environ Microbiol **59:**3840-3849.

224.   **Ren, D., L. A. Bedzyk, P. Setlow, S. M. Thomas, R. W. Ye, and T. K. Wood.** 2004. Gene expression in *Bacillus subtilis* surface biofilms with and without sporulation and the importance of yveR for biofilm maintenance. Biotechnol Bioeng **86:**344-364.

225.   **Ren, D., L. A. Bedzyk, S. M. Thomas, R. W. Ye, and T. K. Wood.** 2004. Gene expression in *Escherichia coli* biofilms. Appl Microbiol Biotechnol **64:**515-524.

226.   **Rieger, G., R. Rachel, R. Hermann, and K. O. Stetter.** 1995. Ultrastructure of the hyperthermophilic archaeon *Pyrodictium abyssi*. Journal of Structural Biology **115:**78-87.

227.   **Rinker, K. D., and R. M. Kelly.** 1996. Growth Physiology of the Hyperthermophilic Archaeon *Thermococcus litoralis*: Development of a Sulfur-Free Defined Medium, Characterization of an Exopolysaccharide, and Evidence of Biofilm Formation. Appl Environ Microbiol **62:**4478 - 4485.

228.   **Rivas, L., N. Fegan, and G. A. Dykes.** 2008. Expression and putative roles in attachment of outer membrane proteins of *Escherichia coli* O157 from planktonic and sessile culture. Foodborne Pathog Dis **5:**155-164.

229.   **Rivas, L., N. Fegan, and G. A. Dykes.** 2005. Physicochemical properties of Shiga toxigenic *Escherichia coli*. J Appl Microbiol **99:**716-727.

230.   **Rivera-Marrero, C. A., W. Schuyler, S. Roser, and J. Roman.** 2000. Induction of MMP-9 mediated gelatinolytic activity in human monocytic cells by cell wall components of *Mycobacterium tuberculosis*. Microb Pathog **29:**231-244.

231.   **Rodriguez-Valera, F., G. Juez, and D. Kushner.** 1983. *Halobacterium mediterranei* spec. nov., a new carbohydrate-utilizing extreme halophile. Systematic and applied microbiology **4:**369-381.

232.   **Rudolph, C., G. Wanner, and R. Huber.** 2001. Natural communities of novel archaea and bacteria growing in cold sulfurous springs with a string-of-pearls-like morphology. Appl Environ Microbiol **67:**2336-2344.

233.   **Ryan, R. P., Y. Fouhy, J. F. Lucey, and J. M. Dow.** 2006. Cyclic di-GMP signaling in bacteria: recent advances and new puzzles. J Bacteriol **188:**8327-8334.

234.   **Ryder, C., M. Byrd, and D. J. Wozniak.** 2007. Role of polysaccharides in *Pseudomonas aeruginosa* biofilm development. Curr Opin Microbiol **10:**644-648.

235.   **Sampaio, M. M., F. Chevance, R. Dippel, T. Eppler, A. Schlegel, W. Boos, Y. J. Lu, and C. O. Rock.** 2004. Phosphotransferase-mediated transport of the osmolyte 2-O-alpha-mannosyl-D-glycerate in *Escherichia coli* occurs by the product of the mngA (hrsA) gene and is regulated by the mngR (farR) gene product acting as repressor. J Biol Chem **279:**5537-5548.

236.   **Sara, M., and U. B. Sleytr.** 1996. Crystalline bacterial cell surface layers (S-layers): from cell structure to biomimetics. Prog Biophys Mol Biol **65:**83-111.

237.   **Sara, M., and U. B. Sleytr.** 2000. S-Layer proteins. J Bacteriol **182:**859-868.

238.   **Sauer, K., and A. K. Camper.** 2001. Characterization of phenotypic changes in *Pseudomonas putida* in response to surface-associated growth. J Bacteriol **183:**6579-6589.

239. **Sauer, K., A. K. Camper, G. D. Ehrlich, J. W. Costerton, and D. G. Davies.** 2002. *Pseudomonas aeruginosa* displays multiple phenotypes during development as a biofilm. J Bacteriol **184:**1140-1154.

240. **Schelert, J., V. Dixit, V. Hoang, J. Simbahan, M. Drozda, and P. Blum.** 2004. Occurrence and characterization of mercury resistance in the hyperthermophilic archaeon *Sulfolobus solfataricus* by use of gene disruption. J Bacteriol **186:**427-437.

241. **Schembri, M. A., K. Kjaergaard, and P. Klemm.** 2003. Global gene expression in *Escherichia coli* biofilms. Mol Microbiol **48:**253-267.

242. **Schleper, C., G. Puehler, I. Holz, A. Gambacorta, D. Janekovic, U. Santarius, H. P. Klenk, and W. Zillig.** 1995. *Picrophilus* gen. nov., fam. nov.: a novel aerobic, heterotrophic, thermoacidophilic genus and family comprising archaea capable of growth around pH 0. J Bacteriol **177:**7050-7059.

243. **Schopf, S., G. Wanner, R. Rachel, and R. Wirth.** 2008. An archaeal bi-species biofilm formed by *Pyrococcus furiosus* and *Methanopyrus kandleri*. Arch Microbiol **190:**371-377.

244. **Segerer, A. H., S. Burggraf, G. Fiala, G. Huber, R. Huber, U. Pley, and K. O. Stetter.** 1993. Life in hot springs and hydrothermal vents. Orig Life Evol Biosph **23:**77-90.

245. **Seifert, K. N., E. E. Adderson, A. A. Whiting, J. F. Bohnsack, P. J. Crowley, and L. J. Brady.** 2006. A unique serine-rich repeat protein (Srr-2) and novel surface antigen (epsilon) associated with a virulent lineage of serotype III *Streptococcus agalactiae*. Microbiology **152:**1029-1040.

246. **Severina, L.** 1995. Bacterial S Layers, p. 725-733, vol. 64. Mikrobiologiya.

247. **She, Q., R. K. Singh, F. Confalonieri, Y. Zivanovic, G. Allard, M. J. Awayez, C. C. Chan-Weiher, I. G. Clausen, B. A. Curtis, A. De Moors, G. Erauso, C. Fletcher, P. M. Gordon, I. Heikamp-de Jong, A. C. Jeffries, C. J. Kozera, N. Medina, X. Peng, H. P. Thi-Ngoc, P. Redder, M. E. Schenk, C. Theriault, N. Tolstrup, R. L. Charlebois, W. F. Doolittle, M. Duguet, T. Gaasterland, R. A. Garrett, M. A. Ragan, C. W. Sensen, and J. Van der Oost.** 2001. The complete genome of the crenarchaeon *Sulfolobus solfataricus* P2. Proc Natl Acad Sci U S A **98:**7835-7840.

248. **Sherlock, O., M. A. Schembri, A. Reisner, and P. Klemm.** 2004. Novel roles for the AIDA adhesin from diarrheagenic *Escherichia coli*: cell aggregation and biofilm formation. J Bacteriol **186:**8058-8065.

249. **Sherlock, O., R. M. Vejborg, and P. Klemm.** 2005. The TibA adhesin/invasin from enterotoxigenic *Escherichia coli* is self recognizing and induces bacterial aggregation and biofilm formation. Infect Immun **73:**1954-1963.

250. **Siebers, B., and P. Schonheit.** 2005. Unusual pathways and enzymes of central carbohydrate metabolism in Archaea. Curr Opin Microbiol **8:**695-705.

251. **Simm, R., M. Morr, A. Kader, M. Nimtz, and U. Romling.** 2004. GGDEF and EAL domains inversely regulate cyclic di-GMP levels and transition from sessility to motility. Mol Microbiol **53:**1123-1134.

252. **Simon, G., J. Walther, N. Zabeti, Y. Combet-Blanc, R. Auria, J. van der Oost, and L. Casalot.** 2009. Effect of O2 concentrations on *Sulfolobus solfataricus* P2. FEMS Microbiol Lett **299:**255-260.

253. **Smirnova, T., L. Didenko, R. Azizbekyan, and Y. M. Romanova.** 2010. Structural and functional characteristics of bacterial biofilms. Microbiology **79:**413-423.

254. **Smith, A. W.** 2005. Biofilms and antibiotic therapy: is there a role for combating bacterial resistance by the use of novel drug delivery systems? Adv Drug Deliv Rev **57:**1539-1550.

255. **Solano, C., B. Garcia, J. Valle, C. Berasain, J. M. Ghigo, C. Gamazo, and I. Lasa.** 2002. Genetic analysis of *Salmonella enteritidis* biofilm formation: critical role of cellulose. Mol Microbiol **43:**793-808.

256. **Spoering, A. L., and K. Lewis.** 2001. Biofilms and planktonic cells of *Pseudomonas aeruginosa* have similar resistance to killing by antimicrobials. J Bacteriol **183:**6746-6751.

257. **Stanley, N. R., R. A. Britton, A. D. Grossman, and B. A. Lazazzera.** 2003. Identification of catabolite repression as a physiological regulator of biofilm formation by *Bacillus subtilis* by use of DNA microarrays. J Bacteriol **185:**1951-1957.

258. **Starnbach, M. N., and S. Lory.** 1992. The fliA (rpoF) gene of *Pseudomonas aeruginosa* encodes an alternative sigma factor required for flagellin synthesis. Mol Microbiol **6:**459-469.

259. **Stetter, K. O., G. Fiala, R. Huber, G. Huber, and A. Segerer.** 1986. Life above the boiling point of water? Cellular and Molecular Life Sciences **42:**1187-1191.

260. **Stetter, K. O., A. Segerer, W. Zillig, G. Huber, G. Fiala, R. Huber, and H. König.** 1986. Extremely thermophilic sulfur-metabolizing archaebacteria. Systematic and applied microbiology **7:**393-397.

261. **Stewart, P. S., B. M. Peyton, W. J. Drury, and R. Murga.** 1993. Quantitative observations of heterogeneities in *Pseudomonas aeruginosa* biofilms. Appl Environ Microbiol **59:**327-329.

262. **Stoodley, P., J. D. Boyle, I. Dodds, and H. M. Lappin-Scott.** 1997. Consensus model of biofilm structure.

263. **Stoodley, P., A. Jacobsen, B. C. Dunsmore, B. Purevdorj, S. Wilson, H. M. Lappin-Scott, and J. W. Costerton.** 2001. The influence of fluid shear and AICI3 on the material properties of *Pseudomonas aeruginosa* PAO1 and *Desulfovibrio sp*. EX265 biofilms. Water Sci Technol **43:**113-120.

264. **Stoodley, P., K. Sauer, D. Davies, and J. Costerton.** 2002. Biofilms as complex differentiated communities. Annual Reviews in Microbiology **56:**187-209.

265. **Sumper, M.** 1987. Halobacterial glycoprotein biosynthesis. Biochim Biophys Acta **906:**69-79.

266. **Sumper, M., E. Berg, R. Mengele, and I. Strobel.** 1990. Primary structure and glycosylation of the S-layer protein of *Haloferax volcanii*. J Bacteriol **172:**7111-7118.

267. **Sutherland, I. W.** 2001. The biofilm matrix--an immobilized but dynamic microbial environment. Trends Microbiol **9:**222-227.

268. **Suzuki, K., X. Wang, T. Weilbacher, A. K. Pernestig, O. Melefors, D. Georgellis, P. Babitzke, and T. Romeo.** 2002. Regulatory circuitry of the CsrA/CsrB and BarA/UvrY systems of *Escherichia coli*. J Bacteriol **184:**5130-5140.

269. **Suzuki, T., T. Iwasaki, T. Uzawa, K. Hara, N. Nemoto, T. Kon, T. Ueki, A. Yamagishi, and T. Oshima.** 2002. *Sulfolobus tokodaii* sp. nov. (f. *Sulfolobus sp*. strain 7), a new member of the genus *Sulfolobus* isolated from Beppu Hot Springs, Japan. Extremophiles **6:**39-44.

270. **Szabo, Z., M. Sani, M. Groeneveld, B. Zolghadr, J. Schelert, S. V. Albers, P. Blum, E. J. Boekema, and A. J. Driessen.** 2007. Flagellar motility and structure in the hyperthermoacidophilic archaeon *Sulfolobus solfataricus*. J Bacteriol **189:**4305-4309.

271. **Szabo, Z., A. O. Stahl, S. V. Albers, J. C. Kissinger, A. J. Driessen, and M. Pohlschroder.** 2007. Identification of diverse archaeal proteins with class III signal peptides cleaved by distinct archaeal prepilin peptidases. J Bacteriol **189:**772-778.

272. **Szymanski, C. M., D. H. Burr, and P. Guerry.** 2002. *Campylobacter protein* glycosylation affects host cell interactions. Infect Immun **70:**2242-2244.

273. **Tachdjian, S., and R. M. Kelly.** 2006. Dynamic metabolic adjustments and genome plasticity are implicated in the heat shock response of the extremely thermoacidophilic archaeon *Sulfolobus solfataricus*. J Bacteriol **188:**4553-4559.

274. **Tanaka, G., M. Shigeta, H. Komatsuzawa, M. Sugai, H. Suginaka, and T. Usui.** 1999. Effect of the growth rate of *Pseudomonas aeruginosa* biofilms on the susceptibility to antimicrobial agents: beta-lactams and fluoroquinolones. Chemotherapy **45:**28-36.

275. **Thoma, C., M. Frank, R. Rachel, S. Schmid, D. Nather, G. Wanner, and R. Wirth.** 2008. The Mth60 fimbriae of *Methanothermobacter thermoautotrophicus* are functional adhesins. Environ Microbiol **10:**2785-2795.

276. **Thomas, N. A., S. Mueller, A. Klein, and K. F. Jarrell.** 2002. Mutants in flaI and flaJ of the archaeon *Methanococcus voltae* are deficient in flagellum assembly. Mol Microbiol **46:**879-887.

277. **Thomas, V. C., L. R. Thurlow, D. Boyle, and L. E. Hancock.** 2008. Regulation of autolysis-dependent extracellular DNA release by *Enterococcus faecalis* extracellular proteases influences biofilm development. J Bacteriol **190:**5690-5698.

278. **Thormann, K. M., R. M. Saville, S. Shukla, and A. M. Spormann.** 2005. Induction of rapid detachment in *Shewanella oneidensis* MR-1 biofilms. J Bacteriol **187:**1014-1021.

279. **Tremblay, L. O., and A. Herscovics.** 1999. Cloning and expression of a specific human alpha 1,2-mannosidase that trims Man9GlcNAc2 to Man8GlcNAc2 isomer B during N-glycan biosynthesis. Glycobiology **9:**1073-1078.

280. **Trent, J. D., E. Nimmesgern, J. S. Wall, F. U. Hartl, and A. L. Horwich.** 1991. A molecular chaperone from a thermophilic archaebacterium is related to the eukaryotic protein t-complex polypeptide-1. Nature **354:**490-493.

281. **Tripepi, M., S. Imam, and M. Pohlschroder.** 2010. *Haloferax volcanii* flagella are required for motility but are not involved in PibD-dependent surface adhesion. J Bacteriol **192:**3093-3102.

282. **Ueda, A., C. Attila, M. Whiteley, and T. K. Wood.** 2009. Uracil influences quorum sensing and biofilm formation in *Pseudomonas aeruginosa* and fluorouracil is an antagonist. Microb Biotechnol **2:**62-74.

283. **Ueda, A., and T. K. Wood.** 2009. Connecting quorum sensing, c-di-GMP, pel polysaccharide, and biofilm formation in *Pseudomonas aeruginosa* through tyrosine phosphatase TpbA (PA3885). PLoS Pathog **5:**e1000483.

284. **Ukuku, D. O., and W. F. Fett.** 2002. Relationship of cell surface charge and hydrophobicity to strength of attachment of bacteria to cantaloupe rind. J Food Prot **65:**1093-1099.

285. **Uppuluri, P., C. G. Pierce, D. P. Thomas, S. S. Bubeck, S. P. Saville, and J. L. Lopez-Ribot.** 2010. The transcriptional regulator Nrg1p controls *Candida albicans* biofilm formation and dispersion. Eukaryot Cell **9:**1531-1537.

286. **Van Dellen, K. L., L. Houot, and P. I. Watnick.** 2008. Genetic analysis of *Vibrio cholerae* monolayer formation reveals a key role for DeltaPsi in the transition to permanent attachment. J Bacteriol **190:**8185-8196.

287. **Van der Mei, H., M. Rosenberg, and H. Busscher.** 1991. Assessment of microbial cell surface hydrophobicity. Microbial cell surface analysis. VCH, New York**:**265–287.

288. **van der Veen, S., and T. Abee.** 2011. Mixed species biofilms of *Listeria monocytogenes* and *Lactobacillus plantarum* show enhanced resistance to benzalkonium chloride and peracetic acid. Int J Food Microbiol **144:**421-431.

289. **Van Loosdrecht, M., J. Lyklema, W. Norde, G. Schraa, and A. Zehnder.** 1987. The role of bacterial cell wall hydrophobicity in adhesion. Applied and environmental microbiology **53:**1893.

290. **van Loosdrecht, M. C., J. Lyklema, W. Norde, G. Schraa, and A. J. Zehnder.** 1987. Electrophoretic mobility and hydrophobicity as a measured to predict the initial steps of bacterial adhesion. Appl Environ Microbiol **53:**1898-1901.

291. **Van Oss, C. J., M. K. Chaudhury, and R. J. Good.** 1988. Interfacial Lifshitz-van der Waals and polar interactions in macroscopic systems. Chemical Reviews **88:**927-941.

292. **van Schaik, E. J., C. L. Giltner, G. F. Audette, D. W. Keizer, D. L. Bautista, C. M. Slupsky, B. D. Sykes, and R. T. Irvin.** 2005. DNA binding: a novel function of *Pseudomonas aeruginosa* type IV pili. J Bacteriol **187:**1455-1464.

293.   **Vasseur, P., I. Vallet-Gely, C. Soscia, S. Genin, and A. Filloux.** 2005. The pel genes of the *Pseudomonas aeruginosa* PAK strain are involved at early and late stages of biofilm formation. Microbiology **151:**985-997.

294.   **Vats, N., and S. F. Lee.** 2000. Active detachment of *Streptococcus mutans* cells adhered to epon-hydroxylapatite surfaces coated with salivary proteins in vitro. Arch Oral Biol **45:**305-314.

295.   **Veith, A., A. Klingl, B. Zolghadr, K. Lauber, R. Mentele, F. Lottspeich, R. Rachel, S. V. Albers, and A. Kletzin.** 2009. *Acidianus*, *Sulfolobus* and *Metallosphaera* surface layers: structure, composition and gene expression. Mol Microbiol **73:**58-72.

296.   **Voisin, S., R. S. Houliston, J. Kelly, J. R. Brisson, D. Watson, S. L. Bardy, K. F. Jarrell, and S. M. Logan.** 2005. Identification and characterization of the unique N-linked glycan common to the flagellins and S-layer glycoprotein of *Methanococcus voltae*. J Biol Chem **280:**16586-16593.

297.   **von Eiff, C., G. Peters, and C. Heilmann.** 2002. Pathogenesis of infections due to coagulase-negative *staphylococci*. Lancet Infect Dis **2:**677-685.

298.   **Wagner, M., R. Amann, H. Lemmer, and K. H. Schleifer.** 1993. Probing activated sludge with oligonucleotides specific for proteobacteria: inadequacy of culture-dependent methods for describing microbial community structure. Appl Environ Microbiol **59:**1520-1525.

299.   **Wagner, M., S. Berkner, M. Ajon, A. J. Driessen, G. Lipps, and S. V. Albers.** 2009. Expanding and understanding the genetic toolbox of the hyperthermophilic genus *Sulfolobus*. Biochem Soc Trans **37:**97-101.

300.   **Wai, S. N., Y. Mizunoe, A. Takade, S. I. Kawabata, and S. I. Yoshida.** 1998. *Vibrio cholerae* O1 strain TSI-4 produces the exopolysaccharide materials that determine colony morphology, stress resistance, and biofilm formation. Appl Environ Microbiol **64:**3648-3655.

301.   **Waite, R. D., A. Papakonstantinopoulou, E. Littler, and M. A. Curtis.** 2005. Transcriptome analysis of *Pseudomonas aeruginosa* growth: comparison of gene expression in planktonic cultures and developing and mature biofilms. J Bacteriol **187:**6571-6576.

302.   **Walters, M. C., 3rd, F. Roe, A. Bugnicourt, M. J. Franklin, and P. S. Stewart.** 2003. Contributions of antibiotic penetration, oxygen limitation, and low metabolic activity to tolerance of *Pseudomonas aeruginosa* biofilms to ciprofloxacin and tobramycin. Antimicrob Agents Chemother **47:**317-323.

303.   **Ward, D. M., M. J. Ferris, S. C. Nold, and M. M. Bateson.** 1998. A natural view of microbial biodiversity within hot spring cyanobacterial mat communities. Microbiology and Molecular Biology Reviews **62:**1353.

304.   **Waters, C. M., W. Lu, J. D. Rabinowitz, and B. L. Bassler.** 2008. Quorum sensing controls biofilm formation in *Vibrio cholerae* through modulation of cyclic di-GMP levels and repression of vpsT. J Bacteriol **190:**2527-2536.

305.   **Watnick, P. I., and R. Kolter.** 1999. Steps in the development of a *Vibrio cholerae* El Tor biofilm. Mol Microbiol **34:**586-595.

306.   **Webb, J. S., L. S. Thompson, S. James, T. Charlton, T. Tolker-Nielsen, B. Koch, M. Givskov, and S. Kjelleberg.** 2003. Cell death in *Pseudomonas aeruginosa* biofilm development. J Bacteriol **185:**4585-4592.

307.   **Wei, B. L., A. M. Brun-Zinkernagel, J. W. Simecka, B. M. Pruss, P. Babitzke, and T. Romeo.** 2001. Positive regulation of motility and flhDC expression by the RNA-binding protein CsrA of *Escherichia coli*. Mol Microbiol **40:**245-256.

308.   **Whitaker, R. J., D. W. Grogan, and J. W. Taylor.** 2003. Geographic barriers isolate endemic populations of hyperthermophilic archaea. Science **301:**976-978.

309.   **Whitchurch, C. B., T. Tolker-Nielsen, P. C. Ragas, and J. S. Mattick.** 2002. Extracellular DNA required for bacterial biofilm formation. Science **295:**1487.

310. **Whiteley, M., M. G. Bangera, R. E. Bumgarner, M. R. Parsek, G. M. Teitzel, S. Lory, and E. P. Greenberg.** 2001. Gene expression in *Pseudomonas aeruginosa* biofilms. Nature **413:**860-864.

311. **Woese, C. R., and G. E. Fox.** 1977. Phylogenetic structure of the prokaryotic domain: the primary kingdoms. Proc Natl Acad Sci U S A **74:**5088-5090.

312. **Woese, C. R., O. Kandler, and M. L. Wheelis.** 1990. Towards a natural system of organisms: proposal for the domains Archaea, Bacteria, and Eucarya. Proc Natl Acad Sci U S A **87:**4576-4579.

313. **Wozniak, D. J., T. J. Wyckoff, M. Starkey, R. Keyser, P. Azadi, G. A. O'Toole, and M. R. Parsek.** 2003. Alginate is not a significant component of the extracellular polysaccharide matrix of PA14 and PAO1 *Pseudomonas aeruginosa* biofilms. Proc Natl Acad Sci U S A **100:**7907-7912.

314. **Wu, H., M. Zeng, and P. Fives-Taylor.** 2007. The glycan moieties and the N-terminal polypeptide backbone of a fimbria-associated adhesin, Fap1, play distinct roles in the biofilm development of *Streptococcus parasanguinis*. Infect Immun **75:**2181-2188.

315. **Yang, M., E. M. Frey, Z. Liu, R. Bishar, and J. Zhu.** 2010. The virulence transcriptional activator AphA enhances biofilm formation by *Vibrio cholerae* by activating expression of the biofilm regulator VpsT. Infect Immun **78:**697-703.

316. **Yildiz, F. H.** 2008. Cyclic dimeric GMP signaling and regulation of surface-associated developmental programs. J Bacteriol **190:**781-783.

317. **Yildiz, F. H., X. S. Liu, A. Heydorn, and G. K. Schoolnik.** 2004. Molecular analysis of rugosity in a *Vibrio cholerae* O1 El Tor phase variant. Mol Microbiol **53:**497-515.

318. **Yurist-Doutsch, S., H. Magidovich, V. V. Ventura, P. G. Hitchen, A. Dell, and J. Eichler.** 2010. N-glycosylation in Archaea: On the coordinated actions of *Haloferax volcanii* AglF and AglM. Mol Microbiol.

319. **Yurist Doutsch, S., B. Chaban, D. J. VanDyke, K. F. Jarrell, and J. Eichler.** 2008. Sweet to the extreme: protein glycosylation in Archaea. Molecular microbiology **68:**1079-1084.

320. **Zahringer, U., H. Moll, T. Hettmann, Y. A. Knirel, and G. Schafer.** 2000. Cytochrome b558/566 from the archaeon *Sulfolobus acidocaldarius* has a unique Asn-linked highly branched hexasaccharide chain containing 6-sulfoquinovose. Eur J Biochem **267:**4144-4149.

321. **Zeikus, J., M. Dawson, T. Thompson, K. Ingvorsen, and E. Hatchikian.** 1983. Microbial Ecology of Volcanic Sulphidogenesis: Isolation and Characterization of *Thermodesulfobacterium* commune gen. nov. and sp. nov. Microbiology **129:**1159.

322. **Zhang, Y. Q., S. X. Ren, H. L. Li, Y. X. Wang, G. Fu, J. Yang, Z. Q. Qin, Y. G. Miao, W. Y. Wang, R. S. Chen, Y. Shen, Z. Chen, Z. H. Yuan, G. P. Zhao, D. Qu, A. Danchin, and Y. M. Wen.** 2003. Genome-based analysis of virulence genes in a non-biofilm-forming *Staphylococcus epidermidis* strain (ATCC 12228). Mol Microbiol **49:**1577-1593.

323. **Zhou, M., and H. Wu.** 2009. Glycosylation and biogenesis of a family of serine-rich bacterial adhesins. Microbiology **155:**317-327.

324. **Zhou, M., F. Zhu, S. Dong, D. G. Pritchard, and H. Wu.** 2010. A novel glucosyltransferase is required for glycosylation of a serine-rich adhesin and biofilm formation by *Streptococcus parasanguinis*. J Biol Chem **285:**12140-12148.

325. **Zillig, W., A. Kletzin, C. Schleper, I. Holz, D. Janekovic, J. Hain, M. Lanzendörfer, and J. Kristjansson.** 1994. Screening for *Sulfolobales*, their plasmids and their viruses in Icelandic solfataras. Systematic and applied microbiology **16:**609-628.

326. **Zillig, W., K. O. Stetter, S. Wunderl, W. Schulz, H. Priess, and I. Scholz.** 1980. The *Sulfolobus*-"*Caldariella*" group: taxonomy on the basis of the structure of DNA-dependent RNA polymerases. Archives of Microbiology **125:**259-269.

327. **Zolghadr, B., A. Klingl, A. Koerdt, A. J. Driessen, R. Rachel, and S. V. Albers.** 2010. Appendage-mediated surface adherence of *Sulfolobus solfataricus*. J Bacteriol **192:**104-110.

328. **Zolghadr, B., A. Klingl, R. Rachel, A. J. Driessen, and S. V. Albers.** 2011. The bindosome is a structural component of the *Sulfolobus solfataricus* cell envelope. Extremophiles **15:**235-244.

329. **Zolghadr, B., S. Weber, Z. Szabo, A. J. Driessen, and S. V. Albers.** 2007. Identification of a system required for the functional surface localization of sugar binding proteins with class III signal peptides in *Sulfolobus solfataricus*. Mol Microbiol **64:**795-806.

Acknowlegements

I am very grateful to my supervisor Dr. Sonja-Verena Albers who offered me the opportunity to join her lab and to do my PhD in her group. I am not just thankful for her support and guidance during my research, but also for the extraordinary devotion and the empathy which she demonstrated several times.

I am also thankful to my thesis committee Dr. Sonja-Verena Albers, Prof. Dr. Martin Thanbichler, Prof. Dr. Uwe Maier and Prof. Dr. Hans Ulrich Mösch.

Furthermore, special thanks go to Dr. Kai Thormann and Dr. Julia Gödeke who supported my research especially in the beginning of the work on biofilm. I would like to thank also all my collaborators, who are apparent from the list of publications which were published during my study.

I would like to acknowledge all my colleagues in the MPI, especially the group of the Molecular Biology of Archaea for the inspiring discussions and suggestions. Thanks to Kerstin, Marleen, Thomaz, Sunia, Ankan and Sonja F.

I would particularly like to highlight Michaela (thanks for genetics), Alex (thanks for informatics), Julia and Benjamin (thanks for experimental support), and Anna-Lena (the best Master student ever ☺) Furthermore, the persons who worked with me on the same topic and supported me in several aspects, Alvaro and Vicky.

My sincere thanks go to two persons, who are not just colleagues, but very good friends and who supported me in more than scientific related questions: Abhra and Anne. Thanks that you both were there every time I needed you.

Ich möchte hier ebenfalls meinen Dank an meine Familie richten, die immer an mich geglaubt haben und mich in jeder Ihnen möglichen Weise unterstützt haben. Ich habe euch lieb!!!

Last but for sure not least I want to thank Behnam. You are the best for me and I am very glad to be together with you. I am deeply grateful that you supported me and believed in me!

I could continue the list of thanks without ending, therefore I want to thank all the others which are not named, but still contributed in some way to my study, my scientific and personal life.

Curriculum Vitae

Personal Data

Name: Andrea Koerdt
Date of birth: 24 February 1983
Birthplace: Wickede (Ruhr)
Nationality: German
Marital status: Single

Education

2008-Present   PhD research, Max Planck Institute for terrestrial
                   Microbiology in Marburg, department of Molecular Biology
                   of Archaea, PhD is expected to be finalized in October
                   2011

2003-2008   Diploma theses, Max Planck Institute for terrestrial
                   Microbiology in Marburg, Department of Ecophysiology,
                   Study of biology, Philipps-Universität Marburg, Germany
                   Major: Microbiology
                   Minor subjects: Genetics and Virology.
                   Study completed with distinction.

1994-2002   Highschool, completed with general qualification for
                   university entrance.

Publications

Koerdt, A., A. Orell, T. K. Pham, J. Mukherjee, A. Wlodkowski, E. Karunakaran, C. A. Biggs, P. C. Wright, and S. V. Albers. 2011. Macromolecular Fingerprinting of *Sulfolobus* species in Biofilm: A Transcriptomic and Proteomic Approach Combined with Spectroscopic Analysis. J Proteome Res.

Koerdt, A., J. Godeke, Berger, J, Thormann, K.M. and S. V. Albers (2010). "Crenarchaeal biofilm formation under extreme conditions." PLoS One 5(11): e14104.

Zolghadr B, Klingl A, **Koerdt A**, Driessen AJ, Rachel R, Albers SV. (2010). "Appendage-mediated surface adherence of *Sulfolobus solfataricus*." J Bacteriol 192(1): 104-10.

Koerdt A, Paulick A, Mock M, Jost K, Thormann KM. (2009). "MotX and MotY are required for flagellar rotation in *Shewanella oneidensis* MR-1." J Bacteriol 191(16): 5085-93.

Paulick A, **Koerdt A**, Lassak J, Huntley S, Wilms I, Narberhaus F, Thormann KM. (2009). "Two different stator systems drive a single polar flagellum in *Shewanella oneidensis* MR-1." Mol Microbiol 71(4): 836-50.

Erklärung

Ich versichere, dass ich meine Dissertation:

„Biofilm formation in the thermoacidophilic crenarchaea
***Sulfolobus spp.*„**

selbstständig, ohne unerlaubte Hilfe angefertigt und mich dabei keiner anderen als der von mir ausdrücklich bezeichneten Quellen und Hilfen bedient habe. Die Dissertation wurde in der jetzigen oder einer ähnlichen Form noch bei keiner anderen Hochschule eingereicht und hat noch keinen sonstigen Prüfungszwecken gedient.

Marburg, den 24.08.2011

_____

Andrea Koerdt

Einverständniserklärung

Ich erkläre mich damit einverstanden, dass die vorliegende Dissertation mit dem Titel

**„Biofilm formation in the thermoacidophilic crenarchaea
Sulfolobus spp."**

in Bibliotheken allgemeinzugänglich gemacht wird. Dazu gehört, dass sie

- von der Bibliothek der Einrichtung, in der ich meine Arbeit angefertigt habe, zur Benutzung in ihren Räumen bereitgehalten wird
- in konventionellen und maschinenlesbaren Katalogen, Verzeichnissen und Datenbanken verzeichnet wird,
- der Universitätsbibliothek für die lokale Nutzung und für Fernleihzwecke zur Verfügung steht und
- im Rahmen der urheberrechtlichen Bestimmungen für Kopierzwecke genutzt werden kann.

Marburg, den 24.08.2011

_____	_____
Andrea Koerdt	Dr. Sonja-Verena Albers
(Verfasserin)	(Betreuerin)